**Individual Differences in Nucleus Accumbens Activity and Cue-Reward Learning**

by

Cristina Emma María Ríos

A dissertation submitted in partial fulfillment
of the requirements for the degree of
Doctor of Philosophy
(Neuroscience)
in the University of Michigan
2022

Doctoral Committee:

Associate Professor Jonathan D. Morrow, Co-Chair
Professor Geoffrey G. Murphy, Co-Chair
Professor Kent C. Berridge
Associate Professor Carrie Ferrario
Professor Mark Thomas, University of Minnesota
Associate Professor Natalie Tronson

Cristina Emma María Ríos

cemaria@umich.edu

ORCID iD: 0000-0002-4343-8198

## DEDICATION

This dissertation is dedicated to my mother Emma Margarita. Thank you for walking by me every step of the way and for your truly unconditional love.

*Gracias, Madre*.

## ACKNOWLEDGEMENTS

First and foremost, thank you to my graduate co-mentors: Dr. Jonathan Morrow and Dr. Geoffrey Murphy. Thank you, Dr. Morrow for inspiring in me a true passion for behavioral neuroscience, and Dr. Murphy for always motivating me to dive into neurophysiology no matter how challenging it could sometimes be. Both of you have gifted me with invaluable mentorship over the last six years and I deeply thank you for giving me the freedom and confidence to explore my own curiosities and progressively develop into a neuroscientist. I also want to thank all the past and current members of the Morrow and Murphy Labs for sharing your knowledge and providing such a positive and nourishing environment. I have gathered beautiful friendships and priceless experiences that I will always hold dearly. I want to especially thank Frankie Czesak for collaborating with me on all the chemogenetic behavioral experiments. All your hard work is deeply appreciated. I am grateful to post-doctoral and research mentors Dr. Shannon Moore, Dr. Ali Gheidi, Dr. Paolo Campus, Dr. Victor Cazares, and Dr. Kasia Glanowska; former graduate student, Dr. Christopher Fitzpatrick; all undergraduates that have been involved in my journey, but especially Jordan Gregory, Coltrane Groves, and Jacklyn Staffeld; as well as past and current lab managers Tyler Allerton, Aidan Horvath, and Prableen Singh, for all your time and support over the years.

I would like to thank the members of my dissertation committee, Dr. Kent Berridge, Dr. Carrie Ferrario, Dr. Mark Thomas, and Dr. Natalie Tronson for your

guidance and input. I also want to thank Dr. Thomas for taking me in your laboratory at the University of Minnesota under the guidance of Dr. Manny Esguerra, who patiently taught me how to perform whole-cell patch clamp recordings, an experience that I will forever cherish. I want to especially thank Dr. Carlos Jiménez-Rivera, my first research mentor. I would not have undertaken this journey if it had not been for your encouragement and contagious passion for science. I will be forever grateful and hope to someday provide the same inspiration you did for me to another young aspiring student.

To my cohort and all my dearest friends, especially Yanaira Alonso, Sofia López, Normarie Herrera, Marlian Montesinos, and Andrea Delgado, thank you for never failing to brighten my days, especially during those hard ones.

To my parents Emma and Clemente†, my stepdad Alirio, and my brother José, *los amo,* thank you for walking by me every step of the way. Each new day you inspire me to follow my passions and keep moving forward, always ensuring that I remain confident in myself. To my godparents Nydia and Norman, my aunt Mayra, my uncles Eddie and Rubén, my brother Moisés, and the rest of my family, thank you for showing me unconditional love and support.

Finally, *gracias a mi Isla, Puerto Rico*. I hope to give it all back one day.

This work was supported by The National Science Foundation (NSF)-Graduate Research Fellowship Program (GRFP), The National Institute of Neurological Disorders and Stroke [5F99-NS120544-02], The National Institute on Drug Abuse (NIDA) [R01-DA-044960], The National Institute on Aging [R01-AG-074552; R01-AG-052934], and The National Institute of Mental Health [U19-MH-106434].

## TABLE OF CONTENTS

## LIST OF FIGURES

### Chapter I



### Chapter II

**Chapter III**



**Chapter IV**

## LIST OF TABLES

### Chapter II



### Chapter III



### Chapter IV

**Chapter V**

## ABSTRACT

The nucleus accumbens (NAc) and its population of GABAergic medium spiny neurons (MSNs) converge inputs from cortical and subcortical structures to modulate behavioral responses associated with reward and motivation. In particular, the NAc plays a crucial role in cue-reward learning by linking appetitive unconditioned stimuli with external and internal cues to later drive conditioned responses (CR). For decades, much attention has been focused on understanding this carefully coordinated process that supports elemental associative learning mechanisms. We hypothesize that variations in NAc activity can contribute to aberrant and maladaptive behaviors. For example, evidence suggests that behavioral endophenotypes such as impulsivity and heightened cue reactivity – traits that have a neurobiological footprint on NAc activity during cue-reward learning – may predispose certain individuals to develop disorders like addiction.

"Sign-tracker" (ST) and "goal-tracker" (GT) rats can be used as a behavioral model of individual differences in cue reactivity. During a Pavlovian conditioned approach (PavCA) procedure, GTs only use the reward cues as predictors, resulting in a CR directed toward the site of impending reward delivery ("goal-tracking"). In contrast, STs also attribute cues with incentive salience and find them rewarding, resulting in increased motivation towards and fixation on these cues measured by a CR directed toward the cue ("sign-tracking"). STs are more impulsive as well as susceptible to cue-

induced reinstatement or “relapse” of drugs of abuse compared to GTs, making them an excellent model to study predisposition to addiction-like behaviors. Sign- and goal-tracking behaviors exhibit different levels of dependence on NAc activity, and this is reflected by differences in cue- and reward-evoked patterns of neuronal activity and dopamine release during Pavlovian learning. Why these distinct patterns of activity emerge is unknown, but we hypothesize that both the excitability state of MSNs in the NAc as well as the synaptic influence from glutamatergic sources, such as the ventral hippocampus (vHPC), could impact how sensitive the NAc is to input signals carrying cue-related information.

To test this hypothesis, we began by establishing a physiological profile of the subregional membrane excitability of MSNs in the core and shell subdivisions of the NAc of naïve and behaviorally experienced rats. We found that MSNs in the shell consistently exhibited greater intrinsic excitability than those in the core, which supports that subregional excitability across the NAc may be important for understanding differences in NAc dynamics and reward-processing. We also found that STs had significantly lower firing capacity than GTs only in the NAc core, suggesting that individual differences in NAc excitability may be important for different expressions of conditioned responses toward rewarding cues and addiction susceptibility. Focusing on the vHPC-NAc projection, which is thought to regulate conditioned responses based on contextual information processing during cue-reward learning, we found that sign-tracking behavior is associated with reduced vHPC-NAc activity compared to goal-tracking. Collectively, these findings demonstrate that differences in NAc neuronal excitability and synaptic activity are present between STs and GTs. This work highlights

the importance of individual differences in NAc physiology and activity during cue-reward learning for understanding how properties of emotionally salient cues are encoded and contribute to disease susceptibility.

# CHAPTER I

## Introduction

*Note: Portions of the text within Chapter I have appeared previously in print (María-Ríos & Morrow, 2020, Front. Behav. Neurosci.) and are reproduced here with permission from the authors.*

Our brains have evolved systems to operate a range of sensory, cognitive, emotional, and motor processes in response to natural reinforcers. By definition, positive reinforcers are desirable stimuli that increase the likelihood of a behavior to reoccur. Reinforcers are able to exert behavioral control because they can invoke dopamine transmission within brain reward regions like the nucleus accumbens (NAc) and facilitate associative learning processes (Berridge and Kringelbach, 2015). Drug addiction has been previously described as a disorder of associative learning (Di Chiara et al., 1999). This is because addictive drugs can hijack the brain systems naturally evolved for conventional reinforcers and overstimulate dopamine transmission. The consequence is heightened or excessive associative learning to drug-related stimuli that predict drug availability. The excessive motivational value attributed to these drug-related stimuli results in their ability to steer an individual's behavior toward compulsive drug-seeking and use (Robinson and Berridge, 1993; Di Chiara et al., 1999).

Addiction can be a devastating disorder in part because its etiology is rooted in such fundamental and essential neural processes. Around 21 million people in the United States are suffering from addiction (Addiction Center, 2019), and overdose deaths have more than tripled over the last two decades from around 20,000 deaths in 1999 to over 90,000 in 2020 (National Institute on Drug Abuse, 2022). Only around 10% of people meeting criteria for addiction receive treatment and, from those up to 60% relapse within a year (National Institute on Drug Abuse, 2020).

Although substance use is a universal human behavior, and we might expect its associated effects on the reward system and reward processing to also be universal across all individuals, not all who are exposed to addictive substances develop addiction. It is reported that within a given year about 21% of people over the age of 12 use an illicit drug (i.e., cocaine, heroin, opioids, methamphetamine, etc.) (National Survey on Drug Use and Health, 2019), but only about 4% of Americans meet criteria for a drug use disorder within a year (National Institute on Alcohol Abuse and Alcoholism, 2015). This suggests that those who develop addiction may represent a specifically vulnerable population of individuals with greater risk for the disorder compared to others. One possibility is that there are individual differences in how the NAc and other brain reward centers are affected by drug exposure (Volkow et al., 2019). Furthermore, since drug addiction has been conceptualized as a disorder of associative learning (Di Chiara et al., 1999), we might expect these individual differences to manifest in associative learning processes. Even in the absence of drug exposure, some individuals may differ in the way their NAc encodes properties of stimuli that predict positive and negative reinforcers (María-Ríos and Morrow, 2020). Studying

behavioral endophenotypes linked to increased addiction risk and other aberrant associative learning disorders could help determine the potential clinical relevance of individual differences in NAc activity.

**Behavioral endophenotypes as predictors of disease susceptibility**

Because of the often-complex interactions between relevant genetic and environmental factors, it can be difficult to recognize individual factors that affect vulnerability to addiction. Behavioral endophenotypes are more closely related to the abnormalities that characterize these disorders and have the potential to integrate many different underlying genetic and environmental factors, in effect providing a valuable summary of data that might otherwise be prohibitively difficult or impossible to get (Gottesman and Gould, 2003). One such endophenotype that has been consistently associated with addiction is impulsivity (Jentsch and Taylor, 1999; Belin et al., 2008; Crews and Boettiger, 2009; Ersche et al., 2010; Rodríguez-Cintas et al., 2016; Chuang et al., 2017; Thomsen et al., 2018). Impulsivity is a multifaceted concept in research but can be broadly defined as a tendency to engage in risky, premature, or situationally inappropriate actions that are characterized by a lack of planning or forethought (Robbins et al., 2012; Jentsch et al., 2014; Dalley and Robbins, 2017). As has been found in patients with addiction, impulsivity is associated with lower dopaminergic activity in the NAc at baseline and in response to neutral cues but exaggerated striatal responses to more salient cues (Forbes et al., 2009; Hahn et al., 2009; Lee et al., 2009; Colzato et al., 2010; O'Sullivan et al., 2011; Reeves et al., 2012). Impulsivity is also thought to result from impaired prefrontal cortical control over motivationally relevant signals from the NAc and other subcortical structures (Rolls et al., 1994; Aron et al.,

2004; Schmaal et al., 2012; Davis et al., 2013). This same pattern of prefrontal hypoactivity that is insufficient to restrain subcortical impulses has been identified in functional neuroanatomical studies as a key etiologic factor for addiction in preclinical studies (Peters et al., 2009; Goode and Maren, 2019).

Another related behavioral trait is “cue reactivity,” or a tendency towards exaggerated neuronal, emotional and motivational responses to stimuli that have been associated with emotionally salient events. Cue reactivity to drug-related stimuli predicts relapse in patients with addiction (Rohsenow et al., 1991; Carter and Tiffany, 1999; Janes et al., 2010). It also seems to extend to negative stimuli, suggesting cross-sensitization and what may be common neurobiological processes. For example, patients with comorbid addiction and post-traumatic stress disorder (PTSD) exhibit more intense drug cue reactivity, including increased cravings to use drugs, when exposed to personalized trauma cues (Coffey et al., 2010; Tull et al., 2011; Read et al., 2017). Addiction patients also have a tendency to act impulsively in response to emotionally charged stimuli, a trait that is known as “emotional urgency” (Whiteside and Lynam, 2001; Cyders and Smith, 2008), and this tendency correlates with symptom severity and functional impairment (Smith and Cyders, 2016). These findings suggest that symptoms of emotional urgency, impulsivity, and cue reactivity are interrelated and may cross-sensitize in addiction, thereby exacerbating the severity of the illness.

**Individual differences in cue reactivity as a model of addiction vulnerability**

In addition to its role in the pathophysiology of addiction, cue reactivity may also be a pre-existing behavioral trait that predisposes individuals to develop these disorders. This possibility has mainly been explored in preclinical studies by comparing

animals that exhibit individual variation in their reactivity to conditioned cues. An example of this is “sign-trackers” (STs) and “goal-trackers” (GTs) which can be identified using a Pavlovian conditioned approach procedure (PavCA) **(Fig 1.1)**. When a food reward (unconditioned stimulus, US) is repeatedly paired with a localizable cue such as a retractable lever (conditioned stimulus, CS), STs approach and are attracted to the cue itself (“sign-tracking” CR), whereas GTs direct their attention away from the cue and towards the location of impending reward delivery (“goal-tracking” CR) (Flagel et al., 2009; Tomie and Morrow, 2018). Sign-tracking is thought to indicate vulnerability to addiction because STs exhibit increased psychomotor sensitization to cocaine (Flagel et al., 2008), have higher preference for cocaine over food (Tunstall and Kearns, 2015) and exhibit increased cue-induced reinstatement of nicotine (Versaggi et al., 2016) and cocaine (Saunders and Robinson, 2011). In addition, it has been demonstrated that STs, identified by the high levels of incentive salience they attribute to reward-related cues, also have elevated fear responses to a tone that has been paired to a foot-shock (Morrow et al., 2011). This indicates that the sign-tracking trait may represent a more general tendency to attribute excessive motivational salience to cues paired with biologically relevant events, regardless of emotional valence. Sign-tracking may therefore also be a risk factor for PTSD, as suggested by evidence that repeated exposure of STs to aversive stimuli results in a fear response that increases over time, instead of decreasing or remaining stable as is the case for GTs (Morrow et al., 2015). It is important to note that the exaggerated emotional and motivational cue reactivity of STs is specifically tied to discrete, localizable cues. There are no differences between STs and GTs in learning instrumental tasks, so general associative learning and

memory processes appear to be intact in both phenotypes (Ahrens et al., 2016; Fitzpatrick et al., 2019). However, STs exhibit decreased context-induced reinstatement of drug self-administration, as well as lower levels of contextual fear than GTs (Morrow et al., 2011; Saunders et al., 2014). Thus, STs tend to react strongly to conditioned cues regardless of the circumstances under which they are encountered, whereas GTs use contextual cues to modulate their conditioned emotional responses (Pitchers et al., 2017).

Drug use is a normal human behavior, as evidenced by lifetime use estimates in the United States of 48% for illicit drugs, 63% for tobacco products, and 80% for alcohol (Substance Abuse and Mental Health Services Administration, 2018). However, over the course of addiction substance use occurs in increasingly inappropriate contexts, such that it comes to interfere with work, relationships, and other important responsibilities. Though there is substantial evidence that physiological and behavioral consequences of drug use can be highly context-dependent (Crombag et al., 2001; Badiani, 2013), there is also evidence of decreased contextual modulation of responses to drug cues among addiction patients as compared to subjects who used drugs but do not have addiction (Garland et al., 2018). Patients with PTSD express exactly these kinds of deficits as well; their learned fear responses are insensitive to contextual shifts, safety signals, or other indicators of whether the present circumstances are “safe” or “unsafe” (Maren et al., 2013; Garfinkel et al., 2014; Liberzon and Abelson, 2016). Thus, a failure to use contextual information in order to appropriately modify conditioned responses to emotionally salient cues may be a common feature of both addiction and

PTSD, and the ST/GT model seems to accurately represent this trait regardless of the valence.

**The "sign-tracker" and "goal-tracker" model of associative learning**

During associative learning, cues acquire predictive value, meaning they become linked to an explicit representation of the outcome, but in some instances they may also acquire incentive salience, meaning they take on some of the attractive and motivational properties of the reward and become "wanted" targets (Berridge et al., 2009). The propensity to attribute cues with incentive salience is highly variable between individuals, and because cues normally acquire both predictive and incentive value together, it is difficult to dissociate these properties and the underlying neurobiological processes that govern them (Flagel et al., 2009). Because of this caveat, most of the literature on the neurobiology of cue-reward learning and motivation has not taken into consideration individual differences in the attribution of predictive versus incentive value which may even follow distinct rules of reinforcement learning (Maria-Rios et al., 2019). The ST/GT model provides the means to dissociate between these two properties and understand the neurobiological mechanisms responsible for these different forms of learning (Flagel and Robinson, 2017).

What we would now call sign- and goal-tracking behavior was first described by Zener in 1937 in a publication in which he detailed the behavioral responses accompanying the salivary response of freely moving dogs to a bell predicting food availability. Following the initial classical conditioning studies by Pavlov published in 1927 (Pavlov, 1927), Zener reported that while some dogs exhibited goal-directed behaviors in response to the CS by approaching the site of reward delivery, other dogs

were fixated on the CS, approaching it and interacting with it before reward delivery (Zener, 1937). The term “sign-tracking” was first introduced to describe the “keypecking” behavior of pigeons toward an illuminated key when it was positively correlated with food delivery (Hearst and Jenkins, 1974; Wasserman et al., 1974). Shortly after, both “sign-tracking” and “goal-tracking” were used to describe “competing” conditioned behaviors in rats in response to CS presentations. “Sign-tracking” described behavior directed to the CS itself (e.g. lever pressing), while “goal-tracking” described behavior directed toward the site of impending food delivery upon CS presentations (e.g. tray-entry) (Boakes, 1977).

Evidence suggests that STs and GTs differ not only in the form of their behavioral response to the CS, but also in the type of information they are gleaning from the association between the CS and US. While some theorize that both STs and GTs learn the predictive association of the cue and the reward, only for STs does the cue transform into a “wanted” stimuli, sometimes termed a “motivational magnet” (Berridge et al., 2009; Flagel et al., 2009). For instance, the way in which STs interact with the CS can differ depending on the nature of the US: eating behaviors will be directed toward a CS paired with solid food, but drinking behaviors will be directed toward a CS paired with liquid (Jenkins and Moore, 1973). This indicates that for STs, but not GTs, the CS may be taking on some of the motivational properties of the US and thereby gains its own incentive value.

For a cue to be considered an incentive stimulus, three criteria must be met (Saunders and Robinson, 2010; Robinson et al., 2014; Flagel and Robinson, 2017). First, the cue must bias attention and elicit approach. Second, the cue must become

desirable in and of itself, meaning that individuals are willing to work solely for its presentation. Third, the cue can invigorate ongoing operant behavior or reward-seeking. All these properties have been reported to a greater extent in STs than in GTs, providing evidence that different forms of cue-outcome representations are guiding their conditioned responses. As measured using PavCA, if a lever-cue is repeatedly paired with a food reward delivered into a magazine, upon cue presentations STs will approach and engage with the lever (sign-tracking), while GTs go toward the magazine to await the reward (goal-tracking) **(Fig 1.1)**. The response of STs toward the lever illustrates the first property of an incentive stimulus, eliciting approach (Robinson and Berridge, 1993; Flagel et al., 2008). After PavCA training, STs are much more likely than GTs to learn a new operant response and work for the presentation of the CS alone when tested on a conditioned reinforcement procedure. In one such task, used to test for the second property of an incentive stimulus, STs learn to “nosepoke” into an active port which results in the presentation of the previously reward-paired lever (Robinson and Flagel, 2009; Villaruel and Chaudhri, 2016). Finally, the third property is typically tested using a Pavlovian-instrumental transfer (PIT) procedure, in which the previously learned Pavlovian cue may invigorate instrumental learning for either the same reward or a general reward. Although PIT has not been directly demonstrated in ST and GT rats classified using the lever-CS PavCA procedure, a study of ST and GT humans using a monetary reward and visual cues demonstrated that STs had a stronger PIT effect than GTs (Garofalo and di Pellegrino, 2015). Furthermore, it has been shown indirectly that STs engage more than GTs in food- and drug-seeking operant responses following PavCA (Yager and Robinson, 2010; Saunders and Robinson, 2011; Saunders et al.,

2013), suggesting a direct link between the attribution of incentive salience to Pavlovian cues and the vigor of cue-driven, reward-seeking operant responses.

Based on experiments outlined above, the ST/GT behavioral model provides a direct link between individual differences in associative learning (i.e., attribution of incentive salience) and vulnerability to cue-driven psychopathologies like addiction and PTSD. One corollary hypothesis is that differences in cue reactivity may actually stem from differences in the processing of contextual information necessary for modulating conditioned responses to discrete cues (María-Ríos and Morrow, 2020). This has also been conceptualized as a “top-down” cortical control over goal-tracking behavior versus a “bottom-up” subcortical control over sign-tracking behavior (Flagel and Robinson, 2017; Pitchers et al., 2017; Kuhn et al., 2018; Sarter and Phillips, 2018), meaning that less higher-order cortical control in STs results in a lack of restraint on subcortical emotionally-driven impulses. Accordingly, individual differences in reward centers, and specifically the NAc, have been identified using the ST/GT model. This suggests that reward information can be differentially encoded (i.e., incentive vs predictive) in the NAc, and this in turn may determine whether certain individuals are more susceptible or resilient to aberrant associative learning disorders.

**Early evidence of NAc and mesolimbic dopamine in reward**

In the last four to five decades, intense research efforts have been dedicated to understanding the key brain structures and systems responsible for encoding reward information during associative learning, and later eliciting and modulating motivated behaviors (Berridge and Kringelbach, 2015). Early studies indicated a central role for the NAc in reward processing. In 1973, Pijnenburg and van Rossum found that

intracranial injections of dopamine directly into the NAc of rats induced an increase in locomotor activity (Pijnenburg and van Rossum, 1973). At that time, it had been proposed that dopamine played a role in the psychomotor effect of stimulant drugs (van Rossum and Hurkmans, 1964), so this observation led to the hypothesis that certain drugs might exert their psychomotor effect through action on dopamine receptors in the NAc (Pijnenburg and van Rossum, 1973). Shortly thereafter, it was demonstrated that increased locomotion produced by systemic administration of d-amphetamine could indeed be blocked by injections of dopamine antagonists such as trifluoperazine (Jackson et al., 1975) and haloperidol (Pijnenburg et al., 1975) into the NAc.

Over the years, intracranial self-stimulation, lesion, and dopamine ablation studies of the NAc began to reveal its role in reward- and addiction-related behaviors. Rats and monkeys would engage in operant behaviors to self-stimulate the NAc, and dopamine agonism or antagonism/ablation would significantly enhance or reduce these responses respectively (Phillips et al., 1975; Phillips and Fibiger, 1978; Robertson and Mogenson, 1978; Seeger and Gardner, 1979; Rolls et al., 1980; Takigawa and Mogenson, 1980). Furthermore, self-stimulation of dopaminergic cells in the ventral tegmental area (VTA), which send dopamine to the NAc through mesolimbic projections, was also enhanced by dopamine agonism in the NAc (Broekkamp et al., 1975) and blocked by dopamine antagonism (Broekkamp and Van Rossum, 1975; Mogenson et al., 1979), highlighting the importance of the mesolimbic system in reward regulation. It was also demonstrated that self-administration of drugs like cocaine (Roberts et al., 1977, 1980), heroin (Zito et al., 1985; Alderson et al., 2001), nicotine (Singer et al., 1982), and morphine (Dworkin et al., 1988) could be significantly impaired

by lesions of the NAc and mesolimbic projections, strongly suggesting the importance of NAc activity and dopamine transmission for the reinforcing properties of drugs of abuse.

**Effects of drugs in the mesolimbic system and incentive-sensitization**

It is now well-established that the dopaminergic system, and more specifically dopaminergic projections from the VTA in the midbrain to the striatum – the mesolimbic system – is highly involved in regulating behavioral responses to rewarding stimuli (Olsen, 2011; Schultz, 2002). Not only is the mesolimbic system involved in mediating responses to natural rewards (e.g., eating, sexual behavior, and exercising), but it has also been proposed as the final common pathway for the rewarding properties of substances of abuse (Pierce and Kumaresan, 2006). These include psychostimulants (e.g., cocaine and amphetamine), ethanol, opioids, cannabinoids, and nicotine with all exerting pharmacological and physiological effects primarily by increasing dopamine transmission in the mesolimbic system either directly or indirectly (Pierce and Kumaresan, 2006). This reward-induced dopaminergic activity promotes motivated behaviors and links those behaviors to cues associated with the reward (Wyvell and Berridge, 2000; Sotak et al., 2005; Hamid et al., 2016).

Chronic drug use has been characterized by a sensitized, hyperdopaminergic response to drug-related cues, with associated increases in motor activity and motivated behaviors including drug self-administration (Kalivas and Stewart, 1991; Robinson and Berridge, 1993; Vezina, 2004). Though most of the original evidence for sensitization was derived from animal research (Robinson and Becker, 1986), behavioral and dopaminergic sensitization to drug cues has now been reported in several human studies as well (Boileau et al., 2006; O'Daly et al., 2011; Booij et al.,

2016). The dopaminergic incentive-sensitization theory attempts to explain both a general loss of interest in motivated behaviors and a simultaneous increase in one specific type of motivated behavior, namely substance use. The sensitization effect appears very specific to drug-related cues, because evidence of tolerance, rather than sensitization, is generally observed when such cues are absent (Leyton and Vezina, 2013).

Glutamatergic synapses in the NAc that are involved in linking drug-related stimuli to drug-taking behavioral responses are active at the time of this dopamine release and are therefore strengthened every time the drug is used due to activation of relatively low-affinity dopamine type 1 ($D_1$) receptors. In contrast, synapses representing non-drug related stimuli and actions are preferentially active in the presence of lower concentrations of dopamine that are more likely to activate high-affinity dopamine type 2 ($D_2$) receptors, which will progressively weaken the synaptic strength in those circuits (Grace et al., 2007; Surmeier et al., 2007; Lovinger, 2010). Over time, the drug user's thoughts and behaviors become increasingly funneled toward the drug and its related stimuli, at the expense of all other non-drug rewards regardless of how motivating they may have been in the past (Leyton and Vezina, 2014; Berridge and Robinson, 2016).

**NAc activity and dopamine release during Pavlovian learning**

Based on anatomical differences in cellular arrangement and connectivity, the NAc has been subdivided into two main regions: the core and the shell (Záborszky et al., 1985; Berendse and Groenewegen, 1990; Zahm and Heimer, 1990). Perhaps unsurprisingly, these anatomical differences are also accompanied by distinct functional roles in reward and motivation (Zahm, 1999; Day and Carelli, 2007). Since the late

1990's, studies began to establish the role of the NAc as part of a "motive circuit". This is a set of interconnected cortical and subcortical structures that process both external and internal information to modulate motivated behaviors such as reward seeking and avoidance (Kalivas and Volkow, 2005). The NAc is a central component of this circuit as it is thought to integrate cortical and subcortical input during associative learning to initiate and modulate conditioned behaviors (Day and Carelli, 2007; Floresco, 2015; Salgado and Kaplitt, 2015). This form of learning is highly dependent on cues encoding information about the availability, the value, and also the context of the associated stimuli, and whether these associations have been successfully acquired or not is conventionally measured by the presence of a conditioned response to the cue (Day and Carelli, 2007). To decode this information, the NAc relies on synaptic inputs from regions like the prefrontal cortex (PFC), the basolateral amygdala (BLA), and the hippocampus (HPC), which are received by medium spiny neurons (MSNs) – the main neuronal population of the NAc. These inputs are also modulated by dopaminergic input from the VTA through mesolimbic projections (Day and Carelli, 2007; Britt et al., 2012). It is important to note that dopamine in the NAc is thought to encode the "wanting" aspect of rewarding stimuli, while not necessarily impacting the "liking" or hedonic property of rewards (Berridge et al., 2009). Thus the NAc role is crucial for generating the motivation behind goal-directed behaviors in response to appetitive cues, a process also described as limbic-motor integration (Mogenson and Yang, 1991; Morrison et al., 2017).

As mentioned above, the core and shell subregions are thought to be functionally distinct. Studies have consistently demonstrated that dopamine levels in the NAc rise in

response to a range of rewards including drugs (Di Chiara and Imperato, 1986, 1988; Hernandez and Hoebel, 1988; Kalivas and Duffy, 1990), liquid (Young et al., 1992; Norgren et al., 2006), and food (Schultz et al., 1997; Day et al., 2007; Flagel et al., 2011b). Nonetheless, this increase in reward-evoked dopamine may be more selective to the NAc shell. Meanwhile, conditioned stimuli, or cues associated with rewards, tend to increase dopamine more in the NAc core (Bassareo and Di Chiara, 1999; Ito et al., 2000; Stelly et al., 2021). Over the years, it has been postulated that while the core is responsible for the associative learning process, particularly by encoding the motivational value of conditioned cues, the shell has more influence over unconditioned responses (Day and Carelli, 2007; Meredith et al., 2008). This view is supported by behavioral studies demonstrating that discriminative Pavlovian conditioned approach is only impaired by lesions of the NAc core, while lesions of the shell impair the ability of such Pavlovian cues to invigorate instrumental responses as conditioned reinforcers (Parkinson et al., 1999, 2000). Impairments in conditioned approach behavior have also been reported following glutamate and dopamine antagonism in the NAc core (Ciano et al., 2001; Saunders and Robinson, 2012; Fraser and Janak, 2017; Dobrovitsky et al., 2019). More recent studies have demonstrated that optogenetic stimulation of VTA-NAc core neurons, but not VTA-NAc shell evokes conditioned behavior toward a paired cue, demonstrating that dopamine release in the core, but not shell, seems to encode the motivational aspect of Pavlovian cues (Saunders et al., 2018).

As informative as these studies have been, they have not taken into consideration individual differences in conditioned approach behavior. That is, only one type of conditioned response has been assessed, and therefore it is less clear how the

NAc may encode different properties of the reward-paired cue that favor “sign-tracking” (i.e. incentive) or “goal-tracking” (i.e. predictive) responses. For example, total NAc lesions have been found to impair the acquisition of a “sign-tracking” response (Chang et al., 2012). However, selective lesions of the core or shell have not affected the acquisition of “sign-tracking” (Chang and Holland, 2013), even though core lesions have been found to impair “sign-tracking” expression (Cardinal et al., 2002). In contrast, selective lesions/inactivation of the NAc core have been found to impair both the acquisition (Parkinson et al., 2000) and expression of “goal-tracking” behavior (Parkinson et al., 1999; Blaiss and Janak, 2009), while selective lesions of the shell have impaired only the expression (Blaiss and Janak, 2009) but not the acquisition of “goal-tracking” (Parkinson et al., 1999, 2000). When different types of conditioned responses are considered, the role of the NAc and its subregions becomes more complex, and the sensory nature of the conditioned stimulus may also have a powerful effect on how this information is processed (Chow et al., 2016). Even in these examples, individual differences were not considered, and although different conditioned responses were evaluated, they were not studied based on the behavior bias of each subject. This is important because different neurobiological mechanisms may govern the behavioral responses of ST and GT rats. In particular, activity in the NAc may vary based on the properties they are gleaning from the reward-paired cues, and these differences may be relevant to disease vulnerability.

**Individual differences in NAc activity and dopamine transmission in STs and GTs**

Although certain aspects of conditioned approach behavior rely on glutamatergic and dopaminergic transmission in the NAc, there are individual differences in the extent

of this dependence. For instance, a study in which extracellular glutamate was measured in the NAc core during a PavCA procedure demonstrated that sign-tracking behavior – but not goal-tracking – toward a conditioned stimulus caused an increase in glutamate levels in the NAc core (Batten et al., 2018). Not surprisingly then, systemic and intra-accumbal NMDA receptor antagonism preferentially impair sign-tracking behavior (Ciano et al., 2001; Fitzpatrick and Morrow, 2017; Chow and Beckmann, 2018). These findings suggest that glutamatergic signaling, likely in the NAc, may be a substrate for the incentive properties of rewarding stimuli.

Sign- and goal-tracking behavior also seem to be differentially sensitive to dopaminergic transmission. At the molecular level, STs and GTs differ in dopamine receptor and dopamine transporter expression, which can have significant impacts on dopamine signaling and sensitivity (Flagel et al., 2007; Singer et al., 2016). Behaviorally, dopamine antagonism by intra-accumbal flupenthixol administration specifically impairs STs in the expression of sign-tracking behavior without affecting GTs (Saunders and Robinson, 2012). This has led to the hypothesis that the attribution of incentive properties to reward-paired cues may be dopamine-dependent, but not necessarily the other classic associative learning properties that have been linked to prediction errors. A comprehensive study investigated the role of NAc $D_1$ and $D_2$ dopamine receptors in the acquisition and expression of sign- and goal-tracking behavior (Chow et al., 2016). They used a behavioral paradigm in which both a lever and a tone CS were individually presented to elicit sign-tracking and goal-tracking responses respectively in the same rats, and they found that the two behaviors were differentially sensitive to dopamine transmission. Although $D_1$ and $D_2$ receptor

antagonism affected the acquisition of both sign- and goal-tracking responses to the lever and the tone CS, subsequent expression tests in the absence of dopamine antagonism suggested that specifically the incentive properties of the reward-paired cue were affected as sign- but not goal-tracking performance was inhibited. Furthermore, dopamine antagonism affected the ability of the lever CS to support conditioned reinforcement, as evidenced by a significant decrease in lever versus tone preference in a two-choice CS preference test. Dopamine ablation in the NAc using 6-OHDA lesions also impaired the acquisition of sign-tracking behavior, while goal-tracking to the tone was unaffected (Chow et al., 2016). This study highlights the complexity of the role of dopaminergic transmission in sign- and goal-tracking conditioned approach responses, but further suggests that dopamine transmission in the NAc encodes the attribution of incentive salience and not solely the predictive CS-US association.

Consistent with the previously described findings in glutamate and dopamine transmission, learning-related neuronal activity in the NAc differs between STs and GTs. Specifically, STs exhibit increased cue-evoked c-fos expression in the NAc core and shell when compared to GTs (Flagel et al., 2011a). Single-unit recordings have also revealed that STs and GTs exhibit different cue- and reward-evoked patterns of activity in the NAc during Pavlovian learning, with a much more pronounced reduction in reward-evoked activity over the course of training in STs compared to GTs (Gillis and Morrison, 2019). Moreover, STs and GTs exhibit differences in mesolimbic dopamine release during Pavlovian learning. Specifically, the patterns of dopamine release seem to mimic cue- and reward-evoked activity in the NAc core and shell (Flagel et al., 2011b; Campus et al., 2019). Together, these data have led to the hypothesis that a shift of

dopamine release and NAc activity from the reward to the cue – commonly interpreted as a prediction error signal – must instead reflect the attribution of the incentive properties to reward-paired cues. It would otherwise be difficult to explain why the shift in dopamine-prediction error signals is largely absent in GTs that are clearly learning a predictive relationship between the cue and reward.

A neurobiological basis for the distinct patterns of NAc activity observed between STs and GTs so far remains elusive. One possibility is that there are intrinsic differences between STs and GTs in the membrane properties of MSNs – GABAergic projection neurons that comprise around 95% of the total neuronal population in the core and shell of the NAc (Matamales et al., 2009). The sensitivity of MSNs in the core and shell to changes in membrane potential caused by input stimuli could affect how the NAc integrates and relays reward information (O'Donnell and Grace, 1996; Nicola et al., 2000; Planert et al., 2013; Dorris et al., 2015). As part of the "motive circuit", the NAc receives synaptic glutamatergic inputs carrying information about the value and context of emotionally salient stimuli, allowing it to modulate conditioned behavioral responses. Therefore, the characteristic patterns of NAc activity and dopamine release in STs and GTs may also be influenced by the efficacy of synaptic inputs to the NAc during associative learning (Britt et al., 2012).

**Glutamatergic input from the ventral hippocampus to the NAc**

The NAc receives dense glutamatergic input from the PFC, the BLA, and the HPC (Brog et al., 1993; Britt et al., 2012). As mentioned earlier, glutamate transmission in the NAc is thought to be necessary for Pavlovian conditioned approach behavior (Ciano et al., 2001; Dalley et al., 2005) and other forms of associative learning such as

context-dependent reward learning (Layer et al., 1993; Kaddis et al., 1995; Baharlouei et al., 2015). Specifically, glutamatergic input from the ventral hippocampus (vHPC) is thought to be critical for encoding context-specific fear and reward information (Turner et al., 2022). Stimulation of the vHPC to NAc projection can induce conditioned place preference, suggesting that it encodes context-specific reward information (Britt et al., 2012; LeGates et al., 2018). Spatial information encoded by the vHPC is thought to be decoded by the NAc in order to modulate context-specific responses such as cocaine-induced conditioned place preference (Zhou et al., 2019). This is thought to be true not only for reward learning but also fear learning, as it is hypothesized that this projection encodes a general property of salience regardless of the valence of the associated stimuli (Loureiro et al., 2016; Muir et al., 2020). This may be of relevance to the ST/GT model because for both appetitive (Saunders and Robinson, 2011; Saunders et al., 2014; Pitchers et al., 2017) and aversive (Morrow et al., 2011, 2015) behaviors, STs are hypersensitive to discrete cues while GTs are more influenced by contextual information. Contextual information about appetitive and aversive stimuli is necessary for modulating conditioned responses to the associated cues. Therefore, increased cue reactivity could be a sign that context-related information is not being properly retrieved to appropriately modulate conditioned responses, and that is a function served by activity in the vHPC-NAc pathway. So far, studies of the vHPC on sign- and goal-tracking behavior have been somewhat conflicting. While total lesions of the HPC have been found to facilitate sign-tracking behavior (Ito et al., 2005), selective vHPC lesions have been found to abolish sign-tracking and favor goal-tracking behavior (Fitzpatrick et al., 2016). No studies have explored the direct influence of vHPC input to the NAc on

the attribution of incentive salience and individual differences in Pavlovian conditioned approach. While glutamatergic activity in the NAc seems to be different between STs and GTs, the source of this variability remains largely unknown.

**Conclusion**

Although NAc activity has been consistently associated with reward learning and implicated in addiction and other cue-driven psychopathologies, individual differences in the degree of NAc involvement have been less explored. This is in part due to a lack of literature on models of individual differences in associative learning and disease vulnerability. How individuals learn about emotionally salient cues significantly impacts their behavioral responses once these cues are encountered in both normal and disease states. While many studies on addiction and anxiety vulnerability have focused on how drugs and trauma affect brain structures like the NAc, pre-existent functional differences may also influence how the NAc responds to such insults. Specifically, models of individual differences in cue reactivity suggest that the NAc has the potential to encode reward information in different ways, and this may be the cause or the result of differences in conditioned responses and other associated behaviors. However, the neurobiological basis of this variability is unclear, and questions remain as to whether these differences are innate or experience-dependent. This dissertation was designed to test for possible mechanisms that could lead to differential learning-related NAc activity patterns between STs and GTs. To begin, Chapter II establishes a baseline profile for the intrinsic excitability properties of MSNs in the NAc core and shell in both naïve and behaviorally experienced rats to understand the stability of NAc physiology. Chapter III extends this physiological profile of the excitability of core and shell MSNs to

include a direct comparison of STs and GTs. Finally, we focus on the influence of glutamatergic input from the vHPC to the NAc on the attribution of incentive salience from both a behavioral (Chapter IV) and synaptic (Chapter V) level. We selected this particular projection due to its importance in cue- versus context-induced behavior, which relates to both addiction and PTSD vulnerability. Overall, we aim to further dissect the role of the NAc in encoding specific properties of emotionally salient cues to better understand vulnerability to psychopathology. Taking advantage of a model of individual variation in associative learning allows us to address this question while avoiding the potential confounds that can arise from actual trauma or drug exposure.

## References


Ahrens AM, Singer BF, Fitzpatrick CJ, Morrow JD, Robinson TE (2016) Rats that sign-track are resistant to Pavlovian but not instrumental extinction. Behav Brain Res 296:418–430.

Alderson HL, Parkinson JA, Robbins TW, Everitt BJ (2001) The effects of excitotoxic lesions of the nucleus accumbens core or shell regions on intravenous heroin self-administration in rats. Psychopharmacology (Berl) 153:455–463.

Aron AR, Robbins TW, Poldrack RA (2004) Inhibition and the right inferior frontal cortex. Trends Cogn Sci 8:170–177.

Badiani A (2013) Substance-specific environmental influences on drug use and drug preference in animals and humans. Curr Opin Neurobiol 23:588–596.

Baharlouei N, Sarihi A, Komaki A, Shahidi S, Haghparast A (2015) Blockage of acquisition and expression of morphine-induced conditioned place preference in rats due to activation of glutamate receptors type II/III in nucleus accumbens. Pharmacol Biochem Behav 135:192–198.

Bassareo V, Di Chiara G (1999) Differential responsiveness of dopamine transmission to food-stimuli in nucleus accumbens shell/core compartments. Neuroscience 89:637–641.

Batten SR, Pomerleau F, Quintero J, Gerhardt GA, Beckmann JS (2018) The role of glutamate signaling in incentive salience: second-by-second glutamate recordings in awake Sprague Dawley rats. J Neurochem 145:276–286.

Belin D, Mar AC, Dalley JW, Robbins TW, Everitt BJ (2008) High impulsivity predicts the switch to compulsive cocaine-taking. Science 320:1352–1355.

Berendse HW, Groenewegen HJ (1990) Organization of the thalamostriatal projections in the rat, with special emphasis on the ventral striatum. J Comp Neurol 299:187–228.

Berridge KC, Kringelbach ML (2015) Pleasure systems in the brain. Neuron 86:646–664.

Berridge KC, Robinson TE (2016) Liking, wanting, and the incentive-sensitization theory of addiction. Am Psychol 71:670–679.

Berridge KC, Robinson TE, Aldridge JW (2009) Dissecting components of reward: 'liking', 'wanting', and learning. Curr Opin Pharmacol 9:65–73.

Blaiss CA, Janak PH (2009) The nucleus accumbens core and shell are critical for the expression, but not the consolidation, of Pavlovian conditioned approach. Behav Brain Res 200:22–32.

Boakes RA (1977) Performance on learning to associate a stimulus with positive reinforcement. in: operant-pavlovian interactions. Routledge.

Boileau I, Dagher A, Leyton M, Gunn RN, Baker GB, Diksic M, Benkelfat C (2006) Modeling sensitization to stimulants in humans: an [11C]raclopride/positron emission tomography study in healthy men. Arch Gen Psychiatry 63:1386–1395.

Booij L, Welfeld K, Leyton M, Dagher A, Boileau I, Sibon I, Baker GB, Diksic M, Soucy J-P, Pruessner JC, Cawley-Fiset E, Casey KF, Benkelfat C (2016) Dopamine cross-sensitization between psychostimulant drugs and stress in healthy male volunteers. Transl Psychiatry 6:e740–e740.

Britt JP, Benaliouad F, McDevitt RA, Stuber GD, Wise RA, Bonci A (2012) Synaptic and behavioral profile of multiple glutamatergic inputs to the nucleus accumbens. Neuron 76:790–803.

Broekkamp CL, Pijnenburg AJ, Cools AR, Van Rossum JM (1975) The effect of microinjections of amphetamine into the neostriatum and the nucleus accumbens on self-stimulation behaviour. Psychopharmacologia 42:179–183.

Broekkamp CL, Van Rossum JM (1975) The effect of microinjections of morphine and haloperidol into the neostriatum and the nucleus accumbens on self-stimulation behaviour. Arch Int Pharmacodyn Ther 217:110–117.

Brog JS, Salyapongse A, Deutch AY, Zahm DS (1993) The patterns of afferent innervation of the core and shell in the “accumbens” part of the rat ventral striatum: immunohistochemical detection of retrogradely transported fluoro-gold. J Comp Neurol 338:255–278.

Campus P, Covelo IR, Kim Y, Parsegian A, Kuhn BN, Lopez SA, Neumaier JF, Ferguson SM, Solberg Woods LC, Sarter M, Flagel SB (2019) The paraventricular thalamus is a critical mediator of top-down control of cue-motivated behavior in rats Schoenbaum G, Wassum KM, Calu D, Coutureau E, eds. eLife 8:e49041.

Cardinal RN, Parkinson JA, Lachenal G, Halkerston KM, Rudarakanchana N, Hall J, Morrison CH, Howes SR, Robbins TW, Everitt BJ (2002) Effects of selective excitotoxic lesions of the nucleus accumbens core, anterior cingulate cortex, and central nucleus of the amygdala on autoshaping performance in rats. Behav Neurosci 116:553–567.

Carter BL, Tiffany ST (1999) Meta-analysis of cue-reactivity in addiction research. Addiction 94:327–340.

Chang SE, Holland PC (2013) Effects of nucleus accumbens core and shell lesions on autoshaped lever-pressing. Behav Brain Res 256:10.1016/j.bbr.2013.07.046.

Chang SE, Wheeler DS, Holland PC (2012) Roles of nucleus accumbens and basolateral amygdala in autoshaped lever pressing. Neurobiol Learn Mem 97:441–451.

Chow JJ, Beckmann JS (2018) NMDA receptor blockade specifically impedes the acquisition of incentive salience attribution. Behav Brain Res 338:40–46.

Chow JJ, Nickell JR, Darna M, Beckmann JS (2016) Toward isolating the role of dopamine in the acquisition of incentive salience attribution. Neuropharmacology 109:320–331.

Chuang C-WI, Sussman S, Stone MD, Pang RD, Chou C-P, Leventhal AM, Kirkpatrick MG (2017) Impulsivity and history of behavioral addictions are associated with drug use in adolescents. Addict Behav 74:41–47.

Ciano PD, Cardinal RN, Cowell RA, Little SJ, Everitt BJ (2001) Differential involvement of nmda, ampa/kainate, and dopamine receptors in the nucleus accumbens core in the acquisition and performance of pavlovian approach behavior. J Neurosci 21:9471–9477.

Coffey SF, Schumacher JA, Stasiewicz PR, Henslee AM, Baillie LE, Landy N (2010) Craving and physiological reactivity to trauma and alcohol cues in posttraumatic stress disorder and alcohol dependence. Exp Clin Psychopharmacol 18:340–349.

Colzato LS, van den Wildenberg WPM, Van der Does AJW, Hommel B (2010) Genetic markers of striatal dopamine predict individual differences in dysfunctional, but not functional impulsivity. Neuroscience 170:782–788.

Crews FT, Boettiger CA (2009) Impulsivity, frontal lobes and risk for addiction. Pharmacol Biochem Behav 93:237–247.

Crombag HS, Badiani A, Chan J, Dell'Orco J, Dineen SP, Robinson TE (2001) The ability of environmental context to facilitate psychomotor sensitization to amphetamine can be dissociated from its effect on acute drug responsiveness and on conditioned responding. Neuropsychopharmacology 24:680–690.

Cyders MA, Smith GT (2008) Emotion-based dispositions to rash action: Positive and negative urgency. Psychol Bull 134:807–828.

Dalley JW, Lääne K, Theobald DEH, Armstrong HC, Corlett PR, Chudasama Y, Robbins TW (2005) Time-limited modulation of appetitive Pavlovian memory by D1 and NMDA receptors in the nucleus accumbens. Proc Natl Acad Sci U S A 102:6189–6194.

Dalley JW, Robbins TW (2017) Fractionating impulsivity: neuropsychiatric implications. Nat Rev Neurosci 18:158–171.

Davis FC, Knodt AR, Sporns O, Lahey BB, Zald DH, Brigidi BD, Hariri AR (2013) Impulsivity and the modular organization of resting-state neural networks. Cereb Cortex 23:1444–1452.

Day JJ, Carelli RM (2007) The nucleus accumbens and pavlovian reward learning. The Neuroscientist 13:148–159.

Day JJ, Roitman MF, Wightman RM, Carelli RM (2007) Associative learning mediates dynamic shifts in dopamine signaling in the nucleus accumbens. Nat Neurosci 10:1020–1028.

Di Chiara G, Imperato A (1986) Preferential stimulation of dopamine release in the nucleus accumbens by opiates, alcohol, and barbiturates: studies with transcerebral dialysis in freely moving rats. Ann N Y Acad Sci 473:367–381.

Di Chiara G, Imperato A (1988) Drugs abused by humans preferentially increase synaptic dopamine concentrations in the mesolimbic system of freely moving rats. Proc Natl Acad Sci U S A 85:5274–5278.

Di Chiara G, Tanda G, Bassareo V, Pontieri F, Acquas E, Fenu S, Cadoni C, Carboni E (1999) Drug addiction as a disorder of associative learning. Role of nucleus accumbens shell/extended amygdala dopamine. Ann N Y Acad Sci 877:461–485.

Dobrovitsky V, West MO, Horvitz JC (2019) The role of the nucleus accumbens in learned approach behavior diminishes with training. Eur J Neurosci 50:3403–3415.

Dorris DM, Cao J, Willett JA, Hauser CA, Meitzen J (2015) Intrinsic excitability varies by sex in prepubertal striatal medium spiny neurons. J Neurophysiol 113:720–729.

Dworkin SI, Guerin GF, Goeders NE, Smith JE (1988) Kainic acid lesions of the nucleus accumbens selectively attenuate morphine self-administration. Pharmacol Biochem Behav 29:175–181.

Ersche KD, Turton AJ, Pradhan S, Bullmore ET, Robbins TW (2010) Drug addiction endophenotypes: impulsive versus sensation-seeking personality traits. Biol Psychiatry 68:770–773.

Fitzpatrick CJ, Creeden JF, Perrine SA, Morrow JD (2016) Lesions of the ventral hippocampus attenuate the acquisition but not expression of sign-tracking behavior in rats. Hippocampus 26:1424–1434.

Fitzpatrick CJ, Geary T, Creeden JF, Morrow JD (2019) Sign-tracking behavior is difficult to extinguish and resistant to multiple cognitive enhancers. Neurobiol Learn Mem 163:107045.

Fitzpatrick CJ, Morrow JD (2017) Subanesthetic ketamine decreases the incentive-motivational value of reward-related cues. J Psychopharmacol Oxf Engl 31:67–74.

Flagel SB, Akil H, Robinson TE (2009) Individual differences in the attribution of incentive salience to reward-related cues: Implications for addiction. Neuropharmacology 56:139–148.

Flagel SB, Cameron CM, Pickup KN, Watson SJ, Akil H, Robinson TE (2011a) A food predictive cue must be attributed with incentive salience for it to induce c-fos mRNA expression in cortico-striatal-thalamic brain regions. Neuroscience 196:80–96.

Flagel SB, Clark JJ, Robinson TE, Mayo L, Czuj A, Willuhn I, Akers CA, Clinton SM, Phillips PEM, Akil H (2011b) A selective role for dopamine in stimulus-reward learning. Nature 469:53–57.

Flagel SB, Robinson TE (2017) Neurobiological Basis of Individual Variation in Stimulus-Reward Learning. Curr Opin Behav Sci 13:178–185.

Flagel SB, Watson SJ, Akil H, Robinson TE (2008) Individual differences in the attribution of incentive salience to a reward-related cue: Influence on cocaine sensitization. Behav Brain Res 186:48–56.

Flagel SB, Watson SJ, Robinson TE, Akil H (2007) Individual differences in the propensity to approach signals vs goals promote different adaptations in the dopamine system of rats. Psychopharmacology (Berl) 191:599–607.

Floresco SB (2015) The nucleus accumbens: an interface between cognition, emotion, and action. Annu Rev Psychol 66:25–52.

Forbes EE, Brown SM, Kimak M, Ferrell RE, Manuck SB, Hariri AR (2009) Genetic variation in components of dopamine neurotransmission impacts ventral striatal reactivity associated with impulsivity. Mol Psychiatry 14:60–70.

Fraser KM, Janak PH (2017) Long-lasting contribution of dopamine in the nucleus accumbens core, but not dorsal lateral striatum, to sign-tracking. Eur J Neurosci 46:2047–2055.

Garfinkel SN, Abelson JL, King AP, Sripada RK, Wang X, Gaines LM, Liberzon I (2014) Impaired contextual modulation of memories in PTSD: An fMRI and psychophysiological study of extinction retention and fear renewal. J Neurosci 34:13435–13443.

Garland EL, Bryan CJ, Kreighbaum L, Nakamura Y, Howard MO, Froeliger B (2018) Prescription opioid misusing chronic pain patients exhibit dysregulated context-dependent associations: Investigating associative learning in addiction with the cue-primed reactivity task. Drug Alcohol Depend 187:13–21.

Garofalo S, di Pellegrino G (2015) Individual differences in the influence of task-irrelevant Pavlovian cues on human behavior. Front Behav Neurosci 9:163.

Gillis ZS, Morrison SE (2019) Sign tracking and goal tracking are characterized by distinct patterns of nucleus accumbens activity. eNeuro 6.

Goode TD, Maren S (2019) Common neurocircuitry mediating drug and fear relapse in preclinical models. Psychopharmacology (Berl) 236:415–437.

Gottesman II, Gould TD (2003) The endophenotype concept in psychiatry: Etymology and strategic intentions. Am J Psychiatry 160:636–645.

Grace AA, Floresco SB, Goto Y, Lodge DJ (2007) Regulation of firing of dopaminergic neurons and control of goal-directed behaviors. Trends Neurosci 30:220–227.

Hahn T, Dresler T, Ehlis A-C, Plichta MM, Heinzel S, Polak T, Lesch K-P, Breuer F, Jakob PM, Fallgatter AJ (2009) Neural response to reward anticipation is modulated by Gray's impulsivity. NeuroImage 46:1148–1153.

Hamid AA, Pettibone JR, Mabrouk OS, Hetrick VL, Schmidt R, Vander Weele CM, Kennedy RT, Aragona BJ, Berke JD (2016) Mesolimbic dopamine signals the value of work. Nat Neurosci 19:117–126.

Hearst E, Jenkins HM (1974) Sign-tracking: the stimulus-reinforcer relation and directed action. Austin, Tex.: Psychonomic Society.

Hernandez L, Hoebel BG (1988) Food reward and cocaine increase extracellular dopamine in the nucleus accumbens as measured by microdialysis. Life Sci 42:1705–1712.

Ito R, Dalley JW, Howes SR, Robbins TW, Everitt BJ (2000) Dissociation in conditioned dopamine release in the nucleus accumbens core and shell in response to cocaine cues and during cocaine-seeking behavior in rats. J Neurosci Off J Soc Neurosci 20:7489–7495.

Ito R, Everitt BJ, Robbins TW (2005) The hippocampus and appetitive Pavlovian conditioning: Effects of excitotoxic hippocampal lesions on conditioned locomotor activity and autoshaping. Hippocampus 15:713–721.

Jackson DM, Andén NE, Dahlström A (1975) A functional effect of dopamine in the nucleus accumbens and in some other dopamine-rich parts of the rat brain. Psychopharmacologia 45:139–149.

Janes AC, Pizzagalli DA, Richardt S, Frederick B deB., Chuzi S, Pachas G, Culhane MA, Holmes AJ, Fava M, Evins AE, Kaufman MJ (2010) Brain reactivity to smoking cues prior to smoking cessation predicts ability to maintain tobacco Abstinence. Biol Psychiatry 67:722–729.

Jenkins HM, Moore BR (1973) The form of the auto-shaped response with food or water reinforcers. J Exp Anal Behav 20:163–181.

Jentsch JD, Ashenhurst JR, Cervantes MC, Groman SM, James AS, Pennington ZT (2014) Dissecting impulsivity and its relationships to drug addictions. Ann N Y Acad Sci 1327:1–26.

Jentsch JD, Taylor JR (1999) Impulsivity resulting from frontostriatal dysfunction in drug abuse: implications for the control of behavior by reward-related stimuli. Psychopharmacology (Berl) 146:373–390.

Kaddis FG, Uretsky NJ, Wallace LJ (1995) DNQX in the nucleus accumbens inhibits cocaine-induced conditioned place preference. Brain Res 697:76–82.

Kalivas PW, Duffy P (1990) Effect of acute and daily cocaine treatment on extracellular dopamine in the nucleus accumbens. Synap N Y N 5:48–58.

Kalivas PW, Stewart J (1991) Dopamine transmission in the initiation and expression of drug- and stress-induced sensitization of motor activity. Brain Res Rev 16:223–244.

Kalivas PW, Volkow ND (2005) The neural basis of addiction: A pathology of motivation and choice. Am J Psychiatry 162:1403–1413.

Kuhn B, Campus P, Flagel S (2018) Neurobiological mechanisms underlying sign-tracking behavior.

Layer RT, Uretsky NJ, Wallace LJ (1993) Effects of the AMPA/kainate receptor antagonist DNQX in the nucleus accumbens on drug-induced conditioned place preference. Brain Res 617:267–273.

Lee B, London ED, Poldrack RA, Farahi J, Nacca A, Monterosso JR, Mumford JA, Bokarius AV, Dahlbom M, Mukherjee J, Bilder RM, Brody AL, Mandelkern MA (2009) Striatal dopamine D2/D3 receptor availability is reduced in methamphetamine dependence and is linked to impulsivity. J Neurosci 29:14734–14740.

LeGates TA, Kvarta MD, Tooley JR, Francis TC, Lobo MK, Creed MC, Thompson SM (2018) Reward behaviour is regulated by the strength of hippocampus–nucleus accumbens synapses. Nature 564:258–262.

Leyton M, Vezina P (2013) Striatal ups and downs: Their roles in vulnerability to addictions in humans. Neurosci Biobehav Rev 37:1999–2014.

Leyton M, Vezina P (2014) Dopamine ups and downs in vulnerability to addictions: a neurodevelopmental model. Trends Pharmacol Sci 35:268–276.

Liberzon I, Abelson JL (2016) Context processing and the neurobiology of post-traumatic stress disorder. Neuron 92:14–30.

Loureiro M, Kramar C, Renard J, Rosen LG, Laviolette SR (2016) Cannabinoid transmission in the hippocampus activates nucleus accumbens neurons and modulates reward and aversion-related emotional salience. Biol Psychiatry 80:216–225.

Lovinger DM (2010) Neurotransmitter roles in synaptic modulation, plasticity and learning in the dorsal striatum. Neuropharmacology 58:951–961.

Maren S, Phan KL, Liberzon I (2013) The contextual brain: implications for fear conditioning, extinction and psychopathology. Nat Rev Neurosci 14:417–428.

Maria-Rios CE, Fitzpatrick CJ, Morrow JD (2019) Effects of predictive and incentive value manipulation on sign- and goal-tracking behavior. bioRxiv 767095.

María-Ríos CE, Morrow JD (2020) Mechanisms of shared vulnerability to post-traumatic stress disorder and substance use disorders. Front Behav Neurosci 14:6.

Matamales M, Bertran-Gonzalez J, Salomon L, Degos B, Deniau J-M, Valjent E, Hervé D, Girault J-A (2009) Striatal medium-sized spiny neurons: Identification by nuclear staining and study of neuronal subpopulations in BAC transgenic mice. PLoS ONE 4:e4770.

Meredith GE, Baldo BA, Andrezjewski ME, Kelley AE (2008) The structural basis for mapping behavior onto the striatum and its subdivisions. Brain Struct Funct 213:17–27.

Mogenson GJ, Takigawa M, Robertson A, Wu M (1979) Self-stimulation of the nucleus accumbens and ventral tegmental area of Tsai attenuated by microinjections of spiroperidol into the nucleus accumbens. Brain Res 171:247–259.

Mogenson GJ, Yang CR (1991) The contribution of basal forebrain to limbic-motor integration and the mediation of motivation to action. Adv Exp Med Biol 295:267–290.

Morrison SE, McGinty VB, du Hoffmann J, Nicola SM (2017) Limbic-motor integration by neural excitations and inhibitions in the nucleus accumbens. J Neurophysiol 118:2549–2567.

Morrow JD, Maren S, Robinson TE (2011) Individual variation in the propensity to attribute incentive salience to an appetitive cue predicts the propensity to attribute motivational salience to an aversive cue. Behav Brain Res 220:238–243.

Morrow JD, Saunders BT, Maren S, Robinson TE (2015) Sign-tracking to an appetitive cue predicts incubation of conditioned fear in rats. Behav Brain Res 276:59–66.

Muir J, Tse YC, Iyer ES, Biris J, Cvetkovska V, Lopez J, Bagot RC (2020) Ventral hippocampal afferents to nucleus accumbens encode both latent vulnerability and stress-induced susceptibility. Biol Psychiatry 88:843–854.

Nicola SM, Surmeier DJ, Malenka RC (2000) Dopaminergic modulation of neuronal excitability in the striatum and nucleus accumbens. Annu Rev Neurosci 23:185–215.

Norgren R, Hajnal A, Mungarndee SS (2006) Gustatory reward and the nucleus accumbens. Physiol Behav 89:531–535.

O'Daly OG, Joyce D, Stephan KE, Murray RM, Shergill SS (2011) Functional magnetic resonance imaging investigation of the amphetamine sensitization model of schizophrenia in healthy male volunteers. Arch Gen Psychiatry 68:545–554.

O'Donnell P, Grace AA (1996) Dopaminergic reduction of excitability in nucleus accumbens neurons recorded in vitro. Neuropsychopharmacology 15:87–97.

Olsen CM (2011) Natural rewards, neuroplasticity, and non-drug addictions. Neuropharmacology 61:1109–1122.

O'Sullivan SS, Wu K, Politis M, Lawrence AD, Evans AH, Bose SK, Djamshidian A, Lees AJ, Piccini P (2011) Cue-induced striatal dopamine release in Parkinson's disease-associated impulsive-compulsive behaviours. Brain 134:969–978.

Parkinson JA, Olmstead MC, Burns LH, Robbins TW, Everitt BJ (1999) Dissociation in effects of lesions of the nucleus accumbens core and shell on appetitive pavlovian approach behavior and the potentiation of conditioned reinforcement and locomotor activity by D-amphetamine. J Neurosci Off J Soc Neurosci 19:2401–2411.

Parkinson JA, Willoughby PJ, Robbins TW, Everitt BJ (2000) Disconnection of the anterior cingulate cortex and nucleus accumbens core impairs Pavlovian approach behavior: further evidence for limbic cortical-ventral striatopallidal systems. Behav Neurosci 114:42–63.

Pavlov IP (1927) Conditioned reflexes: an investigation of the physiological activity of the cerebral cortex. Oxford, England: Oxford Univ. Press.

Peters J, Kalivas PW, Quirk GJ (2009) Extinction circuits for fear and addiction overlap in prefrontal cortex. Learn Mem 16:279–288.

Phillips AG, Brooke SM, Fibiger HC (1975) Effects of amphetamine isomers and neuroleptics on self-stimulation from the nucleus accumbens and dorsal noradrenergic bundle. Brain Res 85:13–22.

Phillips AG, Fibiger HC (1978) The role of dopamine in maintaining intracranial self-stimulation in the ventral tegmentum, nucleus accumbens, and medial prefrontal cortex. Can J Psychol Can Psychol 32:58–66.

Pierce RC, Kumaresan V (2006) The mesolimbic dopamine system: the final common pathway for the reinforcing effect of drugs of abuse? Neurosci Biobehav Rev 30:215–238.

Pijnenburg AJ, Honig WM, Van Rossum JM (1975) Inhibition of d-amphetamine-induced locomotor activity by injection of haloperidol into the nucleus accumbens of the rat. Psychopharmacologia 41:87–95.

Pijnenburg AJ, van Rossum JM (1973) Letter: Stimulation of locomotor activity following injection of dopamine into the nucleus accumbens. J Pharm Pharmacol 25:1003–1005.

Pitchers KK, Phillips KB, Jones JL, Robinson TE, Sarter M (2017) Diverse roads to relapse: A discriminative cue signaling cocaine availability is more effective in renewing cocaine seeking in goal trackers than sign trackers and depends on basal forebrain cholinergic activity. J Neurosci 37:7198–7208.

Planert H, Berger TK, Silberberg G (2013) Membrane properties of striatal direct and indirect pathway neurons in mouse and rat slices and their modulation by dopamine. PLOS ONE 8:e57054.

Read JP, Bachrach RL, Wardell JD, Coffey SF (2017) Examining cognitive processes and drinking urge in PTSD. Behav Res Ther 90:159–168.

Reeves SJ, Polling C, Stokes PRA, Lappin JM, Shotbolt PP, Mehta MA, Howes OD, Egerton A (2012) Limbic striatal dopamine D2/3 receptor availability is associated with non-planning impulsivity in healthy adults after exclusion of potential dissimulators. Psychiatry Res Neuroimaging 202:60–64.

Robbins TW, Gillan CM, Smith DG, de Wit S, Ersche KD (2012) Neurocognitive endophenotypes of impulsivity and compulsivity: towards dimensional psychiatry. Trends Cogn Sci 16:81–91.

Roberts DC, Corcoran ME, Fibiger HC (1977) On the role of ascending catecholaminergic systems in intravenous self-administration of cocaine. Pharmacol Biochem Behav 6:615–620.

Roberts DC, Koob GF, Klonoff P, Fibiger HC (1980) Extinction and recovery of cocaine self-administration following 6-hydroxydopamine lesions of the nucleus accumbens. Pharmacol Biochem Behav 12:781–787.

Robertson A, Mogenson GJ (1978) Evidence for a role of dopamine in self-stimulation of the nucleus accumbens of the rat. Can J Psychol Can Psychol 32:67–76.

Robinson TE, Becker JB (1986) Enduring changes in brain and behavior produced by chronic amphetamine administration: a review and evaluation of animal models of amphetamine psychosis. Brain Res 396:157–198.

Robinson TE, Berridge KC (1993) The neural basis of drug craving: an incentive-sensitization theory of addiction. Brain Res Brain Res Rev 18:247–291.

Robinson TE, Flagel SB (2009) Dissociating the predictive and incentive motivational properties of reward-related cues through the study of individual differences. Biol Psychiatry 65:869–873.

Robinson TE, Yager LM, Cogan ES, Saunders BT (2014) On the motivational properties of reward cues: Individual differences. Neuropharmacology 76:10.1016/j.neuropharm.2013.05.040.

Rodríguez-Cintas L, Daigre C, Grau-López L, Barral C, Pérez-Pazos J, Voltes N, Braquehais MD, Casas M, Roncero C (2016) Impulsivity and addiction severity in cocaine and opioid dependent patients. Addict Behav 58:104–109.

Rohsenow DJ, Childress AR, Monti PM, Niaura RS, Abrams DB (1991) Cue reactivity in addictive behaviors: Theoretical and treatment implications. Int J Addict 25:957–993.

Rolls ET, Burton MJ, Mora F (1980) Neurophysiological analysis of brain-stimulation reward in the monkey. Brain Res 194:339–357.

Rolls ET, Hornak J, Wade D, McGrath J (1994) Emotion-related learning in patients with social and emotional changes associated with frontal lobe damage. J Neurol Neurosurg Psychiatry 57:1518–1524.

Salgado S, Kaplitt MG (2015) The nucleus accumbens: A comprehensive review. Stereotact Funct Neurosurg 93:75–93.

Sarter M, Phillips KB (2018) The neuroscience of cognitive-motivational styles: Sign- and goal-trackers as animal models. Behav Neurosci 132:1–12.

Saunders BT, O'Donnell EG, Aurbach EL, Robinson TE (2014) A cocaine context renews drug seeking preferentially in a subset of individuals. Neuropsychopharmacology 39:2816–2823.

Saunders BT, Richard JM, Margolis EB, Janak PH (2018) Dopamine neurons create Pavlovian conditioned stimuli with circuit-defined motivational properties. Nat Neurosci 21:1072–1083.

Saunders BT, Robinson TE (2010) A cocaine cue acts as an incentive stimulus in some, but not others: implications for addiction. Biol Psychiatry 67:730–736.

Saunders BT, Robinson TE (2011) Individual variation in the motivational properties of cocaine. Neuropsychopharmacology 36:1668–1676.

Saunders BT, Robinson TE (2012) The role of dopamine in the accumbens core in the expression of Pavlovian-conditioned responses. Eur J Neurosci 36:2521–2532.

Saunders BT, Yager LM, Robinson TE (2013) Cue-evoked cocaine “craving”: Role of dopamine in the accumbens core. J Neurosci 33:13989–14000.

Schmaal L, Goudriaan AE, van der Meer J, van den Brink W, Veltman DJ (2012) The association between cingulate cortex glutamate concentration and delay discounting is mediated by resting state functional connectivity. Brain Behav 2:553–562.

Schultz W (2002) Getting formal with dopamine and reward. Neuron 36:241–263.

Schultz W, Dayan P, Montague PR (1997) A neural substrate of prediction and reward. Science 275:1593–1599.

Seeger TF, Gardner EL (1979) Enhancement of self-stimulation behavior in rats and monkeys after chronic neuroleptic treatment: Evidence for mesolimbic supersensitivity. Brain Res 175:49–57.

Singer BF, Guptaroy B, Austin CJ, Wohl I, Lovic V, Seiler JL, Vaughan RA, Gnegy ME, Robinson TE, Aragona BJ (2016) Individual variation in incentive salience attribution and accumbens dopamine transporter expression and function. Eur J Neurosci 43:662–670.

Singer G, Wallace M, Hall R (1982) Effects of dopaminergic nucleus accumbens lesions on the acquisition of schedule induced self injection of nicotine in the rat. Pharmacol Biochem Behav 17:579–581.

Smith GT, Cyders MA (2016) Integrating affect and impulsivity: The role of positive and negative urgency in substance use risk. Drug Alcohol Depend 163:S3–S12.

Sotak BN, Hnasko TS, Robinson S, Kremer EJ, Palmiter RD (2005) Dysregulation of dopamine signaling in the dorsal striatum inhibits feeding. Brain Res 1061:88–96.

Stelly CE, Girven KS, Lefner MJ, Fonzi KM, Wanat MJ (2021) Dopamine release and its control over early Pavlovian learning differs between the NAc core and medial NAc shell. Neuropsychopharmacology 46:1780–1787.

Surmeier DJ, Ding J, Day M, Wang Z, Shen W (2007) D1 and D2 dopamine-receptor modulation of striatal glutamatergic signaling in striatal medium spiny neurons. Trends Neurosci 30:228–235.

Takigawa M, Mogenson GJ (1980) [Intracranial self-stimulation of the nucleus accumbens of the rat and its associated behavior (author's transl)]. No To Shinkei 32:299–304.

Thomsen KR, Callesen MB, Hesse M, Kvamme TL, Pedersen MM, Pedersen MU, Voon V (2018) Impulsivity traits and addiction-related behaviors in youth. J Behav Addict 7:317–330.

Tomie A, Morrow J (2018) Sign-tracking and drug addiction. Maize Books Available at: https://quod.lib.umich.edu/m/maize/mpub10215070/1:4/--sign-tracking-and-drug-addiction?rgn=div1;view=fulltext [Accessed September 28, 2022].

Tull MT, McDermott MJ, Gratz KL, Coffey SF, Lejuez CW (2011) Cocaine-related attentional bias following trauma cue exposure among cocaine dependent in-patients with and without post-traumatic stress disorder. Addiction 106:1810–1818.

Tunstall BJ, Kearns DN (2015) Sign-tracking predicts increased choice of cocaine over food in rats. Behav Brain Res 281:222–228.

Turner VS, O'Sullivan RO, Kheirbek MA (2022) Linking external stimuli with internal drives: A role for the ventral hippocampus. Curr Opin Neurobiol 76:102590.

van Rossum JM, Hurkmans JAThM (1964) Mechanism of action of psychomotor stimulant drugs: Significance of dopamine in locomotor stimulant action. Int J Neuropharmacol 3:227–239.

Versaggi CL, King CP, Meyer PJ (2016) The tendency to sign-track predicts cue-induced reinstatement during nicotine self-administration, and is enhanced by nicotine but not ethanol. Psychopharmacology (Berl) 233:2985–2997.

Vezina P (2004) Sensitization of midbrain dopamine neuron reactivity and the self-administration of psychomotor stimulant drugs. Neurosci Biobehav Rev 27:827–839.

Villaruel FR, Chaudhri N (2016) Individual differences in the attribution of incentive salience to a Pavlovian alcohol cue. Front Behav Neurosci 10 Available at: https://www.frontiersin.org/articles/10.3389/fnbeh.2016.00238/full [Accessed September 11, 2019].

Volkow ND, Michaelides M, Baler R (2019) The Neuroscience of Drug Reward and Addiction. Physiol Rev 99:2115–2140.

Wasserman EA, Franklin SR, Hearst E (1974) Pavlovian appetitive contingencies and approach versus withdrawal to conditioned stimuli in pigeons. J Comp Physiol Psychol 86:616–627.

Whiteside SP, Lynam DR (2001) The five factor model and impulsivity: using a structural model of personality to understand impulsivity. Personal Individ Differ 30:669–689.

Wyvell CL, Berridge KC (2000) Intra-accumbens amphetamine increases the conditioned incentive salience of sucrose reward: enhancement of reward "wanting" without enhanced "liking" or response reinforcement. J Neurosci Off J Soc Neurosci 20:8122–8130.

Yager LM, Robinson TE (2010) Cue-induced reinstatement of food seeking in rats that differ in their propensity to attribute incentive salience to food cues. Behav Brain Res 214:30–34.

Young AMJ, Joseph MH, Gray JA (1992) Increased dopamine release in vivo in nucleus accumbens and caudate nucleus of the rat during drinking: A microdialysis study. Neuroscience 48:871–876.

Záborszky L, Alheid GF, Beinfeld MC, Eiden LE, Heimer L, Palkovits M (1985) Cholecystokinin innervation of the ventral striatum: a morphological and radioimmunological study. Neuroscience 14:427–453.

Zahm DS (1999) Functional-anatomical Implications of the Nucleus Accumbens Core and Shell Subterritories. Ann N Y Acad Sci 877:113–128.

Zahm DS, Heimer L (1990) Two transpallidal pathways originating in the rat nucleus accumbens. J Comp Neurol 302:437–446.

Zener K (1937) The significance of behavior accompanying conditioned salivary secretion for theories of the conditioned response. Am J Psychol 50:384–403.

Zhou Y, Zhu H, Liu Z, Chen X, Su X, Ma C, Tian Z, Huang B, Yan E, Liu X, Ma L (2019) A ventral CA1 to nucleus accumbens core engram circuit mediates conditioned place preference for cocaine. Nat Neurosci 22:1986–1999.

Zito KA, Vickers G, Roberts DC (1985) Disruption of cocaine and heroin self-administration following kainic acid lesions of the nucleus accumbens. Pharmacol Biochem Behav 23:1029–1036.

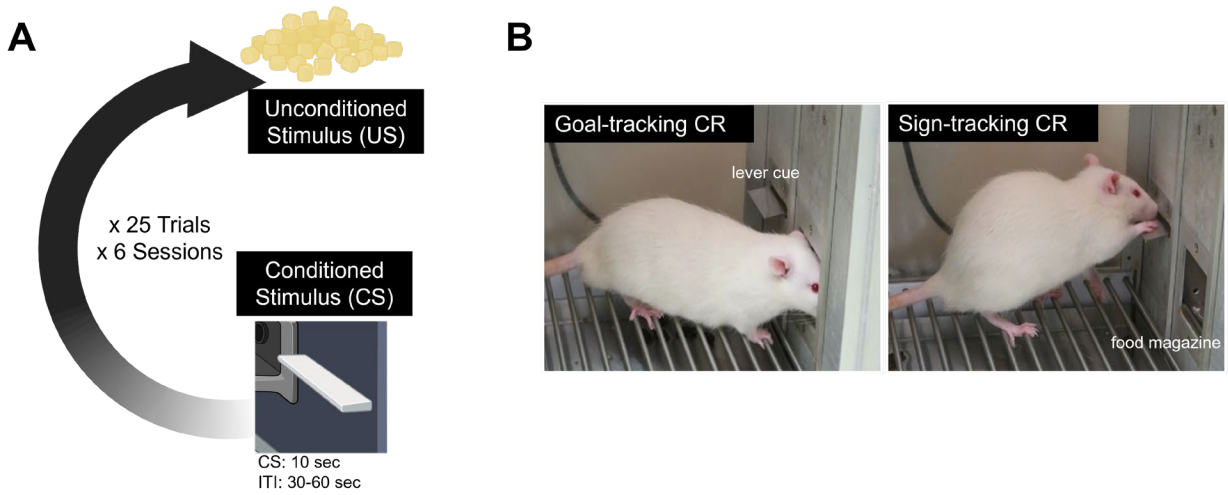


**Figure 1.1.** *Pavlovian conditioned approach (PavCA) procedure and the sign- and goal-tracking behavioral responses.* **A)** All rats undergo six daily sessions of a PavCA procedure**.** Each trial consists of the extension of an illuminated lever-cue (CS) into the chamber for 10 s immediately followed by the delivery of a banana food pellet (US) into the magazine. Each session consists of 25 CS-US pairings with an inter-trial interval of 30-60 s. **B)** Picture representations of goal-tracking (magazine bias) on the left and sign-tracking (lever bias) on the right. In response to the CS, goal-trackers (GTs) approach the magazine, which is the site of impending food delivery, whereas sign-trackers (STs) approach and interact with the lever although no response is necessary for reward delivery. Intermediate responders (IRs) typically engage equally with both the lever and the magazine, exhibiting relatively low bias. Created with BioRender.com (A).

# CHAPTER II

## Subregional Differences in Medium Spiny Neuron Intrinsic Excitability Properties between Nucleus Accumbens Core and Shell in Rats


### Abstract

The nucleus accumbens (NAc) is known for its central role in reward and motivation. Decades of research on the cellular arrangement, density, and connectivity of the NAc have identified two main subregions known as the core and shell. Although anatomically and functionally different, both the NAc core and shell are mainly comprised of GABAergic projection neurons known as medium spiny neurons (MSNs). Several studies have identified key morphological differences between core and shell MSNs, but few studies have directly addressed how core and shell MSNs differ in their intrinsic excitability. Using whole-cell patch clamp recordings in slices prepared from naïve rats and from rats exposed to either a paired CS-US or an unpaired CS-US Pavlovian paradigm, we found that for all groups, regardless of the behavioral experience, MSNs in the NAc shell were significantly more excitable than MSNs in the NAc core. In the shell, MSNs had significantly greater input resistance, lower cell capacitance, and a greater sag. This was accompanied by a lower action potential current threshold, a greater number of action potentials, and faster firing frequency compared to core MSNs. These subregional differences in intrinsic excitability could

provide a potential physiological link to the distinct anatomical characteristics of core and shell MSNs and to their distinct functional roles in reward learning.

## Introduction

The nucleus accumbens (NAc) is a part of the ventral striatum located within the basal forebrain. Decades of research have identified a fundamental role for the NAc in reward and motivation, making it a crucial structure for understanding numerous neuropsychiatric disorders including addiction, anxiety, depression, and bipolar disorder (Day and Carelli, 2007; Floresco, 2015; Salgado and Kaplitt, 2015). Based on differences in cellular arrangement, density, and connectivity, previous anatomical and histological studies have divided the NAc into three subregions: core, shell, and rostral pole, where core and shell are undistinguishable (Záborszky et al., 1985; Berendse and Groenewegen, 1990; Zahm and Heimer, 1990). For example, some studies have found that neurons in the NAc core and shell differ in their morphology with cells in the core having greater total surface area, dendritic branching, and spine density than cells in the shell (Meredith et al., 1992; Forlano and Woolley, 2010). Additionally, core and shell neurons exhibit substantial differences in both afferent and efferent connections with striatal, mesencephalic, hypothalamic, amygdalar, cortical, and hippocampal regions (Záborszky et al., 1985; Berendse and Groenewegen, 1990; Zahm and Heimer, 1990; Heimer et al., 1991; Berendse et al., 1992; Meredith et al., 1992; Britt et al., 2012). Collectively, these subregional differences in NAc anatomy and connectivity may be responsible for the distinctive functional roles in reward and motivation attributed to the core and shell (Zahm, 1999). These include functional differences in instrumental

learning, Pavlovian conditioned approach, reward devaluation, and impulsivity, as well as food- and cocaine-seeking behaviors (Day and Carelli, 2007; Floresco, 2015).

About 95% of the neurons in both the core and the shell of the NAc are GABAergic projection neurons known as medium spiny neurons (MSNs) (Matamales et al., 2009). Within subregions, many electrophysiological studies have thoroughly characterized the intrinsic excitability properties of MSNs in rodents, including how these vary by sex (Dorris et al., 2015; Cao et al., 2018), estrous cycle (Proaño et al., 2018; Proaño and Meitzen, 2020), and neuronal subtype (Planert et al., 2013), how they are modulated by dopamine (O'Donnell and Grace, 1996; Perez et al., 2006; Podda et al., 2010; Planert et al., 2013) and substances like cocaine (Kourrich and Thomas, 2009), and how they are altered in models of addiction (Mu et al., 2010; Graves et al., 2015), obesity (Alonso-Caraballo and Ferrario, 2019; Oginsky and Ferrario, 2019), stress, and depression (Francis et al., 2015, 2019). Despite all the anatomical and functional evidence suggesting physiological differences between NAc subregions, very few studies have directly investigated how core and shell MSNs differ from one another in their passive and active intrinsic excitability properties. Previous findings in mice suggest that differences in input resistance between core and shell MSNs may result in greater excitability in shell MSNs (Kourrich and Thomas, 2009). In comparison, studies in rats have suggested very subtle and contrasting subregional differences, leaving uncertainty as to what the physiological differences between core and shell MSNs may be (Pennartz et al., 1992; O'Donnell and Grace, 1993).

For this study, we used whole-cell patch clamp recordings to conduct a comprehensive electrophysiological analysis of the passive and active membrane

properties of MSNs in the NAc core and shell of adult rats. To explore the stability of core and shell subregional differences, and whether behavioral experiences can differentially impact intrinsic excitability across the NAc (Ziminski et al., 2017; Scala et al., 2018), we studied not only homecage 'naïve' animals, but also rats that underwent either a 'paired' or an 'unpaired' Pavlovian conditioned approach (PavCA) paradigm. We hypothesized that subregional physiological differences would be consistent with previously described morphological and anatomical findings and would remain stable regardless of past behavioral enrichment procedures.

## Materials and Methods

### *Animals*

Sixty-two adult male Sprague Dawley rats (7-8 weeks) were purchased from Charles River Laboratories (C72, R04) and housed in pairs upon arrival. Rats were maintained on a 12:12-hr light/dark cycle, and food and water were available ad libitum for the entirety of experimentation. Rats were divided into three counterbalanced groups before the study began: Naïve (n = 13), Unpaired (n = 18) and Paired (n = 31). Naïve rats remained in their home cages and received no handling prior to electrophysiological recordings. Unpaired and paired rats were acclimatized to the housing colony for at least two days prior to handling. After behavioral testing the rats remained in their home cages for a baseline period of 1-3 weeks before electrophysiological recordings. All animal procedures were previously approved by the University Committee on the Use and Care of Animals (University of Michigan; Ann Arbor, MI).

### *Drugs*

Isoflurane (Fluriso - VetOne; Boise, ID) was administered at 5% via inhalation for inducing anesthesia. Unless otherwise stated, all chemicals were purchased from Tocris Bioscience (Bristol, UK), Sigma-Aldrich (St. Louis, MO), and Fisher Chemical (Pittsburgh, PA).

### *Behavioral Testing Apparatus*

Sixteen modular operant conditioning chambers (24.1 cm width × 20.5 cm depth x 29.2 cm height; MED Associates, Inc.; St. Albans, VT) were used for behavioral testing. Each chamber was in a sound-attenuating cubicle equipped with a ventilation fan to provide ambient background noise. Each chamber was equipped with a food magazine, a retractable lever (counterbalanced on the left or right side of the magazine), and a red house light on the wall opposite of the magazine. The magazine contained an infrared sensor to detect magazine entries, and the levers were calibrated to detect lever deflections in response to 10 g of applied weight. Whenever a lever was extended into the chamber, an LED mounted inside the lever mechanism illuminated the slot through which the lever protruded. The number and latency of lever presses and magazine entries were recorded automatically per each trial (ABET II Software; Lafayette Instrument; Lafayette, IN).

### *Behavioral Testing Procedure*

All rats in the paired and unpaired groups were habituated to the handler and the food reward for two days prior to the start of training. Rats were handled individually and familiarized with banana-flavored pellets (45 mg; Bio-Serv; Frenchtown, NJ) in their home cages. On the third day, rats were placed into the test chambers for one pretraining session during which the red house-light remained on, but the lever was

retracted. Twenty-five food pellets were delivered on a variable time (VT) 30-s schedule (i.e., one pellet was delivered on average every 30 s, but varied 0-60 s).

Next, rats underwent six daily sessions of either a “paired CS-US” or an “unpaired CS-US” PavCA procedure. For the paired group, each trial during a training session consisted of a presentation of the illuminated lever (conditioned stimulus, CS) into the chamber for 10 s on a VT 45-s schedule (i.e., time randomly varied 30-60 s between CS presentations). Immediately after retraction of the lever, there was a response-independent delivery of one pellet into the magazine (unconditioned stimulus, US). The beginning of the next inter-trial interval (ITI) began once both the lever and the pellet had been presented, and each test session consisted of 25 trials of CS-US pairings. For the unpaired group, each trial also consisted of a 10-s presentation of the illuminated lever into the chamber and a response-independent delivery of one pellet into the magazine. However, both stimuli were on independent VT 45-s schedules (i.e., time randomly varied 30-60 s between presentations), meaning that the lever presentations and the food delivery occurred randomly and independent of one another. The beginning of the next (ITI) also began once both the lever and the pellet had been presented, and each test session consisted of 25 trials of random unpaired lever and pellet presentations. All rats consumed all the pellets that were delivered. Rats were not food deprived at any point during experimentation.

### *Electrophysiology*

*Slice preparation.* Rats were deeply anesthetized with isoflurane (Kent Scientific; Torrington, CT) and euthanized by decapitation. The brain was rapidly dissected and glued on a platform, which was then submerged in an ice-cold oxygenated (95% $O_2$/ 5%

$CO_2$) cutting solution containing (in mM): 206 sucrose, 10 d-glucose, 1.25 $NaH_2PO_4$, 26 $NaHCO_3$, 2 KCl, 0.4 sodium ascorbic acid, 2 $MgSO_4$, 1 $CaCl_2$, and 1 $MgCl_2$. A mid-sagittal cut was made to divide the two hemispheres, and coronal brain slices (300 μm) were cut using a vibrating blade microtome (Leica VT1200; Wetzlar, DE). The brain slices were transferred to a holding chamber with oxygenated artificial cerebrospinal fluid (aCSF) containing (in mM): 119 NaCl, 2.5 KCl, 1 $NaH_2PO_4$, 26.2 $NaHCO_3$, 11 d-glucose, 1 sodium ascorbic acid, 1.3 $MgSO_4$, and 2.5 $CaCl_2$ (~295 mOsm, pH 7.2-7.3) at 37ºC for 20 minutes and then room temperature for at least 40 minutes of rest. The slices were kept submerged in oxygenated aCSF in a holding chamber at room temperature for up to 7-8 hours after slicing.

*Electrophysiological recordings*. After at least 1 hour of rest, slices were transferred to the recording chamber where they were perfused with oxygenated aCSF (32ºC) containing 100 μM of $GABA_A$ receptor antagonist, picrotoxin and 5 mM of kynurenic acid to block glutamatergic transmission. Recordings from the NAc core and medial shell were done in the same slices which were obtained between +1.00 mm to +1.70 mm anterior from bregma (Paxinos and Franklin, 2019). Cells were visualized using infrared differential interference contrast (IR-DIC) optics (Microscope: Olympus BX51; Camera: Dage-MIT). Whole-cell current clamp recordings were performed using borosilicate glass pipettes (O.D. 1.5 mm, I.D. 0.86 mm; Sutter Instruments) with a 4-7 MΩ open tip resistance. Pipettes were filled with a potassium gluconate-based internal solution containing (in mM): 122 K-gluconate, 20 HEPES, 0.4 EGTA, 2.8 NaCl, and 2 $Mg^{2+}$ATP/0.3 $Na_2$GTP (~280 mOsm, pH adjusted to 7.2 with KOH). MSNs were identified based on morphology (medium-sized soma) as well as a hyperpolarized

resting potential between -70 to -90 mV and inward rectification. Neurons exhibiting a resting potential out of the desired range, characteristics of fast-spiking interneurons, and irregular firing pattern were excluded. All recordings were obtained using the MultiClamp 700B (Molecular Devices, San Jose, CA) amplifier and Digidata 1550A (Molecular Devices, San Jose, CA) digitizer. Data were filtered at (2 kHz), digitized at 10 kHz, and were collected and analyzed using pClamp 10.0 software (Molecular Devices, San Jose, CA).

To perform whole-cell recordings, membrane seals with a resistance >1 GΩ were achieved prior to breaking into the cell. Membrane capacitance ($C_m$) and series resistance ($R_s$) were compensated under voltage-clamp, and $C_m$ was recorded 1 minute after breaking in. $R_s$ was recorded in voltage-clamp with an average of 29 ± 10 MΩ upon entry and 26 ± 10 MΩ (mean ± SD) once the recordings were finished for the core, and 32 ± 10 MΩ upon entry and 29 ± 10 MΩ once finished, for the shell. Firing properties were recorded under current-clamp, and input resistance ($R_i$) was monitored online during each sweep with a -100-pA, 25-ms current injection separated by 100 ms from the current injection step protocols. The average $R_i$ across all sweeps is reported. Only cells with an $R_i$ that remained stable ($\Delta < 20\%$) were included in the analysis (Naïve: n = 51, Unpaired: n = 78; Paired: n = 131). All neurons underwent two recording protocols from their resting membrane potential (RMP) to assess firing properties. To study spike number, spike frequency, voltage/current relationships, and sag ratios, neurons were subjected once to a step protocol consisting of 500-ms current injections starting from -500 pA to +500 pA in 25-pA increments. Each sweep was separated by 4 seconds. The RMP was reported as the average voltage from all sweeps at 5 ms. The

number of spikes was determined by counting the number of individual spikes at each current injection. Firing frequency was determined by averaging the frequency (in Hz) between each two spikes for a given current injection. If a neuron reached depolarization block, data for that cell were reported until the current injection prior to the depolarization block. The steady-state voltage responses were measured 200 ms from the onset of stimulation for each subthreshold current injection step. Sag ratios were determined by the ratio of the peak voltage at the most hyperpolarized current injection (-500 pA) over the steady-state response. A ratio of 1.0 would represent no sag, and therefore, the greater the ratio, the larger the sag. For voltage/current relationship, the voltage reported is the delta between the steady-state and the baseline voltage 1 ms before onset of stimulation. In a subset of cells (Naïve: n = 25, Unpaired: n = 24, Paired n = 19), the step protocol ranged from -200 pA to +500 pA, and voltage/current relationship and sag ratio for these cells were not included in the analysis.

To study single action potential (AP) firing properties, neurons received 5-ms current injections in 25-pA increments until a single AP was elicited. Each sweep was separated by 4 seconds. Current to threshold (pA) was determined as the minimal current injection necessary to induce a single AP. The AP threshold (mV) was defined from 0 mV as the voltage at the AP inflection point. The Δ RMP/AP threshold (mV) was determined by taking the difference between the RMP and the AP threshold determined by the AP inflection point. The AP amplitude (mV) was defined from 0 mV as the voltage at the peak of the AP overshoot. The Δ RMP/AP amplitude (mV) was determined by taking the difference between the RMP and the AP amplitude measured from 0 mV. The

Δ AP threshold/AP amplitude (mV) was determined by taking the difference between the AP threshold and the AP amplitude. Finally, AP halfwidth (ms) was defined as the duration of the AP at half the voltage of the peak amplitude.

## Experimental Design and Statistical Analysis

### *Behavioral Studies*

Behavioral responses from the paired and unpaired groups in the PavCA procedure were analyzed by session. For each one of the six sessions, the total recorded number of lever presses and magazine entries from all 25 trials were added for each rat and averaged by session and group. Only magazine entries during the time that the lever was present were recorded.

GraphPad Prism 8 (Dotmatics) was used for all the behavioral data statistical analysis. Number of lever presses and number of magazine entries were analyzed separately using mixed-effects model via restricted maximum likelihood (REML). Fixed effects were set for group (unpaired, paired), session (1-6), and group x session. Multiple comparisons were made using Sidak's post-hoc test. Data are presented as mean ± SEM, and significance level was set at $p < 0.05$. A full statistical report for all behavioral data analysis is found in **Table 2.2**.

### *Electrophysiology Studies*

A total of 260 cells from 62 rats were included in the analysis. The naïve group had a total of 13 rats, from which 31 cells were recorded from in the core of 13 rats (1-2 slices/1-4 cells per rat) and 20 cells in the shell of 9 of the rats (1 slice/1-3 cells per rat). The unpaired group had a total of 18 rats, from which 47 cells were recorded from in the core of 18 rats (1-2 slices/1-5 cells per rat) and 31 cells in the shell of 14 of the rats (1-3

slices/1-4 cells per rat). The paired group had a total of 31 rats, from which 73 cells were recorded from in the core of 30 of the rats (1-2 slices/1-5 cells per rat) and 58 cells in the shell of 25 of the rats (1-2 slices/1-6 cells per rat). A total of 68 cells (Naïve: n = 25, Unpaired: n = 24, Paired: n = 19) were excluded from the analyses of sag ratio and voltage/current relationship curves. For these cells the step protocol ranged from -200 pA to +500 pA as opposed to -500 pA to +500 pA. They were excluded to keep the hyperpolarized current injection analysis homogeneous. For a total of 2 cells in the core from naïve rats, 4 cells from the core and 2 from the shell of unpaired rats, and 6 cells from the core and 3 cells from the shell of paired rats, the single action potential protocol was not run.

All offline analysis of electrophysiological recordings was performed using Clampfit 10.7 (Molecular Devices). Statistical analyses were made using GraphPad Prism 8 (Dotmatics) and SPSS Statistics (IBM) software. RMP, $C_m$, $R_i$, sag ratio, current to threshold, AP threshold, ΔRMP/AP threshold, AP amplitude, ΔRMP/AP amplitude, ΔAP threshold/AP amplitude, and AP halfwidth were analyzed using two-way ANOVA with subregion (core vs shell) and group (naïve vs unpaired vs paired) as independent variables. Sidak's post-hoc test was used for multiple comparisons. Data are presented as mean ± SEM with each data point representing an individual cell, and significance level was set at $p < 0.05$. Number of spikes, spike firing frequency, and voltage/current relationship curves (-500 to 0 pA, 0 to +100 pA) were analyzed using linear mixed-effects model via REML. Fixed effects were set for subregion (core, shell), group (naïve, unpaired, paired), current injection (V/I: -500 pA to 0 pA, 0 pA to +100 pA; AP: +50 to +400 pA), subregion x group, subregion x current injection, group x current injection,

and subregion x group x current injection. Multiple comparisons were made using Sidak's post-hoc test. Based on the group x subregion statistical report, planned comparisons using mixed-effects model via REML were done to obtain individual subregion statistics for naïve (core vs shell), unpaired (core vs shell), and paired (core vs shell) rats, and group statistics for core (naïve vs unpaired) and shell (naïve vs paired, unpaired vs paired). Fixed effects to obtain subregion statistics within groups were set for subregion (core, shell), current injection (V/I: -500 pA to 0 pA, 0 pA to +100 pA; AP: +50 to +400 pA), and subregion x current injection. Fixed effects to obtain group statistics within subregion were set for group (naïve, unpaired, paired), current injection (V/I: -500 pA to 0 pA, 0 pA to +100 pA; AP: +50 to +400 pA), and group x current injection. Data are presented as mean ± SEM with significance level set at $p < 0.05$. Full statistical reports for all electrophysiological data analysis are found in **Tables 2.1-2.2**.

## Results

### *Only paired CS-US presentations resulted in rats learning a "sign-tracking" conditioned approach response to the CS*

We wanted to determine whether MSNs in the NAc core and shell exhibit subregional differences in intrinsic excitability. To test the reliability of our findings across subregions, we validated them not only in homecage naïve animals, but also in animals pre-exposed to a behavioral enrichment experience. Moreover, we wanted to test whether a behavioral experience that induces appetitive associative learning would differ from simple reward exposures independent of a conditioned stimulus. Therefore, we performed electrophysiological recordings in naïve rats and in rats exposed to either

a paired or an unpaired Pavlovian conditioning paradigm. With this design, we were also able to explore whether these three different experiences would result in any region-specific changes in intrinsic excitability **(Fig 2.1-2.2)**.

Rats were randomly assigned to either a paired or an unpaired PavCA procedure for six days. For the rats in the paired group, a lever-cue (CS) was immediately followed by a response-independent delivery of a banana-flavored food pellet reward (US). For those in the unpaired group, the lever-cue presentations and the food pellet deliveries occurred randomly and independently of one another (**Fig 2.1-2.2)**. To confirm that rats in the paired group underwent significant associative learning compared to the rats in the unpaired group, we analyzed the number of conditioned lever presses and magazine entries during the CS period over the six training sessions. As expected, the paired group had a significant gradual increase in the number of lever presses, indicating a learned "sign-tracking" conditioned approach response to the lever-cue (**Fig 2.2B**: mixed-effects model: main effect of session, $p < 0.0001$). This learned response was not seen in the unpaired group, which displayed not only significantly lower number of lever presses than the paired group, but also a decline over the course of training (**Fig 2.2B**: mixed-effects model: group x session interaction, $p < 0.0001$).

Neither group exhibited a significant increase in the number of magazine entries during the CS period (**Fig 2.2C**: mixed-effects model: no main effect of session: $p > 0.05$), though overall the unpaired group exhibited a greater number of magazine entries (**Fig 2.2C**: mixed-effects model: main effect of group: $p < 0.01$), suggesting that there was not a prevalent "goal-tracking" learned response when looking at the population as a whole. This is consistent with the paired group exhibiting greater "sign-

tracking" to the interactive lever-cue. For the unpaired group, this may suggest greater time spent in the magazine due to the unpredictability of the reward deliveries. Nonetheless, we confirmed that the paired group displayed a significant associative learned response to the lever-cue, while the unpaired group did not exhibit any signs of associative learning relating to the CS.

***NAc MSNs exhibit distinct passive membrane properties in the core vs shell subregions of all groups regardless of their past experiences***

To characterize the intrinsic excitability properties of MSNs in the NAc core and shell, whole-cell electrophysiological recordings were performed in brain slices from rats in the naïve, unpaired CS-US, and paired CS-US groups. Electrophysiological analysis revealed differences in passive membrane properties between the two subregions in all three experimental groups **(Fig 2.3).** Input resistance was significantly greater in NAc shell MSNs compared to core MSNs (**Fig 2.3C**: two-way ANOVA: main effect of subregion, $p < 0.001$). Consistent with this, cell capacitance was significantly lower in NAc shell MSNs compared to core MSNs in all groups (**Fig 2.3D**: two-way ANOVA: main effect of subregion, $p < 0.0001$). No significant differences were found in resting potential between NAc core and shell MSNs (**Fig 2.3B**: two-way ANOVA: no main effect of subregion, $p > 0.05$). Group differences were also found in input resistance. Specifically, in the NAc shell, MSNs from paired rats had significantly lower input resistance than those from the unpaired group (**Fig 2.3C**: two-way ANOVA: main effect of group, $p < 0.05$)**.**

***MSNs in the NAc shell exhibit greater sag ratios and larger changes in membrane potential in response to current injections than core MSNs across all groups***

To investigate potential subregional differences in active intrinsic excitability properties between the NAc core and shell, we analyzed membrane potential responses of MSNs to current injections from -500 to +100 pA in 25-pA increments, generating a voltage/current relationship curve **(Fig 2.4)**. Consistent with our findings for passive membrane properties, MSNs in the shell exhibited larger responses to current injections compared to responses recorded in core MSNs from rats in the naïve, unpaired, and paired groups. The same hyperpolarizing (-500 to 0 pA) and depolarizing (0 to 100 pA) current injection steps consistently elicited a greater change in membrane potential in the shell than in the core, causing a significant shift of the V/I curve for all groups (**Fig 2.4B**: hyperpolarizing: mixed-effects model: main effect of subregion, $p < 0.0001$; depolarizing: mixed-effects model: main effect of subregion, $p < 0.0001$).

In the shell, MSNs from rats in the paired group exhibited a significantly smaller change in voltage in response to both hyperpolarizing and depolarizing current injections compared to MSNs from naïve and unpaired rats (**Fig 2.4B**: hyperpolarizing: mixed-effects model: main effect of group, $p < 0.001$; depolarizing: mixed-effects model: main effect of group, $p < 0.01$). This may be related to the lower input resistance seen in the paired group, though this difference was only found between the paired and unpaired group **(Fig 2.3C)**.

In addition, we tested whether MSNs in the NAc core versus shell had a significant difference in their voltage sag response to a -500-pA current injection **(Fig 2.5)**. To examine this, a sag ratio was calculated by dividing the peak voltage response to -500 pA over the steady-state response 200 ms from the onset of stimulation. In all three groups, MSNs in the NAc shell exhibited a greater sag ratio, representative of a

larger sag, compared to MSNs in the NAc core (**Fig 2.5B**: two-way ANOVA: main effect of subregion, $p < 0.0001$). No group differences were found in sag ratio.

***NAc MSNs in the shell exhibit higher firing frequencies than core MSNs of naïve, unpaired, and paired rats as well as differences in action potential properties***

To further examine the intrinsic excitability of core and shell MSNs, we measured firing rates in response to current injections from +50 to +400 pA in 25-pA increments **(Fig 2.6A)**. We found that in all three groups, MSNs in the shell had a significantly higher number of spikes (**Fig 2.6B**: mixed-effects model: main effect of subregion, $p < 0.0001$) and greater firing frequency (**Fig 2.6C**: mixed-effects model: main effect of subregion, $p < 0.0001$) compared to core MSNs in response to current injection steps of the same magnitude.

Medium spiny neurons in the core of naïve rats exhibited lower number of spikes and slower firing frequency when specifically compared to those in the unpaired group (**Fig 2.6B-C**: mixed-effects model: main effect of group; $p < 0.0001$). On the other hand, in the NAc shell, MSNs from the paired group had lower number of spikes and firing frequency compared to both naïve and unpaired rats (**Fig 2.6B-C**: mixed-effects model: main effect of group; $p < 0.0001$), suggesting that the paired paradigm may have caused a reduction in the excitability of MSNs in the NAc shell.

To study single spike properties in MSNs in the NAc core and shell, neurons received 5-ms current injections in 25-pA increments until a single AP was elicited **(Fig 2.7A)**. We found significant subregional differences in all groups for most action potential properties **(Fig 2.7, Table 2.1)**. Consistent with the results above, the current necessary to elicit a single action potential was significantly lower in shell MSNs

compared to core MSNs (**Fig 2.7B**: two-way ANOVA: main effect of subregion, $p < 0.0001$). Additionally, the AP threshold was significantly more depolarized in the shell compared to the core (**Fig 2.7C**: two-way ANOVA: main effect of subregion, $p < 0.001$). The peak amplitude of the AP measured from the threshold potential was lower in the shell than in the core in rats from the naïve and unpaired group (**Fig 2.7D**: two-way ANOVA: main effect of subregion, $p < 0.0001$), which is consistent with a more depolarized AP threshold in shell MSNs. The AP halfwidth was not significantly different between the core and the shell in any group (**Fig 2.7E**: two-way ANOVA: no main effect of subregion, $p > 0.05$)**.** Main effects of subregion (**Table 2.2**) were also obtained for Δ RMP/AP threshold, AP amplitude, and Δ RMP/AP amplitude, which all indicate a generally more depolarized action potential threshold and smaller AP amplitude for shell MSNs compared to core MSNs (data not shown in figure).

**Discussion**

Our data demonstrate that MSNs in the core and shell differ in their passive and active membrane properties. Overall, MSNs within the NAc shell, specifically within the medial portion, are significantly more excitable that MSNs in the NAc core. In particular, we found that shell MSNs had greater input resistance and lower cell capacitance compared to core MSNs. We also found a significant difference in the voltage/current relationship, with shell MSNs consistently exhibiting a greater deflection in membrane potential in response to hyperpolarizing and depolarizing current injections. This was accompanied by a greater sag ratio for shell MSNs, which is a measure of the hyperpolarization-activated cation current, or Ih (Pape, 1996; Robinson and Siegelbaum, 2003). As expected, we also found that shell MSNs exhibited a greater

number of action potentials in response to current injection steps as well as greater firing frequency compared to core MSNs. The current necessary to induce a single action potential was also lower for shell MSNs. Interestingly, we also found subregional differences between the action potential properties. Core MSNs had a significantly more hyperpolarized action potential threshold, and overall, a larger action potential amplitude as measured from zero, resting, and the threshold potential. These subregional differences were extremely stable across all experimental groups, suggesting that they may be a defining feature of NAc physiology.

The reported findings are consistent with previous anatomical and morphological differences between core and shell MSNs. Some studies have found that neurons in the shell have significantly fewer dendritic arbors, branch segments, terminal segments, and lower spine densities than those in the core (Meredith et al., 1992; O'Donnell and Grace, 1993; Forlano and Woolley, 2010; Wissman et al., 2011). These morphological differences result in some shell MSNs having up to ~50% less surface area than core MSNs (Meredith et al., 1992). A lower surface area can result in lower cell capacitance and consequently greater input resistance, providing a direct link between morphological and physiological properties. These marked differences in input resistance may be the primary cause of the greater excitability exhibited by shell MSNs compared to core MSNs. Similarly, a greater hyperpolarized response to negative current injections could be activating more hyperpolarization-activated cation channels (HCN) – which are known to be expressed in the NAc (Uchimura et al., 1990; Monteggia et al., 2000; Notomi and Shigemoto, 2004; Santos-Vera et al., 2013) – thus resulting in a greater sag response in shell MSNs (Robinson and Siegelbaum 2003).

Although many electrophysiological studies in MSNs have measured the sag index (Belleau and Warren, 2000; Dehorter et al., 2009; Dorris et al., 2015; Proaño and Meitzen, 2020), to our knowledge this is the first study reporting a significant subregional difference in sag between core and shell MSNs. Studies have identified striatal cholinergic neurons whose spontaneous tonic firing is regulated by Ih and is sensitive to dopaminergic modulation (Bennett et al., 2000; Deng et al., 2007). Interestingly, the mRNA and protein expression of HCN subunits in the NAc is thought to be very low (Monteggia et al., 2000; Santos-Vera et al., 2013), and the role of the Ih current in the MSN neuronal population remains largely unknown (Uchimura et al., 1990; Inoue et al., 2012). Nonetheless, it has been found that cocaine sensitization increases the expression of $HCN_2$ in the NAc without affecting the surface/intracellular ratio (Santos-Vera et al., 2013, 2019), and inhibition of HCN in the NAc significantly reduces methamphetamine self-administration (Cao et al., 2016). Therefore, Ih in the NAc may have an important role in modulating the reinforcing effect of drugs. The subregional differences found in our study could provide insight into how the Ih current may modulate neuronal excitability and network dynamics in the NAc and its functional impact on reward- and motivation-related behaviors.

Our data are consistent with previous electrophysiological studies in mice, which also reported shell MSNs to exhibit greater input resistance and overall greater number of action potentials compared to core MSNs (Kourrich and Thomas, 2009). In rats, direct core versus shell intrinsic excitability comparisons have been somewhat contradictory. Consistent with our findings and those found in mice, one study reported that core MSNs had lower input resistance as well as a more negative resting

membrane potential compared to shell MSNs (Pennartz et al., 1992). Conversely, another study found that overall core and shell MSNs had very similar passive membrane properties, and that shell MSNs were less excitable than core MSNs (O'Donnell and Grace, 1993). These apparent inconsistencies could be due to methodological differences in slice electrophysiology. Nonetheless, some anatomical studies have also reported contrasting findings in the differences between core and shell MSN morphology (Záborszky et al., 1985). Interestingly, it seems that a medial to lateral gradient in spine density and branching exists within the shell. Neurons in the lateral portion of the shell more closely resemble the morphology of neurons in the core (Meredith et al., 1992) meaning that if these physiological differences are linked to morphological differences, the location within each subregion is crucial for detecting specific differences in core versus shell intrinsic excitability properties. This could at least partially explain incongruent findings regarding core versus shell neuronal morphology and physiology.

In the core and shell of the NAc, MSNs differ not only in their morphology, but also in their distinctive patterns of connectivity with mesencephalic regions (Groenewegen and Russchen, 1984; Deutch et al., 1988; Heimer et al., 1991; Berendse et al., 1992; Meredith et al., 1995; Zahm, 1999). Importantly, medial shell MSNs are primarily innervated by mesolimbic dopaminergic projections, while those in the core mainly receive mesostriatal dopaminergic innervation (Brog et al., 1993; Groenewegen et al., 1999). These anatomical differences are accompanied by heterogeneity in dopamine $D_1$ and $D_2$ receptor expression as well as dopamine levels and utilization in the core and shell subregions. Several studies have found that $D_1$ receptors outnumber

$D_2$ receptors in the shell, while in the core $D_2$ receptors are more abundant (Bardo and Hammer, 1991; Lu et al., 1997; Hasbi et al., 2020). In addition, tyrosine hydroxylase immunoreactivity indicates that the shell is more densely innervated by dopaminergic terminals (Zahm, 1992), and dopamine levels are greater in the shell compared to the core (Deutch and Cameron, 1992). These differences in $D_1$ and $D_2$ receptor expression can functionally impact neuronal excitability (Planert et al., 2013). For example, activation of $D_1$-like receptors of MSNs can increase MSN depolarization by inhibiting Kir-channel K+ currents (Podda et al., 2010) and by enhancing L-type $Ca^{2+}$ currents (Hernández-López et al., 1997). Although activation of $D_2$ in MSNs of the NAc can also increase depolarization of the resting membrane potential by decreasing K+ leak currents, it has been found to significantly decrease action potential firing via A-type K+ currents (Perez et al., 2006) and L-type $Ca^{2+}$ currents (Hernández-López et al., 2000). Therefore, morphological differences between core and shell MSNs might not be the only cause for the subregional differences in membrane properties, but distinctive modulation from the dopaminergic system may also impact neuronal excitability. Substances like cocaine (Kourrich and Thomas, 2009), morphine (Madayag et al., 2019), and nicotine (Nisell et al., 1997) have distinctive impacts on core and shell MSN intrinsic excitability and synaptic activity, providing further evidence of physiological and functional differences in neuronal properties.

Since appetitive associative learning can induce acute changes in MSN intrinsic excitability (Ziminski et al., 2017), we studied not only homecage ‘naïve’ animals, but also rats that underwent an appetitive Pavlovian conditioning procedure. Moreover, behavioral and environmental enrichment on its own has been previously reported to

induce changes and adaptations in neuronal excitability in pyramidal neurons in the hippocampus (Malik and Chattarji, 2012; Valero-Aracama et al., 2015) as well as in MSNs in the NAc (Scala et al., 2018). Therefore, in addition to a 'paired' CS-US group that engaged in associative learning, we included another group of rats that underwent the same handling and level of cue/reward exposures, but the CS and US presentations were unpaired to prevent learning to the cue. This allowed us to directly compare whether a behavioral experience that invokes appetitive associative learning would differ from simple reward exposures independent of a conditioned stimulus. In addition, we could test whether these three different experiences would result in any region-specific changes in intrinsic excitability. Although the reported subregional differences were stable regardless of the past behavioral experience of the rat, we did find subtle group differences.

The most significant and consistent differences appeared to be in the NAc shell. Specifically, MSNs from paired animals exhibited a reduced number of action potentials and firing frequency compared to both the naïve and unpaired groups. This suggests that the associative learning procedure may have induced some subregion-specific, long-lasting changes in NAc intrinsic excitability. A previous study in the NAc shell demonstrated that a paired CS-US Pavlovian procedure can acutely increase the firing capacity of specific MSNs that were activated during the task compared to those that were not activated. Interestingly, they report that this increase in firing capacity is not seen following unpaired CS-US exposures (Ziminski et al., 2017). However, the Pavlovian conditioning procedure used in that study only allowed measurement of a "goal-tracking" conditioned response directed toward the magazine as the reward

delivery becomes more predictable. This was because they used a tone and not a localizable interactive cue such as a lever, which supports “sign-tracking” conditioned response. Sign-tracking is uniquely thought to involve some motivational/incentive value transfer from the reward to the cue, resulting in the cue becoming attractive in and of itself. We found that our task did not result in a significant increase in magazine entries, suggesting that this form of predictive learning was not the most prevalent among this sample of rats. Therefore, this finding may suggest that different forms of associative learning that promote or favor different types of associative learning (i.e., incentive vs. predictive), may differentially impact intrinsic excitability in the NAc shell. It is important to note, however, that Ziminski et al. specifically recorded from *Fos-GFP* mice, which allowed them to compare MSNs that were engaged during the paired and unpaired Pavlovian task (GFP+) versus MSNs what were not (GFP-). The reported increase in excitability was selective to specific neuronal ensembles in the paired group that had been active during the task. Furthermore, although the authors do not report any direct group comparisons of paired versus unpaired GFP+ and paired versus unpaired GFP- MSN excitability, firing capacity of MSNs in the paired group and particularly within GFP- neurons seemed to have a lower baseline than those from unpaired rats. This would more closely resemble our findings, though more studies would be needed in order to draw direct parallels.

In the next data chapter, we will explore whether individual differences in the behavioral response during our PavCA procedure affect NAc neuronal excitability in a subregion-specific manner. That is, do “sign-tracking” rats that attribute the reward-paired cue with incentive value, “goal-tracking” rats that only attribute cues with

predictive value, or rats with more intermediate behaviors exhibit differences in the intrinsic membrane properties of the NAc core and shell?

In summary, the NAc is a critical structure of the motive circuit as it converges both cortical and subcortical information during associative learning to ultimately process and regulate motivated behaviors (Day and Carelli, 2007; Floresco, 2015; Salgado and Kaplitt, 2015). The intrinsic excitability state of MSNs – how sensitive neurons are to changes in potential in response to input stimuli – can heavily influence how the NAc encodes and relays reward information (O'Donnell and Grace, 1996; Nicola et al., 2000; Planert et al., 2013; Dorris et al., 2015). The subregional differences in intrinsic excitability reported here provide a potential physiological link to the different morphological and anatomical characteristics of core and shell MSNs. Furthermore, differences between naïve, unpaired, and paired rats suggest that the intrinsic excitability in the NAc is sensitive to long-lasting changes from associative learned experiences. These findings can be used to further inform investigations of the distinct roles of the NAc core and shell in reward learning (Zahm, 1999; Ito and Hayen, 2011; Saddoris et al., 2015; West and Carelli, 2016) and in generating problematic behavioral responses linked to disorders like addiction (Di Chiara, 2002; Ito et al., 2004), anxiety (Dutta et al., 2021), and impulsivity (Pattij et al., 2007; Feja et al., 2014).

## References


Alonso-Caraballo Y, Ferrario CR (2019) Effects of the estrous cycle and ovarian hormones on cue-triggered motivation and intrinsic excitability of medium spiny neurons in the Nucleus Accumbens core of female rats. Horm Behav 116:104583.

Bardo MT, Hammer RP (1991) Autoradiographic localization of dopamine D1 and D2 receptors in rat nucleus accumbens: Resistance to differential rearing conditions. Neuroscience 45:281–290.

Belleau ML, Warren RA (2000) Postnatal development of electrophysiological properties of nucleus accumbens neurons. J Neurophysiol 84:2204–2216.

Bennett BD, Callaway JC, Wilson CJ (2000) Intrinsic membrane properties underlying spontaneous tonic firing in neostriatal cholinergic interneurons. J Neurosci Off J Soc Neurosci 20:8493–8503.

Berendse HW, Groenewegen HJ (1990) Organization of the thalamostriatal projections in the rat, with special emphasis on the ventral striatum. J Comp Neurol 299:187–228.

Berendse HW, Groenewegen HJ, Lohman AH (1992) Compartmental distribution of ventral striatal neurons projecting to the mesencephalon in the rat. J Neurosci Off J Soc Neurosci 12:2079–2103.

Britt JP, Benaliouad F, McDevitt RA, Stuber GD, Wise RA, Bonci A (2012) Synaptic and behavioral profile of multiple glutamatergic inputs to the nucleus accumbens. Neuron 76:790–803.

Brog JS, Salyapongse A, Deutch AY, Zahm DS (1993) The patterns of afferent innervation of the core and shell in the “Accumbens” part of the rat ventral striatum: Immunohistochemical detection of retrogradely transported fluoro-gold. J Comp Neurol 338:255–278.

Cao D-N, Song R, Zhang S-Z, Wu N, Li J (2016) Nucleus accumbens hyperpolarization-activated cyclic nucleotide-gated channels modulate methamphetamine self-administration in rats. Psychopharmacology (Berl) 233:3017–3029.

Cao J, Dorris DM, Meitzen J (2018) Electrophysiological properties of medium spiny neurons in the nucleus accumbens core of prepubertal male and female Drd1a-tdTomato line 6 BAC transgenic mice. J Neurophysiol 120:1712–1727.

Day JJ, Carelli RM (2007) The nucleus accumbens and Pavlovian reward learning. The Neuroscientist 13:148–159.

Dehorter N, Guigoni C, Lopez C, Hirsch J, Eusebio A, Ben-Ari Y, Hammond C (2009) Dopamine-deprived striatal GABAergic interneurons burst and generate repetitive gigantic IPSCs in medium spiny neurons. J Neurosci 29:7776–7787.

Deng P, Zhang Y, Xu ZC (2007) Involvement of Ih in dopamine modulation of tonic firing in striatal cholinergic interneurons. J Neurosci 27:3148–3156.

Deutch AY, Cameron DS (1992) Pharmacological characterization of dopamine systems in the nucleus accumbens core and shell. Neuroscience 46:49–56.

Deutch AY, Goldstein M, Baldino F, Roth RH (1988) Telencephalic projections of the A8 dopamine cell group. Ann N Y Acad Sci 537:27–50.

Di Chiara G (2002) Nucleus accumbens shell and core dopamine: differential role in behavior and addiction. Behav Brain Res 137:75–114.

Dorris DM, Cao J, Willett JA, Hauser CA, Meitzen J (2015a) Intrinsic excitability varies by sex in prepubertal striatal medium spiny neurons. J Neurophysiol 113:720–729.

Dutta S, Beaver J, Halcomb CJ, Jasnow AM (2021) Dissociable roles of the nucleus accumbens core and shell subregions in the expression and extinction of conditioned fear. Neurobiol Stress 15:100365.

Feja M, Hayn L, Koch M (2014) Nucleus accumbens core and shell inactivation differentially affects impulsive behaviours in rats. Prog Neuropsychopharmacol Biol Psychiatry 54:31–42.

Floresco SB (2015) The nucleus accumbens: an interface between cognition, emotion, and action. Annu Rev Psychol 66:25–52.

Forlano PM, Woolley CS (2010) Quantitative analysis of pre- and postsynaptic sex differences in the nucleus accumbens. J Comp Neurol 518:1330–1348.

Francis TC, Chandra R, Friend DM, Finkel E, Dayrit G, Miranda J, Brooks JM, Iñiguez SD, O'Donnell P, Kravitz A, Lobo MK (2015) Nucleus accumbens medium spiny neuron subtypes mediate depression-related outcomes to social defeat stress. Biol Psychiatry 77:212–222.

Francis TC, Gaynor A, Chandra R, Fox ME, Lobo MK (2019) The selective RhoA inhibitor rhosin promotes stress resiliency through enhancing D1-medium spiny neuron plasticity and reducing hyperexcitability. Biol Psychiatry 85:1001–1010.

Graves SM, Clark MJ, Traynor JR, Hu X-T, Napier TC (2015) Nucleus accumbens shell excitability is decreased by methamphetamine self-administration and increased by 5-HT2C receptor inverse agonism and agonism. Neuropharmacology 89:113–121.

Groenewegen H, Russchen FT (1984) Organization of the efferent projections of the nucleus accumbens to pallidal, hypothalamic, and mesencephalic structures: A tracing and immunohistochemical study in the cat. J Comp Neurol.

Groenewegen HJ, Wright CI, Beijer AV j., Voorn P (1999) Convergence and segregation of ventral striatal inputs and outputs. Ann N Y Acad Sci 877:49–63.

Hasbi A, Sivasubramanian M, Milenkovic M, Komarek K, Madras BK, George SR (2020) Dopamine D1-D2 receptor heteromer expression in key brain regions of rat and higher species: Upregulation in rat striatum after cocaine administration. Neurobiol Dis 143:105017.

Heimer L, Zahm DS, Churchill L, Kalivas PW, Wohltmann C (1991) Specificity in the projection patterns of accumbal core and shell in the rat. Neuroscience 41:89–125.

Hernández-López S, Bargas J, Surmeier DJ, Reyes A, Galarraga E (1997) $D_1$ receptor activation enhances evoked discharge in neostriatal medium spiny neurons by modulating an L-type $Ca^{2+}$ conductance. J Neurosci 17:3334–3342.

Hernández-López S, Tkatch T, Perez-Garci E, Galarraga E, Bargas J, Hamm H, Surmeier DJ (2000) D2 dopamine receptors in striatal medium spiny neurons reduce L-type Ca2+ currents and excitability via a novel PLCβ1–IP3–calcineurin-signaling cascade. J Neurosci 20:8987–8995.

Inoue R, Aosaki T, Miura M (2012) Protein kinase C activity alters the effect of μ-opioid receptors on inhibitory postsynaptic current in the striosomes. NeuroReport 23:184–188.

Ito R, Hayen A (2011) Opposing roles of nucleus accumbens core and shell dopamine in the modulation of limbic information processing. J Neurosci 31:6001–6007.

Ito R, Robbins TW, Everitt BJ (2004) Differential control over cocaine-seeking behavior by nucleus accumbens core and shell. Nat Neurosci 7:389–397.

Kourrich S, Thomas MJ (2009) Similar neurons, opposite adaptations: psychostimulant experience differentially alters firing properties in accumbens core versus shell. J Neurosci 29:12275.

Lu X-Y, Behnam Ghasemzadeh M, Kalivas PW (1997) Expression of D1 receptor, D2 receptor, substance P and enkephalin messenger RNAs in the neurons projecting from the nucleus accumbens. Neuroscience 82:767–780.

Madayag AC, Gomez D, Anderson EM, Ingebretson AE, Thomas MJ, Hearing MC (2019) Cell-type and region-specific nucleus accumbens AMPAR plasticity associated with morphine reward, reinstatement, and spontaneous withdrawal. Brain Struct Funct 224:2311–2324.

Malik R, Chattarji S (2012) Enhanced intrinsic excitability and EPSP-spike coupling accompany enriched environment-induced facilitation of LTP in hippocampal CA1 pyramidal neurons. J Neurophysiol 107:1366–1378.

Matamales M, Bertran-Gonzalez J, Salomon L, Degos B, Deniau J-M, Valjent E, Hervé D, Girault J-A (2009) Striatal medium-sized spiny neurons: identification by nuclear staining and study of neuronal subpopulations in BAC transgenic mice. PloS One 4:e4770.

Meredith GE, Agolia R, Arts MP, Groenewegen HJ, Zahm DS (1992) Morphological differences between projection neurons of the core and shell in the nucleus accumbens of the rat. Neuroscience 50:149–162.

Meredith GE, Ypma P, Zahm DS (1995) Effects of dopamine depletion on the morphology of medium spiny neurons in the shell and core of the rat nucleus accumbens. J Neurosci 15:3808–3820.

Monteggia LM, Eisch AJ, Tang MD, Kaczmarek LK, Nestler EJ (2000) Cloning and localization of the hyperpolarization-activated cyclic nucleotide-gated channel family in rat brain. Mol Brain Res 81:129–139.

Mu P, Moyer JT, Ishikawa M, Zhang Y, Panksepp J, Sorg BA, Schlüter OM, Dong Y (2010) Exposure to cocaine dynamically regulates the intrinsic membrane excitability of nucleus accumbens neurons. J Neurosci 30:3689–3699.

Nicola SM, Surmeier DJ, Malenka RC (2000) Dopaminergic modulation of neuronal excitability in the striatum and nucleus accumbens. Annu Rev Neurosci 23:185–215.

Nisell M, Marcus M, Nomikos GG, Svensson TH (1997) Differential effects of acute and chronic nicotine on dopamine output in the core and shell of the rat nucleus accumbens. J Neural Transm 104:1–10.

Notomi T, Shigemoto R (2004) Immunohistochemical localization of Ih channel subunits, HCN1–4, in the rat brain. J Comp Neurol 471:241–276.

O'Donnell P, Grace AA (1993) Physiological and morphological properties of accumbens core and shell neurons recorded in vitro. Synapse 13:135–160.

O'Donnell P, Grace AA (1996) Dopaminergic reduction of excitability in nucleus accumbens neurons recorded in vitro. Neuropsychopharmacology 15:87–97.

Oginsky MF, Ferrario CR (2019) Eating "junk food" has opposite effects on intrinsic excitability of nucleus accumbens core neurons in obesity-susceptible versus -resistant rats. J Neurophysiol 122:1264–1273.

Pape HC (1996) Queer current and pacemaker: the hyperpolarization-activated cation current in neurons. Annu Rev Physiol 58:299–327.

Pattij T, Janssen MCW, Vanderschuren LJMJ, Schoffelmeer ANM, van Gaalen MM (2007) Involvement of dopamine D1 and D2 receptors in the nucleus accumbens core and shell in inhibitory response control. Psychopharmacology (Berl) 191:587–598.

Paxinos G, Franklin KBJ (2019) Paxinos and Franklin's the Mouse Brain in Stereotaxic Coordinates. Academic Press.

Pennartz CMA, Dolleman-Van der Weel MJ, da Silva FHL (1992) Differential membrane properties and dopamine effects in the shell and core of the rat nucleus accumbens studied in vitro. Neurosci Lett 136:109–112.

Perez MF, White FJ, Hu X-T (2006) Dopamine D2 receptor modulation of K+ channel activity regulates excitability of nucleus accumbens neurons at different membrane potentials. J Neurophysiol 96:2217–2228.

Planert H, Berger TK, Silberberg G (2013) Membrane properties of striatal direct and indirect pathway neurons in mouse and rat slices and their modulation by dopamine. PLOS ONE 8:e57054.

Podda MV, Riccardi E, D'Ascenzo M, Azzena GB, Grassi C (2010) Dopamine D1-like receptor activation depolarizes medium spiny neurons of the mouse nucleus accumbens by inhibiting inwardly rectifying K+ currents through a cAMP-dependent protein kinase A-independent mechanism. Neuroscience 167:678–690.

Proaño SB, Meitzen J (2020) Estradiol decreases medium spiny neuron excitability in female rat nucleus accumbens core. J Neurophysiol 123:2465–2475.

Proaño SB, Morris HJ, Kunz LM, Dorris DM, Meitzen J (2018) Estrous cycle-induced sex differences in medium spiny neuron excitatory synaptic transmission and intrinsic excitability in adult rat nucleus accumbens core. J Neurophysiol 120:1356–1373.

Robinson RB, Siegelbaum SA (2003) Hyperpolarization-activated cation currents: From molecules to physiological function. Annu Rev Physiol 65:453–480.

Saddoris MP, Cacciapaglia F, Wightman RM, Carelli RM (2015) Differential dopamine release dynamics in the nucleus accumbens core and shell reveal complementary signals for error prediction and incentive motivation. J Neurosci Off J Soc Neurosci 35:11572–11582.

Salgado S, Kaplitt MG (2015) The nucleus accumbens: A comprehensive review. Stereotact Funct Neurosurg 93:75–93.

Santos-Vera B, Vaquer-Alicea A del C, Maria-Rios CE, Montiel-Ramos A, Ramos-Cardona A, Vázquez-Torres R, Sanabria P, Jiménez-Rivera CA (2019) Protein

and surface expression of HCN2 and HCN4 subunits in mesocorticolimbic areas after cocaine sensitization. Neurochem Int 125:91–98.

Santos-Vera B, Vázquez-Torres R, García Marrero HG, Ramos Acevedo JM, Arencibia-Albite F, Vélez-Hernández ME, Miranda JD, Jiménez-Rivera CA (2013) Cocaine sensitization increases Ih current channel subunit 2 (HCN2) protein expression in structures of the Mesocorticolimbic System. J Mol Neurosci MN 50:234–245.

Scala F et al. (2018) Environmental enrichment and social isolation mediate neuroplasticity of medium spiny neurons through the GSK3 pathway. Cell Rep 23:555–567.

Uchimura N, Cherubini E, North RA (1990) Cation current activated by hyperpolarization in a subset of rat nucleus accumbens neurons. J Neurophysiol 64:1847–1850.

Valero-Aracama MJ, Sauvage MM, Yoshida M (2015) Environmental enrichment modulates intrinsic cellular excitability of hippocampal CA1 pyramidal cells in a housing duration and anatomical location-dependent manner. Behav Brain Res 292:209–218.

West EA, Carelli RM (2016) Nucleus accumbens core and shell differentially encode reward-associated cues after reinforcer devaluation. J Neurosci 36:1128–1139.

Wissman AM, McCollum AF, Huang G-Z, Nikrodhanond AA, Woolley CS (2011) Sex differences and effects of cocaine on excitatory synapses in the nucleus accumbens. Neuropharmacology 61:217–227.

Záborszky L, Alheid GF, Beinfeld MC, Eiden LE, Heimer L, Palkovits M (1985) Cholecystokinin innervation of the ventral striatum: a morphological and radioimmunological study. Neuroscience 14:427–453.

Zahm DS (1992) An electron microscopic morphometric comparison of tyrosine hydroxylase immunoreactive innervation in the neostriatum and the nucleus accumbens core and shell. Brain Res 575:341–346.

Zahm DS (1999) Functional-anatomical implications of the nucleus accumbens core and shell subterritories. Ann N Y Acad Sci 877:113–128.

Zahm DS, Heimer L (1990) Two transpallidal pathways originating in the rat nucleus accumbens. J Comp Neurol 302:437–446.

Ziminski JJ, Hessler S, Margetts-Smith G, Sieburg MC, Crombag HS, Koya E (2017) Changes in appetitive associative strength modulates nucleus accumbens, but not orbitofrontal cortex neuronal ensemble excitability. J Neurosci 37:3160–3170.

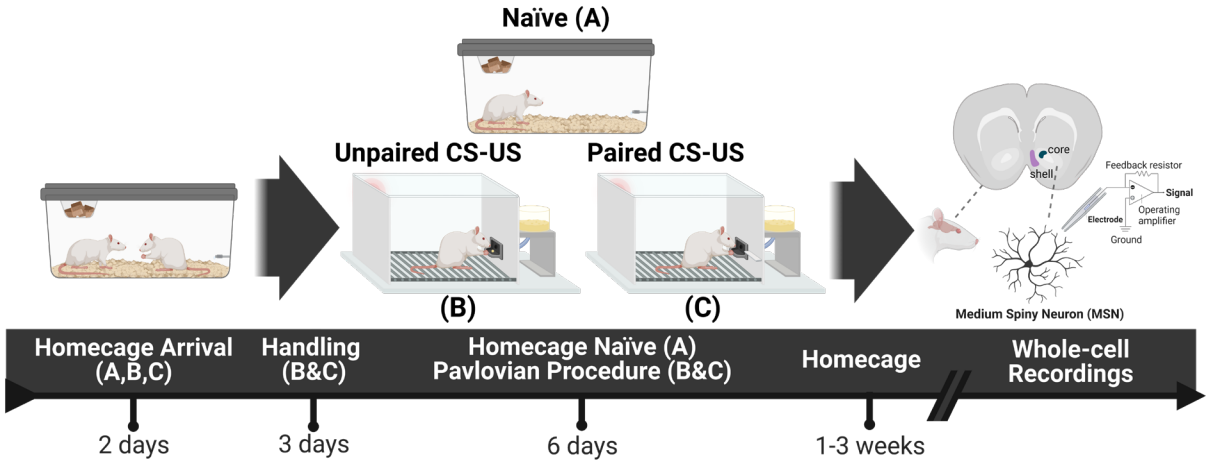


**Figure 2.1**. *Experimental timeline.* All rats were housed in pairs upon arrival. A randomly selected group of rats remained in their homecages for the entirety of the experiment and received no handling prior to the day on which the electrophysiological recordings were performed (Naïve). The other two groups (Unpaired and Paired) were handled for two days after at least two days of acclimation to the housing room. Rats were then exposed to a pre-training session in the behavioral test apparatus where they received 25 pellets into a magazine (food-cup) over the course of 30 min. For the following six days, the "Paired" group underwent a daily Pavlovian conditioned approach (PavCA) procedure in which a neutral lever-cue (CS) was presented, and following its retraction a banana-flavored food pellet (US) was immediately delivered into the magazine. Each session consisted of 25 trials of CS-US pairings (ITI: 30-60s). The "Unpaired" group underwent a similar daily behavioral experience in which a neutral lever-cue was also presented, but the food pellet rewards were delivered into the magazine randomly and independently of the lever presentations. Each session consisted of 25 independent trials of lever and reward presentations (ITI: 30-60s). After the last session of the paired and unpaired behavioral procedure, both groups of rats remained in their homecages for a period of 1-3 weeks. Subsequently, nucleus accumbens slices were prepared for whole-cell recordings of medium spiny neurons in the core and shell subregions. Created with BioRender.com.

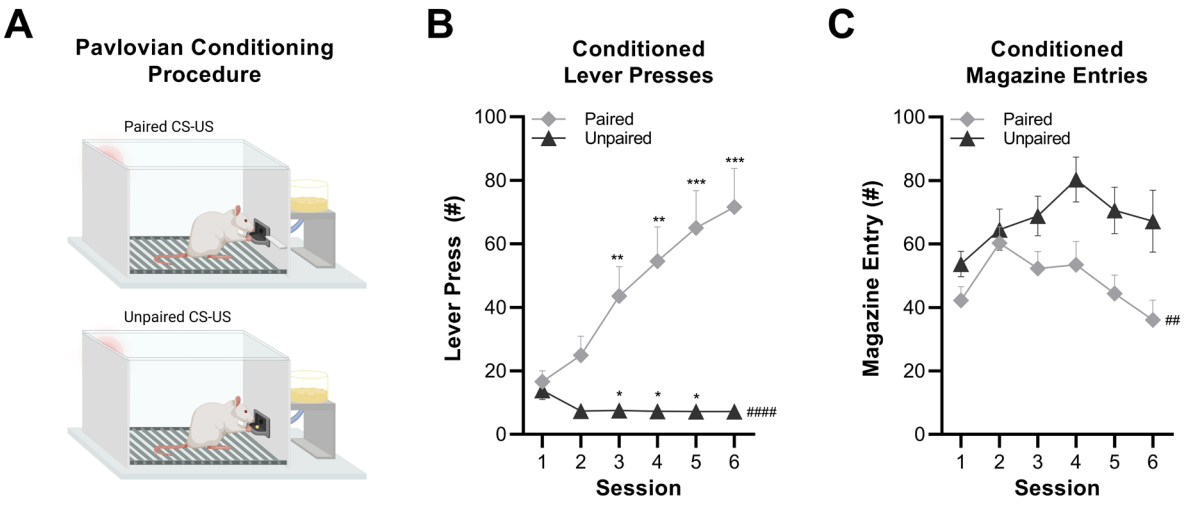


**Figure 2.2.** *Rats in the paired group learned a "sign-tracking" conditioned approach response to the lever-cue (CS) over the course of training, while those in the unpaired group did not.* **A)** Two separate groups of rats underwent six daily sessions of either a 'paired' or an 'unpaired' CS-US Pavlovian conditioned approach (PavCA) procedure. For the paired CS-US group (top), a lever-cue (CS) was paired with a banana-flavored food pellet (US). For the unpaired CS-US group (bottom), lever-cue presentations and food pellet deliveries occurred randomly. For each one of the six sessions, the total number of lever presses and magazine entries from all 25 trials were added for each rat and averaged by session. **B)** Conditioned lever presses: Over the course of training, rats in the paired group exhibited a significant increase in the number of conditioned lever presses compared to the first training session, while lever presses in the unpaired group significantly decreased (mixed-effects model: group x session interaction: $p < 0.0001$). Additionally, the overall number of lever presses was significantly greater for rats in the paired group compared to those in the unpaired group (mixed-effects model: main effect of group: $p < 0.001$). **C)** Conditioned magazine entries: The number of magazine entries during CS presentations did not change over the six training sessions for either group (mixed-effects model: no main effect of session: $p > 0.05$). Overall magazine entries during the CS period were less in the paired group than they were in the unpaired group (mixed-effects model: main effect of group: $p < 0.01$). Significance for Sidak's post-hoc test is shown as * - $p < 0.05$, ** - $p < 0.01$, *** - $p < 0.001$ for group x session multiple comparisons and as ## - $p < 0.01$, ### - $p < 0.001$ for group multiple comparisons. Data are presented as mean ± S.E.M. Created with BioRender.com (A).

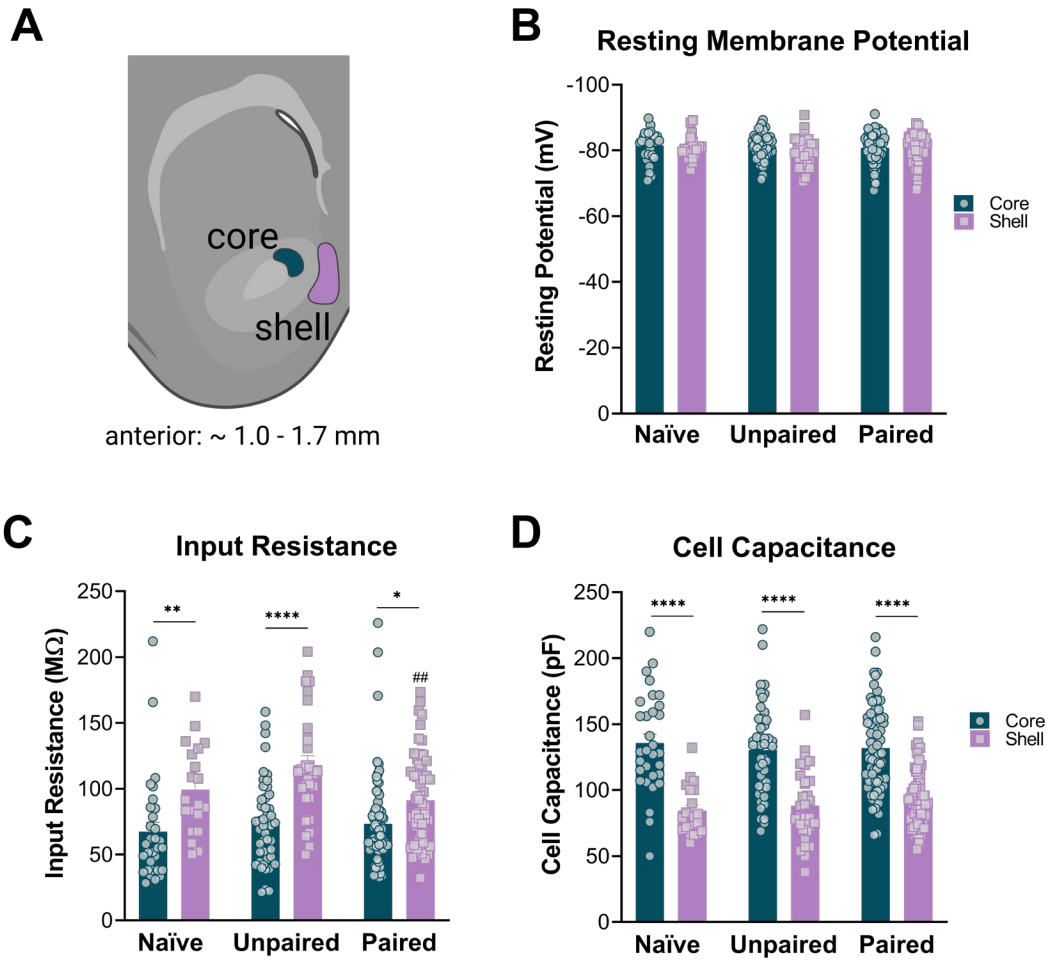


**Figure 2.3.** *Nucleus accumbens (NAc) medium spiny neurons (MSNs) exhibit distinct passive membrane properties in the core vs shell subregions of naïve, unpaired, and paired rats.* **A)** Representative diagram of a coronal brain section containing the NAc core (green) and medial shell (purple) subregions. Whole-cell patch clamp recordings from MSNs were obtained from the highlighted areas. **B)** Resting potential: No significant differences were found in resting potential between NAc core and shell (two-way ANOVA: no main effect of subregion, $p > 0.05$) **C)** Input resistance: For all naïve, unpaired, and paired groups, input resistance was significantly greater in NAc shell MSNs compared to core MSNs (two-way ANOVA: main effect of subregion, $p < 0.0001$). In the shell, MSN input resistance was greater for the unpaired group compared to the paired group (two-way ANOVA: main effect of group, $p < 0.05$). **D)** Cell capacitance was significantly lower in NAc shell MSNs compared to core MSNs for all groups (two-way ANOVA: main effect of subregion, $p < 0.0001$). Significance for Sidak's post-hoc test is shown as * - $p < 0.05$, ** - $p < 0.01$, **** - $p < 0.0001$ for subregion comparisons and as ## - $p < 0.01$ for group comparison. Each data point represents a single cell. Data are presented as mean ± S.E.M. Created with BioRender.com (A).

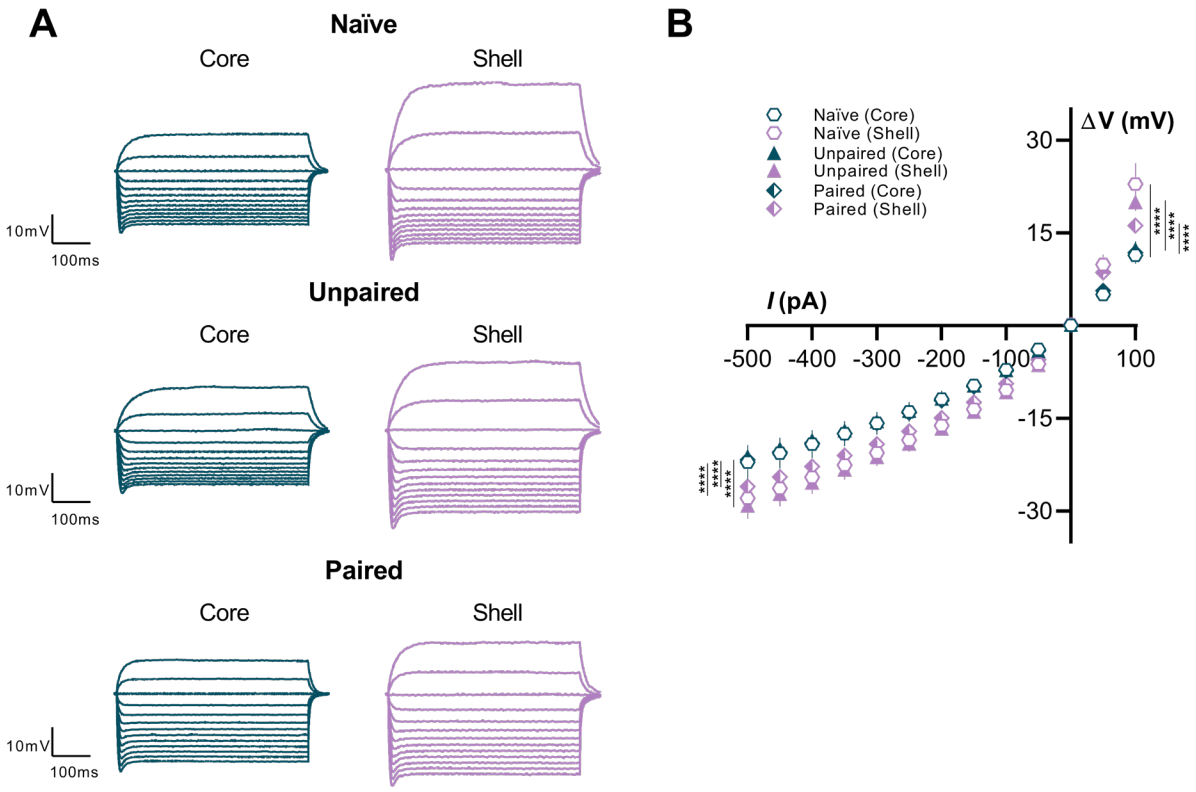


**Figure 2.4.** *Nucleus accumbens (NAc) medium spiny neurons (MSNs) in the shell exhibit larger changes in membrane potential in response to current injections than core MSNs of naïve, unpaired, and paired rats.* **A)** Representative voltage response traces from current-clamp recordings of MSNs in NAc core (left) and shell (right) slices from all groups. Current injection step protocol ranged from -500 to +100pA and is shown here in 50-pA increments. **B)** Voltage/current (V/I) relationship curve is significantly different between NAc shell and core MSNs of naïve, paired, and unpaired rats. The same hyperpolarizing (-500 to 0 paA) and depolarizing (0 to 100 pA) current injection steps consistently elicited a greater change in membrane potential in the shell vs in the core, causing a significant shift of the V/I curve (hyperpolarizing: mixed-effects model: main effect of subregion, $p < 0.0001$; depolarizing: mixed-effects model: main effect of subregion, $p < 0.0001$). In the shell, MSNs from paired group rats exhibited a significantly smaller change in voltage in response to both hyperpolarizing and depolarizing current injections compared to MSNs from naïve and unpaired rats (hyperpolarizing: mixed-effects model: main effect of group, $p < 0.001$; depolarizing: mixed-effects model: main effect of group, $p < 0.01$). Significance for mixed-effect model subregional planned comparisons is shown as **** - $p < 0.0001$. Data are presented as mean ± S.E.M.

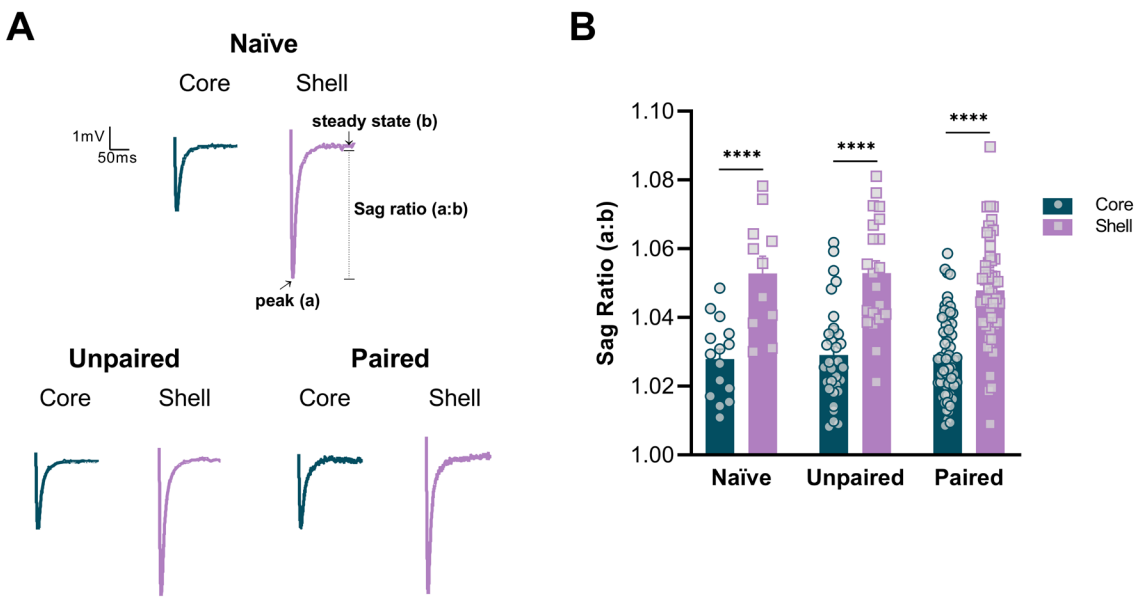


**Figure 2.5.** *Nucleus accumbens (NAc) medium spiny neurons (MSNs) in the shell exhibit greater sag ratios than core MSNs of naïve, unpaired, and paired rats.* **A)** Representative current-clamp recordings of voltage sag response to a -500-pA current injection from MSNs of NAc core and shell slices from naïve (top), unpaired (bottom left), and paired (bottom right) rats. Traces are shown as the average from all cells for each group and subregion. **B)** Sag ratio (a:b) was calculated by dividing the peak voltage response to a -500-pA current injection (a) over the steady-state response 200 ms from the onset of stimulation (b). For all groups, MSNs in the NAc shell exhibited a greater sag ratio, representative of a larger sag, compared to MSNs in the NAc core (two-way ANOVA: main effect of subregion, $p < 0.0001$). Significance for Sidak's post-hoc test is shown as **** - $p < 0.0001$. Each data point represents a single cell. Data are presented as mean ± S.E.M.

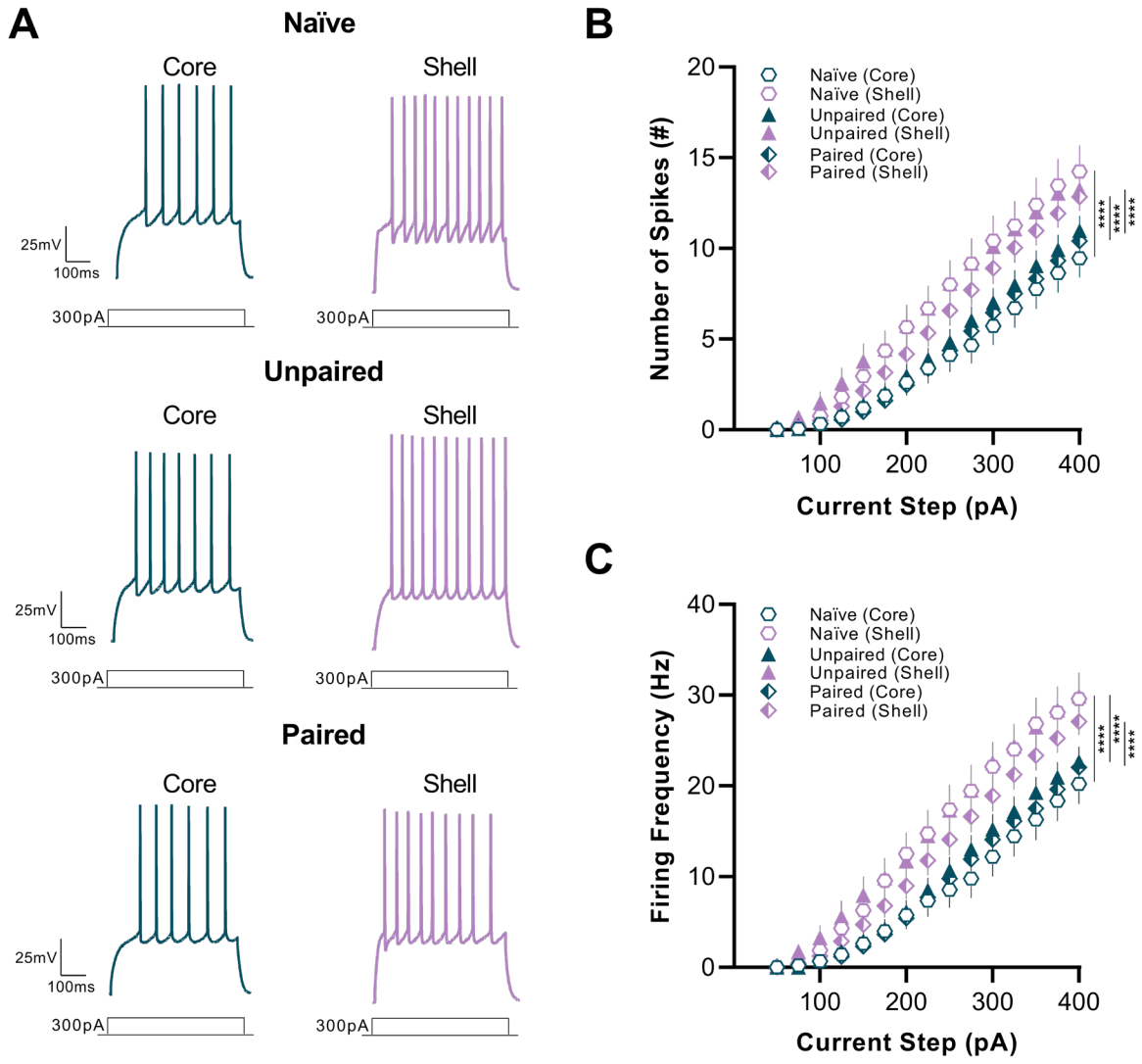


**Figure 2.6.** *Medium spiny neurons (MSNs) located in the shell exhibit greater excitability than core MSNs of naïve, unpaired, and paired rats.* **A)** Representative traces of current-clamp recordings from MSNs in NAc core (left) and shell (right) slices from all groups in response to a 300-pA current injection. **B)** Number of spikes: For all groups, MSNs in the NAc shell exhibited higher number of spikes compared to MSNs in the NAc core in response to current injection steps of the same magnitude (mixed-effects model: main effect of subregion, $p < 0.0001$). MSNs in the core of naïve rats had lower number of spikes compared to those in the unpaired group. In the shell, paired rats had lower number of spikes compared to both naïve and unpaired rats (mixed-effects model: main effect of group; $p < 0.0001$). **D)** Firing frequency: Similarly, for all groups, MSNs in the NAc shell exhibited greater firing frequency compared to MSNs in the NAc core in response to current injection steps of the same magnitude (mixed-effects model: main effect of subregion, $p < 0.0001$). MSNs in the core of naïve rats also had lower firing frequency compared to those in the unpaired group. In the shell, paired rats had lower firing frequency compared to naïve and unpaired rats (mixed-effects model: main effect of group; $p < 0.0001$). Significance for mixed-effect model subregional planned comparisons is shown as **** - $p < 0.0001$. Data are presented as mean ± S.E.M.

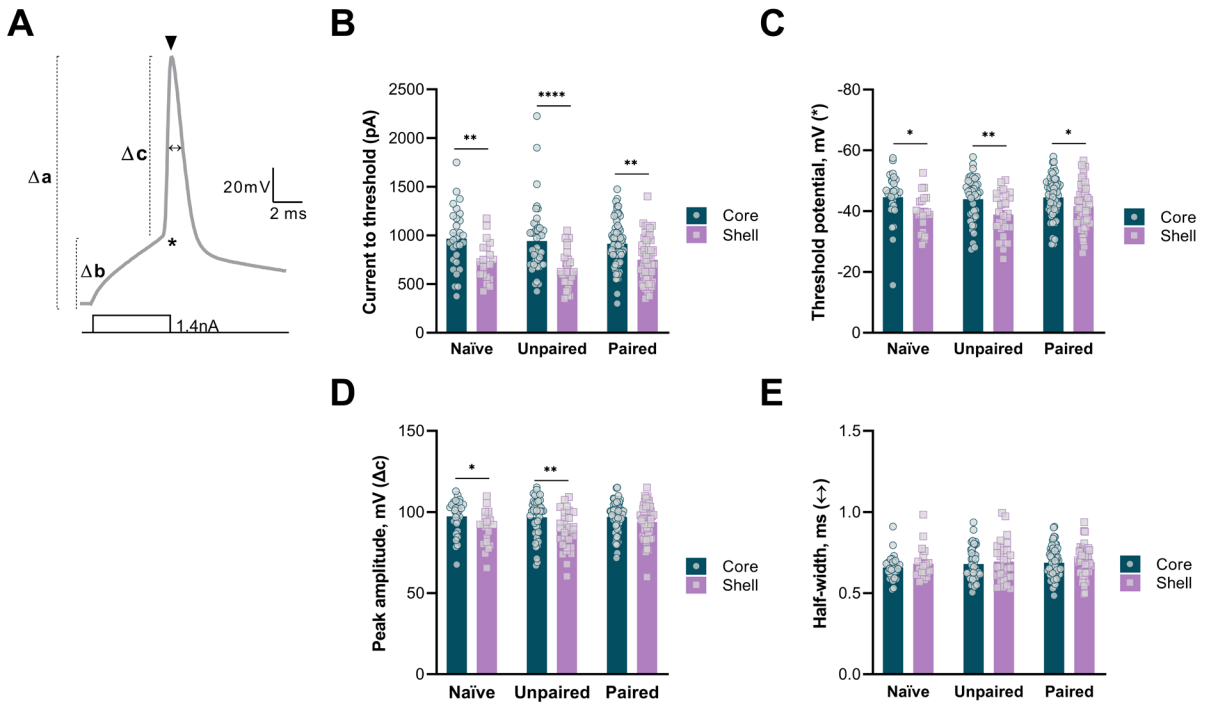


**Figure 2.7.** *Nucleus accumbens (NAc) medium spiny neurons (MSNs) exhibit distinct action potential properties in the core vs shell subregions of naïve, unpaired, and paired rats.* **A)** Representative single action potential trace of current-clamp recording from NAc MSN. Symbols illustrated on trace represent: * = AP threshold (mV), Δb = Δ RMP/AP threshold (mV), ▼ = AP amplitude (mV), Δa = Δ RMP/AP amplitude (mV), Δc = Δ AP threshold/AP amplitude (mV), ↔ = AP halfwidth (ms). **B)** Current to threshold: For naïve, unpaired, and paired groups, the current necessary to elicit a single action potential was significantly lower in NAc shell MSNs compared to core MSNs (two-way ANOVA: main effect of subregion, $p < 0.0001$). **C)** Action potential threshold: AP threshold was significantly more depolarized in NAc shell MSNs compared to core MSNs for all groups (two-way ANOVA: main effect of subregion, $p < 0.0001$). **D)** Action potential peak amplitude from threshold (Δc): For naïve and unpaired rats, Δc was lower in shell MSNs compared to core MSNs (two-way ANOVA: main effect of subregion, $p < 0.0001$). **E)** Action potential halfwidth: No significant differences were found in AP halfwidth between NAc core and shell (two-way ANOVA: no main effect of subregion, $p > 0.05$). No significant group differences were seen across any of the measured AP properties. Significance for Sidak's post-hoc test is shown as * - $p < 0.05$, ** - $p < 0.01$, **** - $p < 0.0001$. Each data point represented a single cell. Data are presented as mean ± S.E.M.

**Table 2.1.** *Electrophysiological passive and active properties of medium spiny neurons (MSNs) in the core and shell of nucleus accumbens of naïve, unpaired, and paired rats.* Table lists mean ± S.E.M. (sample size) for passive and active properties of core and shell MSNs for all three groups. Statistics for core vs shell comparisons were obtained from Sidak's post-hoc test (t value, P value) and mixed-effects model planned comparisons (F value, P value). Main effects and interactions are detailed in Table 2.2.

| | Naïve | | Statistics | Unpaired | | Statistics | Paired | | Statistics |
|---|---|---|---|---|---|---|---|---|---|
| | **Core** | **Shell** | ***t/F, P*** | **Core** | **Shell** | ***t/F, P*** | **Core** | **Shell** | ***t/F, P*** |
| ***Passive membrane properties*** | | | | | | | | | |
| **Resting membrane potential, mV** | -81.5 ± 0.8 (31) | -81.0 ± 0.8 (20) | 0.47, 0.95 | -81.2 ± 0.6 (47) | -79.7 ± 0.8 (31) | 1.55, 0.33 | -80.8 ± 0.5 (73) | -80.8 ± 0.6 (58) | 0.08, 0.99 |
| **Cell capacitance, pF** | 136 ± 7 (31) | 84 ± 4 (20) | 5.95, <0.0001 | 131 ± 5 (47) | 88 ± 5 (31) | 6.08, <0.0001 | 132 ± 4 (73) | 94 ± 3 (58) | 7.13, <0.0001 |
| **Input resistance, MΩ** | 67 ± 7 (31) | 99 ± 8 (20) | 3.16, 0.0053 | 74 ± 5 (47) | 118 ± 7 (31) | 5.39, <0.0001 | 73 ± 4 (73) | 91 ± 4 (58) | 2.87, 0.013 |
| ***Active membrane properties*** | | | | | | | | | |
| **V/I curve (-500 pA to 0 pA)** | -13.0 ± 0.3 (15) | -17.2 ± 0.4 (11) | 55.8, $3.61 \times 10^{-13}$ | -12.7 ± 0.2 (33) | -17.7 ± 0.3 (21) | 227, $8.66 \times 10^{-47}$ | -13.0 ± 0.1 (61) | -15.9 ± 0.2 (51) | 187, $4.92 \times 10^{-41}$ |
| **V/I curve (0 pA to +100 pA)** | 5.4 ± 0.5 (15) | 10.8 ± 0.6 (11) | 40.4, $4.11 \times 10^{-9}$ | 6.1 ± 0.3 (33) | 9.8 ± 0.4 (21) | 47.3, $4.65 \times 10^{-11}$ | 5.8 ± 0.3 (61) | 8.4 ± 0.3 (51) | 51.3, $2.60 \times 10^{-12}$ |
| **Sag ratio at -500 pA, mV** | 1.028 ± 0.003 (15) | 1.053 ± 0.005 (11) | 4.50, <0.0001 | 1.029 ± 0.002 (33) | 1.053 ± 0.004 (21) | 6.09, <0.0001 | 1.029 ± 0.002 (61) | 1.048 ± 0.002 (51) | 7.08, <0.0001 |
| **Number of spikes, AP#** | 3.2 ± 0.2 (31) | 6.7 ± 0.3 (20) | 72.8, $8.57 \times 10^{-17}$ | 4.5 ± 0.2 (46) | 6.8 ± 0.2 (31) | 66.6, $8.93 \times 10^{-16}$ | 4.1 ± 0.1 (71) | 5.7 ± 0.2 (57) | 62.4, $4.64 \times 10^{-15}$ |
| **Firing frequency, Hz** | 8.1 ± 0.4 (31) | 14.5 ± 0.6 (20) | 81.7, $1.48 \times 10^{-18}$ | 9.6 ± 0.4 (46) | 14.9 ± 0.4 (31) | 84.1, $2.25 \times 10^{-19}$ | 8.8 ± 0.3 (71) | 12.2 ± 0.3 (57) | 62.4, $4.82 \times 10^{-15}$ |
| **Current to threshold, pA** | 966 ± 59 (29) | 738 ± 45 (20) | 3.00, 0.0030 | 943 ± 53 (43) | 644 ± 36 (29) | 4.75, <0.0001 | 915 ± 29 (67) | 750 ± 31 (55) | 3.46, 0.0013 |
| **AP threshold, mV (*)** | -45 ± 2 (29) | -40 ± 1 (20) | 2.50, 0.026 | -44 ± 1 (43) | -39 ± 1 (29) | 3.01, 0.0086 | -44.6 ± 0.8 (67) | -41.6 ± 0.9 (55) | 2.30, 0.026 |
| **Δ RMP/AP threshold, mV (Δb)** | 36 ± 2 (29) | 41 ± 2 (20) | 2.29, 0.068 | 37 ± 1 (43) | 40 ± 2 (29) | 1.69, 0.16 | 36.5 ± 0.9 (67) | 39 ± 1 (55) | 1.74, 0.16 |
| **AP amplitude, mV (▼)** | 53 ± 1 (29) | 50 ± 1 (20) | 1.28, 0.37 | 53 ± 1 (43) | 50 ± 1 (29) | 2.08, 0.11 | 52.4 ± 0.7 (67) | 52.1 ± 0.9 (55) | 0.25, 0.80 |
| **Δ RMP/AP amplitude, mV (Δa)** | 134 ± 2 (29) | 131 ± 2 (20) | 1.08, 0.48 | 134 ± 1 (43) | 129 ± 2 (29) | 2.83, 0.015 | 133.4 ± 0.8 (67) | 133 ± 1 (55) | 0.55, 0.58 |
| **Δ AP threshold/AP amplitude, mV (Δc)** | 97 ± 2 (29) | 90 ± 2 (20) | 2.36, 0.037 | 97 ± 2 (43) | 88 ± 2 (29) | 3.17, 0.0052 | 97 ± 1 (67) | 94 ± 1 (55) | 1.63, 0.10 |
| **AP halfwidth, ms (↔)** | 0.66 ± 0.01 (29) | 0.68 ± 0.02 (20) | 0.80, 0.81 | 0.68 ± 0.02 (43) | 0.70 ± 0.02 (29) | 0.65, 0.81 | 0.69 ± 0.01 (67) | 0.69 ± 0.01 (55) | 0.05, 0.96 |

**Table 2.2.** *Full statistical report for behavioral responses and electrophysiological passive and active properties of medium spiny neurons (MSNs) in the core and shell of nucleus accumbens of naïve, unpaired, and paired rats.* Table is organized by figures and lists analyses performed, main effects and interactions, as well as post-hoc and planned comparisons for group and subregion effects.

| | Analysis | Effects | *F, df, P* | Post-hoc | Comparison | *t/F, df, P* |
|---|---|---|---|---|---|---|
| **Figure 2.2** | | | | | | |
| **2.2B. Conditioned Lever Presses** | mixed-effects model | group (main effect)<br>session (main effect)<br>group x session (interaction) | F(2.02, 94) = 9.58, p = 0.0002<br>F(1, 47) = 12.2, p = 0.0010<br>F(5, 233) = 13.2, p < 0.0001 | Sidak's | Paired Sessions:<br>1vs.3, 1vs.4, 1vs.5, 1vs.6<br><br>Unpaired Sessions:<br>1vs.3, 1vs.4, 1vs.5 | t(30) = 4.23, p = 0.0030; t(30) = 4.49, p = 0.0015; t(30) = 5.02, p = 0.0003; t(28) = 5.25, p = 0.0002<br><br>t(17) = 3.62, p = 0.032; t(17) = 3.40, p = 0.050; t(17) = 3.44, p = 0.046 |
| **2.2C. Conditioned Magazine Entries** | mixed-effects model | group (main effect) | F(1, 43) = 12.2, p = 0.0027 | - | - | - |
| **Figure 2.3** | | | | | | |
| **2.3B. Resting membrane potential** | 2-way ANOVA | subregion (no main effect) | F(1, 254) = 1.53, p = 0.22 | - | - | - |
| **2.3C. Input resistance** | 2-way ANOVA | subregion (main effect)<br>group (main effect)<br>subregion x group (interaction) | F(1, 254) = 42.4, p < 0.0001<br>F(2, 254) = 3.77, p = 0.024<br>F(2, 254) = 3.35, p = 0.037 | Sidak's | naïve: core vs shell<br>unpaired: core vs shell<br>paired: core vs shell<br><br>shell: unpaired vs paired | t(254) = 3.16, p = 0.0053<br>t(254) = 5.39, p <0.0001<br>t(254) = 2.87, p = 0.013<br><br>t(254) = 3.41, p = 0.0023 |
| **2.3D. Cell capacitance** | 2-way ANOVA | subregion (main effect) | F(2, 254) = 114, p < 0.0001 | Sidak's | naïve: core vs shell<br>unpaired: core vs shell<br>paired: core vs shell | t(254) = 5.95, p <0.0001<br>t(254) = 6.08, p <0.0001<br>t(254) = 7.13, p <0.0001 |
| **Figure 2.4** | | | | | | |
| **2.4B. Voltage/Current curve** | | | | | | |
| Hyperpolarizing: -500 to 0 pA | mixed-effects model | subregion (main effect)<br>current injection (main effect)<br>group (main effect)<br>subregion x current injection (interaction)<br>group x subregion (interaction) | F(1, 3906) = 390, p = $7.55x10^{-83}$<br>F(20, 3906) = 242, p = $0.0x10^{0}$<br>F(2, 3906) = 8.70, p = 0.00017<br>F(20, 3906) = 2.92, p = 0.000014<br><br>F(2, 3906) = 15.7, p = $1.60x10^{-7}$ | mixed-effects model planned comparison | naïve: core vs shell<br>unpaired: core vs shell<br>paired: core vs shell<br><br>shell: naïve vs paired<br>shell: unpaired vs paired | F(1, 504) = 55.8, p = $3.61x10^{-13}$<br>F(1, 1092) = 227, p = $8.66x10^{-47}$<br>F(1, 2310) = 187, p = $4.92x10^{-41}$<br><br>F(1, 1260) = 10.8, p = 0.0010<br>F(1, 1470) = 33.5, p = $8.50x10^{-9}$ |
| Depolarizing: 0 to 100 pA | mixed-effects model | subregion (main effect)<br>current injection (main effect)<br>group (main effect)<br>subregion x current injection (interaction)<br>group x subregion (interaction) | F(1, 911) = 132, p = $1.27x10^{-28}$<br>F(4, 911) = 264, p = $1.35x10^{-150}$<br>F(2, 911) = 4.86, p = 0.0079<br>F(4, 911) = 16.5, p = $4.45x10^{-13}$<br><br>F(2, 911) = 5.57, p = 0.0039 | mixed-effects model planned comparison | naïve: core vs shell<br>unpaired: core vs shell<br>paired: core vs shell<br><br>shell: naïve vs paired<br>shell: unpaired vs paired | F(1, 117) = 40.4, p = $4.11x10^{-9}$<br>F(1, 258) = 47.3, p = $4.65x10^{-11}$<br>F(1, 536) = 51.3, p = $2.60x10^{-12}$<br><br>F(1, 288) = 9.56, p = 0.0022<br>F(1, 340) = 7.27, p = 0.0074 |

| | | | | | | |
|---|---|---|---|---|---|---|
| **Figure 2.5** | | | | | | |
| **2.5B. Sag ratio** | 2-way ANOVA | subregion (main effect) | $F(1, 186) = 85.9$, $p < 0.0001$ | Sidak's | naïve: core vs shell<br>unpaired: core vs shell<br>paired: core vs shell | $t(186) = 4.496$, $p < 0.0001$<br>$t(186) = 6.092$, $p < 0.0001$<br>$t(186) = 7.084$, $p < 0.0001$ |
| **Figure 2.6** | | | | | | |
| **2.6B. Number of spikes** | mixed-effects model | subregion (main effect)<br>current injection (main effect)<br>group (main effect)<br>subregion x current injection (interaction)<br>group x subregion (interaction) | $F(1, 3658) = 198$, $p = 8.25 \times 10^{-44}$<br>$F(14, 3658) = 167$, $p = 0.0 \times 10^{0}$<br>$F(2, 3658) = 9.31$, $p = 0.000093$<br>$F(14, 3658) = 3.92$, $p = 0.000001$<br>$F(2, 3658) = 5.62$, $p = 0.0037$ | mixed-effects model<br>planned comparison | naïve: core vs shell<br>unpaired: core vs shell<br>paired: core vs shell<br><br>core: naïve vs unpaired<br>shell: naïve vs paired<br>shell: unpaired vs paired | $F(1, 706) = 72.8$, $p = 8.57 \times 10^{-17}$<br>$F(1, 1087) = 66.6$, $p = 8.93 \times 10^{-16}$<br>$F(1, 1865) = 62.4$, $p = 4.64 \times 10^{-15}$<br><br>$F(1, 1097) = 6.87$, $p = 0.0089$<br>$F(1, 1104) = 8.82$, $p = 0.0030$<br>$F(1, 1256) = 13.3$, $p = 0.00027$ |
| **2.6C. Firing frequency** | mixed-effects model | subregion (main effect)<br>current injection (main effect)<br>group (main effect)<br>subregion x current injection (interaction)<br>group x subregion (interaction) | $F(1, 3658) = 224$, $p = 3.61 \times 10^{-49}$<br>$F(14, 3658) = 178$, $p = 0.0 \times 10^{0}$<br>$F(2, 3658) = 11.3$, $p = 0.000013$<br>$F(14, 3658) = 4.29$, $p = 1.32 \times 10^{-7}$<br>$F(2, 3658) = 7.77$, $p = 0.00043$ | mixed-effects model<br>planned comparison | naïve: core vs shell<br>unpaired: core vs shell<br>paired: core vs shell<br><br>core: naïve vs unpaired<br>shell: naïve vs paired<br>shell: unpaired vs paired | $F(1, 706) = 81.7$, $p = 1.48 \times 10^{-18}$<br>$F(1, 1087) = 84.1$, $p = 2.25 \times 10^{-19}$<br>$F(1, 1865) = 62.4$, $p = 4.82 \times 10^{-15}$<br><br>$F(1, 1097) = 7.38$, $p = 0.0067$<br>$F(1, 1104) = 10.6$, $p = 0.0012$<br>$F(1, 1256) = 19.0$, $p = 0.000014$ |
| **Figure 2.7** | | | | | | |
| **2.7B. Current to threshold** | 2-way ANOVA | subregion (main effect) | $F(1, 237) = 39.9$, $p < 0.0001$ | Sidak's | naïve: core vs shell<br>unpaired: core vs shell<br>paired: core vs shell | $t(237) = 3.00$, $p = 0.0030$<br>$t(237) = 4.75$, $p < 0.0001$<br>$t(237) = 3.46$, $p = 0.0013$ |
| **2.7C. Threshold potential** | 2-way ANOVA | subregion (main effect) | $F(1, 237) = 19.9$, $p < 0.0001$ | Sidak's | naïve: core vs shell<br>unpaired: core vs shell<br>paired: core vs shell | $t(237) = 2.50$, $p = 0.026$<br>$t(237) = 3.01$, $p = 0.0086$<br>$t(237) = 2.30$, $p = 0.026$ |
| **2.7D. Δ AP threshold/AP amplitude** | 2-way ANOVA | subregion (main effect) | $F(1, 237) = 17.4$, $p < 0.0001$ | Sidak's | naïve: core vs shell<br>unpaired: core vs shell<br>paired: core vs shell | $t(237) = 2.36$, $p = 0.037$<br>$t(237) = 3.17$, $p = 0.0052$<br>$t(237) = 1.63$, $p = 0.10$ |
| **2.7E. AP halfwidth** | 2-way ANOVA | subregion (no main effect) | $F(1, 237) = 0.90$, $p = 0.34$ | - | - | - |
| **Table 2.1 (not in figure)** | | | | | | |
| **Δ RMP/AP threshold** | 2-way ANOVA | subregion (main effect) | $F(1, 237) = 11.0$, $p = 0.0011$ | Sidak's | naïve: core vs shell<br>unpaired: core vs shell<br>paired: core vs shell | $t(237) = 2.29$, $p = 0.068$<br>$t(237) = 1.69$, $p = 0.16$<br>$t(237) = 1.74$, $p = 0.16$ |
| **AP amplitude** | 2-way ANOVA | subregion (main effect) | $F(1, 237) = 4.79$, $p = 0.030$ | Sidak's | naïve: core vs shell<br>unpaired: core vs shell<br>paired: core vs shell | $t(237) = 1.28$, $p = 0.37$<br>$t(237) = 2.08$, $p = 0.11$<br>$t(237) = 0.25$, $p = 0.80$ |
| **Δ RMP/AP amplitude** | 2-way ANOVA | subregion (main effect) | $F(1, 237) = 6.81$, $p = 0.0096$ | Sidak's | naïve: core vs shell<br>unpaired: core vs shell<br>paired: core vs shell | $t(237) = 1.08$, $p = 0.48$<br>$t(237) = 2.83$, $p = 0.015$<br>$t(237) = 0.55$, $p = 0.58$ |

## CHAPTER III

# Individual Variation in Intrinsic Neuronal Properties of Nucleus Accumbens Core and Shell Medium Spiny Neurons in Animals Prone to Sign- or Goal-Track


## Abstract

The “sign-tracking” and “goal-tracking” model of individual variation in associative learning allows us to identify rats with different cue-reactivity and predisposition to addiction-like behaviors. Certainly, compared to “goal-trackers” (GTs), “sign-trackers” (STs) exhibit more susceptibility traits such as increased cue-induced ‘relapse’ of drugs of abuse. Different cue- and reward-evoked patterns of activity in the nucleus accumbens (NAc) have been a hallmark of the ST/GT phenotype. However, it is unknown whether differences in the intrinsic neuronal properties of NAc medium spiny neurons (MSNs) in the core and shell subregions are also a physiological correlate of these phenotypes. We performed whole-cell slice electrophysiology in outbred rats and found that STs exhibited the lowest excitability in the NAc core, with lower number of action potentials and firing frequency as well as a blunted voltage/current relationship curve in response to hyperpolarized potentials in both the NAc core and shell. Although firing properties of shell MSNs did not differ between STs and GTs, intermediate responders that engage in both behaviors exhibited greater excitability compared to

both STs and GTs. These findings suggest that intrinsic excitability in the NAc may contribute to individual differences in the attribution of incentive salience.

## Introduction

The ability to develop adaptive responses to cues that signal the availability of food, safety, mating opportunities, and other rewards is essential for survival. The nucleus accumbens (NAc) plays a central role in this learning process. Individual variations in the way information about the environment is processed through the NAc could contribute to a variety of traits associated with neuropsychiatric disorders including impulsivity, hyperactivity, and cue-reactivity (Robinson and Berridge, 1993; Berridge et al., 2009; Flagel and Robinson, 2017). However, linking such behaviorally complex predisposing factors to specific neurobiological processes has proven difficult. Because cues normally acquire both predictive and incentive value together, it is difficult to dissociate these properties and disambiguate the neurobiological processes that govern them. However, such a dissociation can be achieved in rats by using Pavlovian conditioned approach (PavCA) procedure to isolate and study individual variation in associative learning styles known as “sign-tracking” and “goal-tracking”. During a Pavlovian conditioning task, “sign-trackers” (STs) will reliably approach the reward-paired cue and interact with it (“sign-tracking”), whereas “goal-trackers” (GTs) will instead direct their behavior away from the cue and towards the site of impending reward delivery (“goal-tracking”). The key difference between these phenotypes is that GTs only use reward cues as predictors, but STs also attribute them with incentive salience, meaning the cues become irresistible and rewarding in and of themselves (Berridge et al., 2009). Intermediate responders (IRs) are rats that exhibit a relatively

low bias toward sign- or goal-tracking behavior and tend to alternate between both conditioned responses. Compared to GTs, STs are more impulsive (Lovic et al., 2011), have less attentional control (Paolone et al., 2013), and are more susceptible to cue-induced “relapse” of drug self-administration (Saunders and Robinson, 2011; Versaggi et al., 2016) making it a useful model for studying the neurobiological basis of incentive salience attribution and its contribution to disorders like addiction.

Perhaps unsurprisingly, neuronal activity in the NAc seems to be particularly important for individual differences in the attribution of incentive salience. STs exhibit increased cue-evoked c-fos expression in the NAc when compared to GTs (Flagel et al., 2011a), and single-unit recordings and *in vivo* voltammetry have also revealed that STs and GTs exhibit different cue- and reward-evoked patterns of activity and dopamine release in the NAc during Pavlovian learning (Flagel et al., 2011b; Gillis and Morrison, 2019). Over the years, particular attention has been given to the NAc – including its molecular and chemical composition – with the goal of dissecting the neurocircuitry responsible for biasing sign- and goal-tracking behavior (for review see Flagel and Robinson, 2017). Nonetheless, it remains unknown whether the observed variation in NAc activity between STs and GTs actually reflect phenotypic differences in the fundamental intrinsic neuronal excitability of these neurons.

The NAc consists of two subregions known as the core and shell with distinct anatomical features (Záborszky et al., 1985; Zahm and Heimer, 1990; Heimer et al., 1991; Meredith et al., 1992; Britt et al., 2012) and functional roles in Pavlovian learning and motivation (Zahm, 1999; Bassareo et al., 2002; Day and Carelli, 2007; West and Carelli, 2016). GABAergic projection neurons known as medium spiny neurons (MSNs)

comprise about 95% of the total neuronal population in both the core and the shell (Pennartz et al., 1994; Matamales et al., 2009). Therefore, the intrinsic excitability state of MSNs – how sensitive they are to changes in membrane potential caused by input stimuli – may reveal important functional differences between STs, GTs, and IRs in how the NAc integrates and relays reward information (O'Donnell and Grace, 1996; Nicola et al., 2000; Planert et al., 2013; Dorris et al., 2015).

The present study used whole-cell patch-clamp recordings to conduct an electrophysiological characterization of the passive and active membrane properties of MSNs in the NAc core and shell of ST, GT, and IR rats. We hypothesize that MSNs from these three phenotypes will express basal differences in intrinsic excitability and that these will contribute to our understanding of how the NAc, particularly of STs and GTs, differentially encodes predictive and incentive value of appetitive cues.

## Materials and Methods

### *Animals*

Thirty-one adult male Sprague Dawley rats (8-10 weeks) were purchased from Charles River Laboratories (C72, R04) and housed in pairs. Rats were maintained on a 12:12-hr light/dark cycle, with food and water available ad libitum for the entirety of the experiment. All rats were acclimatized to the housing colony for at least two days prior to handling. After behavioral testing the rats remained in their home cages for a resting period of 1-3 weeks before electrophysiological recordings. All animal procedures were previously approved by the University Committee on the Use and Care of Animals (University of Michigan; Ann Arbor, MI).

### *Drugs*

Isoflurane (Fluriso - VetOne; Boise, ID) was administered at 5% via inhalation for inducing anesthesia. Unless otherwise stated, all chemicals were purchased from Tocris Bioscience (Bristol, UK), Sigma-Aldrich (St. Louis, MO), and Fisher Chemical (Pittsburgh, PA).

### *Behavioral Testing Apparatus*

Sixteen modular operant conditioning chambers (24.1 cm width × 20.5 cm depth x 29.2 cm height; MED Associates, Inc.; St. Albans, VT) were used for behavioral testing. Each chamber was inside a sound-attenuating cubicle with a ventilation fan providing ambient background noise during testing. Each chamber was equipped with a food magazine, a retractable lever (counterbalanced on the left or right side of the magazine), and a red house light on the wall opposite to the magazine. An infrared sensor in the magazines detected magazine entries, and the levers were calibrated to detect lever deflections in response to a minimum of 10 g of applied weight. The inside of the lever mechanism contained a mounted LED to illuminate the slot through which the lever protruded each time the lever was extended into the chamber. The number and latency of lever presses and magazine entries were recorded automatically (ABET II Software; Lafayette Instrument; Lafayette, IN).

### *Behavioral Testing Procedure*

For two days prior to the start of training, all rats were habituated to the handler and the food reward. Rats were handled individually and were given banana-flavored pellets (45 mg; Bio-Serv; Frenchtown, NJ) in their home cages. On the third day, rats were placed into the test chambers for one pre-training session during which the red house-light remained on, but the lever was retracted. Twenty-five food pellets were

delivered on a variable time (VT) 30-s schedule (i.e., one pellet was delivered on average every 30 s, but varied 0-60 s). Following the pre-training session, all rats underwent six daily sessions of behavioral training. Each trial during a training session consisted of a presentation of the illuminated lever (conditioned stimulus, CS) into the chamber for 10 seconds on a VT 45-s schedule (i.e., time randomly varied 30-60 s between CS presentations). Immediately after retraction of the lever, there was a response-independent delivery of one pellet into the magazine (unconditioned stimulus, US). The beginning of the next inter-trial interval (ITI) began once both the lever and the pellet had been presented, and each test session consisted of 25 trials of CS-US pairings. All rats consumed all the pellets that were delivered. Rats were not food deprived at any point during experimentation.

***Electrophysiology***

*Slice preparation.* Rats were deeply anesthetized with isoflurane (Kent Scientific; Torrington, CT) and euthanized by decapitation. The brain was rapidly dissected and glued on a platform, which was then submerged in an ice-cold oxygenated (95% $O_2$/ 5% $CO_2$) cutting solution containing (in mM): 206 sucrose, 10 d-glucose, 1.25 $NaH_2PO_4$, 26 $NaHCO_3$, 2 KCl, 0.4 sodium ascorbic acid, 2 $MgSO_4$, 1 $CaCl_2$, and 1 $MgCl_2$. A mid-sagittal cut was made to divide the two hemispheres, and 300-µm coronal brain slices were cut using a vibrating blade microtome (Leica VT1200; Wetzlar, DE). The brain slices were transferred to a holding chamber with oxygenated artificial cerebrospinal fluid (aCSF) containing (in mM): 119 NaCl, 2.5 KCl, 1 $NaH_2PO_4$, 26.2 $NaHCO_3$, 11 d-glucose, 1 sodium ascorbic acid, 1.3 $MgSO_4$, and 2.5 $CaCl_2$ (~295 mOsm, pH 7.2-7.3) at 37ºC for 20 minutes and then room temperature for at least 40 minutes of rest. The

slices were kept submerged in oxygenated aCSF in a holding chamber at room temperature for up to 7-8 hours after slicing.

*Electrophysiological recordings*. After at least 1 hour of rest, slices were individually transferred to the recording chamber where they were perfused with oxygenated aCSF (32 ºC) containing 100 µM of the $GABA_A$ receptor antagonist picrotoxin and 5 mM kynurenic acid to block glutamatergic transmission. Recordings from the NAc core and medial shell were made in the same slices which were obtained between +1.00 mm to +1.70 mm anterior from bregma (Paxinos and Franklin, 2019). Cells were visualized using infrared differential interference contrast (IR-DIC) optics (Microscope: Olympus BX51; Camera: Dage-MIT). Whole-cell current clamp recordings were performed using borosilicate glass pipettes (O.D. 1.5 mm, I.D. 0.86 mm; Sutter Instruments) with a 4-7-MΩ open tip resistance. Pipettes were filled with a potassium gluconate-based internal solution containing (in mM): 122 K-gluconate, 20 HEPES, 0.4 EGTA, 2.8 NaCl, and 2 $Mg^{2+}$ATP/0.3 $Na_2$GTsP (~280 mOsm, pH adjusted to 7.2 with KOH). MSNs were identified based on morphology (medium-sized soma) as well as a hyperpolarized resting potential between -70 to -90 mV and inward rectification. Neurons exhibiting a resting potential out of the desired range, characteristics of fast-spiking interneurons, and irregular firing pattern were excluded. All recordings were obtained using the MultiClamp 700B (Molecular Devices, San Jose, CA) amplifier and Digidata 1550A (Molecular Devices, San Jose, CA) digitizer. Data were filtered at 2 kHz, digitized at 10 kHz, and collected and analyzed using pClamp 10.0 software (Molecular Devices, San Jose, CA).

To perform whole-cell recordings, membrane seals with a resistance >1 GΩ were achieved prior to breaking into the cell. Membrane capacitance ($C_m$) and series resistance ($R_s$) were compensated under voltage-clamp, and $C_m$ was recorded 1 minute after breaking in. $R_s$ was recorded in voltage-clamp with an average of 28 ± 6 MΩ, 28 ± 7 MΩ, and 30 ± 7 MΩ (mean ± SD) upon entry and 26 ± 6 MΩ, 27 ± 7 MΩ, and 26 ± 7 MΩ (mean ± SD) once the recordings were finished, for STs, GTs, and IRs respectively. Firing properties were recorded under current-clamp, and input resistance ($R_i$) was monitored online during each sweep with a -100-pA, 25-ms current injection separated by 100 ms from the current injection step protocols. The average $R_i$ across all sweeps is reported. Only cells with an $R_i$ that remained stable ($\Delta < 20\%$) were included in the analysis (STs: n = 42, GTs: n = 40, IRs: n = 46). All neurons underwent two recording protocols from their resting membrane potential (RMP) to assess firing properties. To study spike number, spike frequency, voltage/current relationships, and sag ratios, neurons were subjected once to a step protocol consisting of 500 ms current injections starting from -500 pA to +500 pA in 25-pA increments. Each sweep was separated by 4 seconds. The RMP was reported as the average voltage from all sweeps at 5 ms. The number of spikes was determined by counting the number of individual spikes at each current injection. Firing frequency was determined by averaging the frequency (in Hz) between each two spikes for a given current injection. If a neuron reached depolarization block, data for that cell were reported until the current injection prior to the depolarization block. The steady-state voltage responses were measured 200 ms from the onset of stimulation for each subthreshold current injection step. Sag ratios were determined by the ratio of the peak voltage at the most hyperpolarized current

injection (-500 pA) over the steady-state response. A ratio of 1.0 would represent no sag, and therefore, the greater the ratio, the larger the sag. For voltage/current relationship, the voltage reported is the delta between the steady-state and the baseline voltage 1 ms before onset of stimulation.

To study single action potential (AP) firing properties, neurons received 5-ms current injections in 25-pA increments until a single AP was elicited. Each sweep was separated by 4 seconds. Current to threshold (pA) was determined as the minimal current injection necessary to induce a single AP. The AP threshold (mV) was defined from 0 mV as the voltage at the AP inflection point. The Δ RMP/AP threshold (mV) was determined by taking the difference between the RMP and the AP threshold determined by the AP inflection point. The AP amplitude (mV) was defined from 0mV as the voltage at the peak of the AP overshoot. The Δ RMP/AP amplitude (mV) was determined by taking the difference between the RMP and the AP amplitude measured from 0 mV. The Δ AP threshold/AP amplitude (mV) was determined by taking the difference between the AP threshold and the AP amplitude. Finally, AP halfwidth (ms) was defined as the duration of the AP at half the voltage of the peak amplitude.

## Experimental Design and Statistical Analysis

### *Behavioral Studies*

The behavioral response in the Pavlovian conditioned approach (PavCA) procedure was scored using an index that integrates the number, latency, and probability of lever presses (sign-tracking conditioned response) and magazine entries (goal-tracking conditioned response) during CS presentations within a session (Meyer et al., 2012). In brief, we averaged the response bias (i.e., number of lever presses and

magazine entries for a session; [lever presses – magazine entries] / [lever presses + magazine entries]), latency score (i.e., average latency to perform a lever press or magazine entry during a session; [magazine entry latency – lever press latency]/10), and probability difference (i.e., proportion of lever presses or magazine entries; lever press probability – magazine entry probability). The index score ranges from +1.0 (absolute sign-tracking) to -1.0 (absolute goal-tracking), with 0 representing no bias. The average PavCA index scores of Sessions 5-6 were used to classify rats as STs (score ≥ 0.5), GTs (score ≤ -0.5), and IRs (-0.5 < score < 0.5). Out of a total of 31 rats, 10 were classified as STs, 7 were GTs, and 14 were IRs.

GraphPad Prism 8 (Dotmatics) was used for all the behavioral data statistical analysis. Number, latency, and probability for lever presses and for magazine entries, as well as PavCA index scores were analyzed using mixed-effects model via restricted maximum likelihood (REML). Fixed effects were set for phenotype (STs, GTs, IRs), session (1-6), and phenotype x session. Multiple comparisons were made using Sidak's post-hoc test. Significance level was set at $p < 0.05$. Full statistical report for all behavioral data analysis is found in **Table 3.2**.

### *Electrophysiology Studies*

A total of 128 cells from 31 rats were included in the analysis. The STs group had a total of 10 rats, from which 23 cells were recorded from in the core of 10 rats (1-2 slices/1-5 cells per rat) and 19 cells in the shell of 9 of the rats (1-2 slices/1-3 cells per rat). The GTs group had a total of 7 rats, from which 17 cells were recorded from in the core of 7 rats (1-2 slices/2-4 cells per rat) and 23 cells in the shell of 7 rats (1-2 slices/2-5 cells per rat). The IRs group had a total of 14 rats, from which 31 cells were recorded

from in the core of 14 rats (1-2 slices/1-5 cells per rat) and 15 cells in the shell of 10 of the rats (1 slice/1-3 cells per rat). A total of 8 cells from STs (Core: n = 4, Shell: n = 4) and 17 cells from IRs (Core: n = 13, Shell: n = 4) were excluded from the analyses of sag ratio and voltage/current relationship curves. For these cells the step protocol ranged from -200 pA to +500 pA as opposed to -500 pA to +500 pA. They were excluded to keep the hyperpolarized current injection analysis homogeneous. For a total of 3 cells in the core from STs, 1 cell from the core of GTs, and 4 cells from the core and 2 cells from the shell of IRs, the single action potential protocol was not run.

All offline analysis of electrophysiological recordings was performed using Clampfit 10.7 (Molecular Devices). Statistical analyses were made using GraphPad Prism 8 (Dotmatics) and SPSS Statistics (IBM) software. RMP, $C_m$, $R_i$, sag ratio, current to threshold, AP threshold, ΔRMP/AP threshold, AP amplitude, ΔRMP/AP amplitude, ΔAP threshold/AP amplitude, and AP halfwidth were analyzed for the core and for the shell separately using one-way ANOVA to test for significant group differences between STs, GTs, and IRs. Tukey's post-hoc test was used for multiple comparisons. Significance level was set at $p < 0.05$. Number of spikes, spike firing frequency, and voltage/current relationship curves (-500 to 0 pA and 0 to +100 pA) were analyzed using linear mixed-effects model via REML. Significance level set at $p < 0.05$. To obtain phenotype statistics within subregion, fixed effects were set for phenotype (STs, GTs, IRs), current injection (V/I: -500 pA to 0 pA, 0 pA to +100 pA; AP: +25 to +500 pA), and phenotype x current injection. Based on significance on Sidak's post hoc test for multiple comparisons, planned comparisons using mixed-effects model via REML were used to obtain specific statistical values (*F/P value*) for STs vs GTs, STs vs IRs, and

GTs vs IRs. Fixed effects were set for phenotype (STs, GTs, IRs), current injection (V/I: -500 pA to 0 pA, 0 pA to +100 pA; AP: +25 to +500 pA), and phenotype x current injection.

For subregional analysis, mixed-effects model via REML was used with fixed effects set for phenotype (STs, GTs, IRs), subregion (core, shell), current injection (V/I: -500 pA to 0 pA, 0 pA to +100 pA; AP: +25 to +500 pA), subregion x phenotype, phenotype x current injection, subregion x current injection, and phenotype x subregion x current injection. Multiple comparisons were made using Sidak's post-hoc test. Based on the phenotype x subregion statistical report, planned comparisons using mixed-effects model via REML, were done to obtain individual subregion statistics for STs (core vs shell), GTs (core vs shell), and IRs (core vs shell). Fixed effects to obtain subregion statistics within phenotypes were set for subregion (core, shell), current injection (V/I: -500 pA to 0 pA, 0 pA to +100 pA), and subregion x current injection. For subregional differences within phenotypes in number of spikes and firing frequency, statistical values (*F/P value*) for STs (core vs shell), GTs (core vs shell), and IRs (core vs shell), were obtained from the phenotype x subregion Sidak's post-hoc test. Full statistical reports for all electrophysiological data analysis are found in **Tables 3.1-3.2**.

## Results

### *Following a PavCA procedure, rats were classified as STs, GTs, or IRs based on their lever and magazine response bias*

To identify rats with ST, GT, and IR behavioral phenotypes in an outbred population, all rats underwent six days of PavCA training with a lever-cue (CS) paired with a response-independent delivery of a banana-flavored food pellet into a magazine

(US) **(Fig 3.2)**. Based on their PavCA index score on Sessions 5-6 (see ***Experimental Design and Statistical Analysis*** session for PavCA index score calculation), rats were classified as either STs (score ≥ 0.5; n = 10), GTs (score ≤ -0.5; n = 7), or IRs (-0.5 < score < 0.5; n = 14) **(Fig 3.2)**. As expected, STs exhibited the highest lever press number (**Fig 3.3A**: mixed-effects model: session x phenotype interaction, $p < 0.0001$), lowest latency (**Fig 3.3A**: mixed-effects model: session x phenotype interaction, $p < 0.0001$), and greatest probability (**Fig 3.3A**: mixed-effects model: session x phenotype interaction, $p < 0.0001$) compared to GTs and IRs. Compared to GTs, IRs also exhibited greater number, lower latency, and greater probability of lever presses during PavCA (**Fig 3.3A**: mixed-effects model: session x phenotype interaction, $p < 0.0001$). Conversely, compared to STs, GTs and IRs exhibited greater magazine entry number (**Fig 3.3B**: mixed-effects model: session x phenotype interaction, $p < 0.0001$), lower latency (**Fig 3.3B**: mixed-effects model: session x phenotype interaction, $p < 0.0001$), and greater probability (**Fig 3.3B**: mixed-effects model: session x phenotype interaction, $p < 0.0001$), but IRs and GTs did not differ from one another **(Fig 3.3B).** All STs, GTs, and IRs significantly differed from one another in their PavCA index score across the six training sessions (**Fig 3.2E**: mixed-effects model: session x phenotype interaction, $p < 0.0001$) indicating a difference in their behavior response bias toward either the lever or magazine and thereby suggesting different levels of incentive and predictive value attribution to the cue.

***Passive membrane properties of NAc MSNs in the core and shell subregions of STs, GTs, and IRs rats***

To characterize the intrinsic excitability properties of MSNs in the NAc core and shell of STs, GTs, and IRs, whole-cell patch clamp recordings were performed in rat brain slices following a 1-3 week resting period from the last PavCA training session **(Fig 3.1)**. This resting period was intended to provide enough time for training-induced neuronal changes to return to baseline so that our measurements would reflect innate differences between the three phenotypes in NAc intrinsic excitability. We found that MSNs in the NAc core of STs, GTs, and IRs had very similar passive membrane properties, as they did not differ in resting membrane potential or input resistance (**Fig 3.4B-C**: one-way ANOVA: $p > 0.05$). In the NAc shell, MSNs from STs exhibited a more hyperpolarized resting membrane potential than GTs (**Fig 3.4D**: one-way ANOVA: $p < 0.01$), but no significant differences were found compared to IRs. Input resistance in the NAc shell across all phenotypes was not significantly different (**Fig 3.4E**: one-way ANOVA: $p < 0.05$).

***NAc MSNs in the core and shell of STs exhibit less hyperpolarization than GTs and IRs in response to negative current inputs***

Next, we tested whether MSNs from STs, GTs, and IRs differ in their active intrinsic excitability properties in both the NAc core and shell. MSNs were subjected to a current injection step protocol ranging from -500 to +500 pA in 25-pA increments. We analyzed the voltage response of each neuron to the current injections from -500 to +100 pA to generate a voltage/current relationship curve. Interestingly, we found that in both the NAc core and shell, MSNs from STs exhibited less hyperpolarization than MSNs from GTs and IRs in response to negative current inputs. The same hyperpolarizing (-500 to 0 pA) current injection steps elicited a smaller change in

membrane potential in MSNs from STs causing a significant shift of the V/I curve in both the core (**Fig 3.5B**: mixed-effects model: main effects of phenotype, $p < 0.0001$) and shell (**Fig 3.5E**: mixed-effects model: main effects of phenotype, $p < 0.0001$). Although MSNs from STs exhibited a different V/I relationship in response to hyperpolarizing inputs, there were no significant differences between the three phenotypes in the voltage response to depolarizing (0 to 100 pA) current injection steps in the NAc core (**Fig 3.5B**: mixed-effects model: no effect, $p > 0.05$) or shell (**Fig 3.5E**: mixed-effects model: no effect, $p > 0.05$). We also wanted to test whether MSNs from STs, GTs, and IRs had any significant differences in their membrane potential sag response to a -500-pA current injection, a measure of the hyperpolarization-activated cation current (Ih) (Pape, 1996; Robinson and Siegelbaum, 2003). The sag ratio was obtained by dividing the peak voltage response to -500 pA over the steady-state response 200 ms from the onset of stimulation. In both the core **(Fig 3.5C)** and the shell **(Fig 3.5F)**, all phenotypes exhibited sag ratios that were not significantly different from each other (one-way ANOVA: $p > 0.05$).

Overall, we also found that for all STs, GTs, and IRs rats, NAc MSNs in the shell exhibited greater excitability than core MSNs since the same hyper- and de-polarizing current injection steps consistently induced a greater change in membrane potential in the shell (hyperpolarizing: mixed-effects model: main effect of subregion, $p < 0.0001$; depolarizing: mixed-effects model: main effect of subregion, $p < 0.0001$).

### *NAc MSNs in the core and shell of STs, GTs, and IRs exhibit distinct firing properties*

To further characterize the intrinsic excitability of MSNs from the core and shell of STs, GTs, and IRs, we examined the firing properties in response to current injection steps from +25 to +500 pA in 25-pA increments. In the NAc core, we found that MSNs from GTs exhibited the greatest number of spikes (**Fig 3.6B**: mixed-effects model: main effect of phenotype, $p < 0.0001$) and firing frequency (**Fig 3.6C**: mixed-effects model: main effect of phenotype, $p < 0.0001$) compared to both IRs and STs, while STs exhibited the lowest number of spikes and firing frequency in response to current injection steps of the same magnitude. This suggests that overall, in the NAc core, STs have the lowest intrinsic membrane excitability followed by IRs, then GTs with the highest.

Interestingly, in the NAc shell we found that firing properties did not differ between STs and GTs. However, compared to both phenotypes, MSNs from IRs exhibited significantly greater number of spikes (**Fig 3.6E**: mixed-effects model: no effect, $p < 0.0001$) and firing frequency (**Fig 3.6F**: mixed-effects model: no effect, $p < 0.0001$), suggesting that in the NAc shell, IRs appear to have the highest intrinsic membrane excitability.

Similar to the subregional differences between core and shell in the V/I relationship curve, we also found subregional differences in firing properties. Interestingly, these differences were present in STs and IRs, but not in GTs. For STs and IRs, MSNs in the shell exhibited significantly greater number of spikes and firing frequency than core MSNs, whereas for GTs, there were no significant differences between the two regions (mixed-effects model: phenotype x subregion interaction, $p < 0.0001$).

Lastly, we examined whether specific properties of the action potentials (AP) of MSNs in the core and shell were different between STs, GTs, and IRs. We delivered 5-ms current injections in 25-pA increments until a single AP was elicited. Upon analysis, we found that the action potential properties in both subregions did not differ between STs and GTs (data not shown in figure; see **Table 3.1** for full list of AP properties and **Table 3.2** for statistical report). In summary, we found no differences in the current necessary to elicit a single AP, AP halfwidth, AP threshold from zero and resting potential, and AP peak amplitude from zero, resting potential, and threshold. However, we did find some subtle differences between STs and IRs. In the core, STs had a significantly longer AP halfwidth than IRs (one-way ANOVA: $p < 0.05$) suggesting slower repolarization. In the shell, IRs had a more depolarized AP threshold value, and consequently a smaller AP peak amplitude measured from threshold (one-way ANOVA: $p < 0.05$).

**Discussion**

This is the first study to demonstrate that MSNs in the NAc of STs, GTs, and IRs exhibit distinct intrinsic membrane properties. Furthermore, these differences vary across the core and shell subregions. Most prominently, we found that STs had the lowest intrinsic excitability in the NAc core, while GTs exhibited the highest. Although STs and GTs exhibited no differences in firing properties in the NAc shell, IRs had greater intrinsic excitability than the ST and GT phenotypes. The NAc core, and particularly dopamine within the core, seems to preferentially encode the motivational value of conditioned cues while the shell has more influence over unconditioned responses (Meredith et al., 2008; Saunders et al., 2018). Therefore, it is not necessarily

surprising that differences between STs and GTs in intrinsic excitability seem to be more pronounced in the core than in the shell.

These findings suggest that the previously reported differences between STs, GTs, and IRs in NAc core and shell activity during Pavlovian learning might stem in part from the intrinsic excitability state of their MSNs. It has been previously observed that STs exhibit an increase in cue-evoked activity in both the NAc core and shell (Flagel et al., 2011a), which is accompanied by a reduction in reward-evoked activity over the course of PavCA training (Gillis and Morrison, 2019). Although this pattern of activity has been commonly interpreted as a prediction error signal, it is largely absent in GTs. Such a result is surprising because GTs are clearly learning a predictive relationship between the cue and reward. This has led to the hypothesis that the shift from reward-evoked to cue-evoked neuronal activity in the NAc may primarily reflect the attribution of incentive properties to a reward-paired cue as opposed to predictive properties. Here, we found that GTs exhibited the highest intrinsic membrane excitability in the NAc core compared to both STs and IRs. This raises the possibility that a higher neuronal excitability state in GTs may make it more difficult for their incentive salience-related NAc core activity to shift away from the reward and toward the cue. Thus, some of the differences in reward learning processes between GTs and STs might be traced to subregional differences in the intrinsic neurophysiological properties of their NAc core neurons.

Decreased intrinsic excitability of MSNs has been extensively described as a feature of cocaine exposure and both short- and long-term cocaine withdrawal (for review see Wolf 2010). For example, lower intrinsic membrane excitability of MSNs has

been directly linked to an increase in cocaine sensitization and self-administration (Dong et al., 2006; Mu et al., 2010). Compared to GTs, STs exhibit greater addictive-like behaviors, including increased psychomotor sensitization to cocaine (Flagel et al., 2008), higher preference for cocaine over food (Tunstall and Kearns, 2015), and increased cue-induced reinstatement of cocaine and nicotine (Saunders and Robinson, 2011; Versaggi et al., 2016). Therefore, it is possible that reduced intrinsic excitability of MSNs may be a key feature of STs that predisposes them to develop more pathological responses to drugs of abuse.

Physiologically, it has been postulated that the decrease in MSN membrane excitability following cocaine exposure and withdrawal may be due to a decrease in voltage-dependent $Na^+$ (Zhang et al., 1998) and $Ca^{2+}$ (Zhang et al., 2002) currents, as well as an increase in the activity of various $K^+$ channels (Hu et al., 2004). One class is thought to be the SK-type $Ca^{2+}$-activated $K^+$ channels, since the SK channel-selective antagonist apamin has been found to partially prevent cocaine from reducing MSN excitability (Ishikawa et al., 2009). Interestingly, neurochemicals like inositol and corticosterone – which are thought to be differentially expressed between STs and GTs (Flagel et al., 2009; Fitzpatrick et al., 2016) – can affect SK channel activity, leading to an increase in $K^+$ currents and decreased neuronal output (Yamada et al., 2004; Kye et al., 2007; Clements et al., 2013). Therefore, further studies could explore whether the decreased intrinsic excitability we observed in STs even in the absence of drug exposure might be linked to differential activity and expression of $K^+$ channels such as the SK-type class.

It is important to note that most of the mentioned studies reporting a reduction in MSN excitability have been in the NAc shell. Although STs and GTs only exhibited differences in firing properties in the core, MSNs in the shell of STs also exhibited a significantly more hyperpolarized resting membrane potential, suggesting that they might also exist at a lower baseline state and further contribute to this phenotype. In addition, relative to IRs, both STs and GTs exhibit reduced excitability in the NAc shell. Not many studies investigating behavioral and neurobiological drug- and non-drug related effects on STs and GTs have included IRs in their analysis, which makes it hard to predict how this may relate to the behavioral responses associated with this phenotype. It is known that appetitive Pavlovian conditioning can increase the intrinsic excitability of specific neuronal ensembles of MSNs in the NAc shell (Ziminski et al., 2017). It is possible that an overall greater intrinsic excitability in the NAc shell of IRs may facilitate the attribution of both predictive and incentive properties to cues, giving them more flexibility in their conditioned responses. However, many more studies need to be performed to characterize IRs at this level.

It is widely known that dopaminergic transmission onto the NAc can have a significant impact on the intrinsic excitability of MSNs in the NAc (O'Donnell and Grace, 1996; Nicola et al., 2000; Surmeier et al., 2007; Planert et al., 2013). During Pavlovian learning, STs and GTs exhibit differences in mesolimbic dopamine (DA) release. Specifically, the patterns of DA release seem to mimic cue- and reward-evoked activity in the NAc (Flagel et al., 2011b). Moreover, DA agonists and antagonists seem to differentially affect STs and GTs (Saunders and Robinson, 2012; Chow et al., 2016), suggesting that there might be pre-existing differences in the dopaminergic system.

Indeed, some studies have reported differences in the DA system of STs and GTs that may differentially modulate the way MSNs respond to DA, and therefore affect their intrinsic membrane excitability properties (Flagel et al., 2007; Singer et al., 2016). For example, compared to GTs, STs have greater levels of dopamine transporter (DAT) in the NAc core (Singer et al., 2016). As a consequence, STs seem to clear DA from the synapse at a faster rate than GTs independent of baseline differences in DA release (Singer et al., 2016). This fast re-uptake of DA is thought to be important for more time-locked responses of MSNs to phasic DA release during cue presentations and may help potentiate the value of incentive stimuli and attribution of incentive salience (Wieland et al., 2015; Singer et al., 2016). Interestingly, it has been demonstrated that activation of $D_1$-like receptors in MSNs can cause an increase in MSN depolarization by inhibiting Kir-channel $K^+$ currents (Podda et al., 2010) and by enhancing L-type $Ca^{2+}$ currents (Hernández-López et al., 1997). Therefore, if GTs have greater tonic levels of DA at the synapse it may allow for DA to activate these receptors at a greater degree and increase the membrane excitability in comparison to STs. Both reduced intrinsic excitability in STs and a more fine-tuned response to DA release may selectively enhance the response of MSNs to only the most salient stimuli and thereby promote the attribution of incentive salience to specific stimuli. In addition, several studies have demonstrated that this $D_1$-mediated increase in intrinsic excitability seems to occur mainly when MSNs are at an up-state (near threshold potentials), which may explain why MSNs from GTs are observed to be more excitable in depolarized but not hyperpolarized states.

We also found that subregional differences between the excitability of core versus shell MSNs were stronger for STs and IRs than they were for GTs. Specifically, MSNs in the shell of STs and IRs had greater number and frequency of action potentials than the core, whereas GTs exhibited no significant subregional difference. It is interesting that IRs share this feature with STs. In this case, this shared characteristic may suggest that a subregional difference might be important for sign-tracking responses. Future studies are needed to test whether experimental manipulation of subregional differences between core and shell excitability can affect individual differences in the attribution of incentive salience.

The overwhelming evidence suggests that neuronal activity in the NAc is particularly important for individual differences in the attribution of incentive salience. It is very likely that the distinct patterns of activity during PavCA, are the collective result of differences in inputs to the NAc modulated by both internal and external stimuli in STs and GTs. However, our results suggest that these characteristic patterns of activity can be directly influenced by differences in the intrinsic neuronal properties of MSNs in the NAc of STs and GTs. This in turn may help understand how inputs to the NAc may exert different synaptic influence because of baseline differences in its excitability state. We intend for these studies to aid in our understanding on the neurobiology of individual differences in incentive salience attribution and endophenotypes associated with addiction vulnerability.

## References


Bassareo V, De Luca MA, Di Chiara G (2002) Differential expression of motivational stimulus properties by dopamine in nucleus accumbens shell versus core and prefrontal cortex. J Neurosci Off J Soc Neurosci 22:4709–4719.

Berridge KC, Robinson TE, Aldridge JW (2009) Dissecting components of reward: 'liking', 'wanting', and learning. Curr Opin Pharmacol 9:65–73.

Britt JP, Benaliouad F, McDevitt RA, Stuber GD, Wise RA, Bonci A (2012) Synaptic and behavioral profile of multiple glutamatergic inputs to the nucleus accumbens. Neuron 76:790–803.

Chow JJ, Nickell JR, Darna M, Beckmann JS (2016) Toward isolating the role of dopamine in the acquisition of incentive salience attribution. Neuropharmacology 109:320–331.

Clements MA, Swapna I, Morikawa H (2013) Inositol 1,4,5-triphosphate drives glutamatergic and cholinergic inhibition selectively in spiny projection neurons in the striatum. J Neurosci Off J Soc Neurosci 33:2697–2708.

Day JJ, Carelli RM (2007) The nucleus accumbens and Pavlovian reward learning. Neurosci Rev J Bringing Neurobiol Neurol Psychiatry 13:148–159.

Dong Y, Green T, Saal D, Marie H, Neve R, Nestler EJ, Malenka RC (2006) CREB modulates excitability of nucleus accumbens neurons. Nat Neurosci 9:475–477.

Dorris DM, Cao J, Willett JA, Hauser CA, Meitzen J (2015) Intrinsic excitability varies by sex in prepubertal striatal medium spiny neurons. J Neurophysiol 113:720–729.

Fitzpatrick CJ, Perrine SA, Ghoddoussi F, Galloway MP, Morrow JD (2016) Sign-trackers have elevated myo-inositol in the nucleus accumbens and ventral hippocampus following Pavlovian conditioned approach. J Neurochem 136:1196–1203.

Flagel SB, Akil H, Robinson TE (2009) Individual differences in the attribution of incentive salience to reward-related cues: Implications for addiction. Neuropharmacology 56 Suppl 1:139–148.

Flagel SB, Cameron CM, Pickup KN, Watson SJ, Akil H, Robinson TE (2011a) A food predictive cue must be attributed with incentive salience for it to induce c-fos mRNA expression in cortico-striatal-thalamic brain regions. Neuroscience 196:80–96.

Flagel SB, Clark JJ, Robinson TE, Mayo L, Czuj A, Willuhn I, Akers CA, Clinton SM, Phillips PEM, Akil H (2011b) A selective role for dopamine in stimulus-reward learning. Nature 469:53–57.

Flagel SB, Robinson TE (2017) Neurobiological Basis of Individual Variation in Stimulus-Reward Learning. Curr Opin Behav Sci 13:178–185.

Flagel SB, Watson SJ, Akil H, Robinson TE (2008) Individual differences in the attribution of incentive salience to a reward-related cue: influence on cocaine sensitization. Behav Brain Res 186:48–56.

Flagel SB, Watson SJ, Robinson TE, Akil H (2007) Individual differences in the propensity to approach signals vs goals promote different adaptations in the dopamine system of rats. Psychopharmacology (Berl) 191:599–607.

Gillis ZS, Morrison SE (2019) Sign tracking and goal tracking are characterized by distinct patterns of nucleus accumbens activity. eNeuro 6.

Heimer L, Zahm DS, Churchill L, Kalivas PW, Wohltmann C (1991) Specificity in the projection patterns of accumbal core and shell in the rat. Neuroscience 41:89–125.

Hernández-López S, Bargas J, Surmeier DJ, Reyes A, Galarraga E (1997) $D_1$ receptor activation enhances evoked discharge in neostriatal medium spiny neurons by modulating an L-type $Ca^{2+}$ conductance. J Neurosci 17:3334–3342.

Hu X-T, Basu S, White FJ (2004) Repeated cocaine administration suppresses HVA-Ca2+ potentials and enhances activity of K+ channels in rat nucleus accumbens neurons. J Neurophysiol 92:1597–1607.

Ishikawa M, Mu P, Moyer JT, Wolf JA, Quock RM, Davies NM, Hu X, Schlüter OM, Dong Y (2009) Homeostatic synapse-driven membrane plasticity in nucleus accumbens neurons. J Neurosci 29:5820–5831.

Kye M-J, Spiess J, Blank T (2007) Transcriptional regulation of intronic calcium-activated potassium channel SK2 promoters by nuclear factor-kappa B and glucocorticoids. Mol Cell Biochem 300:9–17.

Lovic V, Saunders BT, Yager LM, Robinson TE (2011) Rats prone to attribute incentive salience to reward cues are also prone to impulsive action. Behav Brain Res 223:255–261.

Matamales M, Bertran-Gonzalez J, Salomon L, Degos B, Deniau J-M, Valjent E, Hervé D, Girault J-A (2009) Striatal medium-sized spiny neurons: identification by nuclear staining and study of neuronal subpopulations in BAC transgenic mice. PloS One 4:e4770.

Meredith GE, Agolia R, Arts MP, Groenewegen HJ, Zahm DS (1992) Morphological differences between projection neurons of the core and shell in the nucleus accumbens of the rat. Neuroscience 50:149–162.

Meredith GE, Baldo BA, Andrezjewski ME, Kelley AE (2008) The structural basis for mapping behavior onto the ventral striatum and its subdivisions. Brain Struct Funct 213:17–27.

Meyer PJ, Lovic V, Saunders BT, Yager LM, Flagel SB, Morrow JD, Robinson TE (2012) Quantifying individual variation in the propensity to attribute incentive salience to reward cues. PLOS ONE 7:e38987.

Mu P, Moyer JT, Ishikawa M, Zhang Y, Panksepp J, Sorg BA, Schlüter OM, Dong Y (2010) Exposure to cocaine dynamically regulates the intrinsic membrane excitability of nucleus accumbens neurons. J Neurosci 30:3689–3699.

Nicola SM, Surmeier DJ, Malenka RC (2000) Dopaminergic modulation of neuronal excitability in the striatum and nucleus accumbens. Annu Rev Neurosci 23:185–215.

O'Donnell P, Grace AA (1996) Dopaminergic reduction of excitability in nucleus accumbens neurons recorded in vitro. Neuropsychopharmacology 15:87–97.

Paolone G, Angelakos CC, Meyer PJ, Robinson TE, Sarter M (2013) Cholinergic control over attention in rats prone to attribute incentive salience to reward cues. J Neurosci Off J Soc Neurosci 33:8321–8335.

Pape HC (1996) Queer current and pacemaker: the hyperpolarization-activated cation current in neurons. Annu Rev Physiol 58:299–327.

Paxinos G, Franklin KBJ (2019) Paxinos and Franklin's the Mouse Brain in Stereotaxic Coordinates. Academic Press.

Pennartz CM, Groenewegen HJ, Lopes da Silva FH (1994) The nucleus accumbens as a complex of functionally distinct neuronal ensembles: an integration of behavioural, electrophysiological and anatomical data. Prog Neurobiol 42:719–761.

Planert H, Berger TK, Silberberg G (2013) Membrane properties of striatal direct and indirect pathway neurons in mouse and rat slices and their modulation by dopamine. PLOS ONE 8:e57054.

Podda MV, Riccardi E, D'Ascenzo M, Azzena GB, Grassi C (2010) Dopamine D1-like receptor activation depolarizes medium spiny neurons of the mouse nucleus accumbens by inhibiting inwardly rectifying K+ currents through a cAMP-dependent protein kinase A-independent mechanism. Neuroscience 167:678–690.

Robinson RB, Siegelbaum SA (2003) Hyperpolarization-activated cation currents: From molecules to physiological function. Annu Rev Physiol 65:453–480.

Robinson TE, Berridge KC (1993) The neural basis of drug craving: an incentive-sensitization theory of addiction. Brain Res Brain Res Rev 18:247–291.

Saunders BT, Richard JM, Margolis EB, Janak PH (2018) Dopamine neurons create Pavlovian conditioned stimuli with circuit-defined motivational properties. Nat Neurosci 21:1072–1083.

Saunders BT, Robinson TE (2011) Individual Variation in the Motivational Properties of Cocaine. Neuropsychopharmacology 36:1668–1676.

Saunders BT, Robinson TE (2012) The role of dopamine in the accumbens core in the expression of Pavlovian-conditioned responses. Eur J Neurosci 36:2521–2532.

Singer BF, Guptaroy B, Austin CJ, Wohl I, Lovic V, Seiler JL, Vaughan RA, Gnegy ME, Robinson TE, Aragona BJ (2016) Individual variation in incentive salience attribution and accumbens dopamine transporter expression and function. Eur J Neurosci 43:662–670.

Surmeier DJ, Ding J, Day M, Wang Z, Shen W (2007) D1 and D2 dopamine-receptor modulation of striatal glutamatergic signaling in striatal medium spiny neurons. Trends Neurosci 30:228–235.

Tunstall BJ, Kearns DN (2015) Sign-tracking predicts increased choice of cocaine over food in rats. Behav Brain Res 281:222–228.

Versaggi CL, King CP, Meyer PJ (2016) The tendency to sign-track predicts cue-induced reinstatement during nicotine self-administration, and is enhanced by nicotine but not ethanol. Psychopharmacology (Berl) 233:2985–2997.

West EA, Carelli RM (2016) Nucleus accumbens core and shell differentially encode reward-associated cues after reinforcer devaluation. J Neurosci 36:1128–1139.

Wieland S, Schindler S, Huber C, Köhr G, Oswald MJ, Kelsch W (2015) Phasic dopamine modifies sensory-driven output of striatal neurons through synaptic plasticity. J Neurosci 35:9946–9956.

Wolf ME (2010) The Bermuda triangle of cocaine-induced neuroadaptations. Trends Neurosci 33:391–398.

Yamada S-I, Takechi H, Kanchiku I, Kita T, Kato N (2004) Small-conductance Ca2+-dependent K+ channels are the target of spike-induced Ca2+ release in a feedback regulation of pyramidal cell excitability. J Neurophysiol 91:2322–2329.

Záborszky L, Alheid GF, Beinfeld MC, Eiden LE, Heimer L, Palkovits M (1985) Cholecystokinin innervation of the ventral striatum: a morphological and radioimmunological study. Neuroscience 14:427–453.

Zahm DS (1999) Functional-anatomical implications of the nucleus accumbens core and shell subterritories. Ann N Y Acad Sci 877:113–128.

Zahm DS, Heimer L (1990) Two transpallidal pathways originating in the rat nucleus accumbens. J Comp Neurol 302:437–446.

Zhang X-F, Cooper DC, White FJ (2002) Repeated cocaine treatment decreases whole-cell calcium current in rat nucleus accumbens neurons. J Pharmacol Exp Ther 301:1119–1125.

Zhang XF, Hu XT, White FJ (1998) Whole-cell plasticity in cocaine withdrawal: reduced sodium currents in nucleus accumbens neurons. J Neurosci Off J Soc Neurosci 18:488–498.

Ziminski JJ, Hessler S, Margetts-Smith G, Sieburg MC, Crombag HS, Koya E (2017) Changes in appetitive associative strength modulates nucleus accumbens, but not orbitofrontal cortex neuronal ensemble excitability. J Neurosci 37:3160–3170.

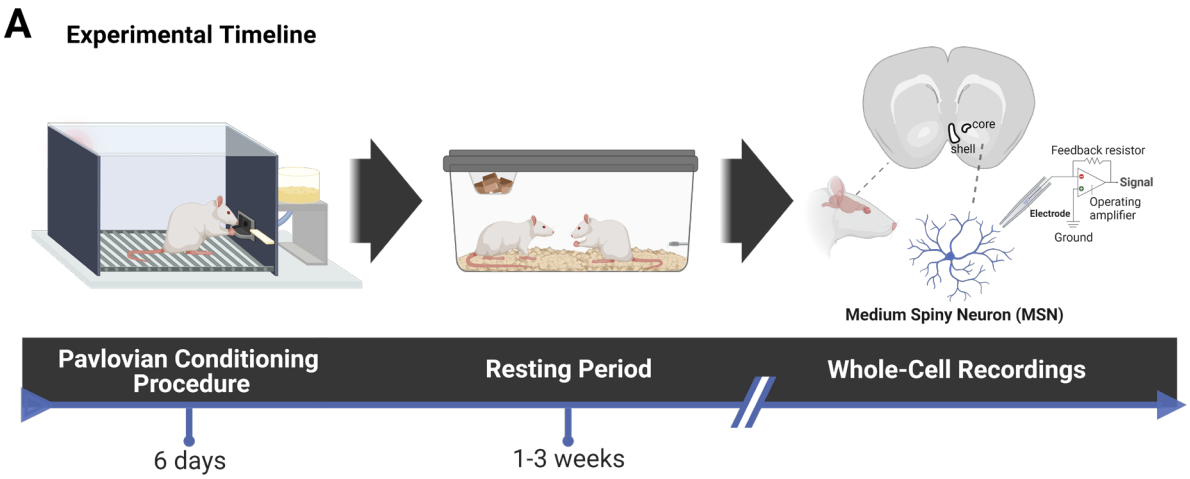


**Figure 3.1.** Experimental timeline. For six days, all rats underwent a daily Pavlovian conditioned approach (PavCA) procedure in which a neutral lever-cue (CS) was presented and following its retraction, a banana-flavored food pellet reward (US) was immediately delivered into the magazine. Each session consisted of 25 trials of CS-US pairings (ITI: 30-60 s). After the last PavCA session, the rats remained in their home cages for a period of 1-3 weeks before slice preparation for whole-cell recordings of medium spiny neurons in the nucleus accumbens core and shell subregions. Created with BioRender.com.

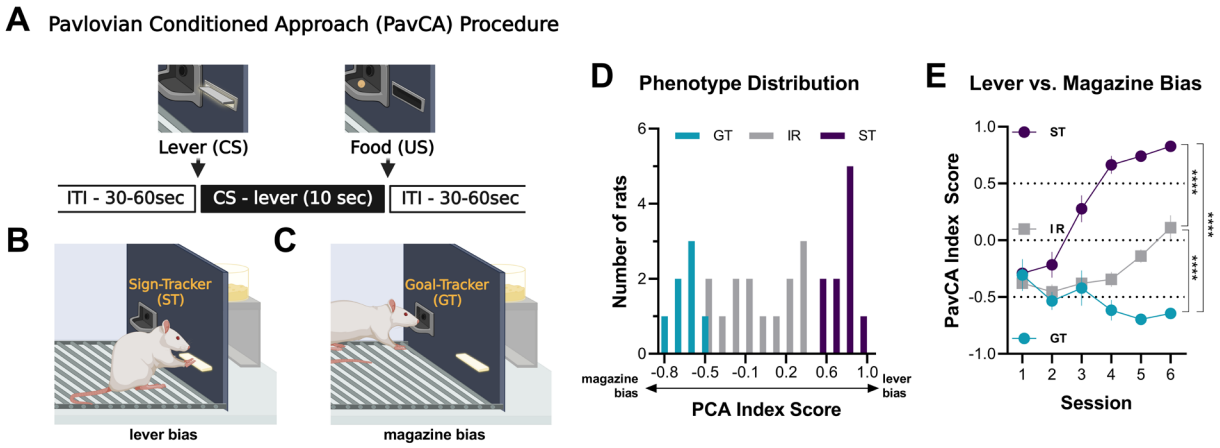


**Figure 3.2**. *Rats were classified as sign-trackers (STs), goal-trackers (GTs), or intermediate responders (IRs) based on their lever and magazine bias during the Pavlovian conditioned approach (*PavCA*) procedure*. **A)** Each trial in the PavCA procedure consisted of the extension of an illuminated lever-cue (CS) into the chamber for 10 seconds immediately followed by the delivery of a banana-flavored food pellet (US) into the magazine (inter-trial interval: 30-60 sec). **B)** Cartoon representation of sign-tracking (lever bias): In response to the CS, STs approach and interact with the lever although no response is necessary for reward delivery. **C)** Cartoon representation of goal-tracking (magazine bias): In response to the CS, GTs approach the magazine which is the site of impending food delivery. IRs typically engage equally with both the lever and the magazine, exhibiting relatively low bias. **D)** Distribution of STs (score ≥ 0.5; n = 10), GTs (score ≤ -0.5; n = 7), and IRs (-0.5 < score < 0.5; n = 14) phenotypes: A score of +1.0 is absolute sign-tracking, while -1.0 is absolute goal-tracking (0 represents no bias). **E)** Lever vs. magazine bias for all three phenotypes over the course of training: STs, GTs, and IRs significantly differed between one another in their PavCA index score across the six training sessions (mixed-effects model: session x phenotype interaction, $p < 0.0001$). Significance for Sidak's post-hoc test is shown as **** - $p < 0.0001$. Data are presented as mean ± S.E.M. Created with BioRender.com (A-C).

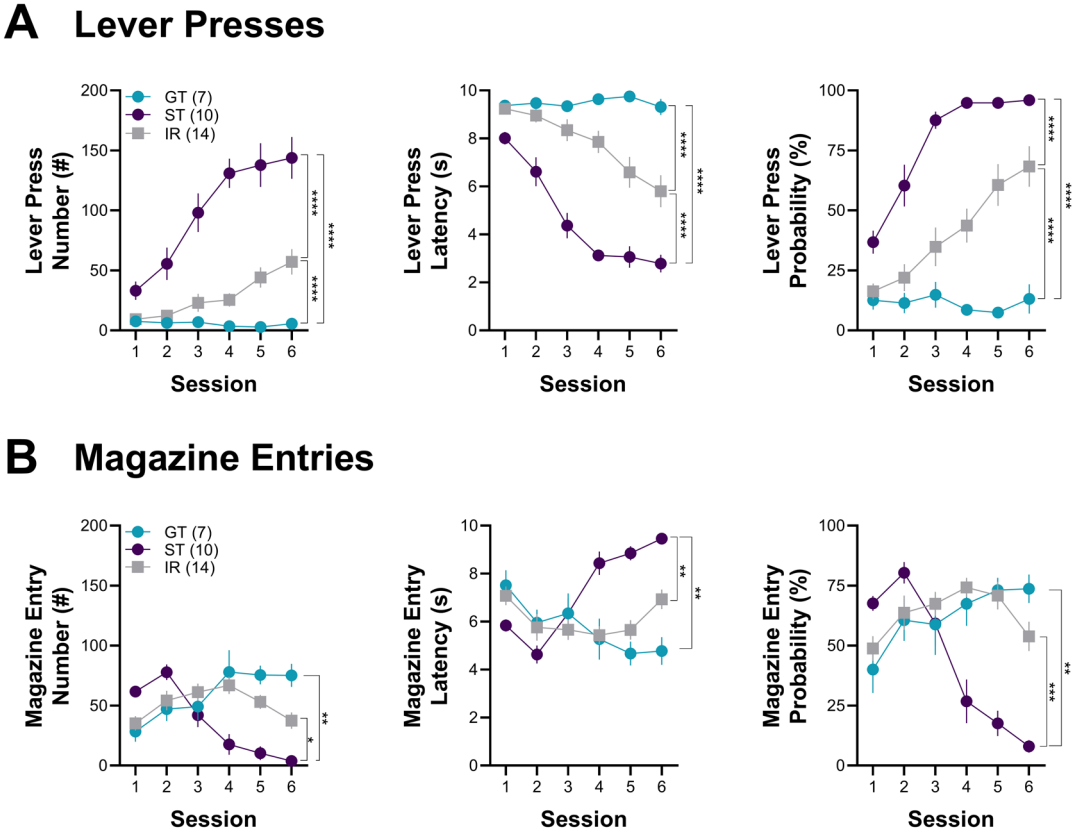


**Figure 3.3.** *In a Pavlovian conditioned approach (*PavCA*) procedure, sign-trackers (STs) and goal-trackers (GTs) differ in the number, latency, and probability of lever presses and magazine entries.* All rats underwent six sessions of PavCA and were classified as STs, GTs, or IRs based on their lever press and magazine entry number (left), latency (center), and probability (right) during Sessions 5-6. **A)** Across all six sessions STs exhibited greater lever press number (mixed-effects model: session x phenotype interaction, $p < 0.0001$), lower latency (mixed-effects model: session x phenotype interaction, $p < 0.0001$), and greater probability (mixed-effects model: session x phenotype interaction, $p < 0.0001$) compared to both GTs and IRs. IRs also exhibited greater lever press number, lower latency, and greater probability than GTs (mixed-effects model: session x phenotype interaction, $p < 0.0001$). **B)** Across all six sessions GTs and IRs exhibited greater magazine entry number (mixed-effects model: session x phenotype interaction, $p < 0.0001$), lower latency (mixed-effects model: session x phenotype interaction, $p < 0.0001$), and greater probability (mixed-effects model: session x phenotype interaction, $p < 0.0001$) compared to STs, but IRs and GTs did not differ from one another. Significance for Sidak's post-hoc test is shown as * - $p < 0.05$, ** - $p < 0.01$, *** - $p < 0.001$, **** - $p < 0.0001$. Data are presented as mean ± S.E.M.

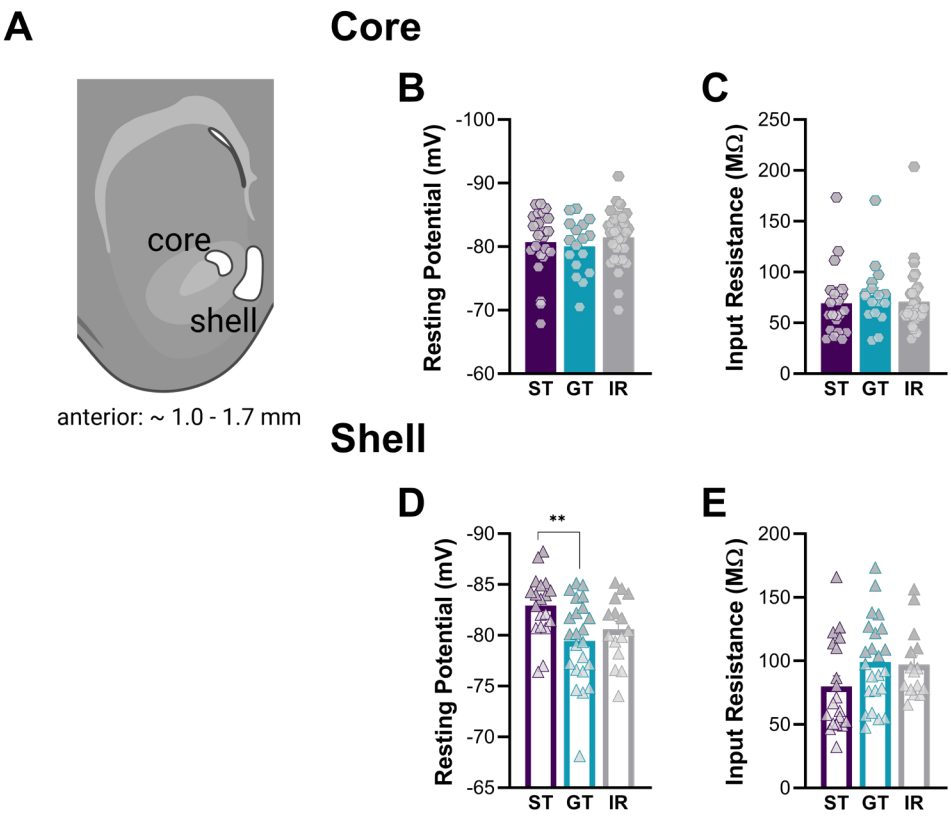


**Figure 3.4.** *Passive membrane properties of nucleus accumbens (NAc) medium spiny neurons (MSNs) in the core and shell subregions of sign-tracker (STs), goal-tracker (GTs), and intermediate responder (IRs) rats.* **A)** Representative diagram of coronal brain section containing the NAc core and medial shell subregions. Whole-cell electrophysiological recordings from MSNs were obtained from the areas highlighted in white. In the NAc core, no significant differences were found between STs, GTs, and IRs in MSNs **B)** resting membrane potential or **C)** input resistance (one-way ANOVA: $p > 0.05$). In the NAc shell, **D)** the resting membrane potential of MSNs was significantly more hyperpolarized in STs compared to GTs (one-way ANOVA: $p < 0.05$). **E)** Input resistance was not significantly different between STs, GTs, and IRs (one-way ANOVA: $p > 0.05$). Significance for Tukey's post hoc test is shown as ** - $p < 0.01$. Each data point represents a single cell. Data are presented as mean ± S.E.M. Created with BioRender.com (A).

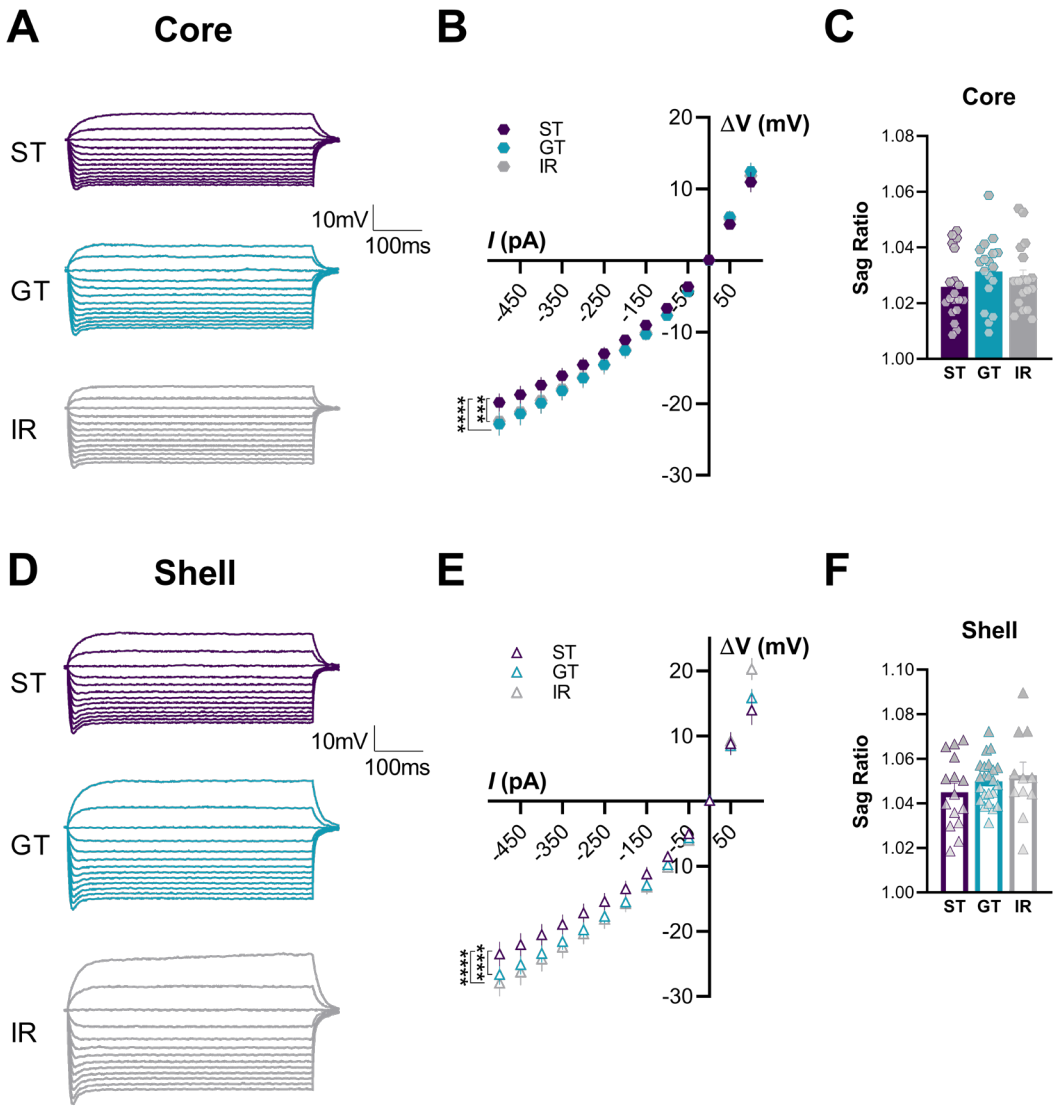


**Figure 3.5.** *In response to negative current injections medium spiny neurons (MSNs) in the core and shell of sign-trackers (STs) exhibit less hyperpolarization than goal-trackers (GTs) and intermediate responders (IRs).* Representative voltage response traces from current-clamp recordings of MSNs in NAc core **(A)** and shell **(D)** slices from STs (purple), GTs (blue), and IRs (gray). **B, E)** Voltage/current (V/I) relationship curve: The same hyperpolarizing (-500 to 0 pA) current injection steps elicited a significantly lower change in voltage in MSNs from STs compared to both GTs and IRs in the NAc core (mixed-effects model: main effect of phenotype, $p < 0.0001$) and shell (mixed-effects model: main effect of phenotype, $p < 0.0001$). No significant differences were found between STs, GTs, and IRs in response to depolarizing (0 to 100 pA) current injection steps in the NAc core (mixed-effects model: no effect, $p > 0.05$) or shell (mixed-effects model: no effect, $p > 0.05$). **C, F)** Sag ratio: Sag ratio was obtained by dividing the peak voltage response to a -500pA current injection over the steady-state response 200ms from the onset of stimulation. There were no significant differences between STs, GTs, and IRs in sag ratio in the NAc core (one-way ANOVA: $p > 0.05$) or shell (one-way ANOVA: $p > 0.05$). Significance for mixed-effect model planned comparisons is shown as *** - $p < 0.001$, **** - $p < 0.0001$. Each data point in bar graphs represents a single cell. Data are presented as mean ± S.E.M.

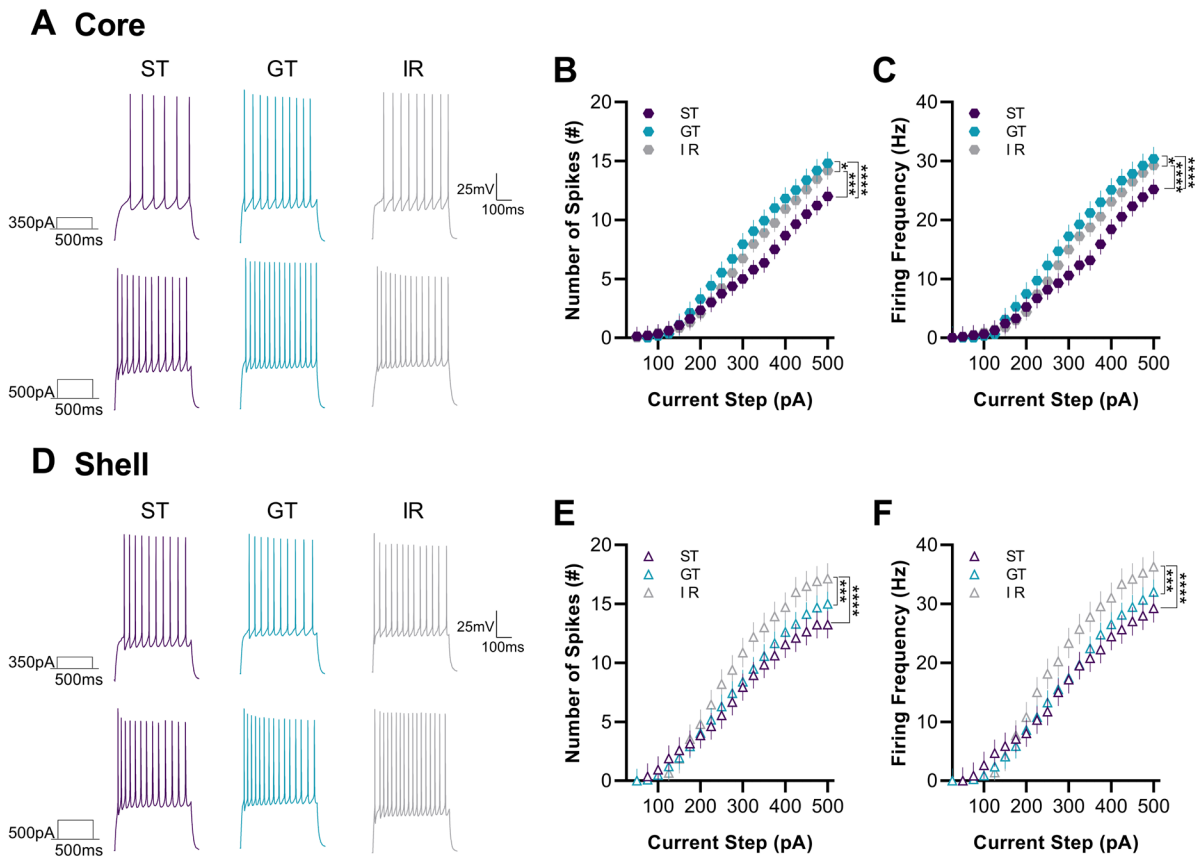


**Figure 3.6.** *Nucleus accumbens (NAc) medium spiny neurons (MSNs) in the core and shell of sign-trackers (STs), goal-trackers (GTs), and intermediate responders (IRs) exhibit distinctive firing properties.* Representative traces of current-clamp recordings from MSNs in NAc core **(A)** and shell **(D)** slices from STs (purple), GTs (blue), and IRs (gray) in response to 350-pA (top) and 500-pA (bottom) current injections. **B)** Number of spikes and **C)** firing frequency in NAc core: in response to current injection steps of the same magnitude, MSNs from GTs exhibited the greatest number of spikes (mixed-effects model: main effect of phenotype, $p < 0.0001$) and firing frequency (mixed-effects model: main effect of phenotype, $p < 0.0001$) compared to IRs and STs, while STs had the lowest number of spikes and firing frequency compared to IRs and GTs. **E)** Number of spikes and **F)** firing frequency in NAc shell: While there were no significant differences between STs and GTs in the number of spikes or firing frequency, MSNs from IRs had significantly greater number of spikes (mixed-effects model: no effect, $p < 0.0001$) and firing frequency (mixed-effects model: no effect, $p < 0.0001$) compared to both STs and GTs in the NAc shell. Significance for mixed-effect model planned comparisons is shown as * - $p < 0.05$, *** - $p < 0.001$, **** - $p < 0.0001$. Data are presented as mean ± S.E.M.

**Table 3.1.** *Electrophysiological passive and active properties of medium spiny neurons (MSNs) in the core and shell of nucleus accumbens of sign-tracker (STs), goal-tracker (GTs), and intermediate responder (IRs) rats.* Table lists mean ± S.E.M. (sample size) for passive and active properties of core and shell MSNs for STs, GTs, and IRs. Main effects statistics for STs vs GTs vs IRs comparisons were obtained using one-way ANOVA and linear mixed-effects models via REML (F value, P value). Significance for group comparisons were obtained from Tukey's post-hoc test for one-way ANOVA analysis and from Sidak's post-hoc test for mixed-effects model analysis. Main effects, interactions, multiple comparisons, and planned comparisons are detailed in Table 3.2.

| | Core | | | Statistics | Shell | | | Statistics |
|---|---|---|---|---|---|---|---|---|
| | **Sign-trackers** | **Goal-trackers** | **Intermediates** | ***F, P*** | **Sign-trackers** | **Goal-trackers** | **Intermediates** | ***F, P*** |
| ***Passive membrane properties*** | | | | | | | | |
| **Resting membrane potential, mV** | -81 ± 1 (23) | -80 ± 1 (17) | -81.5 ± 0.8 (31) | 0.55, 0.58 | -82.9 ± 0.7 (19) ** | -79.4 ± 0.9 (23) ** | -80.6 ± 0.8 (15) | 4.98, 0.010 |
| **Cell capacitance, pF** | 150 ± 8 (23) †† | 130 ± 7 (17) | 122 ± 5 (31) †† | 5.47, 0.0063 | 105 ± 6 (19) * † | 88 ± 4 (23) * | 86 ± 6 (15) † | 4.12, 0.022 |
| **Input resistance, MΩ** | 69 ± 7 (23) | 77 ± 7 (17) | 71 ± 6 (31) | 0.33, 0.72 | 80 ± 8 (19) | 99 ± 7 (23) | 97 ± 7 (15) | 1.96, 0.15 |
| ***Active membrane properties*** | | | | | | | | |
| **V/I curve (-500pA to 0pA)** | -11.9 ± 0.2 (19) **** ††† | -13.6 ± 0.2 (18) **** | -13.3 ± 0.2 (18) ††† | 13.4, 0.000002 | -14.3 ± 0.3 (15) **** †††† | -16.4 ± 0.2 (23) **** | -16.9 ± 0.3 (11) †††† | 20.9, $1.30x10^{-9}$ |
| **V/I curve (0pA to +100pA)** | 5.3 ± 0.4 (19) | 6.2 ± 0.4 (18) | 5.6 ± 0.4 (18) | 1.60, 0.20 | 7.7 ± 0.6 (15) | 8.4 ± 0.5 (23) | 9.8 ± 0.6 (11) | 2.81, 0.063 |
| **Sag ratio at -500pA, mV** | 1.026 ± 0.003 (19) | 1.031 ± 0.003 (18) | 1.029 ± 0.003 (18) | 1.01, 0.37 | 1.045 ± 0.004 (15) | 1.050 ± 0.002 (23) | 1.053 ± 0.006 (11) | 0.97, 0.39 |
| **Number of spikes, AP#** | 4.7 ± 0.2 (23) **** ††† | 6.4 ± 0.2 (17) **** ^ | 5.7 ± 0.2 (31) ††† ^ | 19.3, $5.53x10^{-9}$ | 6.5 ± 0.3 (19) †††† | 7.0 ± 0.2 (23) ^^^ | 8.3 ± 0.3 (15) †††† ^^^ | 12.1, 0.000006 |
| **Firing frequency, Hz** | 10.0 ± 0.4 (23) **** †††† | 13.7 ± 0.4 (17) **** ^ | 12.2 ± 0.3 (31) †††† ^ | 20.4, $1.81x10^{-9}$ | 14.0 ± 0.5 (19) †††† | 14.6 ± 0.5 (23) ^^^ | 17.7 ± 0.6 (15) †††† ^^^ | 12.6, 0.000004 |
| **Current to threshold, pA** | 981 ± 56 (20) | 875 ± 60 (16) | 879 ± 42 (27) | 1.35, 0.27 | 836 ± 63 (19) | 711 ± 45 (23) | 694 ± 40 (13) | 2.13, 0.13 |
| **AP threshold, mV** | -45 ± 1 (20) | -44 ± 1 (16) | -45 ± 1 (27) | 0.12, 0.89 | -45 ± 2 (19) † | -41 ± 1 (23) | -39 ± 2 (13) † | 3.72, 0.031 |
| **Δ RMP/AP threshold, mV** | 36 ± 2 (20) | 35 ± 1 (16) | 37 ± 8 (27) | 0.14, 0.87 | 37 ± 2 (19) | 38 ± 1 (23) | 42 ± 2 (13) | 1.76, 0.18 |
| **AP amplitude, mV** | 53.9 ± 0.9 (20) | 53 ± 1 (16) | 51 ± 1 (27) | 1.89, 0.16 | 53 ± 1 (19) | 53 ± 2 (23) | 49 ± 2 (13) | 1.84, 0.17 |
| **Δ RMP/AP amplitude, mV** | 135 ± 1 (20) | 132 ± 2 (16) | 132 ± 1 (27) | 1.28, 0.29 | 135 ± 1 (19) | 133 ± 2 (23) | 130 ± 2 (13) | 1.65, 0.20 |
| **Δ AP threshold/AP amplitude, mV** | 99 ± 2 (20) | 97 ± 2 (16) | 96 ± 2 (27) | 0.74, 0.48 | 97 ± 2 (19) † | 94 ± 2 (23) | 88 ± 3 (13) † | 3.62, 0.034 |
| **AP halfwidth, ms** | 0.72 ± 0.02 (20) † | 0.68 ± 0.02 (16) | 0.65 ± 0.01 (27) † | 4.16, 0.020 | 0.70 ± 0.02 (19) | 0.68 ± 0.02 (23) | 0.69 ± 0.02 (13) | 0.33, 0.72 |

* significance from post-hoc comparison between ST and GT ($p < 0.05$)
† significance from post-hoc comparison between ST and IR ($p < 0.05$)
^ significance from post-hoc comparison between GT and IR ($p < 0.05$)

**Table 3.2.** *Full statistical report for behavioral responses and electrophysiological passive and active properties of medium spiny neurons (MSNs) in the core and shell of nucleus accumbens of sign-tracker (STs), goal-tracker (GTs), and intermediate responder (IRs) rats.* Table is organized by figures and lists analyses performed, main effects and interactions, as well as post-hoc and planned comparisons for group and subregion effects.

| | Analysis | Effects | *F, (df), P* | Post-hoc | Comparison | *t/q/F, (df), P* |
|---|---|---|---|---|---|---|
| **Figure 3.2** | | | | | | |
| **3.2E. PavCA Index Score** | mixed-effects model | session (main effect)<br>phenotype (main effect)<br>session x phenotype (interaction) | F(2.74, 75.6) = 20.8, p < 0.0001<br>F(2, 28) = 56.6, p < 0.0001<br>F(10, 138) = 19.0, p < 0.0001 | Sidak's | GTs vs IRs<br>GTs vs STs<br>IR vs STs | t(91.6) = 4.72, p < 0.0001<br>t(94.3) = 10.7, p < 0.0001<br>t(90.0) = 7.82, p < 0.0001 |
| **Figure 3.3** | | | | | | |
| **3.3A. Lever Press Analysis** | | | | | | |
| **Number** | mixed-effects model | session (main effect)<br>phenotype (main effect)<br>session x phenotype (interaction) | F(2.24, 61.9) = 28.6, p < 0.0001<br>F(2, 28) = 36.6, p < 0.0001<br>F(10, 138) = 12.9, p < 0.0001 | Sidak's | GTs vs IRs<br>GTs vs STs<br>IR vs STs | t(93.8) = 6.66, p < 0.0001<br>t(59.5) = 11.7, p < 0.0001<br>t(78.0) = 8.25, p < 0.0001 |
| **Latency** | mixed-effects model | session (main effect)<br>phenotype (main effect)<br>session x phenotype (interaction) | F(2.67, 73.6) = 35.8, p < 0.0001<br>F(2, 28) = 41.6, p < 0.0001<br>F(10, 138) = 12.4, p < 0.0001 | Sidak's | GTs vs IRs<br>GTs vs STs<br>IR vs STs | t(102) = 6.74, p < 0.0001<br>t(66.4) = 14.9, p < 0.0001<br>t(115) = 8.10, p < 0.0001 |
| **Probability** | mixed-effects model | session (main effect)<br>phenotype (main effect)<br>session x phenotype (interaction) | F(2.93, 80.8) = 25.5, p < 0.0001<br>F(2, 28) = 42.0, p < 0.0001<br>F(10, 138) = 8.06, p < 0.0001 | Sidak's | GTs vs IRs<br>GTs vs STs<br>IR vs STs | t(112) = 7.55, p < 0.0001<br>t(82.4) = 17.5, p < 0.0001<br>t(137) = 7.65, p < 0.0001 |
| **3.3B. Magazine Entry Analysis** | | | | | | |
| **Number** | mixed-effects model | session (main effect)<br>phenotype (main effect)<br>session x phenotype (interaction) | F(3.28, 90.4) = 4.25, p = 0.0059<br>F(2, 28) = 4.06, p = 0.028<br>F(10, 138) = 13.7, p < 0.0001 | Sidak's | GTs vs IRs<br>GTs vs STs<br>IR vs STs | t(68.95) = 1.22, p = 0.54<br>t(88.73) = 3.31, p = 0.0041<br>t(107.7) = 2.86, p = 0.015 |
| **Latency** | mixed-effects model | session (main effect)<br>phenotype (main effect)<br>session x phenotype (interaction) | F(3.38, 93.4) = 6.85, p = 0.0002<br>F(2, 28) = 4.37, p = 0.022<br>F(10, 138) = 15.1, p < 0.0001 | Sidak's | GTs vs IRs<br>GTs vs STs<br>IR vs STs | t(73.5) = 0.92, p = 0.74<br>t(93.4) = 3.59, p = 0.0016<br>t(106) = 3.42, p = 0.0027 |
| **Probability** | mixed-effects model | session (main effect)<br>phenotype (main effect)<br>session x phenotype (interaction) | F(3.73, 103) = 8.50, p < 0.0001<br>F(2, 28) = 4.72, p = 0.017<br>F(10, 138) = 20.3, p < 0.0001 | Sidak's | GTs vs IRs<br>GTs vs STs<br>IR vs STs | t(74.2) = 0.22, p = 0.99<br>t(98.6) = 3.19, p = 0.0058<br>t(94.1) = 3.92, p = 0.0005 |
| **Figure 3.4** | | | | | | |
| **Core (3.4 B-D)** | | | | | | |

| | | | | | | |
|---|---|---|---|---|---|---|
| **3.4B. Resting Potential** | one-way ANOVA | no effect | $F(2, 68) = 0.55$, $p = 0.58$ | - | - | - |
| **3.4C. Input Resistance** | one-way ANOVA | no effect | $F(2, 68) = 0.33$, $p = 0.72$ | - | - | - |
| **3.4D. Cell Capacitance** | one-way ANOVA | phenotype (main effect) | $F(2, 68) = 5.47$, $p = 0.0063$ | Tukey's | core: STs vs IRs | $q(68) = 4.62$, $p = 0.0048$ |
| **Shell (3.4 E-G)** | | | | | | |
| **3.4E. Resting Potential** | one-way ANOVA | phenotype (main effect) | $F(2, 54) = 4.98$, $p = 0.010$ | Tukey's | shell: STs vs GTs | $q(54) = 4.42$, $p = 0.0079$ |
| **3.4F. Input Resistance** | one-way ANOVA | no effect | $F(2, 54) = 1.96$, $p = 0.15$ | - | - | - |
| **3.4G. Cell Capacitance** | one-way ANOVA | phenotype (main effect) | $F(2, 54) = 4.16$, $p = 0.022$ | Tukey's | shell: STs vs GT<br>shell: STs vs IRs | $q(54) = 3.53$, $p = 0.041$<br>$q(54) = 3.48$, $p = 0.045$ |
| **Figure 3.5** | | | | | | |
| **Core – Phenotype Analysis (3.5 B-C)** | | | | | | |
| **3.5B. Voltage/Current curve** | | | | | | |
| Hyperpolarizing: -500 to 0pA | mixed-effects model | phenotype (main effect)<br>current injection (main effect) | $F(2, 1134) = 13.4$, $p = 0.000002$<br>$F(20, 1134) = 101$, $p = 1.47 \times 10^{-234}$ | mixed-effects model planned comparison | core: STs vs GTs<br>core: STs vs IRs | $F(1, 735) = 28.0$, $p = 1.64 \times 10^{-7}$<br>$F(1, 777) = 16.4$, $p = 0.000057$ |
| Depolarizing: 0 to 100pA | mixed-effects model | phenotype (no main effect)<br>current injection (main effect) | $F(2, 265) = 1.60$, $p = 0.20$<br>$F(4, 265) = 84.0$, $p = 5.58 \times 10^{-46}$ | -<br>- | - | - |
| **3.5C. Sag ratio** | one-way ANOVA | no effect | $F(2, 52) = 1.01$, $p = 0.37$ | - | - | - |
| **Shell – Phenotype Analysis (3.5 E-F)** | | | | | | |
| **3.5E. Voltage/Current curve** | | | | | | |
| Hyperpolarizing: -500 to 0pA | mixed-effects model | phenotype (main effect)<br>current injection (main effect) | $F(2, 966) = 20.9$, $p = 1.30 \times 10^{-9}$<br>$F(20, 966) = 94.4$, $p = 5.83 \times 10^{-211}$ | mixed-effects model planned comparison | shell: STs vs GTs<br>shell: STs vs IRs | $F(1, 756) = 29.1$, $p = 9.13 \times 10^{-8}$<br>$F(1, 504) = 34.7$, $p = 7.20 \times 10^{-9}$ |
| Depolarizing: 0 to 100pA | mixed-effects model | phenotype (no main effect)<br>current injection (main effect) | $F(2, 221) = 2.81$, $p = 0.063$<br>$F(4, 221) = 85.7$, $p = 8.02 \times 10^{-44}$ | -<br>- | - | - |
| **3.5F. Shell – Sag ratio** | one-way ANOVA | no effect | $F(2, 46) = 0.97$, $p = 0.39$ | - | - | - |
| **Core vs Shell – Subregional Analysis** | | | | | | |
| **3.5 B, E. Voltage/Current curve** | | | | | | |

| | | | | | | |
|---|---|---|---|---|---|---|
| Hyperpolarizing: -500 to 0pA | mixed-effects model | subregion (main effect)<br>phenotype (main effect)<br>current injection (main effect) | $F(1, 2100) = 175, p = 1.63x10^{-38}$<br>$F(2, 2100) = 34.6, p = 1.67x10^{-15}$<br>$F(20, 2100) = 195, p = 0.0x10^{0}$ | mixed-effects model planned comparison | STs: core vs shell<br>GTs: core vs shell<br>IRs: core vs shell | $F(1, 672) = 47.4, p = 1.33x10^{-11}$<br>$F(1, 819) = 62.0, p = 1.09x10^{-14}$<br>$F(1, 609) = 65.6, p = 2.98x10^{-15}$ |
| Depolarizing: 0 to 100pA | mixed-effects model | subregion (main effect)<br>phenotype (main effect)<br>current injection (main effect)<br>subregion x current injection (interaction) | $F(1, 486) = 59.7, p = 6.47x10^{-14}$<br>$F(2, 486) = 3.10, p = 0.046$<br>$F(4, 486) = 173, p = 6.17x10^{-92}$<br>$F(4, 486) = 6.40, p = 0.000050$ | mixed-effects model planned comparison | STs: core vs shell<br>GTs: core vs shell<br>IRs: core vs shell | $F(1, 155) = 10.5, p = 0.0015$<br>$F(1, 190) = 14.1, p = 0.00023$<br>$F(1, 141) = 48.3, p = 1.23x10^{-10}$ |
| **Figure 3.6** | | | | | | |
| **Core – Phenotype Analysis (3.6 B-C)** | | | | | | |
| **3.6B. Number of spikes** | mixed-effects model | phenotype (main effect)<br>current injection (main effect) | $F(2, 1316) = 19.3, p = 5.53x10^{-9}$<br>$F(19, 1316) = 97.3, p = 1.31x10^{-234}$ | mixed-effects model planned comparison | core: STs vs GTs<br>core: STs vs IRs<br>core: GTs vs IRs | $F(1, 750) = 39.0, p = 6.95x10^{-10}$<br>$F(1, 999) = 16.4, p = 0.000055$<br>$F(1, 883) = 6.70, p = 0.0098$ |
| **3.6C. Firing frequency** | mixed-effects model | phenotype (main effect)<br>current injection (main effect) | $F(2, 1316) = 20.4, p = 1.81x10^{-9}$<br>$F(19, 1316) = 97.5, p = 5.72x10^{-235}$ | mixed-effects model planned comparison | core: STs vs GTs<br>core: STs vs IRs<br>core: GTs vs IRs | $F(1, 750) = 41.4, p = 2.17x10^{-10}$<br>$F(1, 999) = 17.8, p = 0.000027$<br>$F(1, 883) = 6.75, p = 0.0096$ |
| **Shell – Phenotype Analysis (3.6 E-F)** | | | | | | |
| **3.6E. Number of spikes** | mixed-effects model | phenotype (main effect)<br>current injection (main effect) | $F(2, 1058) = 12.1, p = 0.000006$<br>$F(19, 1058) = 70.9, p = 2.38x10^{-173}$ | mixed-effects model planned comparison | shell: STs vs IRs<br>shell: GTs vs IRs | $F(1, 620) = 23.2, p = 0.000002$<br>$F(1, 714) = 14.8, p = 0.00013$ |
| **3.6F. Firing frequency** | mixed-effects model | phenotype (main effect)<br>current injection (main effect) | $F(2, 1058) = 12.6, p = 0.000004$<br>$F(19, 1058) = 74.6, p = 5.13x10^{-180}$ | mixed-effects model planned comparison | shell: STs vs IRs<br>shell: GTs vs IRs | $F(1, 620) = 22.0, p = 0.000003$<br>$F(1, 714) = 19.0, p = 0.000015$ |
| **Core vs Shell – Subregional Analysis** | | | | | | |
| **3.6 B, E. Number of spikes** | mixed-effects model | phenotype (main effect)<br>subregion (main effect)<br>current injection (main effect)<br>phenotype x subregion (interaction) | $F(2, 2374) = 23.2, p = 1.03x10^{-10}$<br>$F(1, 2374) = 83.5, p = 1.31x10^{-19}$<br>$F(19, 2374) = 166, p = 0.0x10^{-0}$<br>$F(2, 2374) = 10.8, p = 0.000022$ | Sidak's | STs: core vs shell<br>GTs: core vs shell<br>IRs: core vs shell | $F(1, 2374) = 33.5, p = 8.05x10^{-9}$<br>$F(1, 2374) = 3.11, p = 0.078$<br>$F(1, 2374) = 69.0, p = 1.66x10^{-16}$ |
| **3.6 C, F. Firing frequency** | mixed-effects model | phenotype (main effect)<br>subregion (main effect)<br>current injection (main effect)<br>phenotype x subregion (interaction) | $F(2, 2374) = 22.8, p = 1.59x10^{-10}$<br>$F(1, 2374) = 88.9, p = 9.58x10^{-21}$<br>$F(19, 2374) = 171, p = 0.0x10^{-0}$<br>$F(1, 2374) = 12.8, p = 0.000003$ | Sidak's | STs: core vs shell<br>GTs: core vs shell<br>IRs: core vs shell | $F(1, 2374) = 40.0, p = 3.07x10^{-10}$<br>$F(1, 2374) = 2.25, p = 0.13$<br>$F(1, 2374) = 73.0, p = 2.32x10^{-17}$ |
| **Table 3.1 (not in figure)** | | | | | | |
| **Current to threshold** | | | | | | |

| | | | | | | |
|---|---|---|---|---|---|---|
| **Core** | one-way ANOVA | no effect | F(2, 60) = 1.35, p = 0.27 | - | - | - |
| **Shell** | one-way ANOVA | no effect | F(2, 52) = 2.13, p = 0.13 | - | - | - |
| **AP threshold** | | | | | | |
| **Core** | one-way ANOVA | no effect | F(2, 60) = 0.12, p = 0.89 | - | - | - |
| **Shell** | one-way ANOVA | phenotype (main effect) | F(2, 52) = 3.72, p = 0.031 | Tukey's | shell: STs vs IRs | q(52) = 3.720, p = 0.030 |
| **Δ RMP/AP threshold** | | | | | | |
| **Core** | one-way ANOVA | no effect | F(2, 60) = 0.14, p = 0.87 | - | - | - |
| **Shell** | one-way ANOVA | no effect | F(2, 52) = 1.76, p = 0.18 | - | - | - |
| **AP amplitude** | | | | | | |
| **Core** | one-way ANOVA | no effect | F(2, 60) = 1.89, p = 0.16 | - | - | - |
| **Shell** | one-way ANOVA | no effect | F(2, 52) = 1.84, p = 0.17 | - | - | - |
| **Δ RMP/AP amplitude** | | | | | | |
| **Core** | one-way ANOVA | no effect | F(2, 60) = 1.28, p = 0.29 | - | - | - |
| **Shell** | one-way ANOVA | no effect | F(2, 52) = 1.65, p = 0.20 | - | - | - |
| **Δ AP threshold/AP amplitude** | | | | | | |
| **Core** | one-way ANOVA | no effect | F(2, 60) = 0.74, p = 0.48 | - | - | - |
| **Shell** | one-way ANOVA | phenotype (main effect) | F(2, 52) = 3.62, p = 0.034 | Tukey's | shell: ST vs IRs | q(52) = 3.78, p = 0.027 |
| **AP halfwidth** | | | | | | |
| **Core** | one-way ANOVA | phenotype (main effect) | F(2, 60) = 4.16, p = 0.020 | Tukey's | shell: ST vs IRs | q(60) = 4.08, p = 0.015 |
| **Shell** | one-way ANOVA | no effect | F(2, 52) = 0.33, p = 0.72 | - | - | - |

# CHAPTER IV

## Functional Role of Ventral Hippocampus to Nucleus Accumbens Projections in Pavlovian Conditioned Approach Behaviors


### Abstract

During associative learning discrete and contextual cues gain the ability to elicit and modulate motivated behaviors. Glutamatergic transmission in the nucleus accumbens (NAc) is necessary for generating cue- and context-dependent behavioral responses, and alterations in this system can significantly impact vulnerability to disorders like addiction. The NAc relies on inputs from the ventral hippocampus (vHPC) to encode context-specific reward information, meaning that the vHPC-NAc projection may be important for modulating conditioned responses to discrete cues based on the associated contextual information. Therefore, individual variation in Pavlovian conditioned approach behavior, such as increased cue reactivity, could be due to differences in vHPC-NAc activity during appetitive reward learning. The “sign-tracker” and “goal-tracker” model allows us to classify rats based on their sensitivity to reward-paired cues during a Pavlovian conditioned approach (PavCA) procedure. While “goal-trackers” use the cue solely as a predictor to direct their behavior towards the site of reward delivery, for “sign-trackers” the cue becomes a reward in and of itself. Sign-trackers approach the cue because it has become embedded with the motivational

properties of the reward, i.e. with incentive salience. In this chapter, we investigate the role of the vHPC-NAc projection on sign- and goal-tracking behavior. We used an *in vivo* dual-vector approach of Cre-dependent DREADDs to determine the effects of chemogenetic inhibition and excitation of the vHP*C-NAc* projection during PavCA. Collectively, our data suggest that decreased activity of the vHPC-NAc may favor sign-tracking behavior while increased activity may diminish it. Therefore, the vHPC-NAc projection may play a role in guiding individual differences in reward learning.

**Introduction**

During associative learning, individuals acquire information and infer relationships between elements in their environment to guide future behavioral responses. This process typically involves the interplay between discrete and contextual cues that can both elicit and modulate motivated behaviors. The integration of surrounding stimuli into motivated actions is attributed in part to glutamatergic transmission onto the nucleus accumbens (NAc). Glutamatergic signaling in the NAc is necessary for Pavlovian conditioned approach (Ciano et al., 2001; Dalley et al., 2005) and context-dependent reward learning (Layer et al., 1993; Kaddis et al., 1995; Baharlouei et al., 2015), which encompass a significant range of associative behavioral responses. Understanding glutamate signaling within the NAc is therefore likely to provide insight into the etiology of psychopathologies involving aberrant associative learning (Hearing et al., 2018; Turner et al., 2018).

The NAc receives glutamatergic innervation from a number of regions including the prefrontal cortex, the basolateral amygdala, and the hippocampus (Brog et al., 1993; Britt et al., 2012). The ventral hippocampus (vHPC) is thought to be especially pivotal

for encoding context-specific reward information. For example, drugs of abuse such as cocaine (Bell et al., 2000; Barr et al., 2014; Keralapurath et al., 2017) and morphine (Alvandi et al., 2017) induce synaptic changes in the vHPC that are believed to be necessary for subsequent context-induced reinstatement of drug-seeking (Lasseter et al., 2010). Evidence suggests that this context-specific information is decoded by the NAc through coupling with vHPC neuronal engrams that store spatial information necessary for context-driven responses (Zhou et al., 2019). In fact, stimulation of the vHPC-NAc alone can result in significant conditioned place preference, suggesting that activity in this projection can shape context-dependent reward learning (Britt et al., 2012; LeGates et al., 2018).

Although several studies have highlighted a role for the vHPC-NAc projection in influencing susceptibility and resiliency to stress and depression-like behaviors (Bagot et al., 2015; LeGates et al., 2018; Muir et al., 2020; Williams et al., 2020), not many studies have explored whether individual differences in reward learning and addiction susceptibility can also be influenced by vHPC-NAc activity. The “sign-tracker” and “goal-tracker” behavioral model provides the means to classify rats that react strongly to conditioned cues regardless of the context under which they are encountered, versus rats that use contextual cues to modulate their conditioned emotional responses (Pitchers et al., 2017). This phenotypic distinction can be achieved through a Pavlovian conditioned approach (PavCA) procedure in which a neutral stimulus (i.e., lever) is repeatedly paired with an unconditioned stimulus (i.e., banana-flavored food pellet). “Sign-trackers” (STs) will interact with the reward-paired cue, indicating that the cue itself acquires incentive salience for them. In contrast, “goal-trackers” (GTs) direct their

behavior away from the cue and towards the site of impending food reward (i.e., magazine), indicating that they are using the cue solely as a predictor of the reward (Berridge et al., 2009).

Interestingly, compared to GTs, STs are more impulsive (Lovic et al., 2011), have poorer attentional control (Paolone et al., 2013), and are more sensitive to cue-induced "relapse" or reinstatement of drug self-administration (Saunders and Robinson, 2011; Versaggi et al., 2016). However, STs also exhibit less cocaine context-induced hyperactivity and context-dependent reinstatement of cocaine (Saunders et al., 2014) as well as less cocaine reinstatement induced by "occasion setters" which are discriminative stimuli thought to mimic the properties of contextual cues (Pitchers et al., 2017). As mentioned above, the vHPC is necessary for context-induced reinstatement of cocaine (Lasseter et al., 2010) which is thought to be mediated through input to the NAc (Zhou et al., 2019). Consistent with this, disconnection lesions between the whole hippocampus and NAc shell impede context-dependent cue retrieval (Ito et al., 2008). In addition, lesions of the whole hippocampus have been found to facilitate sign-tracking toward a CS+ (Ito et al., 2005), though another study found that lesions limited to the vHPC can impair sign-tracking and promote goal-tracking (Fitzpatrick et al., 2016). It is thus possible that differences between STs and GTs in vHPC activity may affect processing of context-specific reward information and in turn modulate conditioned responses to discrete cues as seen in PavCA responses.

No study has yet tested whether the vHPC projections affect sign- and goal-tracking behavior through direct modulation of NAc activity. Using a dual-vector chemogenetic approach, we performed a series of three experiments in which we

altered activity in the vHPC-NAc projection during PavCA to test its role in the acquisition and expression of sign- and goal-tracking. We reasoned that isolating the role of this specific projection in driving the two distinct behavioral phenotypes may help determine whether it can influence individual differences in the attribution of incentive salience. Such processes are of both clinical and scientific interest because of their importance in psychiatric disorders such as addiction that are characterized by aberrant associative learning.

## Materials and Methods

### *Animals*

A total of 119 adult male Sprague Dawley rats (7-8 weeks) were purchased from Charles River Laboratories from barriers C72, R04, K90, and K92, to increase phenotypic diversity (Fitzpatrick et al., 2013). Rats were maintained on a 12:12-hr light/dark cycle, with food and water available ad libitum for the entirety of the experiment. All rats were acclimatized to the housing colony for at least two days prior to any handling and surgical procedures. All animal procedures were previously approved by the University Committee on the Use and Care of Animals (University of Michigan; Ann Arbor, MI).

### *Drugs*

For *in vivo* studies, clozapine-N-oxide (CNO) was supplied by the National Institute on Drug Abuse (NIDA) Drug Supply Program. Clozapine-N-oxide was first dissolved in dimethyl sulfoxide (DMSO), then diluted with sterile water to 3 mg/ml CNO and 6% DMSO. This solution was administered intraperitoneally (IP) at a dose of 3

mg/kg (1 ml/kg). Six per cent DMSO was used as a vehicle control (Veh) and administered IP at 1 ml/kg. For *ex vivo* slice electrophysiology, water soluble CNO (Hello Bio; Bristol, UK) was dissolved in artificial cerebrospinal fluid (aCSF) to make a 10- or 20-μM solution. Unless otherwise stated, all chemicals were purchased from Tocris Bioscience (Bristol, UK), Sigma-Aldrich (St. Louis, MO), and Fisher Chemical (Pittsburgh, PA).

### *Viral vectors*

*Designer receptors exclusively activated by designer drugs* (DREADDs): Double-floxed hM4D(Gi) pAAV-hSyn-DIO-hM4D(Gi)-mCherry (Addgene plasmid #44362; http://n2t.net/ addgene:44362; RRID: Addgene_44362) and double-floxed hM3D(Gq) pAAV-hSyn-DIO-hM3D (Gq)-mCherry (Addgene plasmid #44361; http://n2t.net/addgene:44361; RRID: Addgene_ 44361), were a gift from Bryan Roth.

*Cre-recombinase*: Retrograde Cre pENN.AAV.hSyn.HI.eGFP-Cre.WPRE.SV40 was a gift from James M. Wilson (Addgene plasmid #105540; http://n2t.net/addgene:105540; RRID: Addgene_ 105540).

*Control virus*: mCherry pAAV-hSyn-mCherry was a gift from Karl Deisseroth (Addgene plasmid #114472; http://n2t.net/addgene:114472; RRID: Addgene_114472).

*Channelrhodopsin*: pAAV-CaMKIIa-hChR2(H134R)-mCherry was a gift from Karl Deisseroth (Addgene plasmid # 26975; http://n2t.net/addgene:26975; RRID: Addgene_26975).

### *AAV injections*

All rats were anesthetized using 4-5% isoflurane for induction and 1-2% for maintenance (Fluriso - VetOne; Boise, ID). Following anesthesia, rats were given

carprofen (Rimadyl: 5mg/kg; SQ) for analgesia. Rats were then placed in a stereotaxic frame (David Kopf Instruments; Tujunga, CA), and temperature was regulated with a heating pad. Bilateral intracranial viral injections were performed by lowering a 5-µl Hamilton Neuros Syringe (Model 75 RN, 33-gauge; Hamilton, Reno, NV) into the NAc and vHPC. Each virus was infused at a rate of 0.1 µl/min over the course of either 5 or 10 min. The syringe was left in place for 5 min to allow diffusion. Following the surgical procedures, the incisions were closed using sutures. Following surgery, rats received post-operative analgesia for two days and additional monitoring for 7-10 days. A period of 5 weeks was allowed for optimal viral expression before behavioral testing. The following coordinates based on a rat brain atlas (Paxinos and Franklin, 2019) were used in Experiment 1: NAc: AP = +1.7 mm, ML = ±1.8 mm, DV = -7.8 mm, vHPC: AP = -6.0 mm, ML = ±5.4 mm, DV = -8.4 mm. Experiments 2 and 3 utilized the following coordinates: NAc: AP = +1.7 mm, ML = ±0.8 mm, DV = -7.8 mm, and for the vHPC: AP = -6.0 mm, ML = ±4.8 mm, DV = -8.4 mm. In the vHPC, a total of 1.0 µl of a Cre-dependent inhibitory (AAV8-hSyn-DIO-hM4D(Gi)-mCherry) or excitatory (AAV8-hSyn-DIO-hM3D(Gq)-mCherry) DREADD virus was bilaterally injected. As a control, some rats were injected with AAV8-hSyn-mCherry. In the NAc a total of 1.0 µl in Experiment 1, and 0.5 µl in Experiments 2 and 3 of a retrograde Cre-recombinase virus (AAVrg.hSyn.HI.eGFP-Cre), was bilaterally injected. For all rats there were a total of four injection sites.

To verify the inhibitory action of the DREADD-(Gi) virus *ex vivo* (**Table 4.4**), a subset of rats received bilateral injections of the retrograde Cre-recombinase virus into the NAc (stereotaxic coordinates: AP = +1.7 mm, ML = ±1.8 mm, DV = -7.8 mm) and a

combination of the Cre-dependent inhibitory DREADD virus and a channelrhodopsin virus (AAV5-CAMKIIa-hChR2(H134R)-mCherry) into the vHPC (stereotaxic coordinates: AP = -6.0 mm, ML = ±5.4 mm, DV = -8.4 mm). In the NAc all rats received 1.0 µl per side of Cre-recombinase injected at a rate of 0.2 µl/min. In the vHPC two rats (Rat IDs: A and B, **Table 4.4**) received 1.0 µl of the DREADD virus and 0.5 µl of channelrhodopsin for a total of 1.5 µl per side. One rat (Rat ID: C, **Table 4.4**) received 0.5 µl of the DREADD virus and 0.5 µl of channelrhodopsin for a total of 1.0 µl per side. All injections in the vHPC were performed at a rate of 0.1 µl/min.

### *Behavioral Testing Apparatus*

Sixteen modular operant conditioning chambers (24.1 cm width × 20.5 cm depth x 29.2 cm height; MED Associates, Inc.; St. Albans, VT) were used for behavioral testing. Each chamber was inside a sound-attenuating cubicle with a ventilation fan providing ambient background noise during testing. Each chamber was equipped with a food magazine, a retractable lever (counterbalanced on the left or right side of the magazine), and a red house light on the wall opposite of the magazine. An infrared sensor in the magazines detected magazine entries, and the levers were calibrated to detect lever deflections in response to a minimum of 10 g of applied weight. The inside of the lever mechanism contained a mounted LED to illuminate the slot through which the lever protruded each time the lever was extended into the chamber. The number and latency of lever presses and magazine entries were recorded automatically per each trial (ABET II Software; Lafayette Instrument; Lafayette, IN).

### *Behavioral Testing Procedure*

For two days prior to the start of training, all rats were handled individually and were given banana-flavored pellets (45 mg; Bio-Serv; Frenchtown, NJ) in their home cages. On the third day, rats were placed into the test chambers for one pre-training session during which the red house-light remained on, but the lever was retracted. Twenty-five food pellets were delivered on a variable time (VT) 30-s schedule (i.e., one pellet was delivered on average every 30 s, but varied 0-60 s). Pre-training sessions were performed up to three times a day until all rats were consuming all the pellets. Following the pre-training session, all rats underwent six daily sessions of behavioral training. Prior to each training session, rats received either CNO or Veh and remained in a transfer box until 25 minutes had passed. Following this time, rats were placed in their conditioning chambers to begin testing. Each trial during a training session consisted of a presentation of the illuminated lever (conditioned stimulus, CS) into the chamber for 10 seconds on a VT 45-s schedule (i.e., time randomly varied 30-60 s between CS presentations). Immediately after retraction of the lever, there was a response-independent delivery of one pellet into the magazine (unconditioned stimulus, US). The beginning of the next inter-trial interval (ITI) began once both the lever and the pellet had been presented, and each test session consisted of 25 trials of CS-US pairings. Rats were not food deprived at any point during experimentation.

***Perfusions and tissue collection***

Approximately 1 week after completing the behavioral experiments, rats were deeply anesthetized with sodium pentobarbital (39 mg/kg, IP; Euthasol – Virbac; Carros, FR) and transcardially perfused with a 4% formaldehyde solution (pH 7.0-7.4). Following decapitation, brains were dissected and post-fixed in 4% formaldehyde for 24

hours at 4ºC. Brains were then transferred to a 30% sucrose solution made with 0.2 M sodium phosphate buffer (NaPB, pH = 7.0-7.4) and were left at 4ºC for approximately 3-5 days. Brains were then frozen using cooled isopentane (-160ºC) for 20-30 seconds. Coronal sections (35-40 µm) were obtained using a cryostat (Leica CM1860; Leica Biosystems Inc, Wetzlar, DE). Brain slices from the NAc (ranging from +3.20 to -0.30 mm from Bregma) and vHPC (ranging from -3.60 to -7.04 mm from Bregma) were placed into glass vials containing 0.1 M phosphate-buffered saline (PBS) with 0.02% sodium azide to prevent microbial growth and stored at 4ºC until immunohistochemical processing.

***Immunohistochemistry***

An immunohistochemistry protocol for verifying accuracy of DREADD expression in the NAc and vHPC was performed by staining and visualizing mCherry protein. In brief, free-floating coronal sections of NAc and vHPC were rinsed with 0.1 M PBS (pH = 7.4) before blocking the tissue for 1 hr at room temperature (RT) in 0.1 M PBS containing 0.4% Triton X-100 (TX) and 2.5% normal donkey serum (NDS) (Jackson Immuno Research Labs; West Grove, PA). Sections were then incubated overnight (~17 hrs) at RT in rabbit anti-mCherry primary antibody (Abcam, ab167453), diluted 1:1000 in 0.1 M PBS containing 0.4% TX and 1% NDS. The next day, sections were rinsed 3 times with 0.1 M PBS and then incubated for 2 hrs at RT in biotinylated donkey anti-rabbit secondary antibody (Jackson Immuno, 711-065-152), diluted 1:500 in 0.1 M PBS containing 0.4% TX and 1% NDS. Following incubation, sections were rinsed three times and incubated in the dark for 1 hr at RT in Alexa Fluor 594-conjugated streptavidin, (Thermo Fisher Scientific, S11227), diluted 1:1000 in 0.1 M PBS containing

0.4% TX. Sections were rinsed three times and mounted on Fisherbrand +charged slides. Once the sections were fully dried, they were cover-slipped with Vectashield Plus antifade medium with DAPI (Vector Laboratories, H-20000-10) and stored at 4ºC. Fluorescence imaging of sections containing the NAc and vHPC was captured at 4x magnification using the Olympus IX83 inverted microscope and processed using ImageJ. Out of the 100 rats included in the analysis, histological verification of proper DREADD expression was confirmed on 37 rats.

### *Electrophysiology for DREADD validation*

*Slice preparation.* Rats that received viral injections of Cre-recombinase into the NAc plus the combination of the DREADD-(Gi) and channelrhodopsin viruses into the vHPC, were deeply anesthetized with isoflurane (Kent Scientific; Torrington, CT) and euthanized by decapitation. The brain was rapidly dissected and glued on a platform, which was then submerged in an ice-cold oxygenated (95% $O_2$/ 5% $CO_2$) cutting solution containing (in mM): 206 sucrose, 10 d-glucose, 1.25 $NaH_2PO_4$, 26 $NaHCO_3$, 2 KCl, 0.4 sodium ascorbic acid, 2 $MgSO_4$, 1 $CaCl_2$, and 1 $MgCl_2$. A mid-sagittal cut was made to divide the two hemispheres, and coronal brain slices (300 µm) were cut using a vibrating blade microtome (Leica VT1200; Wetzlar, DE). Brain slices were transferred to a holding chamber with oxygenated aCSF containing (in mM): 119 NaCl, 2.5 KCl, 1 $NaH_2PO_4$, 26.2 $NaHCO_3$, 11 d-glucose, 1 sodium ascorbic acid, 1.3 $MgSO_4$, and 2.5 $CaCl_2$ (~295 mOsm, pH 7.2-7.3) at 37ºC for 20 minutes and then room temperature for at least 40 m of rest. The slices were kept submerged in oxygenated aCSF in a holding chamber at room temperature for up to 7-8 h after slicing.

*Optically evoked excitatory post-synaptic currents (EPSC) recordings*. After at least 1 h of rest, slices were transferred to the recording chamber where they were perfused with oxygenated aCSF (32 ºC) containing 100 µM of $GABA_A$ receptor antagonist, picrotoxin. Recordings from the NAc medial shell were made in slices obtained between +1.00 mm to +1.70 mm anterior from bregma (Paxinos and Franklin, 2019). Cells were visualized using infrared differential interference contrast (IR-DIC) optics (Scientifica SlicePro 1000), and optogenetic stimulation was accomplished using a digital micromirror device and a 470 nm LED (Polygon 400, Mightex, Toronto Ontario) controlled by a Mightex BLS-SA/PL series BioLED control module. Whole-cell voltage clamp recordings were performed using borosilicate glass pipettes (O.D. 1.5 mm, I.D. 0.86 mm; Sutter Instruments) with a 4-7-MΩ open-tip resistance. Pipettes were filled with a cesium methanesulfonate-based internal solution containing (in mM): 120 CsMeS, 15 CsCl, 10 TEA-Cl, 8 NaCl, 10 HEPES, 0.4 EGTA, and 2 $Mg^{2+}$ATP/0.3 $Na_2$GTsP (~280 mOsm, pH adjusted to 7.2 with KOH). Medium spiny neurons (MSNs) were identified based on morphology (medium-sized soma) as well as a hyperpolarized resting potential between -70 to -90 mV. All recordings were obtained using a MultiClamp 700B (Molecular Devices, San Jose, CA) amplifier and Digidata 1550A (Molecular Devices, San Jose, CA) digitizer. Recordings were filtered at 2 kHz, digitized at 10 kHz, and were collected and analyzed using pClamp 10.0 software (Molecular Devices, San Jose, CA).

To perform whole-cell recordings, membrane seals with a resistance >1 GΩ were achieved prior to breaking into the cell. Membrane capacitance ($C_m$) and series resistance ($R_s$) were compensated under voltage-clamp. To record optically evoked-

EPSCs, cells were held at -80 mV. An input-output curve was generated by stimulating each cell at five varying LED intensities (20%, 40%, 60%, 80%, 100%). At each intensity, an optical pulse of either 0.5 ms, 1 ms, or 2 ms was delivered six times separated by 20 s. Following the input-output protocol with regular aCSF, CNO (10 μM or 20 μM) was added to the solution and left to perfuse while holding the cell. After 5 min, an optical pulse was delivered at 100% of the LED intensity six times separated by 20 s. Finally, if the cell was still stable the aCSF solution was swapped once more to regular aCSF to wash out CNO. Following 5 min, an optical pulse was delivered at 100% of the LED intensity six times and separated by 20 s. For every cell, all six sweeps were averaged for each stimulation intensity to obtain EPSC amplitude.

## Experimental Design and Statistical Analysis

### *Behavioral Studies*

*Experiment 1*. From a total of 75 rats (Barriers R04/C72), 8 were excluded for lack of proper DREADD expression and 5 were excluded for failing to consume all food pellets by the end of pre-training. A total of 62 rats were included in the analysis. Rats were randomly divided into 3 groups: mCherry/CNO control group (n = 20), Gi/Veh group (n = 21), or Gi/CNO group (n = 21).

*Experiment 2.* From a total of 16 rats (Barriers R04/K97), 1 was excluded for treatment error. A total of 15 rats were included in the analysis. Rats were randomly divided into 3 groups:  mCherry/CNO control group (n = 3), Gq/Veh group (n = 4), or Gq/CNO group (n = 8).

*Experiment 3.* From a total of 25 rats (Barriers R04/K90), 2 were excluded because of adverse reactions to treatment. A total of 23 rats were used in the analysis.

Rats were randomly divided into 4 groups: mCherry/CNO control group (n = 3), Gi/CNO group (n = 7), Gq/CNO group (n = 5), or Veh group (n = 8: 3 Gi, 5 Gq).

The behavioral responses in the PavCA procedure were analyzed by session. For each one of the sessions, the total recorded numbers of lever presses and magazine entries from all 25 trials were added for each rat and averaged by session and group. The latency of lever presses and magazine entries were averaged for each rat across all 25 trials and then averaged by session and group. Probability to lever press or enter the magazine on each trial was also averaged across all 25 trials for each rat and is defined as the number of trials with a lever press or magazine entry, divided by the total number of trials (Meyer et al., 2012). The behavioral response in PavCA was scored using an index that incorporates the number, latency, and probability of lever presses (sign-tracking conditioned response) and magazine entries (goal-tracking conditioned response) during CS presentations within a session (Meyer et al., 2012). In brief, we averaged the response bias (i.e., number of lever presses and magazine entries for a session; [lever presses – magazine entries] / [lever presses + magazine entries]), latency score (i.e., average latency to perform a lever press or magazine entry during a session; [magazine entry latency – lever press latency]/10), and probability difference (i.e., proportion of lever presses or magazine entries; lever press probability – magazine entry probability). The index score ranges from +1.0 (absolute sign-tracking) to -1.0 (absolute goal-tracking), with 0 representing no bias. In Experiment 1, the PavCA index score from Session 6 was used to classify rats as STs (score ≥ 0.3), GTs (score ≤ -0.3), and IRs (-0.3 < score < 0.3). For Experiment 1, out of a total of 21 rats in the CNO

group, 8 were classified as STs, 7 were GTs, and 6 were IRs. From the 21 rats in the Veh group, 6 were classified as STs, 11 were GTs, and 4 were IRs.

GraphPad Prism 8 (Dotmatics) was used for statistical analysis of all the behavioral data. Number, latency, and probability for lever presses and for magazine entries, as well as PavCA index scores were analyzed using mixed-effects model via restricted maximum likelihood (REML). For cross-treatment test analysis, paired t-tests were performed to compare behavioral responses (lever press and magazine entry number, latency, and probability; PavCA index score) on day 6 of original treatment (Pre) with behavioral responses of the same rats on cross-treatment test day (Cross-Tx). No multiple comparison corrections were made for paired t-test analyses. Data are presented as mean ± SEM and significance level was set at $p < 0.05$.

*Experiment 1:* For PavCA acquisition analysis, fixed effects for mixed-effects model via REML were set for group (Gi/CNO vs Veh), session (1-6), and group x session. Cross-treatment analysis was done for all rats in the Gi/CNO and Veh groups and then individually for STs, GTs, and IRs in each of those treatment groups.
*Experiment 2:* For PavCA acquisition analysis, fixed effects for mixed-effects model via REML were set for group (Gq/CNO vs Veh), session (1-6), and group x session.
*Experiment 3:* For PavCA acquisition analysis, fixed effects for mixed-effects model via REML were set for group (Gq/CNO vs Gi/CNO vs Veh), session (1-6), and group x session. Multiple comparisons were performed using Tukey's post hoc test.

To test for non-specific effects of CNO on lever press and magazine entry number, latency, and probability, mCherry/CNO control rats were compared with DREADD/Veh rats using mixed-effects model via REML. Fixed effects were set for

group (mCherry/CNO vs DREADD/Veh), session (1-6), and group x session. In Experiments 2 and 3, the mCherry/CNO group only had 3 rats resulting in very high variability. Full statistical reports for all behavioral data analysis of Experiments 1-3 are found in **Tables 4.1-4.3** respectively.

### *Electrophysiological Studies*

*Optically evoked-EPSC recordings for DREADD virus validation.* A total of 8 cells from 3 rats were included. All offline analysis of electrophysiological recordings was performed using Clampfit 10.7 (Molecular Devices). Statistical analyses were made using GraphPad Prism 8 (Dotmatics). Excitatory postsynaptic current amplitude at 100% of LED intensity before and after CNO application was analyzed using paired t-test. Data are presented for each cell and as mean ± SEM, and significance level was set at $p < 0.05$. Refer to **Table 4.4** for full data summary.

## Results

### *Experiment 1: Effects of chemogenetic inhibition of the vHPC-NAc during PavCA*

Chemogenetic inhibition was used to determine if the vHPC-NAc projection plays a role in biasing sign- and goal-tracking behavior and influencing individual differences in incentive salience attribution. Rats expressing an inhibitory Cre-dependent hM4D-Gi DREADD selectively in NAc-projecting vHPC neurons **(Fig 4.1)** underwent a PavCA procedure with either CNO (3 mg/kg, IP) or Veh (6% DMSO: 1 ml/kg, IP) administered prior to testing **(Fig 4.2)**. We found that inhibition of vHPC-NAc did not affect the acquisition of sign- or goal-tracking behavior as measured by lever-oriented or magazine-oriented behaviors respectively. Across the six training sessions, rats that

received CNO did not display significant differences in the number or latency of lever presses (**Fig 4.3A-B:** mixed-effects model: $p > 0.05$) or magazine entry number and latency (**Fig 4.3C-D:** mixed-effects model: $p > 0.05$) compared to Veh controls. The PavCA index score, which gives a measure of sign- versus goal-tracking bias by incorporating the number, latency, and probability of lever presses and magazine entries during CS presentations (see ***Experimental Design and Statistical Analysis*** session for PavCA index score calculation), did not differ between CNO and Veh treated rats (**Table 4.1**: mixed-effects model, $p > 0.05$). This would suggest that overall, the behavior response bias toward the lever or magazine**,** and therefore, the levels of incentive and predictive value attribution to the cue, were not impacted by vHPC-NAc inhibition during the acquisition of PavCA. Nonetheless, there was a main effect of session for all measures, suggesting that both treatment groups had a progressive change in their behavioral responses, consistent with learning predictive and incentive associations with the lever-cue (**Fig 4.2A-D:** mixed-effects model: main effect of session, $p < 0.05$).

In order to determine whether inhibition of vHPC-NAc can affect the expression or performance of sign-and goal-tracking behavior, we subjected all rats to a cross-treatment PavCA test session in which rats that had received Veh throughout acquisition would receive CNO, and those who received CNO would now receive Veh. For both groups, we compared the behavioral responses of Session 6 (Pre) to their behavioral responses on the cross-treatment test session (Cross-Tx). We found that inhibition of vHPC-NAc for the first time after PavCA acquisition did not affect the expression of sign- or goal-tracking behavior, as measured by the number and latency

of lever presses (**Fig 4.3E-F:** paired t-tests: $p > 0.05$) or magazine entries (**Fig 4.3G-H:** paired t-tests: $p > 0.05$) in the Veh group. Similarly, we found that ceasing inhibition of CNO by giving Veh prior to the PavCA test did not affect the number or latency of lever presses (**Fig 4.3E-F:** paired t-tests: $p > 0.05$) or magazine entries (**Fig 4.3G-H:** paired t-tests: $p > 0.05$) for the CNO group.

It is possible that inhibition of vHPC-NAc could selectively impact either STs and GTs, and such an effect would be difficult to detect by analyzing the entire cohort. Therefore, based on their PavCA index score on Session 6, rats were classified as either STs (score ≥ 0.3; n = 14), GTs (score ≤ -0.3; n = 18), or intermediate responders (-0.3 < score < 0.3; n = 10; not included in the analysis), and the cross-treatment PavCA test was analyzed by phenotype (**Fig 4.4)**. Again, we compared the behavioral responses of Session 6 (Pre) to their behavioral responses on the cross-treatment test session (Cross-Tx) for both STs and GTs in the CNO and Veh groups. We found that ceasing inhibition of vHPC-NAc significantly decreased the number of lever presses for STs that had received CNO during PavCA acquisition (n = 8) (**Fig 4.4A:** paired t-test: $p = 0.03$) but did not affect the latency to lever press (**Fig 4.4B:** paired t-test: $p = 0.65$), suggesting that inhibition of vHPC-NAc may have been increasing sign-tracking behavior within the STs in the CNO group. On the other hand, for GTs (n = 7) ceasing inhibition of vHPC-NAc did not affect the number of magazine entries (**Fig 4.4C:** paired t-tests: $p = 0.17$). The latency to enter the magazine slightly decreased, though this effect did not reach statistical significance (**Fig 4.4D:** paired t-test: $p = 0.06$). This finding may similarly suggest that inhibition of vHPC-NAc during PavCA acquisition may have been slightly suppressing goal-tracking behavior within the GTs receiving CNO. Overall,

these results suggest that decreased activity of vHPC-NAc during PavCA may be increasing sign-tracking in STs and suppressing goal-tracking in GTs, though this effect might be somewhat subtle. We did not find any significant differences or trends for STs (n = 6) and GTs (n = 11) receiving CNO for the first time in the cross-treatment session in the number or latency of lever presses and magazine entries (**Fig 4.4A-D:** paired t-tests: $p > 0.05$). This suggests that once STs and GTs have acquired their learned responses under regular conditions, inhibition of vHPC-NAc does not affect their performance.

***Experiment 2: Effects of chemogenetic excitation of the vHPC-NAc during PavCA***

To expand upon our previous findings and further examine the role of the vHPC-NAc projection in biasing sign- and goal-tracking behavior, a separate cohort of rats expressing an excitatory Cre-dependent hM3D-Gq DREADD selectively in NAc-projecting vHPC neurons **(Fig 4.1)** underwent a PavCA procedure with either CNO (3 mg/kg, IP) or Veh (6% DMSO: 1 ml/kg, IP) administered before testing **(Fig 4.2)**. Compared to Veh controls, CNO treated rats exhibited a slower increase in the number of lever presses (**Fig 4.5A:** mixed-effects model: session x group interaction, $p = 0.0013$), as well as a slower decrease in lever press latency (**Fig 4.5B:** mixed-effects model: session x group interaction, $p = 0.0005$) over the course of PavCA training. However, the effect of CNO was only seen in sign-tracking behavior, as the number and latency of magazine entries were not significantly different compared to Veh treated rats (**Fig 4.5C-D:** mixed-effects model: no effect, $p > 0.05$). Furthermore, our analysis found that there were no main effects of session for the number or latency of magazine entries (**Fig 4.5C-D:** mixed-effects model: no effect of session, $p > 0.05$), but there were for the

number and latency of lever presses (**Fig 4.5A-B:** mixed-effects model: main effect of session, $p < 0.05$), suggesting that goal-tracking was not the predominantly learned response in this cohort of rats. Finally, consistent with greater sign-tracking behavior, the PavCA index score (see ***Experimental Design and Statistical Analysis*** session for PavCA index score calculation) significantly differed between CNO and Veh treated rats (**Table 4.2:** mixed-effects model: session x group interaction, $p = 0.037$). Rats in the Veh group exhibited greater lever-bias compared to CNO rats (more positive PavCA scores), indicating that the level of incentive salience attribution to the lever-cue may have been impacted in the CNO group. Overall, these findings suggest that excitation of the vHPC-NAc projection disrupts the acquisition of sign-tracking behavior without directly impacting goal-tracking. Excitation of vHPC-NAc does not necessarily block sign-tracking, but more seems to delay its acquisition, as evidenced by the sharp increase in lever presses on the last day of training (**Fig 4.5A)**.

To determine whether excitation of vHPC-NAc can affect the expression or performance of sign- and goal-tracking behavior, we subjected all rats to the same cross-treatment PavCA test session done in Experiment 1. We found that ceasing CNO treatment by giving Veh in the cross-treatment PavCA session did not impact the expression of sign- or goal-tracking behavior, as measured by the number and latency of lever presses (**Fig 4.5E-F:** paired t-tests: $p > 0.05$) or magazine entries (**Fig 4.5G-H:** paired t-tests: $p > 0.05$). Giving CNO for the first time to rats that received Veh during acquisition also did not significantly affect the number or latency of lever presses (**Fig 4.5E-F:** paired t-tests: $p > 0.05$) or magazine entries (**Fig 4.5G-H:** paired t-tests: $p >$

0.05) for the CNO group. There was a slight increase in the number of lever presses, though this effect did not reach significance (**Fig 4.5E:** paired t-test: p = 0.058).

### *Experiment 3: Effects of chemogenetic inhibition vs excitation of the vHPC-NAc during PavCA*

For our last experiment, we wanted to directly compare the effects of inhibition and excitation of the vHPC-NAc projection on sign- and goal-tracking behavior. One last separate cohort of rats expressing either an inhibitory Cre-dependent hM4D-Gq DREADD or an excitatory Cre-dependent hM3D-Gq DREADD selectively in NAc-projecting vHPC neurons **(Fig 4.1)**, underwent a PavCA procedure with CNO (3 mg/kg, IP) or Veh (6% DMSO: 1 ml/kg, IP) administered before testing **(Fig 4.2)**. Interestingly, only inhibition of vHPC-NAc had a significant effect on the acquisition of PavCA behavior. Compared to both Gq-CNO rats and Veh controls, Gi-CNO rats exhibited greater number of lever presses (**Fig 4.6A:** mixed-effects model: session x group interaction, p = 0.0005) and lower latency (**Fig 4.6B:** mixed-effects model: session x group interaction, p = 0.0032) over the course of PavCA training, indicating an enhanced acquisition of sign-tracking behavior. No group differences were found in the acquisition of goal-tracking behavior, however for both the number (**Fig 4.6C:** mixed-effects model: session x group interaction, p = 0.0004) and latency (**Fig 4.6D:** mixed-effects model: session x group interaction, p < 0.0001) of magazine entries there was an interaction of session and group, suggesting differences in the rate of acquisition. Overall, mid-way through training, the Gi-CNO group exhibited a sharper decrease in the number of magazine entries and increase in latency compared to Gq-CNO rats and Veh controls. Consistent with differences in lever presses and magazine entries, Gi-

CNO rats exhibited greater lever-bias – particularly compared to Veh controls – as seen by a more positive PavCA index score (see ***Experimental Design and Statistical Analysis*** session for PavCA index score calculation) (**Table 4.3:** mixed-effects model: session x group interaction, $p < 0.0001$). For all lever- and magazine-oriented behaviors, there was a main effect of session, which typically suggests that both sign- and goal-tracking responses were learned (**Fig 4.6A-D:** mixed-effects model: main effect of session, $p < 0.05$), though at a different rate in the Gi-CNO group. Our findings suggest that in this cohort of rats, inhibition of vHPC-NAc enhanced the acquisition of sign-tracking and somewhat hindered goal-tracking behavior. The behavior response bias toward the lever and magazine**,** and therefore the levels of incentive and predictive value attribution to the cue seemed to be impacted by vHPC-NAc reduced activity.

Similar to Experiments 1 and 2, the expression and performance of PavCA was tested using a cross-treatment test session in which CNO treatment was ceased, and rats received Veh. Because the Veh group had a mixture of Gi- and Gq-expressing rats, cross-treatment test session data from this group were not included. Consistent with the acquisition data, we found that ceasing CNO treatment resulted in a slight increase in lever press latency for the Gi-CNO rats (**Fig 4.6F:** paired t-test, $p = 0.053$). Though it did not reach significance, this finding suggests that CNO treatment during acquisition enhanced sign-tracking and was reduced once treatment was ceased. On the other hand, ceasing CNO also caused a significant decrease in the number of magazine entries for Gq-CNO rats (**Fig 4.6G:** paired t-test: $p = 0.0081$), which may also suggest that increased activity in vHPC-NAc promotes goal-tracking while decreased activity

suppresses goal-tracking**.** No other significant effects or trends were found for number of lever presses and magazine entry latency in the cross-treatment test session.

**Optically-evoked EPSC recordings for DREADD-(Gi) *ex vivo* validation**

Although we confirmed the viral expression of DREADDs in vHPC terminals within the NAc through immunohistochemical assays, we also wanted to test whether these receptors were functional in response to CNO. To do this, we used a small subset of rats (n = 3) for intracranial viral injections of retrograde Cre-recombinase in the NAc and Cre-dependent inhibitory DREADD in the vHPC, plus an additional viral injection of channelrhodopsin into the vHPC. This would allow for *ex vivo* optogenetic stimulation of DREADD-expressing vHPC axon terminals during whole-cell recordings of MSNs in the NAc before and after CNO bath application. Since the majority of vHPC inputs innervate the medial shell portion of the NAc, we performed all our recordings in this area. To determine whether CNO could decrease synaptic transmission of vHPC-NAc, we analyzed the amplitude of optically evoked EPSCs before and after adding CNO (10 or 20 μM). We first studied basal synaptic transmission by delivering optical pulses at varying intensities ranging from 20% to 100% of the LED capacity in 20% increments. Following 5 min of CNO application, we delivered optical pulses at 100% LED intensity. Using 100% LED intensity, EPSC amplitudes before and after CNO were compared. The EPSC amplitude after 10 μM CNO application was significantly lower than before CNO (**Table 4.4**: paired t-test: $p = 0.0381$), though it was not significantly different after 20 μM CNO application (**Table 4.4**: paired t-test: $p = 0.4604$). Additionally, in a subset of cells (n = 3), 10 μM CNO was allowed to wash out for at least 5 min and EPSC amplitude did not recover. Partial recovery of baseline neuronal activity has been

previously reported following 4 min (Shipman et al., 2019), though others have reported that at least 60 min are necessary (Pati et al., 2019). Although the reduction reported here may be a result of CNO it is also possible that it was due to a decrease in neuronal health and quality of the seal. See **Table 4.4** for data summary of all cell recordings.

## Discussion

In Experiment 1, we found that inhibition of vHPC-NAc did not affect the acquisition of sign- or goal-tracking behavior, but once vHPC-NAc inhibition was ceased sign-tracking behavior decreased selectively in STs. In Experiment 2, we found that excitation of vHPC-NAc significantly delayed the acquisition of sign-tracking without affecting goal-tracking. Finally, in Experiment 3 which included both inhibition and excitation of vHPC-NAc, inhibition resulted in both an increase in sign-tracking acquisition as well as reduced goal-tracking, whereas excitation had no behavioral effect. Collectively, the findings across all three experiments are inconsistent but not contradictory. The effects or absence of effects may be due to differences in the baseline bias across all three rat cohorts that can either highlight or overshadow the effects of vHPC-NAc manipulation. That being said, this can also suggest that the vHPC-NAc projection may play more of a modulatory role than a deterministic role in influencing ST/GT phenotypes. Furthermore, it is possible that the role of vHPC-NAc may be stronger in rats with a natural bias toward sign-tracking. Despite their differences, the findings from all 3 experiments are consistent with the interpretation that decreased activity in vHPC-NAc may promote sign-tracking behavior and impair goal-tracking, while increased activity may hinder the acquisition of sign-tracking and promote goal-tracking.

In Experiment 1, we found that inhibition of the vHPC-NAc projection during PavCA did not significantly impact the acquisition of sign- or goal-tracking responses (**Fig 4.3 A-D**). However, we found that during the cross-treatment PavCA test session, ceasing vHPC-NAc inhibition by removing CNO treatment caused a significant decrease in the number of lever presses, specifically in rats classified as STs (**Fig 4.4 A**). Furthermore, selectively in GTs, the latency to enter the magazine slightly decreased when treatment with CNO was removed in the cross-treatment test session (**Fig 4.4 D**). These two findings suggest that for rats that developed a strong lever or magazine bias during training, inhibition of vHPC may have influenced their preferred behaviors. For STs, inhibition may have promoted sign-tracking, while for GTs, inhibition may have suppressed goal-tracking. It is unclear why this effect was not observed during acquisition, but the effect on the acquisition of sign-tracking may have been too subtle to detect given the general behavior bias in this cohort of rats. Focusing on the Veh group (14 out of 21 had a negative PavCA index), the number of lever presses were low, particularly compared to the other two experiments, suggesting that this group of rats was not very biased toward sign-tracking. An increase in lever presses may have been difficult to detect in rats that were not naturally biased toward sign-tracking, which might explain why the effect only manifested in STs during the cross-treatment session as a decline in lever presses. Furthermore, the fact that we did not see an effect in STs (**Fig 4.4 A-B**) or GTs (**Fig 4.4 C-D**) from the Veh group that received CNO on the test session suggests that this projection did not impact PavCA expression once it had been established under normal conditions.

In Experiment 2, we tested the effect of excitation of the vHPC-NAc projection during PavCA in a small cohort of rats. We found that excitation of this projection resulted in a delayed sign-tracking response (**Fig 4.5 A-B**), while no effect was seen in goal-tracking (**Fig 4.5 C-D**). These findings are consistent with the results of Experiment 1. If ceasing vHPC-NAc inhibition reduced sign-tracking in STs in Experiment 1, then excitation of this projection may be expected to have a similar effect. This is particularly interesting because in the Veh group, all but one rat were STs, which may suggest that the rats in Experiment 2 may have been more naturally biased toward sign-tracking and therefore manipulation of vHPC-NAc may have been more likely to influence this group of rats. However, it is very important to note that only 4 rats were in the Veh group, which makes it difficult to draw definitive conclusions.

Finally, in Experiment 3 we directly compared excitation to inhibition of vHPC-NAc during PavCA in a modest size cohort of rats. This time, we found that inhibition of vHPC-NAc significantly increased sign-tracking behavior (**Fig 4.6 A-B**), and impaired goal-tracking (**Fig 4.6 C-D**). This was accompanied by a slight increase in lever press latency for Gi-CNO rats in the cross-treatment test session (**Fig 4.6 F**), and by a decrease in magazine entry number for the Gq-CNO group once CNO treatment was ceased (**Fig 4.6 G**). Nonetheless, during PavCA acquisition Gq-CNO rats did not significantly differ from Veh controls (**Fig 4.6 A-D**). Together, the findings in this experiment suggest that inhibition of vHPC-NAc enhanced sign-tracking and impaired goal-tracking. Surprisingly, excitation of vHPC-NAc did not suppress sign-tracking as it did in Experiment 2, though ceasing CNO reduced goal-tracking behavior. Once again, it is important to note that out of all Veh groups, this was the most balanced with 4 STs

and 3 GTs by the end of training, which most likely resulted in lever presses being at a midpoint compared to the other two experiments. A more well-balanced group might have allowed for the increase in lever presses to be observed during acquisition in the Gi-CNO group that could have been overshadowed in Experiment 1. The cause of the lack of sign-tracking suppression in the Gq-CNO group is not clear, but excitation of vHPC-NAc in Experiment 2 only reduced sign-tracking to a level similar to the baseline in Experiment 3. This may suggest that a floor effect may have been reached for the effect of Gq-CNO on sign-tracking in Experiment 3.

Reduced activity of vHPC-NAc as a feature of STs and sign-tracking behavior is not completely unexpected. It has been previously hypothesized that part of the ST phenotype involves reacting strongly to conditioned cues regardless of the context in which they are encountered, whereas GTs more effectively use contextual cues to modulate their conditioned emotional responses (Pitchers et al., 2017; María-Ríos and Morrow, 2020). Evidence for this can be observed during cue- and context-induced reinstatement of drug-seeking. Following self-administration of cocaine and nicotine, STs exhibit increased cue-induced reinstatement compared to GTs (Saunders and Robinson, 2011; Versaggi et al., 2016). However, during context-induced reinstatement of cocaine, GTs exhibit increased hyperactivity and greater cocaine seeking than STs (Saunders et al., 2014). A study using discriminative stimuli or “occasion setters” which are thought to closely resemble contextual cues also found that GTs exhibited greater cocaine reinstatement (Pitchers et al., 2017), further indicating a distinct influence of context versus cues over their behaviors. The vHPC is thought to be necessary for context-induced reinstatement of drug-seeking (Lasseter et al., 2010), and this is at

least in part mediated through input to the NAc (Zhou et al., 2019). This view is further supported by disconnection lesions between the whole hippocampus and NAc shell, which result in impaired context-dependent cue retrieval (Ito et al., 2008). Interestingly, neuronal engrams in the vHPC are thought to encode spatial information that is subsequently decoded by the NAc for context-driven conditioned responses (Zhou et al., 2019). Therefore, reduced vHPC-NAc activity is consistent with blunted context-specific reward-related responses, such as those seen in STs. Furthermore, stimulation of vHPC-NAc has been found to induce conditioned place preference in mice (Britt et al., 2012; LeGates et al., 2018). It is possible that excitation of this projection may have caused a more generalized reward state in the PavCA chamber and reduced the level of incentive salience attributed to the discrete lever cue. Future experiments could be performed to directly measure evidence of conditioned place preference in sign-tracking versus goal-tracking rats during vHPC-NAc excitation.

Although no other study has specifically examined the role of vHPC-NAc in sign- and goal-tracking behavior, one study found that lesioning the whole hippocampus facilitated sign-tracking toward a conditioned stimulus (Ito et al., 2005). They hypothesize that this could have been due to a loss of contextual inhibition which results in the release of excitatory control over conditioned behaviors (Ito et al., 2005), all of which is aligned with the findings reported here. However, another study found that sign-tracking was severely impeded by lesions restricted to the vHPC, while goal-tracking was increased during PavCA (Fitzpatrick et al., 2016). In this study, the investigators also found that vHPC lesions caused a decrease of NAc dopamine metabolites selectively in STs. Several studies have demonstrated that the

glutamatergic projection from the vHPC to the NAc is a potent driver of mesolimbic dopamine release from the ventral tegmental area (VTA) to the NAc (Lipska et al., 1992; Wu and Brudzynski, 1995; Blaha et al., 1997; Legault et al., 2000; Taepavarapruk et al., 2000; Floresco et al., 2001). It is known that the acquisition of sign-tracking is dependent on dopamine in the NAc, while goal-tracking appears to be dopamine-independent (Flagel et al., 2011; Saunders and Robinson, 2012). The authors hypothesize that the loss of this vHPC to NAc connection during Pavlovian conditioning blocked the attribution of incentive salience and favored the development of goal-tracking behavior, and that this could be due at least in part to dopamine dysregulation. However, the effects of a lesion are not necessarily comparable to the temporary inhibition induced by DREADD, especially when the DREADD expression is restricted to one specific efferent pathway. Since our results trend toward the opposite direction than this lesion study, it is probable that the impact of vHPC lesions on sign- and goal-tracking may have been due to more widespread downstream effects not necessarily dependent on this specific projection to the NAc.

Although inhibitory DREADDs reduce neuronal activity, they do not completely abolish natural patterns of neuronal activity. The vHPC is thought to gate activity states of dopamine neurons by regulating spontaneous or ‘tonic’ firing rate of VTA neurons. This is mediated through activation of NAc GABAergic neurons which subsequently inhibit GABAergic ventral pallidum neurons, thereby disinhibiting their hold on dopaminergic VTA neurons (Lodge and Grace, 2006). This spontaneous firing state seems to regulate the ability of VTA neurons to transition into ‘phasic’ dopamine release that is typically driven by behavioral responses. Although the vHPC is a player in this

process, other afferents to the NAc such as the pedunculopontine tegmental nucleus and the laterodorsal tegmentum can directly drive phasic dopamine release in response to reward-related cues (Lodge and Grace, 2006; Grace et al., 2007). It is known that STs exhibit greater cue-evoked phasic dopamine release during PavCA compared to GTs (Flagel et al., 2011). Because the gating role of the vHPC on NAc dopamine release may not be fully tied to behavioral responses, it may not directly modulate transmission during cue presentations. If this was the case, we would have expected vHPC-NAc excitation to enhance cue-evoked dopamine transmission and increase sign-tracking, and vice versa with vHPC-NAc inhibition, which was the opposite of what we found. Our findings might suggest that inhibition of vHPC-NAc regulates more spontaneous or tonic dopamine signaling during PavCA as opposed to directly modulating phasic dopamine release during cue presentations. Whether changes in tonic dopamine signaling could directly impact incentive salience is less clear. Nonetheless, because of differences in dopamine transporter (DAT) expression and dopamine re-uptake between STs and GTs in the NAc, it has been previously suggested that the impact of these differences on tonic dopamine levels may be linked to sign- and goal-tracking behavior (Singer et al., 2016). Specifically, *ex vivo* voltammetry studies found that STs clear dopamine from the synapse at a faster rate than GTs due to greater DAT expression (Singer et al., 2016). The authors suggest that lower DAT expression in GTs may result in higher levels of tonic dopamine and degrade the temporal control of discrete conditioned stimuli. This further favors contextual conditioning and ultimately results in distinct forms of conditioned responding between STs and GTs (Singer et al., 2016). Although this is independent of vHPC modulation, it

supports the idea that higher tonic dopamine in the NAc may be a characteristic of GTs whereas more phasic dopamine release may be more present in STs. Similarly, our findings indirectly suggest that lower vHPC-NAc activity – and consequent lower tonic dopamine – may result in a greater propensity to sign-track and a lower goal-tracking response. However it is also important to note that although NAc plasticity is thought to be important for reward learning and heavily influenced by dopamine, vHPC-NAc plasticity in reward-related behaviors can be dopamine-independent (LeGates et al., 2018), and therefore the effects seen on sign- and goal-tracking behavior in these experiments may not necessarily depend on dopamine signaling.

It has been demonstrated that CNO can have non-specific effects in the brain that can impact behavioral measures (MacLaren et al., 2016; Gomez et al., 2017). We attempted to control for this by adding a group expressing mCherry protein in the vHPC under the same promoter as the DREADD virus and administering the same dose of CNO (3 mg/kg, IP) as the experimental groups during PavCA. Following statistical analyses between control CNO treated rats and DREADD Veh treated rats, we found that in Experiments 1 and 3, the two groups were significantly different in lever presses and magazine entries (see **Tables 4.1-4.3)**. However, upon histological examination, we found extremely high levels of mCherry expression in the control animals that were visible with the naked eye. A previous study found that compared to other monomeric red fluorescent proteins, mCherry caused higher levels of toxicity as measured by a decrease in eye size during development in tadpoles (Shemiakina et al., 2012). Another study in neuron cell cultures from the hippocampus found large aggregates in mCherry-transfected neurons which can typically lead to neuronal death. Again, compared to

other red fluorescent proteins, such as Crimson, mCherry was more toxic leading to lower cell survival rates (Ning et al., 2022). Thus, it is possible that the effects seen in CNO treated control rats could have also been caused by toxicity at the injection site by mCherry and not CNO.

Our data suggest that decreased activity in vHPC-NAc may promote sign-tracking behavior and impair goal-tracking, while increased activity may hinder the acquisition of sign-tracking and promote goal-tracking. It is clear that STs and GTs process contextual reward information differentially. Thus, these findings support the role of the vHPC-NAc as modulator of conditioned responses to discrete cues by means of context-specific reward information. Decreased activity in this projection may contribute to the increased cue reactivity exhibited by STs that is in part thought to predispose them to addiction like behaviors. In the next chapter, we will explore the vHPC-NAc projection from a synaptic level to address whether the findings reported in this chapter correlate with baseline differences in synaptic transmission efficacy. Understanding how this projection can modulate individual differences in reward learning and cue sensitivity in a basic model of associative learning can further inform how it becomes altered in pathological states.

## References


Alvandi MS, Bourmpoula M, Homberg JR, Fathollahi Y (2017) Association of contextual cues with morphine reward increases neural and synaptic plasticity in the ventral hippocampus of rats. Addict Biol 22:1883–1894.

Bagot RC, Parise EM, Peña CJ, Zhang H-X, Maze I, Chaudhury D, Persaud B, Cachope R, Bolaños-Guzmán CA, Cheer JF, Deisseroth K, Han M-H, Nestler EJ (2015) Ventral hippocampal afferents to the nucleus accumbens regulate susceptibility to depression. Nat Commun 6:7062.

Baharlouei N, Sarihi A, Komaki A, Shahidi S, Haghparast A (2015) Blockage of acquisition and expression of morphine-induced conditioned place preference in rats due to activation of glutamate receptors type II/III in nucleus accumbens. Pharmacol Biochem Behav 135:192–198.

Barr JL, Forster GL, Unterwald EM (2014) Repeated cocaine enhances ventral hippocampal-stimulated dopamine efflux in the nucleus accumbens and alters ventral hippocampal NMDA receptor subunit expression. J Neurochem 130:583–590.

Bell K, Duffy P, Kalivas PW (2000) Context-specific enhancement of glutamate transmission by cocaine. Neuropsychopharmacology 23:335–344.

Berridge KC, Robinson TE, Aldridge JW (2009) Dissecting components of reward: 'liking', 'wanting', and learning. Curr Opin Pharmacol 9:65–73.

Blaha CD, Yang CR, Floresco SB, Barr AM, Phillips AG (1997) Stimulation of the ventral subiculum of the hippocampus evokes glutamate receptor-mediated changes in dopamine efflux in the rat nucleus accumbens. Eur J Neurosci 9:902–911.

Britt JP, Benaliouad F, McDevitt RA, Stuber GD, Wise RA, Bonci A (2012) Synaptic and behavioral profile of multiple glutamatergic inputs to the nucleus accumbens. Neuron 76:790–803.

Brog JS, Salyapongse A, Deutch AY, Zahm DS (1993) The patterns of afferent innervation of the core and shell in the "accumbens" part of the rat ventral striatum: immunohistochemical detection of retrogradely transported fluoro-gold. J Comp Neurol 338:255–278.

Ciano PD, Cardinal RN, Cowell RA, Little SJ, Everitt BJ (2001) Differential involvement of NMDA, AMPA/Kainate, and dopamine receptors in the nucleus accumbens core in the acquisition and performance of Pavlovian approach behavior. J Neurosci 21:9471–9477.

Dalley JW, Lääne K, Theobald DEH, Armstrong HC, Corlett PR, Chudasama Y, Robbins TW (2005) Time-limited modulation of appetitive Pavlovian memory by

D1 and NMDA receptors in the nucleus accumbens. Proc Natl Acad Sci U S A 102:6189–6194.

Fitzpatrick CJ, Creeden JF, Perrine SA, Morrow JD (2016) Lesions of the ventral hippocampus attenuate the acquisition but not expression of sign-tracking behavior in rats. Hippocampus 26:1424–1434.

Fitzpatrick CJ, Gopalakrishnan S, Cogan ES, Yager LM, Meyer PJ, Lovic V, Saunders BT, Parker CC, Gonzales NM, Aryee E, Flagel SB, Palmer AA, Robinson TE, Morrow JD (2013) Variation in the form of Pavlovian conditioned approach behavior among outbred male Sprague-Dawley rats from different vendors and colonies: sign-tracking vs. goal-tracking. PLOS ONE 8:e75042.

Flagel SB, Clark JJ, Robinson TE, Mayo L, Czuj A, Willuhn I, Akers CA, Clinton SM, Phillips PEM, Akil H (2011) A selective role for dopamine in stimulus-reward learning. Nature 469:53–57.

Floresco SB, Todd CL, Grace AA (2001) Glutamatergic Afferents from the hippocampus to the nucleus accumbens regulate activity of ventral tegmental area dopamine neurons. J Neurosci 21:4915–4922.

Gomez JL, Bonaventura J, Lesniak W, Mathews WB, Sysa-Shah P, Rodriguez LA, Ellis RJ, Richie CT, Harvey BK, Dannals RF, Pomper MG, Bonci A, Michaelides M (2017) Chemogenetics revealed: DREADD occupancy and activation via converted clozapine. Science 357:503–507.

Grace AA, Floresco SB, Goto Y, Lodge DJ (2007) Regulation of firing of dopaminergic neurons and control of goal-directed behaviors. Trends Neurosci 30:220–227.

Hearing M, Graziane N, Dong Y, Thomas MJ (2018) Opioid and psychostimulant plasticity: targeting overlap in nucleus accumbens glutamate signaling. Trends Pharmacol Sci 39:276–294.

Ito R, Everitt BJ, Robbins TW (2005) The hippocampus and appetitive Pavlovian conditioning: Effects of excitotoxic hippocampal lesions on conditioned locomotor activity and autoshaping. Hippocampus 15:713–721.

Ito R, Robbins TW, Pennartz CM, Everitt BJ (2008) Functional interaction between the hippocampus and nucleus accumbens shell is necessary for the acquisition of appetitive spatial context conditioning. J Neurosci 28:6950–6959.

Kaddis FG, Uretsky NJ, Wallace LJ (1995) DNQX in the nucleus accumbens inhibits cocaine-induced conditioned place preference. Brain Res 697:76–82.

Keralapurath MM, Briggs SB, Wagner JJ (2017) Cocaine self-administration induces changes in synaptic transmission and plasticity in ventral hippocampus. Addict Biol 22:446–456.

Lasseter HC, Xie X, Ramirez DR, Fuchs RA (2010) Sub-region specific contribution of the ventral hippocampus to drug context-induced reinstatement of cocaine-seeking behavior in rats. Neuroscience 171:830–839.

Layer RT, Uretsky NJ, Wallace LJ (1993) Effects of the AMPA/kainate receptor antagonist DNQX in the nucleus accumbens on drug-induced conditioned place preference. Brain Res 617:267–273.

LeGates TA, Kvarta MD, Tooley JR, Francis TC, Lobo MK, Creed MC, Thompson SM (2018) Reward behaviour is regulated by the strength of hippocampus–nucleus accumbens synapses. Nature 564:258–262.

Legault M, Rompré P-P, Wise RA (2000) Chemical stimulation of the ventral hippocampus elevates nucleus accumbens dopamine by activating dopaminergic neurons of the ventral tegmental area. J Neurosci 20:1635–1642.

Lipska BK, Jaskiw GE, Chrapusta S, Karoum F, Weinberger DR (1992) Ibotenic acid lesion of the ventral hippocampus differentially affects dopamine and its metabolites in the nucleus accumbens and prefrontal cortex in the rat. Brain Res 585:1–6.

Lodge DJ, Grace AA (2006) The hippocampus modulates dopamine neuron responsivity by regulating the intensity of phasic neuron activation. Neuropsychopharmacology 31:1356–1361.

Lovic V, Saunders BT, Yager LM, Robinson TE (2011) Rats prone to attribute incentive salience to reward cues are also prone to impulsive action. Behav Brain Res 223:255–261.

MacLaren DAA, Browne RW, Shaw JK, Krishnan Radhakrishnan S, Khare P, España RA, Clark SD (2016) Clozapine N-oxide administration produces behavioral effects in Long–Evans rats: Implications for designing DREADD experiments. eNeuro 3:ENEURO.0219-16.2016.

María-Ríos CE, Morrow JD (2020) Mechanisms of shared vulnerability to post-traumatic stress disorder and substance use disorders. Front Behav Neurosci 14:6.

Meyer PJ, Lovic V, Saunders BT, Yager LM, Flagel SB, Morrow JD, Robinson TE (2012) Quantifying individual variation in the propensity to attribute incentive salience to reward cues. PLOS ONE 7:e38987.

Muir J, Tse YC, Iyer ES, Biris J, Cvetkovska V, Lopez J, Bagot RC (2020) Ventral hippocampal afferents to nucleus accumbens encode both latent vulnerability and stress-induced susceptibility. Biol Psychiatry 88:843–854.

Ning L, Geng Y, Lovett-Barron M, Niu X, Deng M, Wang L, Ataie N, Sens A, Ng H-L, Chen S, Deisseroth K, Lin MZ, Chu J (2022) A bright, nontoxic, and non-

aggregating red fluorescent protein for long-term labeling of fine structures in neurons. Front Cell Dev Biol 10:893468.

Paolone G, Angelakos CC, Meyer PJ, Robinson TE, Sarter M (2013) Cholinergic control over attention in rats prone to attribute incentive salience to reward cues. J Neurosci Off J Soc Neurosci 33:8321–8335.

Pati S, Salvi SS, Kallianpur M, Vaidya B, Banerjee A, Maiti S, Clement JP, Vaidya VA (2019) Chemogenetic activation of excitatory neurons alters hippocampal neurotransmission in a dose-dependent manner. eNeuro 6:ENEURO.0124-19.2019.

Paxinos G, Franklin KBJ (2019) Paxinos and Franklin's the Mouse Brain in Stereotaxic Coordinates. Academic Press.

Pitchers KK, Phillips KB, Jones JL, Robinson TE, Sarter M (2017) Diverse roads to relapse: a discriminative cue signaling cocaine availability is more effective in renewing cocaine seeking in goal trackers than sign trackers and depends on basal forebrain cholinergic activity. J Neurosci 37:7198–7208.

Saunders BT, O'Donnell EG, Aurbach EL, Robinson TE (2014) A cocaine context renews drug seeking preferentially in a subset of individuals. Neuropsychopharmacology 39:2816–2823.

Saunders BT, Robinson TE (2011) Individual variation in the motivational properties of cocaine. Neuropsychopharmacology 36:1668–1676.

Saunders BT, Robinson TE (2012) The role of dopamine in the accumbens core in the expression of Pavlovian-conditioned responses. Eur J Neurosci 36:2521–2532.

Shemiakina I, Ermakova G, Cranfill P, Baird M, Evans RA, Souslova EA, Staroverov DB, Gorokhovatsky AY, Putintseva K, Gorodnicheva TV, Chepurnykh TV, Strukova L, Lukyanov S, Zaraisky A, Davidson M, Chudakov DM, Shcherbo D (2012) A monomeric red fluorescent protein with low cytotoxicity. Nat Commun 3:1204.

Shipman ML, Johnson GC, Bouton ME, Green JT (2019) Chemogenetic silencing of prelimbic cortex to anterior dorsomedial striatum projection attenuates operant responding. eNeuro 6:ENEURO.0125-19.2019.

Singer BF, Guptaroy B, Austin CJ, Wohl I, Lovic V, Seiler JL, Vaughan RA, Gnegy ME, Robinson TE, Aragona BJ (2016) Individual variation in incentive salience attribution and accumbens dopamine transporter expression and function. Eur J Neurosci 43:662–670.

Taepavarapruk P, Floresco SB, Phillips AG (2000) Hyperlocomotion and increased dopamine efflux in the rat nucleus accumbens evoked by electrical stimulation of

the ventral subiculum: role of ionotropic glutamate and dopamine D1 receptors. Psychopharmacology (Berl) 151:242–251.

Turner BD, Kashima DT, Manz KM, Grueter CA, Grueter BA (2018) Synaptic plasticity in the nucleus accumbens: Lessons learned from experience. ACS Chem Neurosci 9:2114–2126.

Versaggi CL, King CP, Meyer PJ (2016) The tendency to sign-track predicts cue-induced reinstatement during nicotine self-administration, and is enhanced by nicotine but not ethanol. Psychopharmacology (Berl) 233:2985–2997.

Williams ES, Manning CE, Eagle AL, Swift-Gallant A, Duque-Wilckens N, Chinnusamy S, Moeser A, Jordan C, Leinninger G, Robison AJ (2020) Androgen-dependent excitability of mouse ventral hippocampal afferents to nucleus accumbens underlies sex-specific susceptibility to stress. Biol Psychiatry 87:492–501.

Wu M, Brudzynski SM (1995) Mesolimbic dopamine terminals and locomotor activity induced from the subiculum. Neuroreport 6:1601–1604.

Zhou Y, Zhu H, Liu Z, Chen X, Su X, Ma C, Tian Z, Huang B, Yan E, Liu X, Ma L (2019) A ventral CA1 to nucleus accumbens core engram circuit mediates conditioned place preference for cocaine. Nat Neurosci 22:1986–1999.

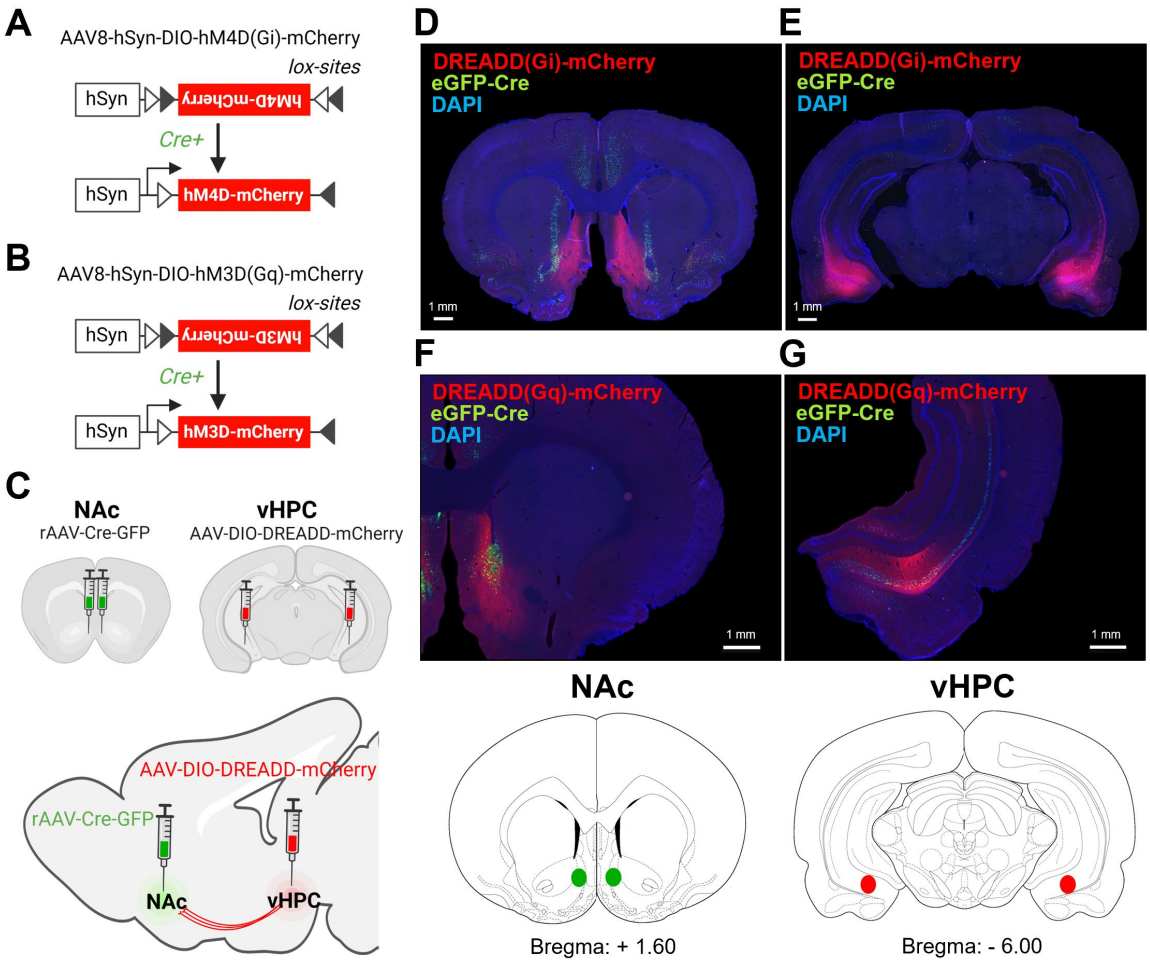


**Figure 4.1**. *Cre-dependent Designer Receptors Exclusively Activated by Designer Drugs (DREADDs) expression in the ventral hippocampus (vHPC) and nucleus accumbens (NAc).* Representative diagram of viral vectors (AAV) containing double-floxed Cre-dependent **A)** inhibitory: hM4D(Gi) and **B)** excitatory: hM3D(Gq) DREADDs. Both viruses contained an mCherry reporter to verify DREADD expression upon Cre-lox recombination. **C)** AAV injections: A retrograde Cre-eGFP was injected into the NAc, and a Cre-dependent DREADD-mCherry was injected into the vHPC to target the vHPC-NAc projection. eGFP+ neurons in the vHPC projecting to the NAc should selectively express DREADDs. Inhibitory **(D-E)** and excitatory **(F-G)** DREADD expression can be seen through mCherry immunohistochemistry in eGFP+ cell bodies within the vHPC and in vHPC axon terminals in the NAc. Created with BioRender.com (A-C).

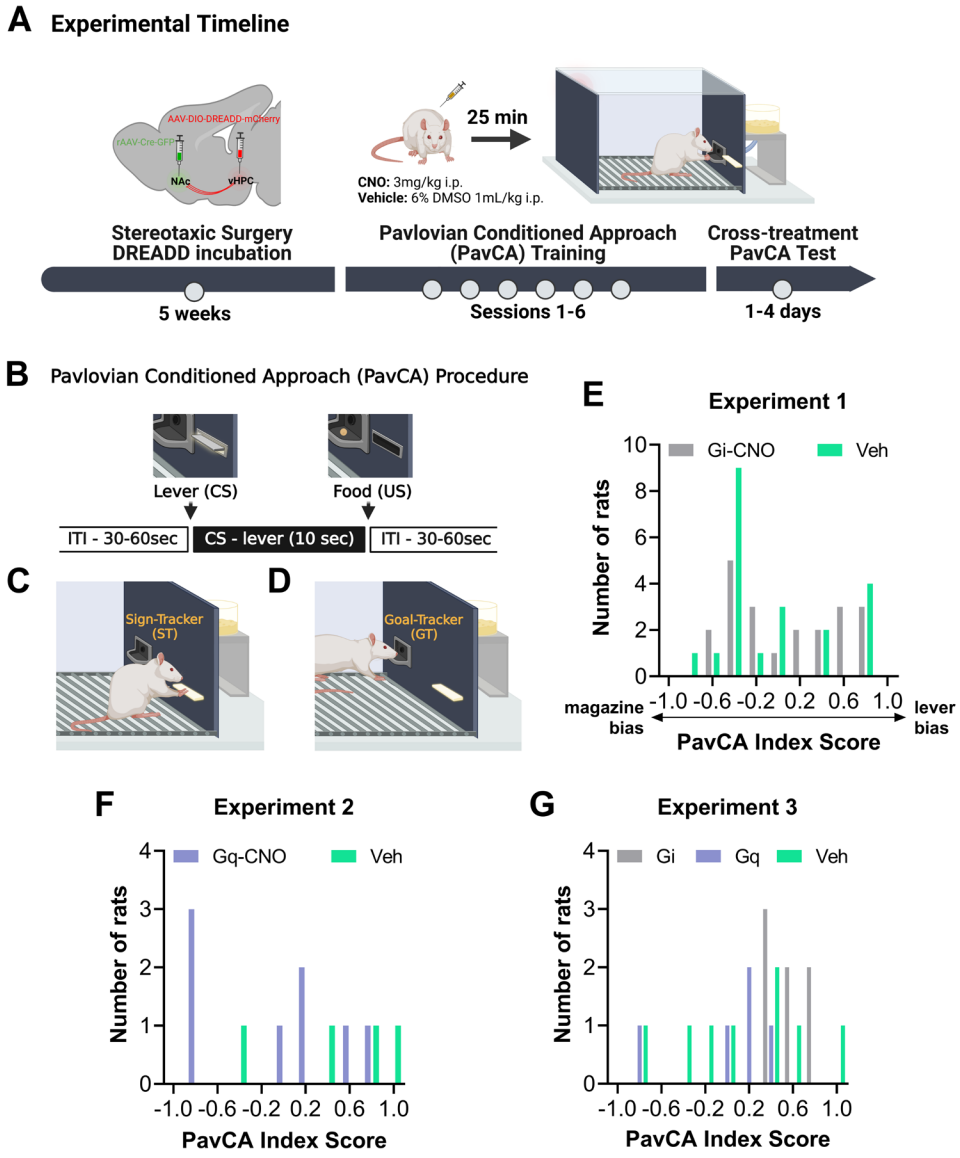


**Figure 4.2**. *Experimental timeline and phenotypic distribution across all three experiments.* **A)** A dual-viral vector approach of Cre-dependent DREADDs was used. Rats underwent stereotaxic surgery to deliver viruses into the nucleus accumbens (NAc) and ventral hippocampus (vHPC). Following a 5-week incubation period, rats underwent six sessions of a daily Pavlovian conditioned approach (PavCA) procedure with either clozapine-n-oxide (CNO; 3 mg/kg, IP) or Veh on-board for time-selective chemogenetic inhibition or excitation of the vHPC to NAc projection. In the cross-treatment PavCA test, rats that received Veh during acquisition received CNO for the first time, and those that received CNO were given Veh. **B)** During PavCA, a neutral lever-cue (CS) was presented, and following its retraction a banana food pellet reward (US) was immediately delivered into the magazine. Each session consisted of 25 trials of CS-US pairings (ITI: 30-60 s). No operant response was required for food reward delivery. **C)** Cartoon representation of sign-tracking (lever bias): In response to the CS, STs approach and interact with the lever although no response is necessary for reward delivery. **D)** Cartoon representation of goal-tracking (magazine bias): In response to the CS, GTs approach the magazine which is the site of impending food delivery. **E, F, G)** The PavCA index incorporates the number, latency, and probability of lever presses and magazine entries during CS presentations within a session. A score of +1.0 is absolute sign-tracking, while -1.0 is absolute goal-tracking (0 represents no bias). Session 6 index scores are shown to illustrate the distribution of rats with lever- vs. magazine-bias in control and experimental groups across all three experiments. Created with BioRender.com (A-D).

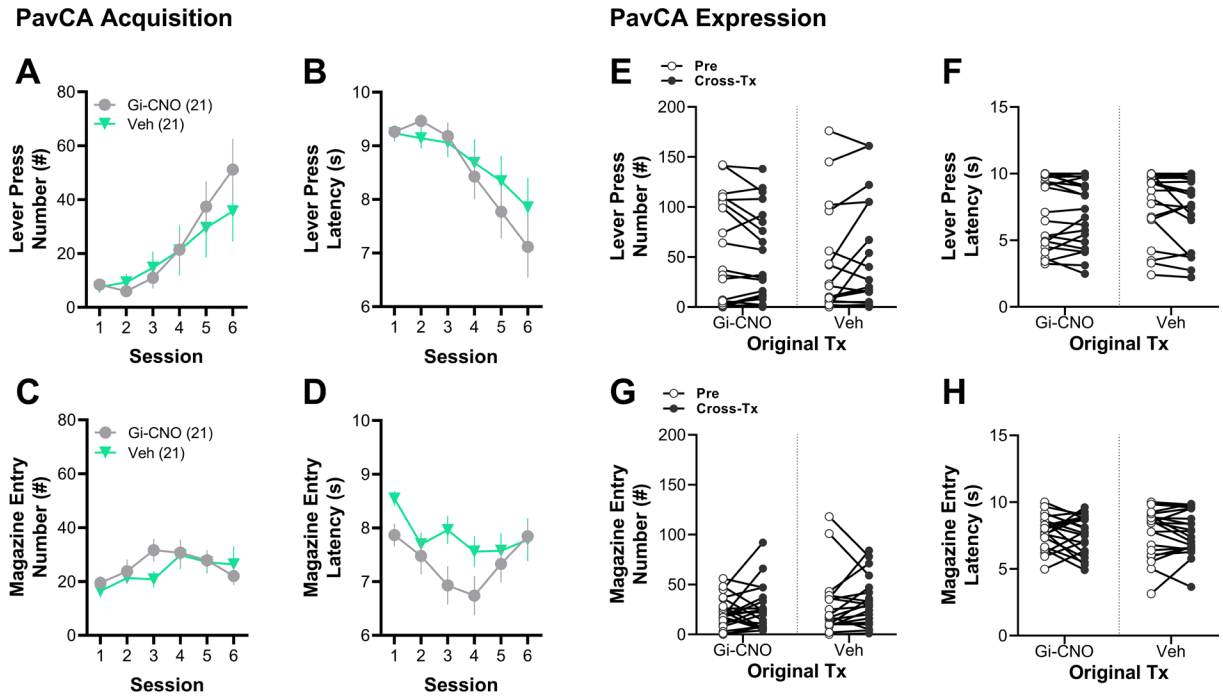


**Figure 4.3.** *Experiment 1: Effects of chemogenetic inhibition of the ventral hippocampus (vHPC) to nucleus accumbens (NAc) projection on Pavlovian conditioned approach (PavCA) behavior.* PavCA Acquisition: Rats expressing an inhibitory Gi-DREADD in vHPC-NAc underwent six sessions of PavCA with either clozapine-N-oxide (CNO; 3 mg/kg, IP) or Veh (6% DMSO; 1 ml/kg, IP) administered prior to testing. No significant differences were found between rats that received CNO and Veh controls in the **(A)** number or **(B)** latency of lever presses during training (mixed-effects model: $p > 0.05$). Magazine entry **(C)** number and **(D)** latency were also not significantly different between the two groups (mixed-effects model: $p > 0.05$). PavCA Expression: Switching treatment did not significantly affect either group in the **(E)** number and **(F)** latency of lever presses (paired t-tests: $p > 0.05$) or in the **(G)** number and **(H)** latency of magazine entries (paired t-tests: $p > 0.05$). Each data point represents a single rat. Data are presented as mean ± S.E.M.

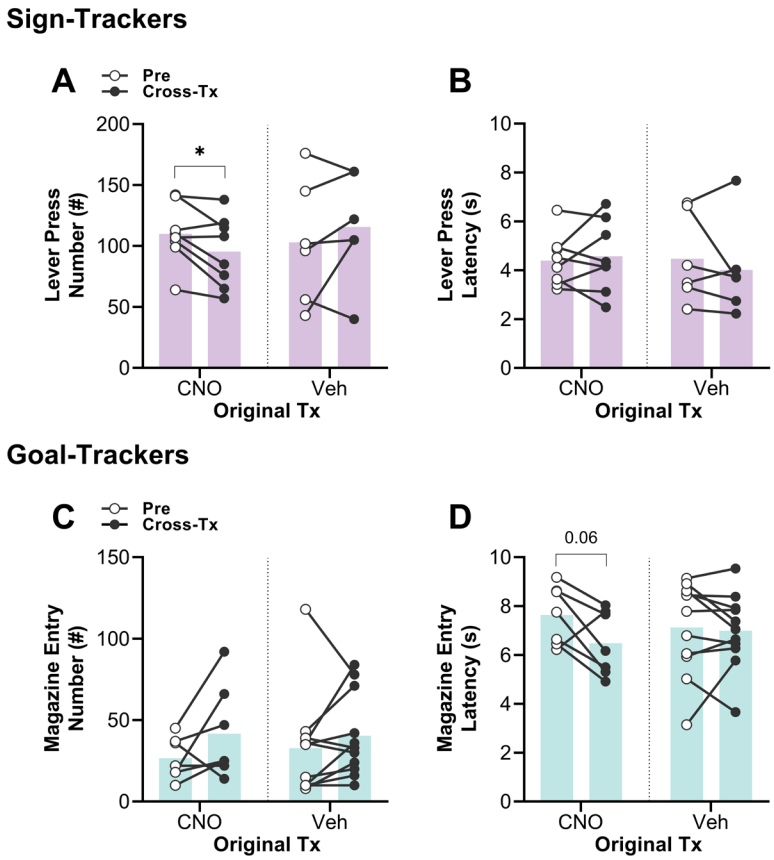


**Figure 4.4.** *Experiment 1: Effects of chemogenetic inhibition of the ventral hippocampus (vHPC) to nucleus accumbens (NAc) projection on the expression of Pavlovian conditioned approach (PavCA) behavior in sign-trackers (STs) and goal-trackers (GTs).* Based on the PavCA index scores of Session 6, rats were classified as STs (score ≥ 0.3), GTs (score ≤ -0.3), or intermediate responders (IRs) (-0.3 < score < 0.3). **A)** Ceasing inhibition of vHPC-NAc by giving Veh instead of CNO significantly decreased the number of lever presses for STs that had received CNO during PavCA acquisition (paired t-test: $p = 0.03$), but did not affect **(B)** latency to lever press. For GTs, ceasing inhibition of vHPC-NAc did not affect the **(C)** number of magazine entries (paired t-tests: $p > 0.05$). The **(D)** latency to enter the magazine slightly decreased, though this effect did not reach significance (paired t-test: $p = 0.06$). For STs and GTs receiving CNO for the first time, the number and latency of lever presses and magazine entries were not affected **(A-D)**. Significance for paired t-test is shown as * - $p < 0.05$. Each data point represents a single rat. Data are presented as mean ± S.E.M.

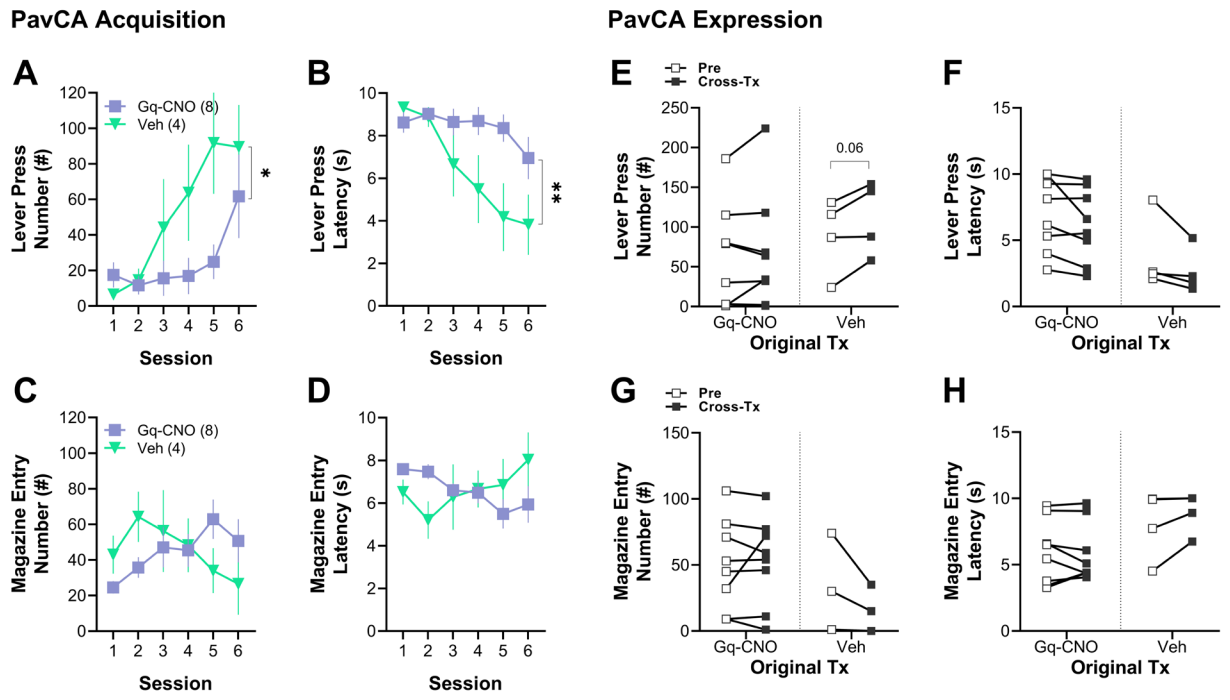


**Figure 4.5.** *Experiment 2: Effects of chemogenetic excitation of the ventral hippocampus (vHPC) to nucleus accumbens (NAc) projection on Pavlovian conditioned approach (PavCA) behavior.* PavCA Acquisition: Rats expressing an excitatory Gq-DREADD in vHPC-NAc underwent six sessions of PavCA with either clozapine-N-oxide (CNO; 3 mg/kg, IP) or Veh (6% DMSO; 1 ml/kg, IP) administered prior to testing. Rats that received CNO exhibited **(A)** lower number of lever presses (mixed-effects model: session x group interaction, $p = 0.03$) and **(B)** higher latency (mixed-effects model: session x group interaction, $p = 0.0013$) than Veh controls over the course of PavCA training. The **(C)** number and **(D)** latency of magazine entries were not significantly different between the two groups (mixed-effects model: $p > 0.05$). PavCA Expression: Switching treatment did not significantly affect either group in the **(F)** latency of lever presses (paired t-tests: $p > 0.05$) or in the **(G)** number and **(H)** latency of magazine entries (paired t-tests: $p > 0.05$). **E)** For rats in the Veh group, treatment with CNO on the test session caused a slight increase in the number of lever presses, though this effect did not reach significance (paired t-test: $p = 0.058$). Significance for mixed-effect model is shown as * - $p < 0.05$, ** - $p < 0.01$. Each data point represents a single rat. Data are presented as mean ± S.E.M.

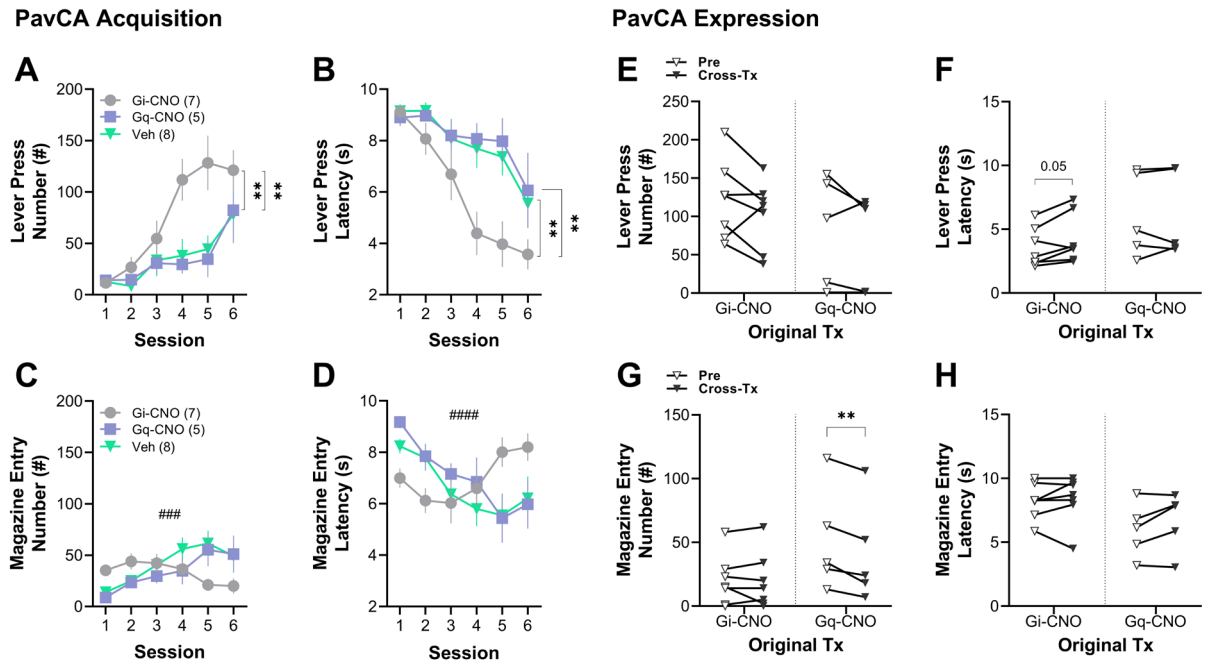


**Figure 4.6.** *Experiment 3: Effects of chemogenetic inhibition vs excitation of the ventral hippocampus (vHPC) to nucleus accumbens (NAc) projection on Pavlovian conditioned approach (PavCA) behavior.* PavCA Acquisition: Rats expressing either an inhibitory Gi-DREADD or an excitatory Gq-DREADD in vHPC-NAc underwent six sessions of PavCA with either clozapine-N-oxide (CNO; 3 mg/kg, IP) or Veh (6% DMSO; 1 ml/kg, IP) administered prior to testing. Inhibition of vHPC-NAc resulted in **(A)** greater number of lever presses (mixed-effects model: session x group interaction, $p = 0.0005$) and **(B)** lower latency (mixed-effects model: session x group interaction, $p = 0.0032$) over the course of PavCA training compared to both Gq-CNO rats and Veh controls. The rate of acquisition for the **(C)** number (mixed-effects model: session x group interaction, $p = 0.0004$) and **(D)** latency (mixed-effects model: session x group interaction, $p < 0.0001$) of magazine entries was significantly different between groups. Overall, the Gi-CNO group exhibited a greater decrease in the number of magazine entries and an increase in the latency compared to Gq-CNO rats and Veh controls. PavCA Expression: Ceasing CNO treatment resulted in a slight increase in lever press latency for the Gi-CNO rats **(F)**, though it did not reach significance (paired t-test: $p = 0.053$). Ceasing CNO also caused a significant decrease in the number of magazine entries for Gq-CNO rats (paired t-test: $p = 0.0081$) **(G).** No other significant effects were found for **(E)** lever press number or **(H)** magazine entry latency on the cross-treatment test session. For mixed-effects model, significance is shown as ### - $p < 0.001$, #### - $p < 0.0001$ for session x group interaction and as ** - $p < 0.01$ for Tukey's post-hoc test. Significance for paired t-test is shown as ** - $p < 0.01$. Each data point represents a single rat. Data are presented as mean ± S.E.M.

**Table 4.1.** *Experiment 1: Full statistical report for behavioral responses of clozapine-n-oxide (CNO) or vehicle (Veh) treated Gi-DREADD in the Pavlovian Conditioned Approach (PavCA) procedure.* Table lists analyses performed, main effects and interactions, as well as post-hoc multiple comparisons.

| | Analysis | Effects | *F/t, (df), P* |
|---|---|---|---|
| **PavCA Acquisition** | | | |
| **Lever Press Analysis** | | | |
| **Number** | mixed-effects model | session (main effect)<br>group (no effect)<br>session x group (no effect) | F(1.76, 70.3) = 14.1, p < 0.0001<br>F (1, 40) = 0.14, p = 0.71<br>F (5, 200) = 0.91, p = 0.48 |
| **Latency** | mixed-effects model | session (main effect)<br>group (no effect)<br>session x group (no effect) | F (1.96, 78.5) = 14.2, p < 0.0001<br>F (1, 40) = 0.21, p = 0.65<br>F (5, 200) = 1.11, p = 0.36 |
| **Probability** | mixed-effects model | session (main effect)<br>group (no effect)<br>session x group (no effect) | F (2.02, 81.0) = 13.6, p < 0.0001<br>F (1, 40) = 0.24, p = 0.63<br>F (5, 200) = 0.98, p = 0.43 |
| **Magazine Entry Analysis** | | | |
| **Number** | mixed-effects model | session (main effect)<br>group (no effect)<br>session x group (no effect) | F (2.97, 118) = 3.32, p = 0.023<br>F (1, 40) = 0.33, p = 0.57<br>F (5, 200) = 1.12, p = 0.35 |
| **Latency** | mixed-effects model | session (main effect)<br>group (no effect)<br>session x group (no effect) | F (3.39, 135) = 4.72, p = 0.0025<br>F (1, 40) = 2.63, p = 0.11<br>F (5, 200) = 1.57, p = 0.17 |
| **Probability** | mixed-effects model | session (main effect)<br>group (no effect)<br>session x group (no effect) | F (3.25, 130) = 2.94, p = 0.032<br>F (1, 40) = 2.44, p = 0.13<br>F (5, 200) = 1.08, p = 0.37 |
| **PavCA Index Score** | mixed-effects model | session (main effect)<br>group (no effect)<br>session x group (no effect) | F (2.27, 90.1) = 6.51, p = 0.0015<br>F (1, 40) = 0.069, p = 0.79<br>F (5, 199) = 1.28, p = 0.27 |
| **PavCA Acquisition (mCherry/CNO vs DREADD/Veh Controls)** | | | |
| **Lever Press Analysis** | | | |
| **Number** | mixed-effects model | session (main effect)<br>group (no effect)<br>session x group (no effect) | F (1.59, 61.9) = 7.86, p = 0.0020<br>F (1, 39) = 0.036, p = 0.85<br>F (5, 195) = 0.24, p = 0.95 |
| **Latency** | mixed-effects model | session (main effect)<br>group (no effect)<br>session x group (no effect) | F (1.69, 65.7) = 9.05, p = 0.0007<br>F (1, 39) = 0.65, p = 0.42<br>F (5, 195) = 0.11, p = 0.99 |
| **Probability** | mixed-effects model | session (main effect)<br>group (no effect)<br>session x group (no effect) | F (1.85, 72.1) = 8.67, p = 0.0006<br>F (1, 39) = 0.94, p = 0.34<br>F (5, 195) = 0.14, p = 0.98 |
| **Magazine Entry Analysis** | | | |
| **Number** | mixed-effects model | session (main effect)<br>group (no effect)<br>session x group (no effect) | F (3.19, 124) = 5.38, p = 0.0013<br>F (1, 39) = 3.81, p = 0.058<br>F (5, 195) = 1.00, p = 0.42 |
| **Latency** | mixed-effects model | session (main effect)<br>group (main effect)<br>session x group (no effect) | F (3.31, 129) = 6.39, p = 0.0003<br>F (1, 39) = 4.40, p = 0.042<br>F (5, 195) = 0.52, p = 0.76 |
| **Probability** | mixed-effects model | session (main effect)<br>group (main effect)<br>session x group (no effect) | F (3.27, 127) = 6.01, p = 0.0005<br>F (1, 39) = 6.34, p = 0.016<br>F (5, 195) = 0.95, p = 0.45 |

| | | | |
|---|---|---|---|
| **PavCA Index Score** | mixed-effects model | session (no effect)<br>group (no effect)<br>session x group (no effect) | F (2.06, 80.1) = 2.90, p = 0.059<br>F (1, 39) = 0.012, p = 0.91<br>F (5, 194) = 0.47, p = 0.80 |
| **PavCA Expression (No Phenotypes)** | | | |
| **Veh to CNO (Cross-Tx)** | | | |
| **Lever Press** | | | |
| **Number** | paired t-test | cross-Tx (no effect) | t=1.79, df=20, p = 0.089 |
| **Latency** | paired t-test | cross-Tx (no effect) | t=1.65, df=20, p = 0.11 |
| **Probability** | paired t-test | cross-Tx (no effect) | t=1.62, df=20, p = 0.12 |
| **Magazine Entry** | | | |
| **Number** | paired t-test | cross-Tx (no effect) | t=0.86, df=20, p = 0.40 |
| **Latency** | paired t-test | cross-Tx (no effect) | t=0.20, df=20, p = 0.85 |
| **Probability** | paired t-test | cross-Tx (no effect) | t=0.61, df=20, p = 0.55 |
| **CNO to Veh (Cross-Tx)** | | | |
| **Lever Press** | | | |
| **Number** | paired t-test | cross-Tx (no effect) | t=1.24, df=20, p = 0.23 |
| **Latency** | paired t-test | cross-Tx (no effect) | t=0.49, df=20, p = 0.63 |
| **Probability** | paired t-test | cross-Tx (no effect) | t=1.21, df=20, p = 0.24 |
| **Magazine Entry** | | | |
| **Number** | paired t-test | cross-Tx (no effect) | t=0.76, df=20, p = 0.45 |
| **Latency** | paired t-test | cross-Tx (no effect) | t=0.88, df=20, p = 0.39 |
| **Probability** | paired t-test | cross-Tx (no effect) | t=0.28, df=20, p = 0.78 |
| **PavCA Expression (By Phenotypes)** | | | |
| **Sign-trackers: Veh to CNO (Cross-Tx)** | | | |
| **Lever Press** | | | |
| **Number** | paired t-test | cross-Tx (no effect) | t=1.06, df=5, p = 0.34 |
| **Latency** | paired t-test | cross-Tx (no effect) | t=0.82, df=5, p = 0.45 |
| **Probability** | paired t-test | cross-Tx (no effect) | t=0.64, df=5, p = 0.55 |
| **Magazine Entry** | | | |
| **Number** | paired t-test | cross-Tx (no effect) | t=0.30, df=5, p = 0.78 |
| **Latency** | paired t-test | cross-Tx (no effect) | t=0.23, df=5, p = 0.82 |
| **Probability** | paired t-test | cross-Tx (no effect) | t=0.00, df=5, p >0.99 |
| **Sign-trackers: CNO to Veh (Cross-Tx)** | | | |
| **Lever Press** | | | |
| **Number** | paired t-test | cross-Tx effect | t=2.67, df=7, p = 0.032 |
| **Latency** | paired t-test | cross-Tx (no effect) | t=0.47, df=7, p = 0.65 |
| **Probability** | paired t-test | cross-Tx (no effect) | t=1.18, df=7, p = 0.28 |
| **Magazine Entry** | | | |
| **Number** | paired t-test | cross-Tx (no effect) | t=0.17, df=7, p = 0.87 |
| **Latency** | paired t-test | cross-Tx (no effect) | t=0.29, df=7, p = 0.78 |
| **Probability** | paired t-test | cross-Tx (no effect) | t=0.33, df=7, p = 0.75 |
| **Goal-trackers: Veh to CNO (Cross-Tx)** | | | |
| **Lever Press** | | | |
| **Number** | paired t-test | cross-Tx (no effect) | t=1.28, df=10, p = 0.23 |
| **Latency** | paired t-test | cross-Tx (no effect) | t=1.19, df=10, p = 0.26 |
| **Probability** | paired t-test | cross-Tx (no effect) | t=1.30, df=10, p = 0.22 |
| **Magazine Entry** | | | |
| **Number** | paired t-test | cross-Tx (no effect) | t=1.12, df=10, p = 0.29 |
| **Latency** | paired t-test | cross-Tx (no effect) | t=0.36, df=10, p = 0.73 |
| **Probability** | paired t-test | cross-Tx (no effect) | t=0.74, df=10, p = 0.47 |
| **Goal-trackers: CNO to Veh (Cross-Tx)** | | | |

| | | | |
|---|---|---|---|
| **Lever Press** | | | |
| **Number** | paired t-test | cross-Tx (no effect) | t=1.96, df=6, p = 0.097 |
| **Latency** | paired t-test | cross-Tx (no effect) | t=1.93, df=6, p = 0.10 |
| **Probability** | paired t-test | cross-Tx (no effect) | t=1.66, df=6, p = 0.15 |
| | | | |
| **Magazine Entry** | | | |
| **Number** | paired t-test | cross-Tx (no effect) | t=1.58, df=6, p = 0.17 |
| **Latency** | paired t-test | cross-Tx (no effect) | t=2.28, df=6, p = 0.063 |
| **Probability** | paired t-test | cross-Tx (no effect) | t=1.40, df=6, p = 0.21 |

**Table 4.2.** *Experiment 2: Full statistical report for behavioral responses of clozapine-n-oxide (CNO) or vehicle (Veh) treated Gq-DREADD in the Pavlovian Conditioned Approach (PavCA) procedure*. Table lists analyses performed, main effects and interactions, as well as post-hoc multiple comparisons.

| | Analysis | Effects | *F/t, (df), P* |
|---|---|---|---|
| **PavCA Acquisition** | | | |
| **Lever Press Analysis** | | | |
| **Number** | mixed-effects model | session (main effect) | F (2.02, 20.2) = 8.15, p = 0.0025 |
| | | group (no effect) | F (1, 10) = 2.61, p = 0.14 |
| | | session x group (interaction) | F (5, 50) = 2.56, p = 0.0013 |
| **Latency** | mixed-effects model | session (main effect) | F (2.14, 21.4) = 10.8, p = 0.0005 |
| | | group (no effect) | F (1, 10) = 4.19, p = 0.068 |
| | | session x group (interaction) | F (5, 50) = 4.72, p = 0.0013 |
| **Probability** | mixed-effects model | session (main effect) | F (2.57, 25.7) = 10.7, p = 0.0002 |
| | | group (no effect) | F (1, 10) = 2.80, p = 0.13 |
| | | session x group (interaction) | F (5, 50) = 3.33, p = 0.011 |
| **Magazine Entry Analysis** | | | |
| **Number** | mixed-effects model | session (no effect) | F (2.35, 23.5) = 0.68, p = 0.54 |
| | | group (no effect) | F (1, 10) = 0.017, p = 0.90 |
| | | session x group (no effect) | F (5, 50) = 1.79, p = 0.13 |
| **Latency** | mixed-effects model | session (no effect) | F (2.25, 22.5) = 0.44, p = 0.67 |
| | | group (no effect) | F (1, 10) = 0.00011, p = 0.99 |
| | | session x group (no effect) | F (5, 50) = 2.21, p = 0.068 |
| **Probability** | mixed-effects model | session (no effect) | F (2.50, 25.0) = 0.51, p = 0.65 |
| | | group (no effect) | F (1, 10) = 0.013, p = 0.91 |
| | | session x group (no effect) | F (5, 50) = 1.92, p = 0.11 |
| **PavCA Index Score** | mixed-effects model | session (main effect) | F (2.24, 24.6) = 4.04, p = 0.027 |
| | | group (no effect) | F (1, 11) = 1.65, p = 0.23 |
| | | session x group (interaction) | F (5, 55) = 2.56, p = 0.037 |
| **PavCA Acquisition (mCherry/CNO vs DREADD/Veh Controls)** | | | |
| **Lever Press Analysis** | | | |
| **Number** | mixed-effects model | session (main effect) | F (1.48, 7.4) = 5.54, p = 0.040 |
| | | group (no effect) | F (1, 5) = 0.35, p = 0.58 |
| | | session x group (no effect) | F (5, 25) = 0.27, p = 0.93 |
| **Latency** | mixed-effects model | session (main effect) | F (1.68, 8.41) = 7.27, p = 0.017 |
| | | group (no effect) | F (1, 5) = 2.80, p = 0.16 |
| | | session x group (no effect) | F (5, 25) = 1.80, p = 0.15 |
| **Probability** | mixed-effects model | session (main effect) | F (2.14, 10.7) = 8.14, p = 0.0065 |
| | | group (no effect) | F (1, 5) = 3.14, p = 0.14 |
| | | session x group (no effect) | F (5, 25) = 1.49, p = 0.23 |
| **Magazine Entry Analysis** | | | |
| **Number** | mixed-effects model | session (no effect) | F (2.03, 12.2) = 0.32, p = 0.74 |
| | | group (no effect) | F (1, 30) = 2.56, p = 0.12 |
| | | session x group (no effect) | F (5, 30) = 1.21, p = 0.33 |
| **Latency** | mixed-effects model | session (no effect) | F (1.95, 9.8) = 0.37, p = 0.69 |
| | | group (no effect) | F (1, 5) = 0.31, p = 0.60 |
| | | session x group (no effect) | F (5, 25) = 1.01, p = 0.44 |
| **Probability** | mixed-effects model | session (no effect) | F (1.91, 9.56) = 0.37, p = 0.69 |
| | | group (no effect) | F (1, 5) = 0.57, p = 0.48 |
| | | session x group (no effect) | F (5, 25) = 0.90, p = 0.50 |

| | | | |
|---|---|---|---|
| **PavCA Index Score** | mixed-effects model | session (no effect)<br>group (no effect)<br>session x group (no effect) | F (1.72, 10.3) = 2.82 p = 0.11<br>F (1, 6) = 0.73, p = 0.43<br>F (5, 194) = 0.47, p = 0.50 |
| **PavCA Expression (No Phenotypes)** | | | |
| **Veh to CNO (Cross-Tx)** | | | |
| **Lever Press** | | | |
| **Number** | paired t-test | cross-Tx (no effect) | t=2.99, df=3, p = 0.058 |
| **Latency** | paired t-test | cross-Tx (no effect) | t=1.97, df=3, p = 0.14 |
| **Probability** | paired t-test | cross-Tx (no effect) | t=1.12, df=3, p = 0.34 |
| **Magazine Entry** | | | |
| **Number** | paired t-test | cross-Tx (no effect) | t=1.56, df=3, p = 0.23 |
| **Latency** | paired t-test | cross-Tx (no effect) | t=1.70, df=3, p = 0.19 |
| **Probability** | paired t-test | cross-Tx (no effect) | t=2.67, df=3, p = 0.076 |
| **CNO to Veh (Cross-Tx)** | | | |
| **Lever Press** | | | |
| **Number** | paired t-test | cross-Tx (no effect) | t=0.90, df=7, p = 0.40 |
| **Latency** | paired t-test | cross-Tx (no effect) | t=1.92, df=7, p = 0.096 |
| **Probability** | paired t-test | cross-Tx (no effect) | t=1.14, df=7, p = 0.29 |
| **Magazine Entry** | | | |
| **Number** | paired t-test | cross-Tx (no effect) | t=0.35, df=7, p = 0.74 |
| **Latency** | paired t-test | cross-Tx (no effect) | t=0.18, df=7, p = 0.86 |
| **Probability** | paired t-test | cross-Tx (no effect) | t=0.32, df=7, p = 0.76 |

**Table 4.3.** *Experiment 3: Full statistical report for behavioral responses of clozapine-n-oxide (CNO) or vehicle (Veh) treated Gi-DREADD vs Gq-DREADD in the Pavlovian Conditioned Approach (PavCA) procedure.* Table lists analyses performed, main effects and interactions, as well as post-hoc multiple comparisons.

| | Analysis | Effects | *F/t, (df), P* | *Post-hoc* | *Comparison* | *q(df), P* |
|---|---|---|---|---|---|---|
| **PavCA Acquisition** | | | | | | |
| **Lever Press Analysis** | | | | | | |
| **Number** | mixed-effects model | session (main effect)<br>group (no effect)<br>session x group (interaction) | F (2.61, 44.4) = 23.8 p < 0.0001<br>F (2, 17) = 3.58, p = 0.051<br>F (10, 85) = 3.63, p = 0.0005 | Tukey's | Gi vs Gq<br>Gi vs Veh<br>Gq vs Veh | q(68.8) = 4.73, p = 0.0038<br>q(70.1) = 4.78, p = 0.0034<br>q(65.3) = 0.23, p = 0.99 |
| **Latency** | mixed-effects model | session (main effect)<br>group (main effect)<br>session x group (interaction) | F (3.03, 51.4) = 26.3, p < 0.0001<br>F (2, 17) = 3.81, p = 0.043<br>F (10, 85) = 2.95, p = 0.0032 | Tukey's | Gi vs Gq<br>Gi vs Veh<br>Gq vs Veh | q(69.8) = 5.22, p = 0.0013<br>q(76.8) = 4.89, p = 0.0026<br>q(68.1) = 0.59, p = 0.91 |
| **Probability** | mixed-effects model | session (main effect)<br>group (main effect)<br>session x group (interaction) | F (3.13, 53.2) = 25.9, p < 0.0001<br>F (2, 17) = 3.65, p = 0.048<br>F (10, 85) = 2.15, p = 0.029 | Tukey's | Gi vs Gq<br>Gi vs Veh<br>Gq vs Veh | q(68.8) = 5.45, p = 0.0007<br>q(84.4) = 4.73, p = 0.0035<br>q(67.9) = 0.99, p = 0.76 |
| **Magazine Entry Analysis** | | | | | | |
| **Number** | mixed-effects model | session (main effect)<br>group (no effect)<br>session x group (interaction) | F (2.84, 48.3) = 4.19, p = 0.011<br>F (2, 17) = 0.55, p = 0.59<br>F (10, 85) = 3.72, p = 0.0004 | Tukey's | Gi vs Gq<br>Gi vs Veh<br>Gq vs Veh | q(48.7) = 0.16, p = 0.99<br>q(81.7) = 2.04, p = 0.33<br>q(65.0) = 1.47, p = 0.56 |
| **Latency** | mixed-effects model | session (main effect)<br>group (no effect)<br>session x group (interaction) | F (2.70, 46.0) = 4.96, p = 0.0059<br>F (2, 17) = 0.27, p = 0.76<br>F (10, 85) = 4.35, p < 0.0001 | Tukey's | Gi vs Gq<br>Gi vs Veh<br>Gq vs Veh | q(56.4) = 0.27, p = 0.98<br>q(87.9) = 1.24, p = 0.66<br>q(62.8) = 1.30, p = 0.63 |
| **Probability** | mixed-effects model | session (main effect)<br>group (no effect)<br>session x group (interaction) | F (2.54, 43.1) = 4.50, p = 0.011<br>F (2, 17) = 0.28, p = 0.76<br>F (10, 85) = 3.67, p = 0.0004 | Tukey's | Gi vs Gq<br>Gi vs Veh<br>Gq vs Veh | q(57.9) = 0.76, p = 0.86<br>q(87.7) = 0.97, p = 0.77<br>q(59.9) = 1.57, p = 0.51 |
| **PavCA Index Score** | mixed-effects model | session (main effect)<br>group (no effect)<br>session x group (interaction) | F (2.94, 49.9) = 7.14, p = 0.0005<br>F (2, 17) = 1.86, p = 0.19<br>F (10, 85) = 4.92, p < 0.0001 | Tukey's | Gi vs Gq<br>Gi vs Veh<br>Gq vs Veh | q(69.8) = 3.08, p = 0.083<br>q(82.7) = 4.12, p = 0.013<br>q(73.1) = 1.24, p = 0.66 |
| **PavCA Acquisition (mCherry/CNO vs DREADD/Veh Controls)** | | | | | | |
| **Lever Press Analysis** | | | | | | |
| **Number** | mixed-effects model | session (main effect)<br>group (main effect)<br>session x group (no effect) | F (2.32, 20.9) = 9.67, p = 0.0007<br>F (1, 9) = 5.66, p = 0.041<br>F (5, 45) = 1.96, p = 0.10 | | | |
| **Latency** | mixed-effects model | session (main effect)<br>group (main effect)<br>session x group (no effect) | F (2.74, 24.7) = 14.5, p < 0.0001<br>F (1, 9) = 9.05, p = 0.015<br>F (5, 45) = 2.17, p = 0.075 | | | |
| **Probability** | mixed-effects model | session (main effect)<br>group (main effect) | F (2.77, 24.9) = 12.1, p < 0.0001<br>F (1, 9) = 8.81, p = 0.016 | | | |

| | | | | |
|---|---|---|---|---|
| | | session x group (no effect) | F (5, 45) = 1.52, p = 0.20 | |
| **Magazine Entry Analysis** | | | | |
| **Number** | mixed-effects model | session (no effect) | F (2.59, 23.3) = 0.66, p = 0.57 | |
| | | group (no effect) | F (1, 9) = 2.46, p = 0.15 | |
| | | session x group (interaction) | F (5, 45) = 3.77, p = 0.0062 | |
| **Latency** | mixed-effects model | session (no effect) | F (2.80, 25.2) = 0.28, p = 0.83 | |
| | | group (no effect) | F (1, 9) = 2.55, p = 0.14 | |
| | | session x group (interaction) | F (5, 45) = 4.00, p = 0.0044 | |
| **Probability** | mixed-effects model | session (no effect) | F (2.71, 24.4) = 0.37, p = 0.76 | |
| | | group (no effect) | F (1, 9) = 1.42, p = 0.26 | |
| | | session x group (interaction) | F (5, 45) = 2.96, p = 0.022 | |
| **PavCA Index Score** | mixed-effects model | session (main effect) | F (2.54, 22.8) = 3.55 p = 0.036 | |
| | | group (main effect) | F (1, 9) = 6.53, p = 0.031 | |
| | | session x group (no effect) | F (5, 45) = 1.97, p = 0.10 | |
| **PavCA Expression (No Phenotypes)** | | | | |
| **Gi-CNO to Veh (Cross-Tx)** | | | | |
| **Lever Press** | | | | |
| **Number** | paired t-test | cross-Tx (no effect) | t=1.60, df=6, p = 0.16 | |
| **Latency** | paired t-test | cross-Tx (no effect) | t=2.40, df=6, p = 0.053 | |
| **Probability** | paired t-test | cross-Tx (no effect) | t=1.69, df=6, p = 0.14 | |
| **Magazine Entry** | | | | |
| **Number** | paired t-test | cross-Tx (no effect) | t=0.18, df=6, p = 0.86 | |
| **Latency** | paired t-test | cross-Tx (no effect) | t=0.52, df=6, p = 0.62 | |
| **Probability** | paired t-test | cross-Tx (no effect) | t=0.68, df=6, p = 0.52 | |
| **Gq-CNO to Veh (Cross-Tx)** | | | | |
| **Lever Press** | | | | |
| **Number** | paired t-test | cross-Tx (no effect) | t=1.13, df=4, p = 0.32 | |
| **Latency** | paired t-test | cross-Tx (no effect) | t=0.11, df=4, p = 0.92 | |
| **Probability** | paired t-test | cross-Tx (no effect) | t=0.93, df=4, p = 0.41 | |
| **Magazine Entry** | | | | |
| **Number** | paired t-test | cross-Tx effect | t=4.89, df=4, p = 0.0081 | |
| **Latency** | paired t-test | cross-Tx (no effect) | t=1.89, df=4, p = 0.13 | |
| **Probability** | paired t-test | cross-Tx (no effect) | t=2.45, df=4, p = 0.071 | |

**Table 4.4.** *Effect of CNO on ventral hippocampus (vHPC) to nucleus accumbens (NAc) synaptic transmission during optical stimulation.* Table summarizes amplitude of optically-evoked excitatory post-synaptic currents (EPSCs) before and after CNO application at varying stimulation intensities. Data is shown for each cell and as mean ± S.E.M. (sample size).

| | | | | Before CNO | | | | | CNO Bath | Wash Out |
|---|---|---|---|---|---|---|---|---|---|---|
| | Stimulation Intensity (LED %) | | | 20 | 40 | 60 | 80 | 100 | 100 | 100 |
| Rat ID* | Cell ID | Pulse (ms) | [CNO] µM | EPSC amplitude (pA) | | | | | | |
| A | 1 | 2 | 10 | 13.4 | 11.2 | 11.9 | 12.8 | 12.3 | 0.91 | 1.16 |
| A | 2 | 0.5 | 10 | 2.61 | 8.07 | 14.9 | 15.1 | 15.1 | 12.4 | 10.2 |
| B | 3 | 1 | 10 | 6.40 | 9.05 | 11.1 | 13.0 | 12.3 | 5.14 | - |
| B | 4 | 2 | 10 | 0.53 | 0.94 | 1.72 | 6.47 | 9.85 | 1.27 | 0.70 |
| B | 5 | 2 | 10 | - | 0.89 | 1.50 | 1.65 | 1.81 | 1.34 | - |
| C | 6 | 2 | 20 | 7.95 | 11.6 | 10.6 | 10.6 | 13.3 | 6.35 | - |
| C | 7 | 2 | 20 | 1.36 | 1.27 | 3.65 | 2.91 | 2.98 | 1.55 | - |
| C | 8 | 1 | 20 | 0.62 | 8.61 | 6.80 | 10.9 | 7.28 | 8.87 | - |
| | | | | | | | | | | |
| | **Mean ± SEM** | | 10 µM | 5.73 ± 2.83 (4) | 6.03 ± 2.15 (5) | 8.23 ± 2.78 (5) | 9.80 ± 2.50 (5) | 10.27 ± 2.27 (5) | 4.22 ± 2.19 (5) | 4.02 ± 3.10 (3) |
| | **Mean ± SEM** | | 20 µM | 3.31 ± 2.22 (3) | 7.15 ± 3.06 (3) | 7.01 ± 2.00 (3) | 8.15 ± 2.62 (3) | 7.85 ± 2.99 (3) | 5.59 ± 2.15 (3) | - |

*Rats A and B received 1.0 µl of DREADD-(Gi) and 0.5 µl of channelrhodopsin into the vHPC. Rat C received 0.5 µl of DREADD-(Gi) and 0.5 µl of channelrhodopsin.

# CHAPTER V

## Synaptic Transmission Efficacy in the Ventral Hippocampus to Nucleus Accumbens Projection of Sign-Trackers and Goal-Trackers


### Abstract

Glutamatergic signaling in the nucleus accumbens (NAc) is an integral component of conditioned behavioral responses. Variations in glutamatergic transmission might help explain how adaptive responses can become maladaptive and lead to disease states. “Sign-tracking” and “goal-tracking” behavior are examples of individual differences in associative learning that have implications for increased vulnerability to disorders like addiction and post-traumatic stress disorder (PTSD). In this chapter, we explore whether fundamental differences in overall baseline excitatory synaptic input into the NAc are a feature of the “sign-tracker” (ST) and “goal-tracker” (GT) phenotype in rats. In the previous chapter, we focused on the role of glutamatergic inputs from the ventral hippocampus (vHPC) to the NAc and found that decreased activity of vHPC-NAc may favor sign-tracking behavior, which is associated with increased cue-reactivity. Here, we test whether behavioral differences between STs and GTs are accompanied by differences in synaptic transmission efficacy in the vHPC-NAc projection. Using *ex vivo* optogenetics, combined with whole-cell electrophysiology of medium spiny neurons (MSNs) in the NAc, we found that STs and GTs exhibit very

similar synaptic transmission efficacy in vHPC-NAc. We also found that in both the NAc core and shell, baseline excitatory synaptic input to MSNs is not fundamentally different between the two phenotypes. These findings may suggest that behavioral differences in STs and GTs are not due to baseline differences in excitatory synaptic transmission and may be more activity- or experience-dependent. These data may be important to aid the development of new prevention strategies and more effective treatments for disorders like addiction and PTSD in vulnerable populations.

**Introduction**

Glutamatergic signaling is required for the nucleus accumbens (NAc) to initiate and modulate conditioned behavioral responses, such as motivated actions and goal-directed behaviors (Ciano et al., 2001; Dalley et al., 2005; Day and Carelli, 2007; Batten et al., 2018). Individual differences in glutamatergic transmission can result in variations in the way that individuals process and respond to stimuli in the environment and form appetitive and aversive associations. This in turn can be directly linked to increased risk or predisposition to disorders that are heavily influenced by this type of learning, such as addiction, anxiety, and depression (Turner et al., 2018). The NAc is centered in the limbic system, which allows it to converge inputs from a range of glutamatergic afferents that feed information about both internal and external states to appropriately modulate behavioral responses (Britt et al., 2012). Models of individual variation in reward and fear learning can be helpful for trying to dissect how this information – in the form of excitatory synaptic inputs – is differentially integrated and translates to measurable behavioral differences such as increased cue-reactivity and the associated risk for addiction and post-traumatic stress disorder (PTSD) (María-Ríos and Morrow, 2020).

In the previous chapter we focused on how glutamatergic input from the ventral hippocampus (vHPC) – a region crucial for feeding context-specific information to the NAc during reward and fear learning (Turner et al., 2022) – can modulate “sign-tracking” and “goal-tracking” behavioral responses to conditioned cues. Our interest in the vHPC-NAc projection is centered on evidence that discrete cues versus contextual information differentially affect the conditioned responses of “sign-tracker” (STs) and “goal-tracker” (GTs) rats (Pitchers et al., 2017; Morrow, 2018; María-Ríos and Morrow, 2020). During a Pavlovian conditioned approach (PavCA) procedure in which a conditioned stimulus such as a lever-cue is paired with an unconditioned stimulus, such as a food reward, STs approach the lever indicating that the cue acquires some rewarding and motivational value to them. GTs on the other hand, use the cue as a predictor of the reward, resulting in a goal-directed behavioral response toward the site of impending food delivery (Berridge et al., 2009; Flagel et al., 2009). Interestingly, the behavioral distinctions between STs and GTs are not isolated to PavCA, suggesting that there are fundamental differences in associative learning that translate to a wide range of behaviors. Focusing on differences in cue- versus context-dependent responses, STs seem to exhibit signs of hyperreactivity to both appetitive and aversive cues as suggested by an increased cue-induced reinstatement of drug-seeking (Saunders and Robinson, 2011; Versaggi et al., 2016) and greater freezing responses during cued fear extinction (Morrow et al., 2011). On the other hand, GTs seem to be more sensitive to context-dependent responses than STs. GTs exhibit greater context-induced reinstatement of cocaine (Saunders et al., 2014; Pitchers et al., 2017) as well as greater freezing following contextual fear conditioning (Morrow et al., 2011). Altogether, this has

led to the hypothesis that regardless of the context in which STs encounter discrete cues, they are hypersensitive to the cue's behavioral influence, while GTs use contextual information to modulate their behavioral responses.

As mentioned in the previous chapter, evidence suggests that neuronal engrams in the vHPC store spatial information during associative learning that is decoded by the NAc in order to guide conditioned behavioral responses (Zhou et al., 2019). Because this process has been implicated in both reward and fear learning, some have proposed that this projection encodes a general property of salience regardless of the valence of the associated stimuli (Loureiro et al., 2016; Muir et al., 2020). For example, increased activity of the vHPC-NAc projection can promote conditioned place preference (Britt et al., 2012; LeGates et al., 2018) and context-dependent drug-seeking (Loureiro et al., 2016; Zhou et al., 2019). Increased activity of the vHPC-NAc projection can also facilitate contextual fear conditioning (Loureiro et al., 2016) and anxiety-like behaviors (Muir et al., 2020). This pattern seems to apply to STs and GTs as both exhibit heightened sensitivity to cue- versus context-dependent influence respectively, regardless of their appetitive or aversive nature. Therefore, this projection may be important for driving or regulating individual differences in the conditioned responses exhibited by STs and GTs.

The findings in the previous chapter suggest that the vHPC-NAc projection may have a functional role in sign- and goal-tracking behavior. Specifically, decreased activity of vHPC-NAc seems to promote sign-tracking behavior, while increased activity seems to suppress it. These findings support a role for the vHPC-NAc as a modulator of conditioned responses to discrete cues by means of context-specific information. Based

on this we postulate that decreased activity in this projection may contribute to the increased cue reactivity exhibited by STs while increased activity in GTs may allow them to use contextual cues more effectively to modulate their conditioned emotional responses. In this chapter, we explore whether these behavioral differences in response to vHPC-NAc *in vivo* manipulation are matched by differences in synaptic strength between STs and GTs. That is, compared to GTs, STs may exhibit weaker synaptic transmission efficacy as this would correlate with increased sign-tracking behavior.

To first assess whether STs and GTs exhibit fundamental differences in excitatory synaptic input to medium spiny neurons (MSNs), we tested for differences in miniature excitatory-post synaptic currents (mEPSCs) in the core and shell of the NAc. Furthermore, using *ex vivo* slice optogenetics, combined with whole-cell voltage-clamp recordings, we tested for differences in vHPC-NAc synaptic transmission efficacy in STs and GTs by studying properties of optically evoked excitatory post-synaptic currents (EPSCs) in MSNs innervated by the vHPC.

## Materials and Methods

### *Animals*

A total of sixty-seven adult male Sprague Dawley rats (7-8 weeks) were purchased from Charles River Laboratories (R04, R08, R09, K90, K97) and housed in pairs. Rats were maintained on a 12:12-hr light/dark cycle, with food and water available ad libitum for the entirety of the experiment. All rats were acclimatized to the housing colony for at least two days prior to any handling and behavioral procedures. Twelve rats were trained and subsequently used for mEPSC recordings. Following behavioral procedures, they remained in their home cages for 1-2 weeks prior to

electrophysiological recordings. Forty-eight rats were trained and subsequently used for evoked-EPSC recordings. Following behavioral procedures, twenty-one rats were selected for surgical procedures, and following surgery they remained in their home cages for a six-week incubation period prior to electrophysiological recordings. All animal procedures were previously approved by the University Committee on the Use and Care of Animals (University of Michigan; Ann Arbor, MI).

### *Viral vectors*

*Channelrhodopsin*: pAAV-CaMKIIa-hChR2(H134R)-mCherry was a gift from Karl Deisseroth (Addgene plasmid # 26975; http://n2t.net/addgene:26975; RRID: Addgene_26975).

### *Behavioral Testing Apparatus*

Sixteen modular operant conditioning chambers (24.1 cm width × 20.5 cm depth x 29.2 cm height; MED Associates, Inc.; St. Albans, VT) were used for behavioral testing. Each chamber was inside a sound-attenuating cubicle with ventilation fan providing ambient background noise during testing. Each chamber was equipped with a food magazine, a retractable lever (counterbalanced on the left or right side of the magazine), and a red house light on the wall opposite of the magazine. An infrared sensor in the magazines detected magazine entries, and the levers were calibrated to detect lever deflections in response to a minimum of 10 g of applied weight. The inside of the lever mechanism contained a mounted LED to illuminate the slot through which the lever protruded each time the lever was extended into the chamber. The number and latency of lever presses and magazine entries were recorded automatically for each trial (ABET II Software; Lafayette Instrument; Lafayette, IN).

### *Behavioral Testing Procedure*

For two days prior to the start of training, all rats were habituated to the investigator and the food reward. Rats were handled individually and were given banana-flavored pellets (45 mg; Bio-Serv; Frenchtown, NJ) in their home cages. On the third day, rats were placed into the test chambers for one pre-training session during which the red house-light remained on, but the lever was retracted. Twenty-five food pellets were delivered on a variable time (VT) 30-s schedule (i.e., one pellet was delivered on average every 30 s, but varied 0-60 s). Following the pre-training session, all rats underwent six daily sessions of behavioral training. Each trial during a training session consisted of a presentation of the illuminated lever (conditioned stimulus, CS) into the chamber for 10 s on a VT 45-s schedule (i.e., time randomly varied 30-60 s between CS presentations). Immediately after retraction of the lever, there was a response-independent delivery of one pellet into the magazine (unconditioned stimulus, US). The beginning of the next inter-trial interval (ITI) began once both the lever and the pellet had been presented, and each test session consisted of 25 trials of CS-US pairings. All rats consumed all the pellets that were delivered. Rats were not food deprived at any point during experimentation.

### *AAV injections*

Out of the 60 rats, 21 underwent surgical procedures following PavCA for optically evoked EPSC recordings. Rats were anesthetized using 4-5% isoflurane for induction and 1-2% for maintenance (Fluriso - VetOne; Boise, ID). Following anesthesia, rats were given carprofen (Rimadyl: 5 mg/kg; SQ) for analgesia. Rats were then placed in a stereotaxic frame (David Kopf Instruments; Tujunga, CA) and

temperature was regulated with a heating pad. Bilateral intracranial viral injections were performed by lowering a 5-µl Hamilton Neuros Syringe (Model 75 RN, 33-gauge; Hamilton, Reno, NV) into the ventral hippocampus (vHPC). Based on the rat brain atlas (Paxinos and Franklin, 2019) the following coordinates were used for the vHPC: AP = -6.0 mm, ML = ±5.4 mm, DV = -8.4 mm. A total of 0.5 µl of a channelrhodopsin virus (AAV5-CAMKIIa-hChR2(H134R)-mCherry) was bilaterally injected. For all rats there were a total of two injection sites. The virus was infused at a rate of 0.1 µl/min over the course of 5 min. The syringe was left in place for 5 min to allow diffusion. Following the surgical procedures, the incisions were closed using sutures. Following surgery, rats received post-operative analgesia for two days and additional monitoring for 7-10 days. A period of 6 weeks was allowed for optimal viral expression before electrophysiological testing. Prior to these surgeries, seven naïve rats underwent viral injections to determine the optimal incubation period and viral volume for ChR2 expression. The injection volume was varied from 0.5 to 1.0 µl bilaterally, and the incubation period varied from 4-8 weeks.

***Histological verification***

To confirm that 0.5 µl of viral volume and 6 weeks of incubation were optimal for ChR2 expression in the vHPC cell bodies and axon terminals within the NAc, histological verification was performed at 4, 6, and 8 weeks following viral injections. Rats were deeply anesthetized with sodium pentobarbital (39 mg/kg, IP; Euthasol – Virbac; Carros, FR) and transcardially perfused with 4% formaldehyde (pH 7.0-7.4). Following decapitation, the brains were dissected and post-fixed in 4% formaldehyde for 24 h at 4ºC. They were then transferred to a 30% sucrose solution made with 0.2 M

sodium phosphate buffer (NaPB, pH = 7.0-7.4) and was left at 4ºC for approximately 3-5 days. The brains were then frozen using cooled isopentane (-160ºC) for 20-30 s, and coronal sections (35-40 µm) were obtained using a cryostat (Leica CM1860; Leica Biosystems Inc, Wetzlar, DE). Brain slices from the NAc (ranging from +3.20 to -0.30 mm from bregma) and vHPC (ranging from -3.60 to -7.04 mm from bregma) were mounted on Fisherbrand +charged slides. Once the sections were fully dried, they were cover-slipped with Vectashield Plus antifade medium with DAPI (Vector Laboratories, H-20000-10). Slides were stored at 4ºC until visualization. Fluorescence images of sections containing the NAc and vHPC were captured at 4x and 10x magnification using the Olympus IX83 inverted microscope and were processed using ImageJ.

### *Electrophysiology*

*Slice preparation.* Rats were deeply anesthetized with isoflurane (Kent Scientific; Torrington, CT) and euthanized by decapitation. The brain was rapidly dissected and glued on a platform submerged in an ice-cold oxygenated (95% $O_2$/ 5% $CO_2$) cutting solution containing (in mM): 206 sucrose, 10 d-glucose, 1.25 $NaH_2PO_4$, 26 $NaHCO_3$, 2 KCl, 0.4 sodium ascorbic acid, 2 $MgSO_4$, 1 $CaCl_2$, and 1 $MgCl_2$. A mid-sagittal cut was made to divide the two hemispheres, and coronal brain slices (300 µm) were cut using a vibrating blade microtome (Leica VT1200; Wetzlar, DE). The brain slices were transferred to a holding chamber with oxygenated artificial cerebrospinal fluid (aCSF) containing (in mM): 119 NaCl, 2.5 KCl, 1 $NaH_2PO_4$, 26.2 $NaHCO_3$, 11 d-glucose, 1 sodium ascorbic acid, 1.3 $MgSO_4$ and 2.5 $CaCl_2$ (~295 mOsm, pH 7.2-7.3) at 37ºC for 20 minutes and then room temperature for at least 40 m of rest. The slices were kept submerged in oxygenated aCSF in a holding chamber at room temperature for up to 7-8

h after slicing. Unless otherwise stated, all chemicals were purchased from Tocris Bioscience (Bristol, UK), Sigma-Aldrich (St. Louis, MO), and Fisher Chemical (Pittsburgh, PA).

*Miniature excitatory post-synaptic currents (mEPSC) recordings*. After at least 1 h of rest, individual slices were transferred to the recording chamber where they were perfused with oxygenated aCSF (32 ºC) containing 100 µM of $GABA_A$ receptor antagonist, picrotoxin and 1 µM of tetrodotoxin to block voltage-gated sodium channels. Recordings from the NAc core and medial shell were done in the same slices which were obtained between +1.00 mm to +1.70 mm anterior from bregma (Paxinos and Franklin, 2019). Cells were visualized using infrared differential interference contrast (IR-DIC) optics (Microscope: Olympus BX51; Camera: IR 1000 Dage-MIT). Whole-cell voltage clamp recordings were performed using borosilicate glass pipettes (O.D. 1.5 mm, I.D. 0.86 mm; Sutter Instruments) with a 4-7-MΩ open-tip resistance. Pipettes were filled with a cesium methanesulfonate-based internal solution containing (in mM): 120 CsMeS, 15 CsCl, 10 TEA-Cl, 8 NaCl, 10 HEPES, 0.4 EGTA, and 2 $Mg^{2+}$ATP/0.3 $Na_2$GTsP (~280mOsm, pH adjusted to 7.2 with KOH). MSNs were identified based on morphology (medium-sized soma) as well as a hyperpolarized resting potential between -70 to -90 mV. All recordings were obtained using the MultiClamp 700B (Molecular Devices, San Jose, CA) amplifier and Digidata 1550A (Molecular Devices, San Jose, CA) digitizer. Data were filtered at 2 kHz, digitized at 10 kHz, and were collected and analyzed using pClamp 10.0 software (Molecular Devices, San Jose, CA).

To perform whole-cell recordings, membrane seals with a resistance >1 GΩ were achieved prior to breaking into the cell. Membrane capacitance ($C_m$) and series

resistance ($R_s$) were compensated under voltage-clamp. $R_s$ was recorded before and after each recording, and only cells with a with an $R_s$ < 40 MΩ were included, with the majority of cells with an $R_s$ between 30-35 MΩ (**STs**: n = 22; **GTs**: n = 16). To record mEPSCs, cells were held at -80mV for a total of five minutes, and the first 500 events were analyzed to obtain mEPSC peak amplitude and frequency.

*Optically evoked excitatory post-synaptic currents (EPSC) recordings*. Recordings were performed as it was described above for mEPSCs with a few modifications. Slices were perfused with oxygenated aCSF (32 ºC) containing 100 µM of picrotoxin (Tocris Bioscience), and all recordings were done in the NAc medial shell (Paxinos and Franklin, 2019). Cell visualization was done with IR-DIC optics (Scientifica SlicePro 1000). Excitatory post synaptic currents were evoked by optogenetic stimulation using a digital micromirror device and a 470 nm LED (Polygon 400, Mightex, Toronto Ontario) controlled by a Mightex BLS-SA/PL series BioLED control module.

As described above $C_m$ and $R_s$ were compensated under voltage-clamp. Only cells with an $R_s$ < 40 MΩ were included, though the majority of cells had an $R_s$ between 20-30 MΩ (**STs**: n = 48; **GTs**: n = 51). To record optically evoked-EPSCs, cells were held at -80mV. An input-output curve was generated by stimulating each cell at four varying LED intensities (25%, 50%, 75%, 100%). At each intensity, a 2-ms optical pulse was delivered six times separated by 20 s. For every cell, all six sweeps were averaged for each stimulation intensity to obtain EPSC amplitude, rise time, halfwidth, and decay time. Paired-pulse ratio recordings were performed by delivering two 3-ms optical pulses separated by 50 ms at 75% of the total LED intensity. Six sweeps separated by 20 s were collected for each cell, and the paired-pulse ratio was calculated by dividing

the amplitude of the second EPSC by the amplitude of the first EPSC for each of the six sweeps. The paired-pulse ratio reported is the average ratio of all six sweeps.

## Experimental Design and Statistical Analysis

### *Behavioral Studies*

The behavioral response in the PavCA procedure was scored using an index that integrates the number, latency, and probability of lever presses (sign-tracking conditioned response) and magazine entries (goal-tracking conditioned response) during CS presentations within a session (Meyer et al., 2012). In brief, we averaged the response bias (i.e., number of lever presses and magazine entries for a session; [lever presses – magazine entries] / [lever presses + magazine entries]), latency score (i.e., average latency to perform a lever press or magazine entry during a session; [magazine entry latency – lever press latency]/10), and probability difference (i.e., proportion of lever presses or magazine entries; lever press probability – magazine entry probability). The index score ranges from +1.0 (absolute sign-tracking) to -1.0 (absolute goal-tracking), with 0 representing no bias. The average PavCA index scores of Sessions 5-6 were used to classify rats as STs (score ≥ 0.5), GTs (score ≤ -0.5), and IRs (-0.5 < score < 0.5). Out of a total of 12 rats used for mEPSC recordings, 3 were classified as STs, 3 were GTs, and 6 were IRs (not included in the analysis). Out of a total of 48 rats used for optically evoked-EPSC recordings, 11 were classified as STs, 10 were GTs, and 27 were IRs. For evoked-EPSCs, only STs and GTs underwent viral injections for further study. Any ST or GT not included in the electrophysiological data analysis was also excluded from the behavioral analysis.

GraphPad Prism 8 (Dotmatics) was used for all the behavioral data statistical analysis. Number, latency, and probability for lever presses and for magazine entries, as well as PavCA index scores, were analyzed using mixed-effects modeling via restricted maximum likelihood (REML). Fixed effects were set for phenotype (STs, GTs), session (1-6), and phenotype x session. Data are presented as mean ± SEM, and significance level was set at $p < 0.05$. Full statistical report for all behavioral data analysis is found in **Table 5.2**.

### *Electrophysiological Studies*

All offline analysis of electrophysiological recordings was performed using Clampfit 10.7 (Molecular Devices). Statistical analyses were made using GraphPad Prism 8 (Dotmatics).

*mEPSC recordings.* A total of 38 cells from 6 rats were included in the analysis. The STs group had a total of 3 rats, from which 12 cells were recorded in the core of 3 rats (1-2 slices/4 cells per rat) and 10 cells in the shell of 3 of the rats (1-2 slices/2-4 cells per rat). The GTs group had a total of 3 rats, from which 8 cells were recorded in the core of 3 rats (1-2 slices/2-3 cells per rat) and 8 cells in the shell of 3 rats (1-2 slices/2-3 cells per rat).

mEPSC peak amplitude and instantaneous frequency were obtained using the template search function on Clampfit 10.7. The first 500 events from each 5-min recording were analyzed for the core and shell separately. Cumulative frequency distribution analysis was performed, and bin size was set automatically on GraphPad Prism 8. Histograms were tested for significant differences using the Kolmogorov-Smirnov test. mEPSC peak and frequency averages were calculated for each cell, and

group differences were assessed by performing two-tailed t-test between STs and GTs. Data are presented as mean ± SEM with each data point representing the average of the first 500 events for an individual cell, and significance level was set at $p < 0.05$.

*Optically evoked-EPSC recordings.* A total of 99 cells from 14 rats were included in the analysis. Out of 21 rats used for evoked-EPSC recordings, optical evocation of EPSCs in slices from 7 of the rats failed for undetermined technical problems. Another rat was excluded due to an inability to evoke sub-threshold EPSCs. No data from these rats were included (5 STs, 3 GTs) in the analysis. The evoked-EPSC data reported here were obtained from the following: the STs group had a total of 6 rats, from which 48 cells were recorded in the NAc of 6 rats (2-4 slices/5-12 cells per rat). The GTs group had a total of 7 rats, from which 51 cells were recorded in the NAc of 7 rats (2-4 slices/5-11 cells per rat). Out of all recorded cells, paired-pulse recordings at 75% stimulation intensity were performed in 31 cells from 6 STs (1-4 slices/4-9 cells per rat), and 26 from 6 GTs (2-4 slices/3-6 cells per rat).

EPSCs amplitude, rise time, halfwidth, and decay time were analyzed using two-way ANOVA to test for significant group differences between STs and GTs. Fixed effects were set for phenotype (STs, GTs), stimulation intensity (25%, 50%, 75%, 100%), and phenotype x stimulation intensity. Based on Sidak's post hoc test for multiple comparisons, planned comparisons using t-test (normal and nested) were performed between STs and GTs for EPSC amplitude and rise time only at 25% stimulation intensity. Cumulative frequency distribution analysis was also performed, and bin size was set to 30 for EPSC amplitude and to 0.25 for rise time. Histograms were tested for significant differences using the Kolmogorov-Smirnov test. Paired-pulse

ratios (PPR) were calculated by dividing the amplitude of the second EPSC by the amplitude of the first EPSC, then averaging for all six sweeps to obtain a single ratio per cell. PPR at 75% stimulation intensity was analyzed using t-test between STs and GTs. Data are presented as mean ± SEM, and significance level was set at $p < 0.05$. Full statistical report for all electrophysiological data analysis is found in **Table 5.2**.

## Results

### *Overall baseline excitatory synaptic input of STs and GTs in the NAc*

We wanted to determine whether "sign-tracking" and "goal-tracking" rats differ in overall baseline excitatory synaptic input to MSNs in both the NAc core and shell. To identify these behavioral phenotypes in an outbred population, a cohort of rats underwent six days of PavCA training with a lever-cue (CS) paired with a response-independent delivery of a banana-flavored food pellet into a magazine (US) **(Fig 5.1)**. Based on their PavCA index score on Sessions 5-6 (see ***Experimental Design and Statistical Analysis*** session for PavCA index score calculation), rats were classified as either STs (score ≥ 0.5; n = 3) or GTs (score ≤ -0.5; n = 3) (**Fig 5.1)**. STs exhibited greater lever press number (**Fig 5.2A:** mixed-effects model: session x phenotype interaction, $p < 0.0001$), lower latency (**Fig 5.2A:** mixed-effects model: session x phenotype interaction, $p < 0.0001$), and greater probability (**Fig 5.2A:** mixed-effects model: session x phenotype interaction, $p < 0.0001$) compared to GTs. Conversely, compared to STs, GTs exhibited greater magazine entry number (**Fig 5.2B:** mixed-effects model: session x phenotype interaction, $p < 0.001$), lower latency (**Fig 5.2B:** mixed-effects model: session x phenotype interaction, $p < 0.01$), and greater probability (**Fig 5.2B:** mixed-effects model: session x phenotype interaction, $p < 0.001$). By

definition, the PavCA index score across the six training sessions significantly differed from one another (**Fig 5.1D:** mixed-effects model: session x phenotype interaction, $p < 0.0001$) confirming their difference in their behavior response bias toward the lever and magazine, which is indicative of different levels of incentive and predictive value attribution to the cue.

To explore whether STs and GTs have fundamental differences in excitatory inputs to the NAc core and shell, we measured miniature excitatory post-synaptic currents (mEPSCs) by performing whole-cell voltage-clamp recordings in rat brain slices following a 1-2 week resting period after the last PavCA training session **(Fig 5.1)**. This resting time was meant to allow for any putative training-induced synaptic changes to return to baseline levels. To capture both pre- and post-synaptic measures of excitatory transmission, we tested for differences in mEPSC frequency and amplitude. While changes in mEPSC frequency are usually thought to reflect altered pre-synaptic glutamatergic vesicle release, changes in mEPSC amplitude are presumed to indicate a change in post-synaptic response. Therefore, together these two measures can provide a general characterization of excitatory transmission dynamics at the synapse. In the NAc shell, we found no significant differences between STs and GTs in the mEPSC amplitude (**Fig 5.3A:** Kolmogorov-Smirnov test: $p = 0.5596$) or frequency (**Fig 5.3C:** Kolmogorov-Smirnov test: $p > 0.9999$) cumulative frequency distribution. The cell average mEPSC amplitude (**Fig 5.3B:** unpaired t-test: $p = 0.2348$) and frequency (**Fig 5.3D:** unpaired t-test: $p = 0.9423$) were also not significantly different between the two phenotypes. In the NAc core, the cumulative frequency distributions of mEPSC amplitude were significantly different between STs and GTs, with GTs exhibiting a slight

shift to the right indicative of greater mEPSC amplitude compared to STs (**Fig 5.3E:** Kolmogorov-Smirnov test: p = 0. 0104). However, STs and GTs did not differ in the cell average mEPSC amplitude suggesting this might be a very subtle difference (**Fig 5.3F:** unpaired t-test: p = 0.1720). Neither the cumulative frequency distribution of mEPSC frequency (**Fig 5.3G:** Kolmogorov-Smirnov test: p = 0. 6208) nor the cell average mEPSC frequency (**Fig 5.3H:** unpaired t-test: p = 0.3561) were significantly different between STs and GTs in the NAc core.

These findings suggest that MSNs from the NAc core and shell of STs and GTs exhibit similar overall excitatory input. However, they do not reveal information about specific excitatory afferents that may differentially modulate NAc activity through variations in synaptic transmission efficacy.

***Synaptic transmission efficacy of the vHPC-NAc projection in STs and GTs***

Previous *in vivo* studies exploring the role of the vHPC-NAc projection in the attribution of incentive salience suggest that there may be functional differences between STs and GTs in how this projection modulates their conditioned responses. Therefore, we now wanted to determine whether STs and GTs also exhibit differences in vHPC-NAc synaptic transmission efficacy, meaning the strength of the communication between these neurons. As described previously, a new cohort of rats underwent six days of PavCA training and were classified as either STs (score ≥ 0.5; n = 6) or GTs (score ≤ -0.5; n = 7) based on their significantly different PavCA index score or behavior bias (**Fig 5.1E:** mixed-effects model: session x phenotype interaction, p < 0.0001). Once again, STs exhibited greater lever press number (**Fig 5.5A:** mixed-effects model: session x phenotype interaction, p < 0.0001), lower latency (**Fig 5.5A:**

mixed-effects model: session x phenotype interaction, $p < 0.0001$), and greater probability (**Fig 5.5A:** mixed-effects model: session x phenotype interaction, $p < 0.0001$) compared to GTs. Conversely, compared to STs, GTs exhibited greater magazine entry number (**Fig 5.5B:** mixed-effects model: session x phenotype interaction, $p < 0.0001$), lower latency (**Fig 5.5B**: mixed-effects model: session x phenotype interaction, $p < 0.0001$), and greater probability (**Fig 5.5B**: mixed-effects model: session x phenotype interaction, $p < 0.0001$).

Following PavCA training, rats received transcranial viral injections of channelrhodopsin into the vHPC to allow for *ex vivo* optogenetic stimulation of vHPC axon terminals during whole-cell recordings of MSNs in the NAc **(Fig 5.4)**. Since the majority of vHPC inputs innervate the medial shell portion of the NAc, we performed all our recordings in this area. To determine whether there were differences in vHPC-NAc synaptic transmission efficacy, we analyzed properties of optically evoked EPSCs **(Fig 5.6E)**. We studied basal synaptic transmission by delivering 2-ms optical pulses at varying intensities ranging from 25% to 100% of the LED capacity in 25% increments. We found that across all stimulation intensities, STs and GTs did not differ in EPSC amplitude (**Fig 5.6A:** 2-way ANOVA: no effect of phenotype, $p = 0.4995$), halfwidth (**Fig 5.6B:** 2-way ANOVA: no effect of phenotype, $p = 0.1749$), rise time (**Fig 5.6C:** 2-way ANOVA: no effect of phenotype, $p = 0.2937$), or decay time (**Fig 5.6D:** 2-way ANOVA: no effect of phenotype, $p = 0.2993$). However, for each EPSC property, there was a main effect of stimulation intensity indicating that there was an increment in the optically evoked-EPSC response (**Fig 5.6A-D:** 2-way ANOVA: main effect of stim. intensity, $p < 0.0001$).

Since most EPSC measures reached a plateau at 50% stimulation intensity, we examined whether any significant differences could be uncovered at the 25% stimulation intensity, particularly the EPSC amplitude and rise time. We found that the cumulative frequency distributions of EPSC amplitude were significantly different, with GTs exhibiting a slight shift to the right indicative of greater EPSC amplitude than STs (**Fig 5.6F:** Kolmogorov-Smirnov test: p = 0.0158). Nonetheless, we also performed normal (**Fig 5.6F inset:** unpaired t-test: p = 0.0821) and nested (**Fig 5.6F inset:** nested t-test: p = 0.4936) mean comparisons and no significant differences were found, suggesting that this may be a very subtle difference between the two phenotypes. For EPSC rise time, the cumulative frequency distributions of STs and GTs did not significantly differ (**Fig 5.6G:** Kolmogorov-Smirnov test: p = 0.7937). However, when we performed mean comparisons, GTs did exhibit significantly greater EPSC rise time compared to STs (**Fig 5.6G inset:** unpaired t-test: p = 0.0136). We also performed a nested mean comparison to control for individual subject effects, (**Fig 5.6G inset:** nested t-test: p = 0.9879), and EPSC rise time was no longer significantly different between the two phenotypes. Again, this suggests that vHPC-NAc synaptic transmission efficacy may be similar for STs and GTs, with the slight differences observed here being driven by a small number of individual rats.

Finally, we wanted to determine whether there were any differences in vHPC-NAc paired-pulse ratio (PPR) which can give information about pre-synaptic glutamate release probability and short-term plasticity in STs and GTs. To test this, we evoked two consecutive EPSCs in a small-time window (50 ms). A high release probability typically causes depletion of a large number of vesicles after the first EPSC (P1), which results in

a smaller second EPSC (P2). We found that both STs and GTs exhibited paired-pulse depression, which suggests that for both phenotypes there is a high release probability (P2/P1 < 1.0) in this projection, though the ratio was not significantly different between the two **(Fig 5.7A-B)**.

**Discussion**

Our findings suggest that overall, MSNs in the NAc of STs and GTs exhibit very similar baseline excitatory synaptic input. In the NAc shell, STs and GTs did not differ in the amplitude and frequency of mEPSCs as indicated by no significant differences in cumulative frequency distributions or mean comparisons of either measure. In the NAc core, however, we found that the cumulative frequency distributions for mEPSC amplitude were slightly different, indicating that for GTs mEPSC amplitude was generally greater than for STs. Nonetheless, mean comparison revealed no significant differences, suggesting that the variation may be very subtle. Furthermore, the mEPSC frequency in NAc core MSNs was not different between the two phenotypes.

Although these findings suggest that the overall, pre-synaptic and post-synaptic excitatory transmission is indistinguishable between STs and GTs, the generally lower mEPSC amplitude in the NAc core of STs is worth discussing. As described in Chapter II, MSNs in the core of STs are less excitable compared to MSN in GTs. However, the intrinsic excitability measures described in Chapter II were studied under both glutamatergic and GABAergic transmission blockers. This suggests that differences in glutamatergic transmission would not have influenced MSN intrinsic excitability in those experiments. We hypothesized that differences between STs and GTs in dopamine transporters (Singer et al., 2016) and receptor activation, could modulate intrinsic

excitability (O'Donnell and Grace, 1996; Nicola et al., 2000; Surmeier et al., 2007; Planert et al., 2013). Studies have demonstrated that although dopamine in the NAc core can significantly reduce mEPSC frequency, it does not affect mEPSC amplitude (Nicola et al., 1996; Nicola and Malenka, 1997). This is thought to occur through activation of pre-synaptic dopamine 1 ($D_1$) receptors that reduce release probability at cortico-accumbal synapses (Nicola et al., 1996). A reduction in mEPSC amplitude, such as the subtle difference observed here, would most likely be due to differences between STs and GTs in glutamate receptor expression and/or activation. Previous studies do suggest that sign- and goal-tracking behavior may be differentially sensitive to glutamatergic transmission in the NAc. For example, during sign-tracking– but not goal-tracking – behavior toward a conditioned stimulus, glutamate levels in the NAc core rise (Batten et al., 2018). Furthermore, both systemic and intra-accumbal NMDA receptor antagonism preferentially impair sign-tracking behavior (Ciano et al., 2001; Fitzpatrick and Morrow, 2017; Chow and Beckmann, 2018). Thus, our finding suggests that post-synaptic differences in the glutamatergic system could provide a physiological explanation for the role of glutamate signaling in the attribution of incentive salience.

In the previous chapter, we demonstrated a role for the vHPC-NAc projection in sign- and goal-tracking behavior *in vivo*. Consistent with the role of the vHPC as a modulator of conditioned responses to discrete cues by means of context-specific information (Turner et al., 2022), we found that decreased activity of vHPC-NAc promotes sign-tracking behavior, while increased activity suppresses it. In this chapter, we explored whether our *in vivo* findings were matched by differences in synaptic strength between STs and GTs. We expected to find that compared to GTs, STs would

exhibit weaker synaptic transmission efficacy in vHPC-NAc. However, our findings suggest that STs and GTs do not exhibit pronounced differences in synaptic strength, as measured by similar optically evoked-EPSC amplitude, halfwidth, rise time, and decay time. We also studied EPSC amplitude and rise time at the 25% stimulation intensity because most properties reached a maximum response at 50% of the stimulation intensity, which might overshadow any subtle differences between STs and GTs. We compared the cumulative frequency distributions of both properties as well as performed normal and nested mean comparisons. Interestingly, and consistent with our prior hypothesis, STs had lower EPSC amplitude and rise time compared to GTs at 25% stimulation intensity. This would suggest weaker synaptic transmission efficacy in vHPC-NAc and would therefore be consistent with the finding that decreased activity in this projection promotes sign-tracking behavior. Nonetheless, because these findings were not consistent upon nested mean comparisons that control for subject variability, it is possible that this effect was driven by a few rats, and definitive conclusions should not be drawn from these findings. Paired-pulse ratios were not significantly different between STs and GTs, which further suggests that the subtle differences in EPSC amplitude and rise time may not be related to changes in vHPC-NAc release probability.

Stronger vHPC-NAc synaptic activity has been associated with both context-driven appetitive and aversive behavioral responses. Stimulation of vHPC-NAc leads to conditioned place preference (Britt et al., 2012; LeGates et al., 2018) and context-driven drug-seeking (Loureiro et al., 2016; Zhou et al., 2019), supporting its role in reward learning. Nonetheless, increasing vHPC-NAc activity can also lead to increased context-dependent fear conditioning (Loureiro et al., 2016), which supports its role in fear

memory formation. These findings have provided evidence that the vHPC-NAc projection serves a role in encoding salience as opposed to valence, as it can store context-specific information necessary to drive both appetitive and aversive motivated behaviors. This same parallel has been proposed for STs and GTs, as they also seem to be differentially sensitive to cues and contexts regardless of their positive or negative valence (Pitchers et al., 2017; Morrow, 2018; María-Ríos and Morrow, 2020). During both context-dependent drug-seeking (Saunders et al., 2014; Pitchers et al., 2017) and context-dependent fear extinction (Morrow et al., 2011), GTs exhibit greater sensitivity than STs. Therefore, decreased vHPC-NAc synaptic strength in STs could be a physiological explanation for the relative inability of contextual information to influence their behavior during both reward and fear learning.

Cannabinoid transmission within the vHPC has been found to reduce local GABAergic feedforward inhibition of glutamatergic projection neurons through cannabinoid type 1 receptors ($CB_1R$) expressed pre-synaptically in the GABAergic neurons (Hájos and Freund, 2002). A study demonstrated that this includes disinhibition of glutamatergic neurons projecting to the NAc shell (Loureiro et al., 2016). They explored the role of the vHPC to NAc projection during context-dependent fear and reward learning by delivering a $CB_1R$ agonist (WIN55) in the vHPC to induce a glutamate-dependent increase in NAc shell activity (Loureiro et al., 2016). Activation of $CB_1$ receptors in the vHPC and subsequent increase in NAc activity resulted in greater context-dependent morphine conditioned place preference and higher freezing responses following contextual fear conditioning (Loureiro et al., 2016). Previous work has demonstrated that systemic administration of the $CB_1R$ agonist CP-55,940 causes

a dose-dependent decrease in sign-tracking behavior and increase in goal-tracking (Gheidi et al., 2020). A potential mechanism for this effect could be increased vHPC-NAc activity which would promote context-driven associative learning responses associated with GTs.

The subtle or unclear differences in vHPC-NAc synaptic strength between STs and GTs might also be due to the way this projection encodes contextual information. Evidence has suggested that neuronal engrams in the vHPC mediate context-driven responses in the NAc through neuronal coupling with MSNs (Zhou et al., 2019). Therefore, it is possible that not all neurons would be equally sensitive to vHPC inputs or would exhibit baseline differences in synaptic activity. Single-unit recordings in STs and GTs during PavCA have demonstrated that not all neurons in the NAc respond equally during cue and reward presentations (Gillis and Morrison, 2019). This may add a level of difficulty in capturing the specific neuronal populations responsible for diverging STs and GTs behavioral responses in different associative learning tasks. Furthermore, it is important to note that both mEPSC and evoked-EPSC recordings in the present study were performed following a long resting period after the last PavCA session as we were interested in capturing baseline or pre-existent differences between STs and GTs. However, the findings in this chapter may highlight that some of the behavioral or *in vivo* differences between STs and GTs may in actuality be linked to activity- or experience-dependent responses or adaptations in the glutamatergic system, meaning that real-time events may influence how these structures are differentially engaged. Further synaptic studies in STs and GTs could try to capture immediate changes in synaptic activity following PavCA and other behavioral tasks or

focus on mechanisms of synaptic plasticity such as long-term potentiation and depression that may differentially modulate neuronal activity.

## References


Batten SR, Pomerleau F, Quintero J, Gerhardt GA, Beckmann JS (2018) The role of glutamate signaling in incentive salience: second-by-second glutamate recordings in awake Sprague Dawley rats. J Neurochem 145:276–286.

Berridge KC, Robinson TE, Aldridge JW (2009) Dissecting components of reward: 'liking', 'wanting', and learning. Curr Opin Pharmacol 9:65–73.

Britt JP, Benaliouad F, McDevitt RA, Stuber GD, Wise RA, Bonci A (2012) Synaptic and behavioral profile of multiple glutamatergic inputs to the nucleus accumbens. Neuron 76:790–803.

Chow JJ, Beckmann JS (2018) NMDA receptor blockade specifically impedes the acquisition of incentive salience attribution. Behav Brain Res 338:40–46.

Ciano PD, Cardinal RN, Cowell RA, Little SJ, Everitt BJ (2001) Differential involvement of NMDA, AMPA/Kainate, and dopamine receptors in the nucleus accumbens core in the acquisition and performance of pavlovian approach behavior. J Neurosci 21:9471–9477.

Dalley JW, Lääne K, Theobald DEH, Armstrong HC, Corlett PR, Chudasama Y, Robbins TW (2005) Time-limited modulation of appetitive Pavlovian memory by D1 and NMDA receptors in the nucleus accumbens. Proc Natl Acad Sci U S A 102:6189–6194.

Day JJ, Carelli RM (2007) The nucleus accumbens and pavlovian reward learning. Neurosci Rev J Bringing Neurobiol Neurol Psychiatry 13:148–159.

Fitzpatrick CJ, Morrow JD (2017) Subanesthetic ketamine decreases the incentive-motivational value of reward-related cues. J Psychopharmacol Oxf Engl 31:67–74.

Flagel SB, Akil H, Robinson TE (2009) Individual differences in the attribution of incentive salience to reward-related cues: Implications for addiction. Neuropharmacology 56 Suppl 1:139–148.

Gheidi A, Cope LM, Fitzpatrick CJ, Froehlich BN, Atkinson R, Groves CK, Barcelo CN, Morrow JD (2020) Effects of the cannabinoid receptor agonist CP-55,940 on incentive salience attribution. Psychopharmacology (Berl) 237:2767–2776.

Gillis ZS, Morrison SE (2019) Sign tracking and goal tracking are characterized by distinct patterns of nucleus accumbens activity. eNeuro 6.

Hájos N, Freund TF (2002) Distinct cannabinoid sensitive receptors regulate hippocampal excitation and inhibition. Chem Phys Lipids 121:73–82.

LeGates TA, Kvarta MD, Tooley JR, Francis TC, Lobo MK, Creed MC, Thompson SM (2018) Reward behaviour is regulated by the strength of hippocampus–nucleus accumbens synapses. Nature 564:258–262.

Loureiro M, Kramar C, Renard J, Rosen LG, Laviolette SR (2016) Cannabinoid transmission in the hippocampus activates nucleus accumbens neurons and modulates reward and aversion-related emotional salience. Biol Psychiatry 80:216–225.

María-Ríos CE, Morrow JD (2020) Mechanisms of shared vulnerability to post-traumatic stress disorder and substance use disorders. Front Behav Neurosci 14:6.

Meyer PJ, Lovic V, Saunders BT, Yager LM, Flagel SB, Morrow JD, Robinson TE (2012) Quantifying individual variation in the propensity to attribute incentive salience to reward cues. PLOS ONE 7:e38987.

Morrow ATJ (2018) Sign-tracking and drug addiction. Available at: http://hdl.handle.net/2027/spo.mpub10215070.

Morrow JD, Maren S, Robinson TE (2011) Individual variation in the propensity to attribute incentive salience to an appetitive cue predicts the propensity to attribute motivational salience to an aversive cue. Behav Brain Res 220:238–243.

Muir J, Tse YC, Iyer ES, Biris J, Cvetkovska V, Lopez J, Bagot RC (2020) Ventral hippocampal afferents to nucleus accumbens encode both latent vulnerability and stress-induced susceptibility. Biol Psychiatry 88:843–854.

Nicola SM, Kombian SB, Malenka RC (1996) Psychostimulants depress excitatory synaptic transmission in the nucleus accumbens via presynaptic D1-like dopamine receptors. J Neurosci 16:1591–1604.

Nicola SM, Malenka RC (1997) Dopamine depresses excitatory and inhibitory synaptic transmission by distinct mechanisms in the nucleus accumbens. J Neurosci 17:5697–5710.

Nicola SM, Surmeier DJ, Malenka RC (2000) Dopaminergic modulation of neuronal excitability in the striatum and nucleus accumbens. Annu Rev Neurosci 23:185–215.

O'Donnell P, Grace AA (1996) Dopaminergic reduction of excitability in nucleus accumbens neurons recorded in vitro. Neuropsychopharmacology 15:87–97.

Paxinos G, Franklin KBJ (2019) Paxinos and Franklin's the Mouse Brain in Stereotaxic Coordinates. Academic Press.

Pitchers KK, Phillips KB, Jones JL, Robinson TE, Sarter M (2017) Diverse roads to relapse: a discriminative cue signaling cocaine availability is more effective in

renewing cocaine seeking in goal trackers than sign trackers and depends on basal forebrain cholinergic activity. J Neurosci 37:7198–7208.

Planert H, Berger TK, Silberberg G (2013) Membrane properties of striatal direct and indirect pathway neurons in mouse and rat slices and their modulation by dopamine. PLOS ONE 8:e57054.

Saunders BT, O'Donnell EG, Aurbach EL, Robinson TE (2014) A cocaine context renews drug seeking preferentially in a subset of individuals. Neuropsychopharmacology 39:2816–2823.

Saunders BT, Robinson TE (2011) Individual variation in the motivational properties of cocaine. Neuropsychopharmacology 36:1668–1676.

Singer BF, Guptaroy B, Austin CJ, Wohl I, Lovic V, Seiler JL, Vaughan RA, Gnegy ME, Robinson TE, Aragona BJ (2016) Individual variation in incentive salience attribution and accumbens dopamine transporter expression and function. Eur J Neurosci 43:662–670.

Surmeier DJ, Ding J, Day M, Wang Z, Shen W (2007) D1 and D2 dopamine-receptor modulation of striatal glutamatergic signaling in striatal medium spiny neurons. Trends Neurosci 30:228–235.

Turner BD, Kashima DT, Manz KM, Grueter CA, Grueter BA (2018) Synaptic plasticity in the nucleus accumbens: Lessons learned from experience. ACS Chem Neurosci 9:2114–2126.

Turner VS, O'Sullivan RO, Kheirbek MA (2022) Linking external stimuli with internal drives: A role for the ventral hippocampus. Curr Opin Neurobiol 76:102590.

Versaggi CL, King CP, Meyer PJ (2016) The tendency to sign-track predicts cue-induced reinstatement during nicotine self-administration, and is enhanced by nicotine but not ethanol. Psychopharmacology (Berl) 233:2985–2997.

Zhou Y, Zhu H, Liu Z, Chen X, Su X, Ma C, Tian Z, Huang B, Yan E, Liu X, Ma L (2019) A ventral CA1 to nucleus accumbens core engram circuit mediates conditioned place preference for cocaine. Nat Neurosci 22:1986–1999.

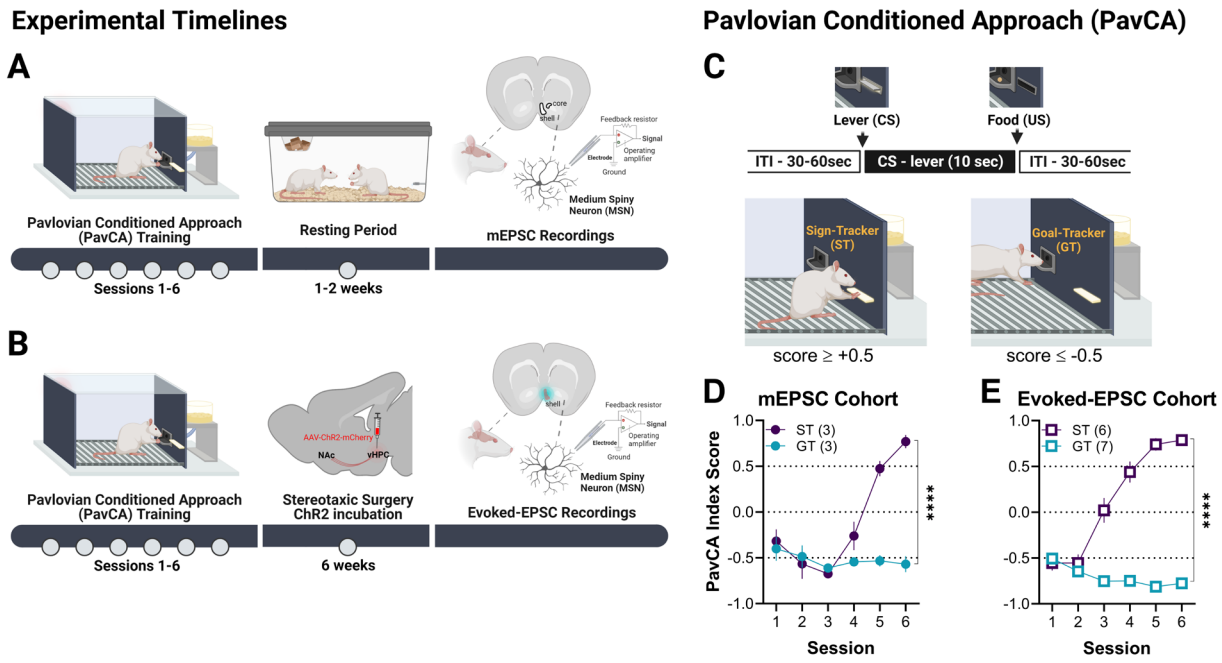


**Figure 5.1**. *Experimental timelines.* **A-B)** Two separate cohort of rats were run. All rats were housed in pairs upon arrival. After at least two days of acclimation to the housing room and pre-training session, rats underwent six daily sessions of a Pavlovian conditioned approach (PavCA) procedure. **C)** During PavCA a neutral lever-cue (CS) was presented and following its retraction a banana-flavored food pellet reward (US) was immediately delivered into the magazine. Each session consisted of 25 trials of CS-US pairings (ITI: 30-60 s). In response to the CS, sign-trackers (STs) approach and interact with the lever although no response is necessary for reward delivery. Goal-trackers (GTs) approach the magazine which is the site of impending food delivery. Rats used for recordings of miniature excitatory post-synaptic currents (mEPSCs) remained in their homecages for 1-2 weeks before electrophysiological recordings **(A)**. Rats used for optically evoked EPSCs in the nucleus accumbens (NAc) underwent stereotaxic surgery to deliver ChR2 virus into the ventral hippocampus (vHPC), followed by a 6-week incubation period before electrophysiological recordings **(B)**. The PavCA index incorporates the number, latency, and probability of lever presses and magazine entries during CS presentations within a session. A score of +1.0 is absolute sign-tracking, while -1.0 is absolute goal-tracking (0 represents no bias). **D-E)** Lever vs. magazine bias over the course of training: STs and GTs significantly differed between one another in their PavCA index score across the six training sessions (mixed-effects model: session x phenotype interaction, $p < 0.0001$) indicating a significant difference between their behavior response bias toward the lever and magazine. Significance for phenotype x session interaction is shown as **** - $p < 0.0001$. Data are presented as mean ± S.E.M. Created with BioRender.com (A-C).

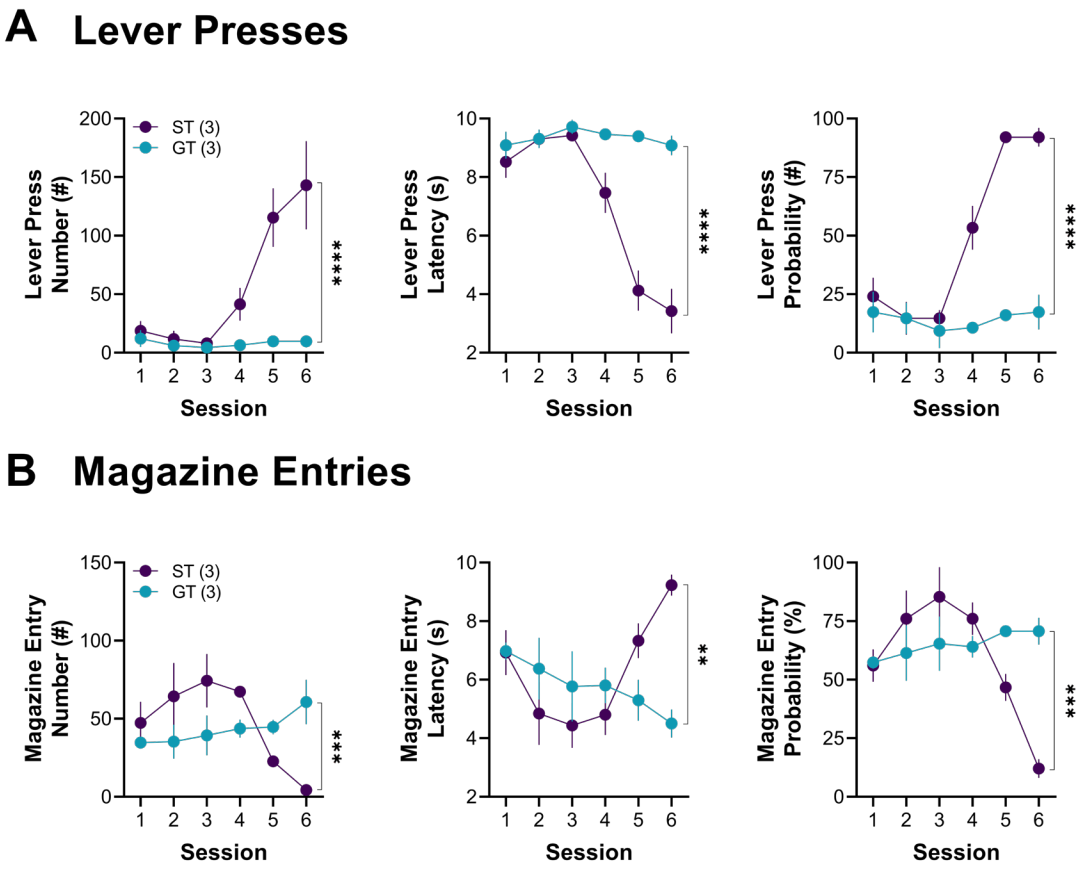


**Figure 5.2**. *Behavioral data from rats used for miniature excitatory post-synaptic currents (mEPSCs).* Sign-trackers (STs) and goal-trackers (GTs) differ in the number, latency, and probability of lever presses and magazine entries during a Pavlovian conditioned approach (PavCA) procedure. All rats underwent six sessions of PavCA and were classified as STs (n = 3) or GTs (n = 3) based on their lever press and magazine entry number (left), latency (center), and probability (right) during Sessions 5-6. **A)** Across all six sessions STs exhibited greater lever press number (mixed-effects model: session x phenotype interaction, $p < 0.0001$), lower latency (mixed-effects model: session x phenotype interaction, $p < 0.0001$), and greater probability (mixed-effects model: session x phenotype interaction, $p < 0.0001$) compared to GTs. **B)** Across all six sessions GTs exhibited greater magazine entry number (mixed-effects model: session x phenotype interaction, $p < 0.001$), lower latency (mixed-effects model: session x phenotype interaction, $p < 0.01$), and greater probability (mixed-effects model: session x phenotype interaction, $p < 0.001$) compared to STs. Significance for phenotype x session interaction is shown as **** - $p < 0.0001$, *** - $p < 0.001$, ** - $p < 0.01$. Data are presented as mean ± S.E.M.

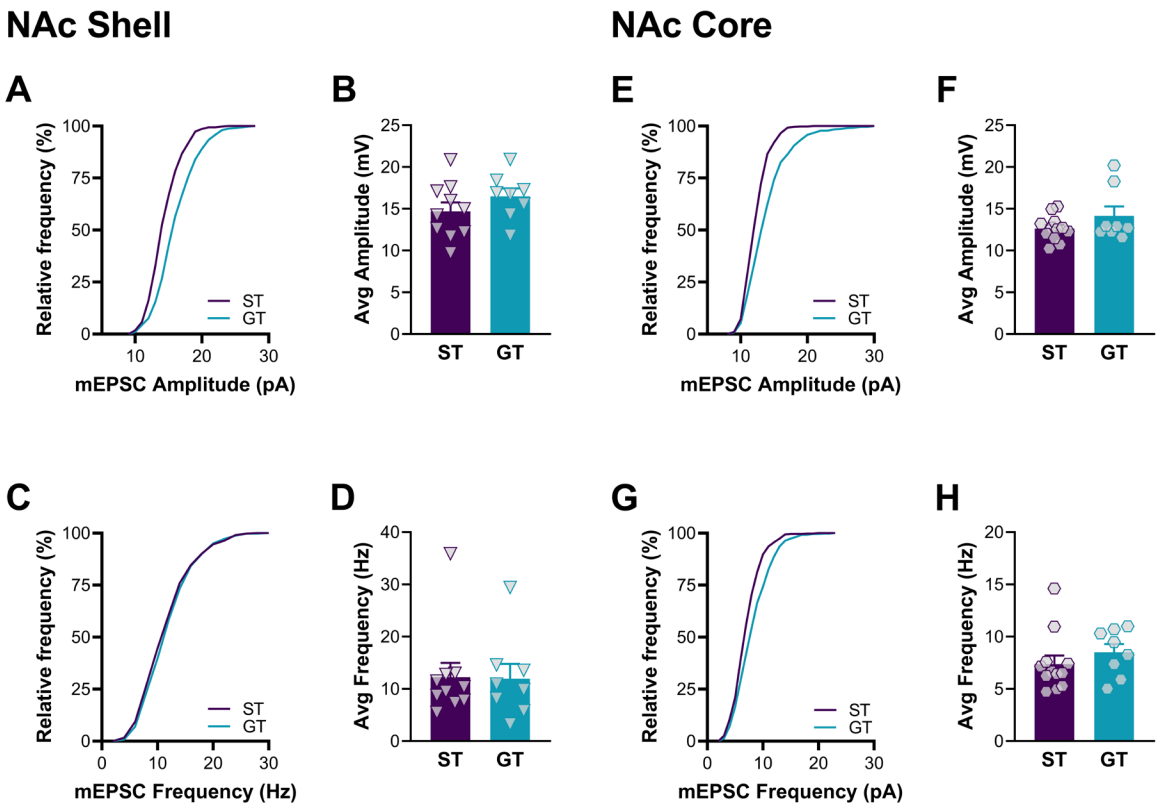


**Figure 5.3.** *Miniature excitatory post-synaptic currents (mEPSCs) in core and shell medium spiny neurons (MSNs) of the nucleus accumbens (NAc) of sign-trackers (STs) and goal-trackers (GTs).* To record mEPSCs, each cell was held at -80mV for 5 min, and the first 500 events were analyzed. **NAc shell: A)** Cumulative frequency distributions of mEPSC amplitude of STs and GTs were not significantly different (Kolmogorov-Smirnov test: p = 0.5596). **B)** No significant differences were seen in the average cell mEPSC amplitude of STs and GTs (unpaired t-test: p = 0.2348). **C)** Cumulative frequency distributions of mEPSC frequency were also not significantly different between STs and GTs (Kolmogorov-Smirnov test: p > 0.9999). **D)** The average cell mEPSC frequency of STs and GTs did not differ (unpaired t-test: p = 0.9423). **NAc core: E)** Cumulative frequency distributions of mEPSC amplitude were significantly different (Kolmogorov-Smirnov test: p = 0.0104), suggesting that GTs exhibited greater mEPSC amplitude than STs. **F)** However, when averaged by cell, mEPSC amplitude of the two phenotypes did not differ (unpaired t-test: p = 0.1720). **G)** Cumulative frequency distributions of mEPSC frequency were not significantly different between STs and GTs (Kolmogorov-Smirnov test: p = 0.6208). **H)** The average cell mEPSC frequency of STs and GTs also did not differ (unpaired t-test: p = 0.3561). Data are presented as mean ± S.E.M, and each data point represents a single cell.

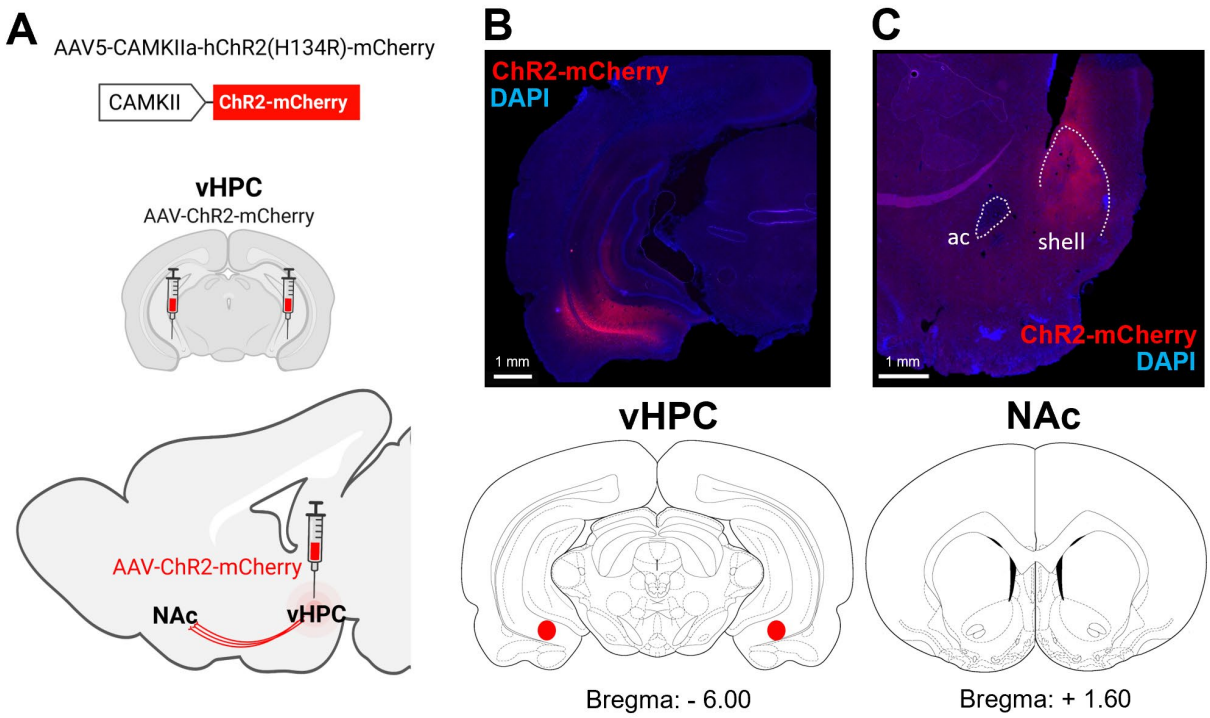


**Figure 5.4**. *Channelrhodopsin (ChR2) expression in the ventral hippocampus (vHPC) and nucleus accumbens (NAc).* **A)** Representative diagram of viral vector (AAV) containing humanized ChR2 with mCherry protein tag injected into the vHPC (0.5 µl). ChR2 expression following a 6-week incubation period can be determined through mCherry visualization in **(B)** vHPC cell bodies and **(C)** vHPC axon terminals in the NAc area. Created with BioRender.com (A).

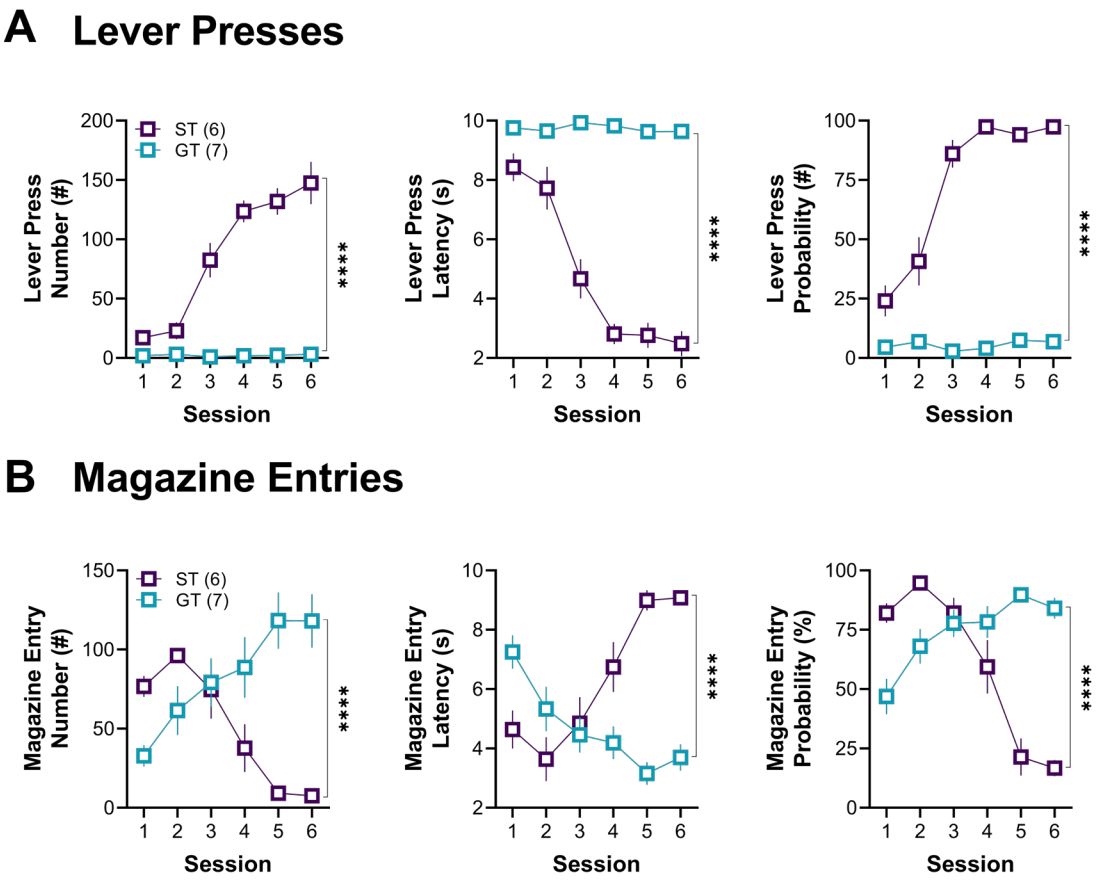


**Figure 5.5.** *Behavioral data from sign-trackers (STs) and goal-trackers (GTs) used for testing synaptic transmission efficacy in the ventral hippocampus (vHPC) to nucleus accumbens (NAc) projection.* STs and GTs differed in the number, latency, and probability of lever presses and magazine entries during a Pavlovian Conditioned Approach (PavCA) procedure. **A)** Across all six sessions STs (n = 6) exhibited greater lever press number (mixed-effects model: session x phenotype interaction, $p < 0.0001$), lower latency (mixed-effects model: session x phenotype interaction, $p < 0.0001$), and greater probability (mixed-effects model: session x phenotype interaction, $p < 0.0001$) compared to GTs (n = 7). **B)** Across all six sessions GTs exhibited greater magazine entry number (mixed-effects model: session x phenotype interaction, $p < 0.0001$), lower latency (mixed-effects model: session x phenotype interaction, $p < 0.0001$), and greater probability (mixed-effects model: session x phenotype interaction, $p < 0.0001$) compared to STs. Significance for phenotype x session interaction is shown as **** - $p < 0.0001$. Data are presented as mean ± S.E.M.

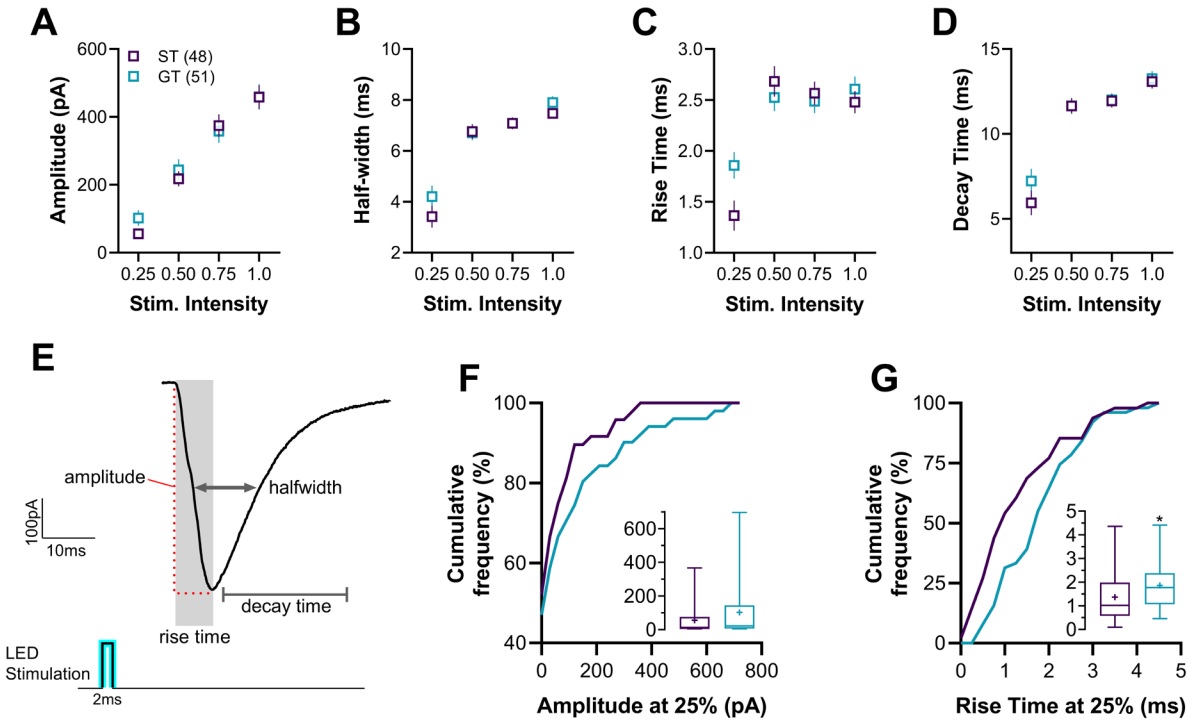


**Figure 5.6.** *Synaptic transmission efficacy in the ventral hippocampus (vHPC) to nucleus accumbens (NAc) projection of sign-trackers (STs) and goal-trackers (GTs).* **E)** Representative excitatory post-synaptic current (EPSC) from voltage-clamp recording of NAc medium spiny neuron (MSN) following a 2-ms optical pulse to depolarize vHPC axon terminals. An input-output curve was generated by stimulating each cell at 25%, 50%, 75%, and 100% of LED intensity. Across all stimulation intensities, STs and GTs did not differ in EPSC **A)** amplitude (2-way ANOVA: no effect of phenotype, $p = 0.4995$), **B)** halfwidth (2-way ANOVA: no effect of phenotype, $p = 0.1749$), **C)** rise time (2-way ANOVA: no effect of phenotype, $p = 0.2937$), and **D)** decay time (2-way ANOVA: no effect of phenotype, $p = 0.2993$). For each EPSC measure, there was a main effect of stimulation intensity indicating an increment in the optically evoked-EPSC response (2-way ANOVA: main effect of stim. intensity, $p < 0.0001$). EPSC amplitude and rise time were further examined at only 25% stimulation intensity. **F)** Cumulative frequency distributions of EPSC amplitude were significantly different between STs and GTs (Kolmogorov-Smirnov test: $p = 0.0158$) suggesting greater EPSC amplitude for GTs. However, the average amplitude (**F** inset of box plot) for STs and GTs did not differ (unpaired t-test: $p = 0.0821$). **G)** Cumulative frequency distributions of EPSC rise time for STs and GTs did not differ (Kolmogorov-Smirnov test: $p = 0.7937$). However, the average rise time (**G** inset of box plot) for STs and GTs was significantly different (unpaired t-test: $p = 0.0136$). Significance for t-test is shown as * - $p < 0.05$. Data are presented as mean ± S.E.M. Mean in box plots is represented as '+'.

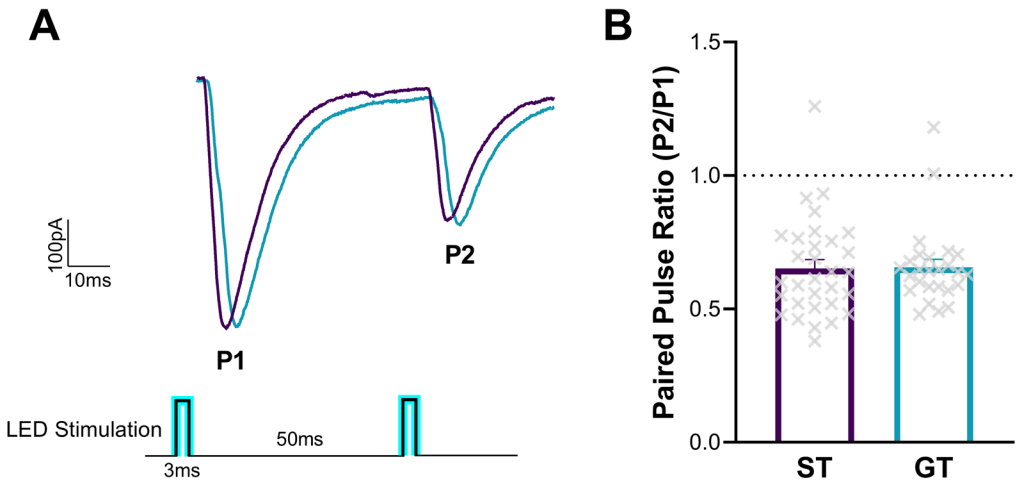


**Figure 5.7.** *Paired-pulse ratio (PPR) analysis of the ventral hippocampus (vHPC) to nucleus accumbens (NAc) projection of sign-trackers (STs) and goal-trackers (GTs).* **A)** Representative voltage-clamp recording of NAc medium spiny neuron (MSN) excitatory post-synaptic currents (EPSCs) following two paired 3-ms optical pulses to depolarize vHPC axon terminals. **B)** PPR (P2/P1) was calculated by dividing the amplitude of the second EPSC (P2) with the amplitude of the first EPSC (P1) at 75% LED intensity. STs and GTs did not significantly differ in vHPC-NAc PPR (unpaired t-test: $p = 0.9205$). Data are presented as mean ± S.E.M, and each data point represents a single cell.

**Table 5.1.** *Overall baseline excitatory synaptic input of shell and core nucleus accumbens (NAc) medium spiny neurons (MSNs), and synaptic transmission efficacy measures of the ventral hippocampus (vHPC) to NAc projection of sign-trackers (STs) and goal-trackers (GTs).* Table lists mean ± S.E.M. (sample size) for properties of miniature excitatory post-synaptic currents (mEPSCs) and for optically evoked-EPSCs in the vHPC-NAc projection.

| | **mEPSC** | |
|---|---|---|
| | **Sign-trackers (ST)** | **Goal-trackers (GT)** |
| ***Shell*** | | |
| **Peak Amplitude (pA)** | 15 ± 1 (10) | 17 ± 1 (8) |
| **Frequency (Hz)** | 12 ± 3 (10) | 12 ± 3 (8) |
| ***Core*** | | |
| **Peak Amplitude (pA)** | 12.6 ± 0.4 (12) | 14 ± 1 (8) |
| **Frequency (Hz)** | 7.4 ± 0.8 (12) | 8.5 ± 0.8 (8) |

| | **vHPC-NAc EPSC** | |
|---|---|---|
| | **Sign-trackers (ST)** | **Goal-trackers (GT)** |
| **Peak Amplitude (pA)** | 276 ± 18 (48) | 291 ± 18 (51) |
| **Rise Time (ms)** | 2.27 ± 0.08 (48) | 2.37 ± 0.07 (51) |
| **Halfwidth (ms)** | 6.2 ± 0.2 (48) | 6.5 ± 0.2 (51) |
| **Decay Time (ms)** | 10.7 ± 0.3 (48) | 11.0 ± 0.3 (51) |
| **Paired Pulse Ratio (75%)** | 0.65 ± 0.03 (31) | 0.66 ± 0.03 (26) |

**Table 5.2.** *Full statistical report for behavioral responses and electrophysiological synaptic properties of medium spiny neurons in the nucleus accumbens of sign-trackers (STs) and goal-trackers (GTs).* Table is organized by figures and lists analyses performed, main effects and interactions.

| | Analysis | Effects | *F, t, (df), P* |
|---|---|---|---|
| **Figure 5.1** | | | |
| **5.1D. PavCA Index Score mEPSC Cohort** | mixed-effects model | session (main effect)<br>phenotype (main effect)<br>session x phenotype (interaction) | F (2.13, 10.2) = 15.6, p = 0.0007<br>F (1, 24) = 51.5, p < 0.0001<br>F (5, 24) = 16.9, p < 0.0001 |
| **5.1E. PavCA Index Score Evoked-EPSC Cohort** | mixed-effects model | session (main effect)<br>phenotype (main effect)<br>session x phenotype (interaction) | F (3.24, 35.7) = 36.3, p < 0.0001<br>F (1, 11) = 184, p < 0.0001<br>F (5, 55) = 69.0, p < 0.0001 |
| **Figure 5.2** | | | |
| **5.2A. Lever Press Analysis** | | | |
| **Number** | mixed-effects model | session (main effect)<br>phenotype (main effect)<br>session x phenotype (interaction) | F (1.19, 4.78) = 11.2, p = 0.020<br>F (1, 4) = 15.6, p = 0.017<br>F (5, 20) = 10.2, p < 0.0001 |
| **Latency** | mixed-effects model | session (main effect)<br>phenotype (main effect)<br>session x phenotype (interaction) | F (1.76, 7.05) = 27.5, p = 0.0005<br>F (1, 4) = 28.9, p = 0.0058<br>F (5, 20) = 23.8, p < 0.0001 |
| **Probability** | mixed-effects model | session (main effect)<br>phenotype (main effect)<br>session x phenotype (interaction) | F (2.17, 8.67) = 25.3, p = 0.0002<br>F (1, 4) = 38.1, p = 0.0035<br>F (5, 20) = 21.6, p < 0.0001 |
| **5.2B. Magazine Entry Analysis** | | | |
| **Number** | mixed-effects model | session (no effect)<br>phenotype (no effect)<br>session x phenotype (interaction) | F (1.59, 6.35) = 2.56, p = 0.16<br>F (1, 4) = 0.13, p = 0.73<br>F (5, 20) = 7.09, p = 0.0006 |
| **Latency** | mixed-effects model | session (no effect)<br>phenotype (no effect)<br>session x phenotype (interaction) | F (1.85, 7.39) = 2.64, p = 0.14<br>F (1, 4) = 0.62, p = 0.48<br>F (5, 20) = 6.23, p = 0.0012 |
| **Probability** | mixed-effects model | session (main effect)<br>phenotype (no effect)<br>session x phenotype (interaction) | F (2.11, 8.45) = 4.79, p = 0.039<br>F (1, 4) = 1.44, p = 0.30<br>F (5, 20) = 7.24, p = 0.0005 |
| **Figure 5.3** | | | |
| **Shell (5.3 A-D)** | | | |
| **5.3A. Cumulative Frequency Distribution (Amplitude)** | Kolmogorov-Smirnov test | no effect | KSD = 0.25, p = 0.56 |
| **5.3B. Average Amplitude** | t-test | no effect | t=1.24, df=16, p = 0.23 |
| **5.3C. Cumulative Frequency Distribution (Frequency)** | Kolmogorov-Smirnov test | no effect | KSD = 0.067, p > 0.99 |
| **5.3D. Average Frequency** | t-test | no effect | t=0.07, df=16, p = 0.94 |
| **Core (5.3 E-H)** | | | |
| **5.3E. Cumulative Frequency Distribution (Amplitude)** | Kolmogorov-Smirnov test | significantly different | KSD = 0.48, p = 0.010 |
| **5.3F. Average Amplitude** | t-test | no effect | t=1.42, df=18, p = 0.17 |
| **5.3G. Cumulative Frequency Distribution (Frequency)** | Kolmogorov-Smirnov test | no effect | KSD = 0.23, p = 0.62 |
| **5.3H. Average Frequency** | t-test | no effect | t=0.95, df=18, p = 0.36 |
| **Figure 5.5** | | | |
| **5.5A. Lever Press Analysis** | | | |
| **Number** | mixed-effects model | session (main effect)<br>phenotype (main effect) | F (1.99, 21.9) = 38.0, p < 0.0001<br>F (1, 11) = 151, p < 0.0001 |

| | | | |
|---|---|---|---|
| | | session x phenotype (interaction) | F (5, 55) = 37.8, p < 0.0001 |
| **Latency** | mixed-effects model | session (main effect)<br>phenotype (main effect)<br>session x phenotype (interaction) | F (2.84, 31.2) = 44.7, p < 0.0001<br>F (1, 11) = 202, p < 0.0001<br>F (5, 55) = 44.4, p < 0.0001 |
| **Probability** | mixed-effects model | session (main effect)<br>phenotype (main effect)<br>session x phenotype (interaction) | F (2.57, 28.2) = 39.2, p < 0.0001<br>F (1, 11) = 419, p < 0.0001<br>F (5, 55) = 39.1, p < 0.0001 |
| **5.5B. Magazine Entry Analysis** | | | |
| **Number** | mixed-effects model | session (no effect)<br>phenotype (no effect)<br>session x phenotype (interaction) | F (3.00, 33.0) = 1.90, p = 0.15<br>F (1, 11) = 4.63, p = 0.054<br>F (5, 55) = 25.8, p < 0.0001 |
| **Latency** | mixed-effects model | session (main effect)<br>phenotype (main effect)<br>session x phenotype (interaction) | F (2.71, 32.5) = 5.41, p = 0.0050<br>F (1, 12) = 7.28, p = 0.019<br>F (5, 60) = 27.9, p < 0.0001 |
| **Probability** | mixed-effects model | session (main effect)<br>phenotype (main effect)<br>session x phenotype (interaction) | F (3.35, 36.9) = 9.89, p < 0.0001<br>F (1, 11) = 8.38, p = 0.015<br>F (5, 55) = 32.0, p < 0.0001 |
| **Figure 5.6 (I-O Curve)** | | | |
| **5.6A. Amplitude** | 2-way ANOVA | stim. intensity (main effect)<br>phenotype (no effect)<br>stim. intensity x phenotype (no effect) | F (3, 388) = 60.9, p < 0.0001<br>F (1, 388) = 0.46, p = 0.50<br>F (3, 388) = 0.44, p = 0.73 |
| **5.6B. Halfwidth** | 2-way ANOVA | stim. intensity (main effect)<br>phenotype (no effect)<br>stim. intensity x phenotype (no effect) | F (3, 388) = 63.8, p < 0.0001<br>F (1, 388) = 1.85, p = 0.17<br>F (3, 388) = 0.83, p = 0.48 |
| **5.6C. Rise Time** | 2-way ANOVA | stim. intensity (main effect)<br>phenotype (no effect)<br>stim. intensity x phenotype (no effect) | F (3, 388) = 27.0, p < 0.0001<br>F (1, 388) = 1.11, p = 0.29<br>F (3, 388) = 2.54, p = 0.056 |
| **5.6D. Decay Time** | 2-way ANOVA | stim. intensity (main effect)<br>phenotype (no effect)<br>stim. intensity x phenotype (no effect) | F (3, 388) = 63.2, p < 0.0001<br>F (1, 388) = 1.08, p = 0.30<br>F (3, 388) = 0.69, p = 0.56 |
| **Figure 5.6 (25% Stim. Intensity)** | | | |
| **5.6F. Cumulative Frequency Distribution (Amplitude)** | Kolmogorov-Smirnov test | significantly different | KSD = 0.44, p = 0.016 |
| **5.6F. Average Amplitude (Inset)** | t-test<br>nested t-test | no effect<br>no effect | t=1.77, df=97, p = 0.080<br>t=0.71, df=11, p = 0.49 |
| **5.6G. Cumulative Frequency Distribution (Rise Time)** | Kolmogorov-Smirnov test | no effect | KSD = 0.21, p = 0.79 |
| **5.6G. Average Rise Time (Inset)** | t-test<br>nested t-test | effect of phenotype<br>no effect | t=2.51, df=97, p = 0.014<br>t=0.02, df=11, p = 0.99 |
| **Figure 5.7** | | | |
| **5.7B – Paired Pulse Ratio** | t-test | no effect | t=0.10, df=55, p = 0.92 |

# CHAPTER VI

## General Discussion

This dissertation aimed to expand our understanding on the role of the nucleus accumbens (NAc) in reward learning and its relevance to addiction predisposition. To this end, we used the "sign-tracker/goal-tracker (ST/GT)" rat model of individual differences in associative learning and cue reactivity. One advantage of this model is that it allows assessment of variations in the way the NAc encodes properties of emotionally salient cues without the confounds of actual drug exposure or disease states. Decades of evidence have demonstrated the importance of the NAc for Pavlovian learning and conditioned approach behavior (Parkinson et al., 1999, 2000; Ciano et al., 2001; Cardinal et al., 2002; Dalley et al., 2005; Blaiss and Janak, 2009; Chang et al., 2012). This literature has directly influenced the study of substance use disorders, leading to the hypothesis that addiction pathophysiology at its heart involves drug-related cues exerting abnormal control over an individual's behavior and driving them toward compulsive drug-seeking and use (Robinson and Berridge, 1993; Di Chiara et al., 1999). These drug-related stimuli initially just predict drug availability, but are thought to specifically acquire incentive or motivational value, and this transition occurs via associative learning processes (Robinson and Berridge, 1993; Di Chiara et al., 1999; Berridge and Robinson, 2016).

During associative learning, cues must acquire predictive value, but the attribution of incentive and motivational value to Pavlovian cues is highly variable. Individual differences in the level of predictive vs incentive value attribution to emotionally salient cues are believed to result in different forms of expression of conditioned approach that can be behaviorally measured (i.e., sign-tracking and goal-tracking) (Berridge et al., 2009; Flagel et al., 2009). It is important to understand how these individual differences in Pavlovian learning arise as they may result in not only differences in personality traits, but also in vulnerability or resilience to disorders like addiction and post-traumatic stress disorder (PTSD) (Flagel and Robinson, 2017; Pitchers et al., 2017a; María-Ríos and Morrow, 2020). The neurophysiology of the NAc has been extensively studied in the context of reward and even fear learning, but evidence using the ST/GT model suggests that NAc activity is not uniform across all individuals or forms of associative learning expressions (Flagel et al., 2011a, 2011b; Gillis and Morrison, 2019). Therefore, we want to further understand differences in how the NAc encodes information about the availability, value, and context of cues to integrate it into action as this may inform the pathways through which disease susceptibility may begin.

In Chapter II, we aimed to create a physiological profile of subregional excitability within the NAc across rats with different levels of behavioral experience (e.g., naïve, paired, unpaired) to shed light on how excitability in the NAc core and shell may contribute to encoding certain aspects of emotionally salient cues.

Next, in Chapter III we explored whether intrinsic differences in NAc excitability between STs and GTs are present, as we hypothesize that the excitability state of

medium spiny neurons (MSNs) in the NAc core and shell could impact how sensitive the NAc is to input stimuli carrying cue-related information during associative learning (Daoudal and Debanne, 2003; Kourrich et al., 2015; Allichon et al., 2021).

Finally, in Chapters IV and V, we tested for differences in the functional role of the ventral hippocampus (vHPC) to NAc pathway *in vivo* during a Pavlovian conditioned approach (PavCA) procedure and also at the synaptic level to test for fundamental differences in transmission efficacy between STs and GTs. Studies have more recently focused on elucidating the neurocircuitry responsible for biasing STs and GTs toward their respective behaviors (Flagel et al., 2011a; Haight et al., 2015, 2017, 2020; Fitzpatrick et al., 2016a; Pitchers et al., 2017a, 2017b; Stringfield et al., 2017; Batten et al., 2018; Campus et al., 2019). We explored the hypothesis that a structure involved in feeding context-specific information during reward and fear learning to the NAc may be differentially engaged between the two phenotypes.

In the next section, we will summarize the rationale and main findings of each chapter in this thesis. These findings will be further discussed in the following sections in relation to the existent literature and future directions.

**Summary of findings**

To better understand NAc MSN excitability in STs and GTs, we first needed to describe the baseline state of membrane properties of MSNs in the core and shell as well as in relation to each other, and how stable this physiological profile is based on the experience of the rat. Thus, the findings in Chapter II are meant to closely inform individual differences in NAc excitability later explored in Chapter III. Using whole-cell patch clamp recordings, we began by measuring the intrinsic excitability properties of

MSNs in the NAc core and shell of naïve rats and rats that underwent either a paired (all phenotypes together) or an unpaired PavCA procedure. Subregional differences were of particular interest because the NAc core and shell are known not only to be anatomically different, but also functionally different (Zahm, 1999; Di Chiara, 2002; Day and Carelli, 2007; Meredith et al., 2008; Ito and Hayen, 2011). Therefore, subregional excitability across the NAc may also be an important consideration for understanding differences in NAc dynamics and reward-processing.

In Chapter II, we first focused on subregional differences in core and shell MSN intrinsic excitability and found stable, pronounced differences in passive and active properties across all three groups regardless of their prior experience. In this analysis, we did not account for any individual differences in conditioned approach in the paired PavCA group. In the NAc shell, MSNs exhibited higher excitability than in the core, and this correlated with what is known about the morphological properties of core vs shell MSNs (Meredith et al., 1992; Forlano and Woolley, 2010).

It has been difficult to measure innate or pre-existent differences in the neurobiology of STs and GTs that may correlate with their behavior bias. This is because there is no known method of distinguishing STs from GTs prior to PavCA training, making it difficult to determine whether any measured differences between STs and GTs in core and shell excitability are pre-existing or are induced or differentially altered by training. First, the training experience itself (e.g., handling, reward exposure) may be enough to alter NAc physiology (Scala et al., 2018) and second, the actual learning component (e.g., CS-US associations) of the task may also have a distinct impact (Ziminski et al., 2017). We attempted to control for these variables by recording

not only from paired rats but also unpaired and naïve rats. Furthermore, we waited a period of at least one week before the electrophysiological recordings with the hopes that any training-induced changes would most likely have returned to baseline by then.

If we assume that STs and GTs are innately different, then we can hypothesize that any rats that could be classified in the paired group as STs and GTs following PavCA would also exist in the naïve and unpaired groups even without the exposure to CS-US pairings. Some studies point to this, specifically when considering there may be genetic influence over sign- and goal-tracking behavior. This is evidenced by the bred high- and low-responder Sprague Dawley rats (Flagel et al., 2010) and by the previously reported variation in these two behavioral phenotypes based on the vendors and colonies of outbred Sprague Dawleys (Fitzpatrick et al., 2013). Without accounting for any individual differences in the paired group, naïve, unpaired, and paired rats had a similar electrophysiological profile of MSN excitability in the NAc with an equal cumulative frequency distribution of action potentials in the core (Kruskal-Wallis test = 0.2575, p = 0.8792; data not shown) and shell (Kruskal-Wallis test = 0.0014, p = 0.9993; data not shown). However, we did find that in the NAc shell, rats in the paired group had lower excitability than both unpaired and naïve rats. Because the innate tendencies toward sign- and goal-tracking should be equivalent in all these groups, these data would suggest that PavCA training may have had some long-lasting effects in MSN excitability.

In Chapter III, rats in the paired group were classified as STs, GTs, and IRs to investigate individual differences in NAc excitability related to encoding the predictive versus incentive properties of reward-paired cues. We found that out of the three

phenotypes, MSNs in the NAc core of STs had the lowest membrane excitability followed by IRs then GTs. In the NAc shell, MSNs from STs and GTs had no significant differences in firing properties, but both had lower action potential number and frequencies compared to IRs. These results revealed that baseline differences between STs, GTs, and IRs are present in NAc membrane excitability. Specifically, our findings in the core suggest that decreased excitability of MSNs may be important for increased attribution of incentive salience to reward-paired cues during associative learning, and may predispose individuals toward addiction-like behaviors.

The neuronal properties of MSNs in the NAc may influence how it encodes synaptic input about the availability, value, and context of emotionally salient cues. However, there may also be individual differences in the synaptic transmission efficacy from other structures in the reward circuit that feed information to the NAc during associative learning (Britt et al., 2012; Floresco, 2015; Salgado and Kaplitt, 2015). The potential relevance of this becomes clear when we consider other behavioral characteristics of STs and GTs. Not only do they differ in conditioned approach behavior, but also in other expressions of associative learning including cue-induced reinstatement of psychostimulants (Saunders and Robinson, 2011; Versaggi et al., 2016), cued fear expression (Morrow et al., 2011), context-dependent cocaine reinstatement (Saunders et al., 2014), as well as context-dependent fear expression (Morrow et al., 2011). From these findings, it has been proposed that cues and context exert different levels of control over STs and GTs behavior (Pitchers et al., 2017b; María-Ríos and Morrow, 2020). Input from the vHPC to the NAc is thought to be especially important for providing contextual information that can modulate conditioned

responses (Loureiro et al., 2016; Zhou et al., 2019; Muir et al., 2020). In Chapters IV and V, we explored differences in the behavioral role of this projection (Chapter IV) as well as its synaptic strength (Chapter V) with the hypothesis that the increased cue reactivity of STs and their blunted responses to contextual information may stem from reduced vHPC-NAc activity relative to GTs, who display high levels of contextual modulation to both appetitive and aversive responses.

In Chapter IV we investigated the role of vHPC-NAc by using cre-dependent DREADDs to selectively target this projection *in vivo* during PavCA acquisition and expression. The data suggested that acquisition of sign-tracking behavior was enhanced by chemogenetic inhibition and impaired by chemogenetic excitation of vHPC-NAc. Goal-tracking behavior was less affected overall, but the data also suggested that chemogenetic inhibition of vHPC-NAc impaired the acquisition of goal-tracking behavior. Manipulation of vHPC-NAc had no significant effects on sign- and goal-tracking behavior expression for rats that had acquired conditioned approach behavior under regular conditions. Based on these results, we further hypothesize that synaptic transmission efficacy from vHPC to NAc would be weaker in STs compared to GTs.

In Chapter V, we used combined *ex vivo* optogenetics with whole-cell patch clamp recordings to measure optically-evoked excitatory post-synaptic currents (EPSCs) from vHPC inputs to MSNs in the NAc shell. Overall, we found no significant differences between STs and GTs in the properties of EPSCs suggesting relatively similar vHPC-NAc synaptic strength. However, subtle differences in EPSC amplitude and rise time, did suggest that synaptic strength in GTs was slightly greater than in STs,

which would align with our behavioral findings in Chapter IV. Altogether, these findings support the role of the vHPC-NAc projection as a modulator of conditioned responses to discrete cues by means of context-specific reward information. Individual differences at the level of this projection may result in different degrees of motivational value attribution to Pavlovian cues, which in turn would affect predisposition to cue-driven psychopathologies.

In the next sections, we will go more in depth into the implications of the findings in this thesis as they relate to previous literature and how they contribute to our understanding of individual differences in NAc activity and associative learning.

**Subregional differences in core and shell MSN intrinsic excitability**

Based on previous anatomical studies (Meredith et al., 1992; Forlano and Woolley, 2010), we speculated that lower dendritic arborization and smaller surface area may be the most direct link to greater input resistance and higher excitability of shell versus core MSNs. These morphological differences can have significant implications on MSN physiology and contribute to functional segregation of the role of the core and the shell based on their excitability thresholds to receive and relay information. These two subregions have been long implicated in distinct aspects of Pavlovian learning (Bassareo and Di Chiara, 1999; Day et al., 2006; Stelly et al., 2021) and addiction pathophysiology (Ito et al., 2004; Kourrich and Thomas, 2009; Wolf, 2010). For example, core and shell MSNs seem to differentially respond to conditioned stimuli during associative learning. A study in which *in vivo* electrophysiological recordings were performed in the core and shell during CS and reward presentations demonstrated that neurons in the core exhibited greater excitation in response to the

CS than did shell neurons (Day et al., 2006). This could be due to differences in dopamine transmission as the same pattern holds true for subregional dopamine release (Bassareo and Di Chiara, 1999; Ito et al., 2000; Stelly et al., 2021). It is possible that baseline differences in excitability are necessary for coordinating these NAc dynamics. Lower baseline membrane excitability in core MSNs may reduce noise and increase their sensitivity to specific reward-related stimuli, while the increased neuronal excitability in the shell may allow these neurons to encode a more generalized reward state.

The responsiveness of core and shell MSNs to drug-induced neuroadaptations is also not uniform across the two subregions (Di Chiara, 2002; Wolf, 2010). One example of this is that cocaine withdrawal causes an increase in firing capacity of core MSNs, while it causes a decrease in that of shell MSNs (Kourrich and Thomas, 2009). If these dynamic subregional adaptations are crucial for drug-seeking and drug-taking behaviors, then the baseline excitability state of MSNs in the core and shell may modulate the impact of drug-induced neuroadaptations in the progression of addiction (Dong et al., 2006; Kourrich et al., 2015; Zinsmaier et al., 2022).

**Individual differences in NAc membrane excitability**

In Chapter II, we found that the cumulative frequency distribution of action potentials in the core and shell were equal for naïve, paired, and unpaired rats. Thus individual differences are present in all groups regardless of the behavioral experience as the Pavlovian learning task did not shift the distribution in any specific direction. However, mean comparisons revealed that the firing capacity of MSNs in the NAc shell of paired rats was lower than those in the naïve and unpaired groups. This challenges

the assumption that the training experience does not directly impact the physiology of STs and GTs and that any measured differences in their physiology must be pre-existent. However, it certainly does not mean that no innate differences between STs and GTs exist. It may mean that a paired PavCA procedure affects the intrinsic excitability of the NAc of rats, and the innate differences may influence how differentially sensitive STs and GTs may be to these changes. Importantly, it has been reported that a paired PavCA paradigm can significantly increase the excitability of MSNs in the NAc shell, compared to an unpaired PavCA task (Ziminski et al., 2017). However, it is important to note that this study took advantage of a *Fos-GFP* transgenic mouse line to measure membrane properties both acutely and in MSNs specifically activated during the Pavlovian procedure. Therefore, although parallels can be drawn, we cannot make definitive comparisons between the two studies. Furthermore, in Chapter III individual differences in NAc MSN intrinsic excitability between STs and GTs were only detected in the core and not the shell, and the paired PavCA procedure did not affect the firing properties of MSNs in the core relative to naïve and unpaired controls.

**Reduced membrane excitability in core MSNs**

In the NAc core, MSNs of STs had the lowest membrane excitability. Compared to GTs, STs are thought to share more traits related to addiction vulnerability including higher impulsivity (Lovic et al., 2011), greater psychomotor sensitization (Flagel et al., 2008), and more robust cue-induced reinstatement of cocaine (Saunders and Robinson, 2011) and nicotine (Versaggi et al., 2016). Addictive substances are thought to affect MSN physiology through neuroadaptations that lead to the development and maintenance of addiction (Wolf, 2010; Kourrich et al., 2015; Zinsmaier et al., 2022).

Therefore, decreased intrinsic excitability of MSNs in the core of STs might be hypothesized to directly contribute to increased susceptibility to addiction-like behaviors. Although decreased membrane excitability has been a defining feature of MSNs following short- and long-term exposure to cocaine (Wolf, 2010), and is even thought to predict a stronger response to the psychostimulant effects of cocaine (Dong et al., 2006; Mu et al., 2010), this is thought to be somewhat selective to MSNs in the NAc shell, not core (Kourrich and Thomas, 2009). Therefore, decreased membrane excitability in the NAc core of STs may not directly relate to this drug-induced neuroadaptation. As discussed above, evidence suggests that the NAc core has a bigger role than the shell in encoding the motivational properties of conditioned stimuli (Day and Carelli, 2007; Meredith et al., 2008). In this sense, greater physiological distinctions between STs and GTs in the NAc core are not surprising. Reduced baseline excitability in the core MSNs of STs relative to GTs may increase the signal-to-noise ratio and potentiate the attribution of motivational value to the most salient cues. It has been proposed that in a state of addiction, responses to non-drug related stimuli get filtered out, and activity in the NAc is funneled towards drug-related stimuli (Kalivas and Hu, 2006; Wolf, 2010; Leyton and Vezina, 2014). Our finding in a non-drug related state may provide a potential physiological parallel to increased cue-reactivity in a drug-related state. Understanding this process in a basic model of associative learning could further reveal neurobiological mechanisms within the NAc that may confer susceptibility to addiction. Future studies could explore whether reduced excitability in the NAc may directly bias rats toward a “sign-tracking” phenotype and whether an increase in baseline excitability in the core can abolish their increased cue-induced reinstatement of drugs.

**Intrinsic excitability of MSNs from IRs**

We also reported in Chapter III that the subregional excitability difference between core and shell MSNs was not present in GT rats. This is most likely a result of the higher membrane excitability in core MSNs of GTs compared to STs and IRs. Not much attention has been previously directed to IR rats. Not only are we less aware of their behavioral characterization in other tasks beside PavCA, but their neurobiology has also been understudied with some few exceptions (Flagel et al., 2009, 2011a; Fitzpatrick et al., 2016b, 2019). This group is particularly important as they have relatively low bias toward sign- or goal-tracking behavior, which also implies that they may be attributing both predictive and incentive value to reward-paired cues. Interestingly, we found that IRs shared features of NAc intrinsic excitability with both GTs and STs. In the NAc core, MSNs from both GTs and IRs had greater excitability than those from STs. Although in GTs this resulted in the loss of a subregional excitability difference between the core and shell, a relatively higher excitability of MSNs in the shell of IRs ensured that this excitability difference was present in both IRs and STs. This subregional NAc dynamic in core and shell excitability as well as in relation to each other may prove important for understanding differences between STs, GTs, and IRs in the way that the NAc encodes predictive and incentive value and modulates their conditioned responses. For example, higher excitability of core MSNs may result in greater engagement of goal-tracking responses, whereas sign-tracking responses may require a greater subregional difference between core and shell excitability.

**Role of vHPC to NAc projections on sign- and goal-tracking**

As previously discussed, our interest in the vHPC mainly developed from its role in providing context-specific information to the NAc for modulating cue-driven conditioned responses (Turner et al., 2022). Behavioral responses from STs and GTs in a range of appetitive and aversive associative learning tasks suggest that STs tend to react strongly to conditioned cues regardless of the circumstances under which they are encountered, whereas GTs use contextual cues to modulate their conditioned emotional responses (Pitchers et al., 2017b; María-Ríos and Morrow, 2020). In Chapter IV, we aimed to explore the functional role of the vHPC in sign- and goal-tracking behavior through *in vivo* chemogenetic manipulation of vHPC-NAc. Our findings support that reduced activity in vHPC-NAc may increase sign-tracking and cue-reactivity. Although we hypothesized that this projection would also exhibit weaker synaptic transmission efficacy in STs, we were not able to conclusively show this in Chapter V. There was a subtle trend suggesting that EPSC amplitude and risetime was greater in GTs, which would support that sign-tracking may result from lower vHPC-NAc activity and synaptic strength.

Decreased engagement of vHPC-NAc in a model of increased cue-reactivity and blunted responses to contextual information provides a promising target for studying mechanisms of addiction and PTSD comorbidity. As discussed in Chapter I, both addiction and PTSD are characterized by an inability to suppress highly emotional responses to trauma- and drug-cues outside of the appropriate contexts (Milad et al., 2009; Wicking et al., 2016; Garland et al., 2018). These drug-seeking behaviors and fear responses are perpetuated if contextual cues are not properly processed. Studies

manipulating vHPC-NAc projections have demonstrated that increased activity in these projections can invigorate context-dependent cocaine and morphine reinstatement (Loureiro et al., 2016; Zhou et al., 2019) and also enhance contextual fear expression (Loureiro et al., 2016). Our findings suggest that the degree of activity in the vHPC-NAc pathway may very well vary across individuals and confer susceptibility to disorders like addiction and PTSD.

**Lower NAc excitability and tonic dopamine in STs**

As we discussed above, lower baseline excitability in core MSNs of STs may increase the signal-to-noise ratio of reward-related versus non-reward related stimuli. If activity in these neurons can confer motivational value to conditioned cues, then this relatively low baseline activity could make reward cues more likely to bias behavioral responses of STs as compared to GTs. Interestingly, the patterns of dopamine transmission between STs and GTs may also reflect differential responsivity to reward cues. For STs, dopamine release is more time-locked to the CS (Flagel et al., 2011b; Singer et al., 2016; Campus et al., 2019). Therefore, both the reduced baseline intrinsic excitability and a more fine-tuned pattern of dopamine release may selectively enhance sign-tracking conditioned responses directed toward the cue. Several lines of evidence support this view. First, STs have higher levels of DAT expression in the NAc core which results in faster dopamine re-uptake compared to GTs (Singer et al., 2016). Second, STs have greater phasic dopamine release than GTs in response to CS presentations (Flagel et al., 2011b). Third, lower dopamine re-uptake in GTs results in higher tonic dopamine release (Singer et al., 2016). Higher levels of tonic dopamine may even modulate MSN membrane excitability more strongly for GTs, increasing firing

capacity at baseline through $D_1$ receptor-mediated modulation of $K^+$ and $Ca^{2+}$ currents (Hernández-López et al., 1997; Podda et al., 2010), though experiments specifically designed to test this have not yet been performed. These differences in tonic versus phasic dopamine release between STs and GTs have been previously proposed to influence their conditioned responses to the cue. In particular, it has been suggested that higher levels of tonic dopamine in GTs may degrade the temporal control of discrete conditioned stimuli enhancing contextual influence over GTs (Singer et al., 2016).

Input from the vHPC to the NAc opens another route for influencing tonic dopamine release. Many studies have demonstrated that the vHPC is a potent driver of mesolimbic dopamine release from the ventral tegmental area (VTA) to the NAc (Lipska et al., 1992; Wu and Brudzynski, 1995; Blaha et al., 1997; Legault et al., 2000; Taepavarapruk et al., 2000; Floresco et al., 2001). However, the role of vHPC-NAc on dopamine transmission seems to be more directly tied to tonic dopamine release from the VTA through modulation of the ventral pallidum (VP) (Lodge and Grace, 2006; Grace et al., 2007). Specifically, VTA dopaminergic neurons silenced by the inhibitory influence of the VP are released from this inhibition by excitatory input from the vHPC to the NAc, resulting in spontaneous spike activity. This vHPC-NAc-VP pathway is therefore thought to control the tonic mesolimbic baseline state (Grace et al., 2007). Our findings in Chapters IV and V suggest that GTs may have greater vHPC-NAc activity compared to STs. This would in turn suggest that GTs have higher levels of tonic dopamine from the VTA to the NAc. Interestingly, a previous study demonstrated that lesions of the vHPC caused a decrease of NAc dopamine metabolites in STs but not

GTs (Fitzpatrick et al., 2016a). This may be an indication that this projection is inherently different between the two phenotypes and undergoes different adaptations during associative learning. Future studies can directly investigate the effects of vHPC-NAc modulation on dopamine release in STs and GTs both at baseline and during PavCA. This would bring more clarity as to how tonic and phasic dopamine signaling may influence sign- and goal-tracking behavior. It may also reveal individual differences in how the different firing states of dopaminergic neurons are gated by input stimuli from the vHPC.

**Limitations and future directions**

Several limitations in the interpretation of our findings highlight the necessity for future studies. One important fact is that although we found clear differences between STs, GTs, and IRs in membrane properties of MSNs, we could not determine whether these are pre-existent differences and conclude that all three phenotypes are innately different. If no significant differences had been present in Chapter II between naïve, unpaired, and paired rats, then this conclusion would have been more justified. To determine whether individual differences in PavCA behavior are innate and caused by intrinsic differences in NAc excitability, some method would be needed to identify STs and GTs prior to PavCA training, and/or measurement of MSN excitability would have to be done *in vivo* to test how it changes over the course of behavioral training. One option would be to use an inbred line such as the high- and low-responder rats, which are known to have a natural tendency toward sign- and goal-tracking behavior respectively (Flagel et al., 2010). These rats are known to exhibit different cue- and reward-evoked patterns of dopamine release in the NAc (Flagel et al., 2011b), and differences in NAc

excitability might also be present in these lines. An additional experiment could be to perform electrophysiological recordings immediately following PavCA. Collectively, the excitability profile of MSNs from STs, GTs, and IRs at baseline and following PavCA would give a much clearer picture of how stable and experience-dependent these membrane properties are.

Because of the known differences between STs and GTs in dopamine neurotransmission (Flagel et al., 2007; Singer et al., 2016) and sensitivity to dopamine (Flagel et al., 2011b; Saunders and Robinson, 2012), it would be informative for future experiments to measure the effect of dopamine and dopamine antagonism on the membrane excitability of MSNs in STs and GTs. This would bring clarity as to how dopamine-dependence at the behavioral and synaptic level may correlate with its influence at the neuronal level.

Although the behavioral effects of vHPC-NAc manipulation suggested that this projection may modulate sign- and goal-tracking, the effects were not as robust and stable as expected. One possible explanation is that the role of this projection may be more temporally selective to cue and reward presentations. To improve temporal control, *in vivo* optogenetics could be performed to specifically increase or decrease vHPC-NAc activity during selected times in the PavCA procedure. Similarly, our results in Chapter V were very subtle, and no definitive conclusions could be made regarding differences in the synaptic transmission efficacy of vHPC-NAc of STs and GTs. However, the subtly of both these findings could be the result of specific, smaller neuronal populations driving the conditioned behavioral responses we measured, as opposed to activity throughout the entire vHPC-NAc pathway. Not only has it been

demonstrated that during Pavlovian conditioning specific neuronal populations are selectively engaged (Ziminski et al., 2017; Gillis and Morrison, 2019), but also modulation from the vHPC in particular is thought to be encoded by neuronal ensembles (Zhou et al., 2019). Therefore, being able to selectively target these neurons or record from neurons solely activated during the task, may also reveal stronger and clearer results on individual differences in this circuit.

All these experiments were meant to capture baseline differences in NAc neuronal and synaptic activity. However, it is also possible that the defining differences between STs and GTs are experience-dependent involving differences in short- and long-term neuroadaptations. Future experiments could investigate differences in synaptic plasticity such as long-term depression and potentiation before and after conditioning to capture differences that arise dynamically in these phenotypes.

Finally, because of the relevance of this model to addiction and PTSD vulnerability, future studies could modulate the vHPC-NAc projection in STs and GTs undergoing drug-self administration and cue-induced reinstatement as well as cued and contextual fear conditioning and expression. Our focus was on studying this model from the level of simple cue-reward associations in order to better understand the elemental mechanics of these predisposing traits. However, it is extremely important that these findings are translated and applied to disease states in the future, as we ultimately hope these studies will result in better prevention and treatment strategies for cue-driven psychopathologies.

## Concluding remarks

Altogether, this thesis demonstrates that individual differences in the NAc are indeed present at baseline between STs and GTs. We propose that variations in NAc activity during associative learning could be associated with differences in both intrinsic neuronal properties of MSNs and with more subtle differences in the level of engagement of vHPC-NAc neurotransmission. These findings highlight the importance of accounting for individual differences in the study of the NAc involvement in cue-reward learning and shed light on how the NAc may differentially encode properties of emotionally salient cues resulting in distinct conditioned responses and disease susceptibility.

## References


Allichon M-C, Ortiz V, Pousinha P, Andrianarivelo A, Petitbon A, Heck N, Trifilieff P, Barik J, Vanhoutte P (2021) Cell-type-specific adaptions in striatal medium-sized spiny neurons and their roles in behavioral responses to drugs of abuse. Front Synaptic Neurosci 13:799274.

Bassareo V, Di Chiara G (1999) Differential responsiveness of dopamine transmission to food-stimuli in nucleus accumbens shell/core compartments. Neuroscience 89:637–641.

Batten SR, Pomerleau F, Quintero J, Gerhardt GA, Beckmann JS (2018) The role of glutamate signaling in incentive salience: second-by-second glutamate recordings in awake Sprague Dawley rats. J Neurochem 145:276–286.

Berridge KC, Robinson TE (2016) Liking, wanting, and the incentive-sensitization theory of addiction. Am Psychol 71:670–679.

Berridge KC, Robinson TE, Aldridge JW (2009) Dissecting components of reward: 'liking', 'wanting', and learning. Curr Opin Pharmacol 9:65–73.

Blaha CD, Yang CR, Floresco SB, Barr AM, Phillips AG (1997) Stimulation of the ventral subiculum of the hippocampus evokes glutamate receptor-mediated changes in dopamine efflux in the rat nucleus accumbens. Eur J Neurosci 9:902–911.

Blaiss CA, Janak PH (2009) The nucleus accumbens core and shell are critical for the expression, but not the consolidation, of Pavlovian conditioned approach. Behav Brain Res 200:22–32.

Britt JP, Benaliouad F, McDevitt RA, Stuber GD, Wise RA, Bonci A (2012) Synaptic and behavioral profile of multiple glutamatergic inputs to the nucleus accumbens. Neuron 76:790–803.

Campus P, Covelo IR, Kim Y, Parsegian A, Kuhn BN, Lopez SA, Neumaier JF, Ferguson SM, Solberg Woods LC, Sarter M, Flagel SB (2019) The paraventricular thalamus is a critical mediator of top-down control of cue-motivated behavior in rats Schoenbaum G, Wassum KM, Calu D, Coutureau E, eds. eLife 8:e49041.

Cardinal RN, Parkinson JA, Lachenal G, Halkerston KM, Rudarakanchana N, Hall J, Morrison CH, Howes SR, Robbins TW, Everitt BJ (2002) Effects of selective excitotoxic lesions of the nucleus accumbens core, anterior cingulate cortex, and central nucleus of the amygdala on autoshaping performance in rats. Behav Neurosci 116:553–567.

Chang SE, Wheeler DS, Holland PC (2012) Effects of lesions of the amygdala central nucleus on autoshaped lever pressing. Brain Res 1450:49–56.

Ciano PD, Cardinal RN, Cowell RA, Little SJ, Everitt BJ (2001) Differential involvement of nmda, ampa/kainate, and dopamine receptors in the nucleus accumbens core in the acquisition and performance of pavlovian approach behavior. J Neurosci 21:9471–9477.

Dalley JW, Lääne K, Theobald DEH, Armstrong HC, Corlett PR, Chudasama Y, Robbins TW (2005) Time-limited modulation of appetitive Pavlovian memory by D1 and NMDA receptors in the nucleus accumbens. Proc Natl Acad Sci U S A 102:6189–6194.

Daoudal G, Debanne D (2003) Long-term plasticity of intrinsic excitability: learning rules and mechanisms. Learn Mem 10:456–465.

Day JJ, Carelli RM (2007) The nucleus accumbens and pavlovian reward learning. The Neuroscientist 13:148–159.

Day JJ, Wheeler RA, Roitman MF, Carelli RM (2006) Nucleus accumbens neurons encode Pavlovian approach behaviors: evidence from an autoshaping paradigm. Eur J Neurosci 23:1341–1351.

Di Chiara G (2002) Nucleus accumbens shell and core dopamine: differential role in behavior and addiction. Behav Brain Res 137:75–114.

Di Chiara G, Tanda G, Bassareo V, Pontieri F, Acquas E, Fenu S, Cadoni C, Carboni E (1999) Drug addiction as a disorder of associative learning. Role of nucleus accumbens shell/extended amygdala dopamine. Ann N Y Acad Sci 877:461–485.

Dong Y, Green T, Saal D, Marie H, Neve R, Nestler EJ, Malenka RC (2006) CREB modulates excitability of nucleus accumbens neurons. Nat Neurosci 9:475–477.

Fitzpatrick CJ, Creeden JF, Perrine SA, Morrow JD (2016a) Lesions of the ventral hippocampus attenuate the acquisition but not expression of sign-tracking behavior in rats. Hippocampus 26:1424–1434.

Fitzpatrick CJ, Geary T, Creeden JF, Morrow JD (2019) Sign-tracking behavior is difficult to extinguish and resistant to multiple cognitive enhancers. Neurobiol Learn Mem 163:107045.

Fitzpatrick CJ, Gopalakrishnan S, Cogan ES, Yager LM, Meyer PJ, Lovic V, Saunders BT, Parker CC, Gonzales NM, Aryee E, Flagel SB, Palmer AA, Robinson TE, Morrow JD (2013) Variation in the form of Pavlovian conditioned approach behavior among outbred male Sprague-Dawley rats from different vendors and colonies: sign-tracking vs. goal-tracking. PLoS ONE 8:e75042.

Fitzpatrick CJ, Perrine SA, Ghoddoussi F, Galloway MP, Morrow JD (2016b) Sign-trackers have elevated myo-inositol in the nucleus accumbens and ventral

hippocampus following Pavlovian conditioned approach. J Neurochem 136:1196–1203.

Flagel SB, Akil H, Robinson TE (2009) Individual differences in the attribution of incentive salience to reward-related cues: Implications for addiction. Neuropharmacology 56:139–148.

Flagel SB, Cameron CM, Pickup KN, Watson SJ, Akil H, Robinson TE (2011a) A food predictive cue must be attributed with incentive salience for it to induce c-fos mRNA expression in cortico-striatal-thalamic brain regions. Neuroscience 196:80–96.

Flagel SB, Clark JJ, Robinson TE, Mayo L, Czuj A, Willuhn I, Akers CA, Clinton SM, Phillips PEM, Akil H (2011b) A selective role for dopamine in stimulus-reward learning. Nature 469:53–57.

Flagel SB, Robinson TE (2017) Neurobiological basis of individual variation in stimulus-reward learning. Curr Opin Behav Sci 13:178–185.

Flagel SB, Robinson TE, Clark JJ, Clinton SM, Watson SJ, Seeman P, Phillips PEM, Akil H (2010) An animal model of genetic vulnerability to behavioral disinhibition and responsiveness to reward-related cues: implications for addiction. Neuropsychopharmacol Off Publ Am Coll Neuropsychopharmacol 35:388–400.

Flagel SB, Watson SJ, Akil H, Robinson TE (2008) Individual differences in the attribution of incentive salience to a reward-related cue: influence on cocaine sensitization. Behav Brain Res 186:48–56.

Flagel SB, Watson SJ, Robinson TE, Akil H (2007) Individual differences in the propensity to approach signals vs goals promote different adaptations in the dopamine system of rats. Psychopharmacology (Berl) 191:599–607.

Floresco SB (2015) The nucleus accumbens: an interface between cognition, emotion, and action. Annu Rev Psychol 66:25–52.

Floresco SB, Todd CL, Grace AA (2001) Glutamatergic afferents from the hippocampus to the nucleus accumbens regulate activity of ventral tegmental area dopamine neurons. J Neurosci 21:4915–4922.

Forlano PM, Woolley CS (2010) Quantitative analysis of pre- and postsynaptic sex differences in the nucleus accumbens. J Comp Neurol 518:1330–1348.

Garland EL, Bryan CJ, Kreighbaum L, Nakamura Y, Howard MO, Froeliger B (2018) Prescription opioid misusing chronic pain patients exhibit dysregulated context-dependent associations: Investigating associative learning in addiction with the cue-primed reactivity task. Drug Alcohol Depend 187:13–21.

Gillis ZS, Morrison SE (2019) Sign tracking and goal tracking are characterized by distinct patterns of nucleus accumbens activity. eNeuro 6.

Grace AA, Floresco SB, Goto Y, Lodge DJ (2007) Regulation of firing of dopaminergic neurons and control of goal-directed behaviors. Trends Neurosci 30:220–227.

Haight JL, Campus P, Maria-Rios CE, Johnson AM, Klumpner MS, Kuhn BN, Covelo IR, Morrow JD, Flagel SB (2020) The lateral hypothalamus and orexinergic transmission in the paraventricular thalamus promote the attribution of incentive salience to reward-associated cues. Psychopharmacology (Berl) 237:3741–3758.

Haight JL, Fraser KM, Akil H, Flagel SB (2015) Lesions of the paraventricular nucleus of the thalamus differentially affect sign- and goal-tracking conditioned responses. Eur J Neurosci 42:2478–2488.

Haight JL, Fuller ZL, Fraser KM, Flagel SB (2017) A food-predictive cue attributed with incentive salience engages subcortical afferents and efferents of the paraventricular nucleus of the thalamus. Neuroscience 340:135–152.

Hernández-López S, Bargas J, Surmeier DJ, Reyes A, Galarraga E (1997) $D_1$ receptor activation enhances evoked discharge in neostriatal medium spiny neurons by modulating an L-type $Ca^{2+}$ conductance. J Neurosci 17:3334–3342.

Ito R, Dalley JW, Howes SR, Robbins TW, Everitt BJ (2000) Dissociation in conditioned dopamine release in the nucleus accumbens core and shell in response to cocaine cues and during cocaine-seeking behavior in rats. J Neurosci Off J Soc Neurosci 20:7489–7495.

Ito R, Hayen A (2011) Opposing roles of nucleus accumbens core and shell dopamine in the modulation of limbic information processing. J Neurosci 31:6001–6007.

Ito R, Robbins TW, Everitt BJ (2004) Differential control over cocaine-seeking behavior by nucleus accumbens core and shell. Nat Neurosci 7:389–397.

Kalivas PW, Hu X-T (2006) Exciting inhibition in psychostimulant addiction. Trends Neurosci 29:610–616.

Kourrich S, Calu DJ, Bonci A (2015) Intrinsic plasticity: an emerging player in addiction. Nat Rev Neurosci 16:173–184.

Kourrich S, Thomas MJ (2009) Similar neurons, opposite adaptations: psychostimulant experience differentially alters firing properties in accumbens core versus shell. J Neurosci 29:12275–12283.

Legault M, Rompré P-P, Wise RA (2000) Chemical stimulation of the ventral hippocampus elevates nucleus accumbens dopamine by activating dopaminergic neurons of the ventral tegmental area. J Neurosci 20:1635–1642.

Leyton M, Vezina P (2014) Dopamine ups and downs in vulnerability to addictions: a neurodevelopmental model. Trends Pharmacol Sci 35:268–276.

Lipska BK, Jaskiw GE, Chrapusta S, Karoum F, Weinberger DR (1992) Ibotenic acid lesion of the ventral hippocampus differentially affects dopamine and its metabolites in the nucleus accumbens and prefrontal cortex in the rat. Brain Res 585:1–6.

Lodge DJ, Grace AA (2006) The hippocampus modulates dopamine neuron responsivity by regulating the intensity of phasic neuron activation. Neuropsychopharmacology 31:1356–1361.

Loureiro M, Kramar C, Renard J, Rosen LG, Laviolette SR (2016) Cannabinoid transmission in the hippocampus activates nucleus accumbens neurons and modulates reward and aversion-related emotional salience. Biol Psychiatry 80:216–225.

Lovic V, Saunders BT, Yager LM, Robinson TE (2011) Rats prone to attribute incentive salience to reward cues are also prone to impulsive action. Behav Brain Res 223:255–261.

María-Ríos CE, Morrow JD (2020) Mechanisms of shared vulnerability to post-traumatic stress disorder and substance use disorders. Front Behav Neurosci 14:6.

Meredith GE, Agolia R, Arts MP, Groenewegen HJ, Zahm DS (1992) Morphological differences between projection neurons of the core and shell in the nucleus accumbens of the rat. Neuroscience 50:149–162.

Meredith GE, Baldo BA, Andrezjewski ME, Kelley AE (2008) The structural basis for mapping behavior onto the striatum and its subdivisions. Brain Struct Funct 213:17–27.

Milad MR, Pitman RK, Ellis CB, Gold AL, Shin LM, Lasko NB, Zeidan MA, Handwerger K, Orr SP, Rauch SL (2009) Neurobiological basis of failure to recall extinction memory in posttraumatic stress disorder. Biol Psychiatry 66:1075–1082.

Morrow JD, Maren S, Robinson TE (2011) Individual variation in the propensity to attribute incentive salience to an appetitive cue predicts the propensity to attribute motivational salience to an aversive cue. Behav Brain Res 220:238–243.

Mu P, Moyer JT, Ishikawa M, Zhang Y, Panksepp J, Sorg BA, Schlüter OM, Dong Y (2010) Exposure to cocaine dynamically regulates the intrinsic membrane excitability of nucleus accumbens neurons. J Neurosci 30:3689–3699.

Muir J, Tse YC, Iyer ES, Biris J, Cvetkovska V, Lopez J, Bagot RC (2020) Ventral hippocampal afferents to nucleus accumbens encode both latent vulnerability and stress-induced susceptibility. Biol Psychiatry 88:843–854.

Parkinson JA, Olmstead MC, Burns LH, Robbins TW, Everitt BJ (1999) Dissociation in effects of lesions of the nucleus accumbens core and shell on appetitive Pavlovian approach behavior and the potentiation of conditioned reinforcement and locomotor activity by D-amphetamine. J Neurosci Off J Soc Neurosci 19:2401–2411.

Parkinson JA, Willoughby PJ, Robbins TW, Everitt BJ (2000) Disconnection of the anterior cingulate cortex and nucleus accumbens core impairs Pavlovian approach behavior: further evidence for limbic cortical-ventral striatopallidal systems. Behav Neurosci 114:42–63.

Pitchers KK, Kane LF, Kim Y, Robinson TE, Sarter M (2017a) “Hot” vs. “cold” behavioural-cognitive styles: motivational-dopaminergic vs. cognitive-cholinergic processing of a Pavlovian cocaine cue in sign- and goal-tracking rats. Eur J Neurosci 46:2768–2781.

Pitchers KK, Phillips KB, Jones JL, Robinson TE, Sarter M (2017b) Diverse roads to relapse: a discriminative cue signaling cocaine availability is more effective in renewing cocaine seeking in goal trackers than sign trackers and depends on basal forebrain cholinergic activity. J Neurosci 37:7198–7208.

Podda MV, Riccardi E, D’Ascenzo M, Azzena GB, Grassi C (2010) Dopamine D1-like receptor activation depolarizes medium spiny neurons of the mouse nucleus accumbens by inhibiting inwardly rectifying K+ currents through a cAMP-dependent protein kinase A-independent mechanism. Neuroscience 167:678–690.

Robinson TE, Berridge KC (1993) The neural basis of drug craving: an incentive-sensitization theory of addiction. Brain Res Brain Res Rev 18:247–291.

Salgado S, Kaplitt MG (2015) The nucleus accumbens: A comprehensive review. Stereotact Funct Neurosurg 93:75–93.

Saunders BT, O’Donnell EG, Aurbach EL, Robinson TE (2014) A cocaine context renews drug seeking preferentially in a subset of individuals. Neuropsychopharmacology 39:2816–2823.

Saunders BT, Robinson TE (2011) Individual variation in the motivational properties of cocaine. Neuropsychopharmacology 36:1668–1676.

Saunders BT, Robinson TE (2012) The role of dopamine in the accumbens core in the expression of Pavlovian-conditioned responses. Eur J Neurosci 36:2521–2532.

Scala F et al. (2018) Environmental enrichment and social isolation mediate neuroplasticity of medium spiny neurons through the GSK3 pathway. Cell Rep 23:555–567.

Singer BF, Guptaroy B, Austin CJ, Wohl I, Lovic V, Seiler JL, Vaughan RA, Gnegy ME, Robinson TE, Aragona BJ (2016) Individual variation in incentive salience attribution and accumbens dopamine transporter expression and function. Eur J Neurosci 43:662–670.

Stelly CE, Girven KS, Lefner MJ, Fonzi KM, Wanat MJ (2021) Dopamine release and its control over early Pavlovian learning differs between the NAc core and medial NAc shell. Neuropsychopharmacology 46:1780–1787.

Stringfield SJ, Palmatier MI, Boettiger CA, Robinson DL (2017) Orbitofrontal participation in sign- and goal-tracking conditioned responses: Effects of nicotine. Neuropharmacology 116:208–223.

Taepavarapruk P, Floresco SB, Phillips AG (2000) Hyperlocomotion and increased dopamine efflux in the rat nucleus accumbens evoked by electrical stimulation of the ventral subiculum: role of ionotropic glutamate and dopamine D1 receptors. Psychopharmacology (Berl) 151:242–251.

Turner VS, O'Sullivan RO, Kheirbek MA (2022) Linking external stimuli with internal drives: A role for the ventral hippocampus. Curr Opin Neurobiol 76:102590.

Versaggi CL, King CP, Meyer PJ (2016) The tendency to sign-track predicts cue-induced reinstatement during nicotine self-administration, and is enhanced by nicotine but not ethanol. Psychopharmacology (Berl) 233:2985–2997.

Wicking M, Steiger F, Nees F, Diener SJ, Grimm O, Ruttorf M, Schad LR, Winkelmann T, Wirtz G, Flor H (2016) Deficient fear extinction memory in posttraumatic stress disorder. Neurobiol Learn Mem 136:116–126.

Wolf ME (2010) The Bermuda triangle of cocaine-induced neuroadaptations. Trends Neurosci 33:391–398.

Wu M, Brudzynski SM (1995) Mesolimbic dopamine terminals and locomotor activity induced from the subiculum. Neuroreport 6:1601–1604.

Zahm DS (1999) Functional-anatomical implications of the nucleus accumbens core and shell subterritories. Ann N Y Acad Sci 877:113–128.

Zhou Y, Zhu H, Liu Z, Chen X, Su X, Ma C, Tian Z, Huang B, Yan E, Liu X, Ma L (2019) A ventral CA1 to nucleus accumbens core engram circuit mediates conditioned place preference for cocaine. Nat Neurosci 22:1986–1999.

Ziminski JJ, Hessler S, Margetts-Smith G, Sieburg MC, Crombag HS, Koya E (2017) Changes in appetitive associative strength modulates nucleus accumbens, but not orbitofrontal cortex neuronal ensemble excitability. J Neurosci 37:3160–3170.

Zinsmaier AK, Dong Y, Huang YH (2022) Cocaine-induced projection- and cell type-specific adaptations in the nucleus accumbens. Mol Psychiatry 27:669–686.